

The Pennsylvania State University
The Graduate School

**ELUCIDATING THE CONSEQUENCES OF DIETARY SUGAR ON HUMAN
GUT COMMENSAL BACTERIA**

A Dissertation in
Biomedical Sciences

by

Victoria H. Pearce

© 2023 Victoria H. Pearce

Submitted in Partial Fulfillment
of the Requirements
for the Degree of

Doctor of Philosophy

December 2023

The dissertation of Victoria H. Pearce was reviewed and approved by the following:

Guy E. Townsend II
Assistant Professor of Biochemistry and Molecular Biology
Dissertation Advisor
Co-Chair of Committee

Amanda Nelson
Assistant Professor of Dermatology
Co-Chair of Committee

Gregory Yochum
Associate Professor of Biochemistry and Molecular Biology, & Surgery

Mauricio H. Pontes
Assistant Professor of Pathology and Laboratory Medicine, Division of
Experimental Pathology, & Microbiology and Immunology

Prashant Nighot
Associate Professor of Medicine, Division of Gastroenterology and
Hepatology

Ralph Keil
Associate Professor of Biochemistry and Molecular Biology
Program Chair, Biomedical Sciences Graduate Program

ABSTRACT

The human gut microbiota is critical to determining human health and development. The gut microbiota composition is variable and can be altered by the host diet, which changes nutrient availability and in turn supports distinct microbial populations. Sugar-rich diet consumption modifies the gut microbiota composition by enriching for microbial populations that drive disease, indicating that abundant human dietary additives increase disease susceptibility by altering the gut microbiota which provides a potential therapeutic target to disease or symptom remediation. To achieve this, microbial metabolic pathways must be explored to identify potential pharmacologic targets.

Diets rich in dietary simple sugars, fructose and glucose, reduce fitness and abundance of a dominant symbiotic gut phylum, Bacteroidetes. In the model organism *Bacteroides thetaiotaomicron*, glucose and fructose silence a critical colonization protein, Roc, via its mRNA leader through an unknown mechanism. I determined that these sugars silence the activity of global transcription factor, BT4338, that I renamed Cur, which indirectly governs Roc synthesis. Further, I demonstrated that this mechanism is conserved across *Bacteroides* species including 3 other abundant human gut commensals.

My findings revealed that Cur activity is interconvertible whereby nutrient availability controls transcription factor binding and introduction of glucose or

fructose rapidly and dramatically reduce synthesis of downstream Cur-dependent products. I utilized forward and reverse genetic approaches to characterize molecular pathways that modulate Cur activity through synthesis of an intracellular metabolite(s) and that a specific phosphofructokinase enzyme mediates Cur silencing during utilization of fructose and glucose. Finally, I determined that increased Cur activity requires a bi-directional ribose-5-phosphate isomerase suggesting that pentose phosphate pathway intermediates are important for controlling activation. My work demonstrates that these enzymes co-ordinate cellular metabolism to regulate Cur activity by modulating a putative intracellular signal.

Together, my work identified a molecular pathway by which dietary sugar alters microbial abundance and fitness by controlling gene expression. Additionally, this work defined metabolic steps required for *Bacteroides* species to control Cur activity and revealed how abundant members of the human gut microbiota coordinate utilization of host dietary components with expression of intestinal colonization factors. Overall, my thesis provides the foundation for identifying targets to modulate microbial populations by way of future therapeutic interventions.

TABLE OF CONTENTS

LIST OF FIGURES	IX
LIST OF TABLES	X
LIST OF ABBREVIATIONS	XI
ACKNOWLEDGMENTS	XIV
CHAPTER 1: LITERATURE REVIEW	1
The human microbiota is a critical health determinant	1
Multi-factorial control of the human gut microbiota.....	9
Host genetics.....	10
Host environment.....	12
Host diet	15
Modulating the gut microbiota can alter disease resolution.....	19
Prebiotics.....	19
Probiotics.....	23
Antibiotics	25
Intra-Intestinal Nutrient Utilization Mechanisms	28
Actinobacteria.....	28
Verrucomicrobia.....	29
Proteobacteria	30
Firmicutes	31
Bacteroidetes.....	32
Non-intestinal microbial mechanisms	33
Importance of nutrient access.....	35
Nutrient Prioritization in a Challenging Environment.....	36
Carbon catabolite repression (CCR).....	36
CCR mechanisms in intestinal microbes	36
CCR influence on host-microbe interactions.....	38
Host Dietary Sugar Consumption Alters the Gut Microbiota	39
Dietary sugar consumption in human populations	39
Microbiota alteration due to high sugar.....	40
Thesis Overview.....	42
CHAPTER 2: DIETARY SUGARS SILENCE THE MASTER REGULATOR OF CARBOHYDRATE UTILIZATION IN HUMAN GUT <i>BACTEROIDES</i> SPECIES ...	44

Abstract.....	44
Introduction	45
Results	48
BT4338 is necessary for Roc synthesis.....	48
BT4338 indirectly controls Roc via its mRNA leader.....	51
EF-G2 and other BT4338 regulated products are dispensable for Roc synthesis.....	55
Candidate <i>Bt</i> sRNAs are insufficient to control Roc levels.....	58
Glucose and fructose rapidly and dominantly silence BT4338 activity.	58
BT4338 orthologs govern a partially conserved regulon.....	61
Dietary sugar silences BT4338-ortholog activity across prominent <i>Bacteroides</i> species.	64
Discussion.....	65
Materials and Methods.....	70
Bacterial culture conditions.....	70
Construction of strains.....	70
Generation of Bt transposon insertion library.....	71
Colony Blotting.	72
Western Blotting.	72
Quantitative PCR (qPCR).....	74
Monitoring growth of bacterial strains <i>in vitro</i>	74
Chromatin Immunoprecipitation.....	75
Carbon limitation experiments.....	75
Examining bacterial abundance in the murine gut.....	76
Measuring BT4338 ortholog silencing by dietary sugar addition.....	76
sRNA binding prediction using IntaRNA.....	77
Statistical analysis.....	77

CHAPTER 3: CARBON UTILIZATION PATHWAYS DIRECT CUR ACTIVITY IN

HUMAN GUT <i>BACTEROIDES</i>	78
Abstract.....	78
Introduction	79
Results	82
Fructose and glucose metabolism is required for Cur silencing.....	82
Disrupting the EMP increases Cur activity in glucose and fructose. ..	84
Reducing specific steps in noPPP reduce Cur activation during carbon starvation.....	86
Discussion.....	91
Material and Methods.....	95
Bacterial culture conditions.....	95
Construction of strains.....	95
Inducible system (CRISPRi).....	96
Western Blotting.....	96

Quantitative PCR (qPCR).....	98
CRISPRi carbon limitation experiments.....	98
Monitoring growth of bacterial strains <i>in vitro</i>	99
Coomassie staining of IPTG induced strains.....	100
Supplemental Tables	101
CHAPTER 4: RESEARCH SUMMARY AND DISCUSSION	106
Summary.....	106
Limitations and future perspectives.....	107
APPENDIX A: HARNESSING GUT MICROBES FOR GLYCAN DETECTION AND QUANTIFICATION.....	115
Introduction	115
Results	116
PUL reporters confer dose-dependent <i>susC</i> transcription	116
<i>pBolux</i> reporter does not inhibit typical glycan-responsive transcription.....	118
PUL reporters confer dose-dependent <i>lux</i> transcription.....	119
Discussion.....	120
Materials and Methods.....	120
Bacterial culture	120
Transcript quantification.....	121
Statistics and reproducibility	122
Supplemental Tables	122
APPENDIX B: GENERATION OF A GDNA LIBRARY IN <i>BACTEROIDES THETAIOAOMICRON</i>.....	124
Introduction	124
Generation of the gDNA library	125
1. Establish the fragmentation method	125
2. Determine the appropriate plasmid.....	126
3. Moving the library into appropriate <i>Bt</i> background.....	127
4. Identify fragments expressing increased Roc	128
Discussion and Future Directions.....	130
Materials and Methods.....	131
Final construction of <i>B. thetaiotaomicron</i> genomic DNA library.	131
Colony Blotting	131
RNA-seq	132
Supplemental Tables	132
APPENDIX C: SUPPLEMENTAL INFORMATION FOR CHAPTER 2.....	134

Supplemental Figures	134
Supplemental Tables	145
REFERENCES	155

LIST OF FIGURES

Figure 1-1: Multifactorial control of the microbiota	9
Figure 1-2: Mechanisms of microbial modulation.....	20
Figure 1-3: High sugar consumption alters microbiota and drives disease.....	41
Figure 2-1: BT4338 is required for Roc synthesis.....	49
Figure 2-2: BT4338 governs Roc levels via its 5' mRNA leader	54
Figure 2-3: BT4338 DNA binding activity is stimulated during carbon starvation.....	56
Figure 2-4: Dietary sugars silence BT4338 activity.....	59
Figure 2-5: BT4338-orthologs govern a conserved regulon among prominent <i>Bacteroides</i> species	63
Figure 2-6: A BT4338-ortholog is silenced by dietary sugar addition in <i>B. fragilis</i>	64
Figure 2-7: Model depicting the consequences of glucose and fructose on Cur activity	67
Figure 3-1: Fructose importation is required for Cur silencing	83
Figure 3-2: EMP disruption increases Cur activity	86
Figure 3-3: Cur activity is differentially stimulated during carbon starvation	87
Figure 3-4: CRISPRi interferes with <i>rpiA</i> transcription	89
Figure A-1: PULs exhibit dose-dependent transcriptional responses	117
Figure A-2: pBolux reporter does not inhibit transcription	118
Figure A-3: PUL reporters confer dose-dependent <i>lux</i> transcription and activity.....	119
Figure B-1: Fragmentation of gDNA using GenomiPhi	126
Figure B-2: Identifying appropriate <i>Bt</i> background	127
Figure B-3: Model for gDNA library generation.....	128
Figure B-4: Identify fragments expressing increased Roc.	129
Figure C-1: BT4338 is required for Roc synthesis through carbon limitation.	134
Figure C-2: Pentose phosphate pathway mutants exhibit reduced Roc amounts	135
Figure C-3: Carbon limitation and various carbon sources change BT4338 activity independent of protein amount.....	136
Figure C-4: The roc mRNA leader is necessary and sufficient for <i>BT4338</i> -dependent control of the downstream ORF	138
Figure C-5: Candidate BT4338 regulated products are not required for Roc synthesis.....	139
Figure C-6: Expression of candidate sRNAs are insufficient to increase Roc amounts.....	140
Figure C-7: BT4338 is dispensable for growth in PMOG and necessary for <i>fusA2</i> and <i>BT4295</i> expression	141
Figure C-8: BT4338 orthologs are dispensable for growth in glucose and fructose	142
Figure C-9: Roc homologs are differentially regulated by BT4338 orthologs.....	143
Figure C-10: PMOGs support <i>B. fragilis</i> growth.....	144

LIST OF TABLES

Table 1-1: Nutrient utilization machinery in gut microbes	34
Table 3-1: Strains and plasmids used in this study	101
Table 3-2: Oligonucleotides used in this study	103
Table A-1: Strains used in this study	122
Table A-2: Oligonucleotides used in this study	123
Table A-3: Plasmids used in this study	123
Table B-1: Strains and plasmids used in this study	132
Table B-2: Oligonucleotides used in this study.....	133
Table C-1: Strains and plasmids used in this study.....	145
Table C-2: Oligonucleotides used in this study	150

LIST OF ABBREVIATIONS

2-DG	2-deoxyglucose
ABC	ATP binding cassette
AD	atopic dermatitis
AMP	adenosine monophosphate
ANOVA	analysis of variance
aTc	anhydrotetracycline
ATP	adenosine triphosphate
<i>Bc</i>	<i>Bacteroides cellulosilyticus</i>
BCFA	branched-chain fatty acid
<i>Bf</i>	<i>Bacteroides fragilis</i>
BHI-B	brain heart infusion-blood
<i>Bo</i>	<i>Bacteroides ovatus</i>
<i>Bt</i>	<i>Bacteroides thetaiotaomicron</i>
BV	bacterial vaginosis
<i>Bv</i>	<i>Bacteroides vulgatus</i>
cAMP	cyclic-AMP
CAZymes	carbohydrate-active enzymes
CBM	carbohydrate binding molecule
CcpA	catabolite control protein A
CCR	carbon catabolite repression
CD	Crohn's disease
CD25	cluster of differentiation 25
CD4	cluster of differentiation 4
cDNA	copy DNA
CE	carbohydrate esterase
ChIP	chromatin immunoprecipitation
ChIP-seq	ChIP-sequencing
Cre	catabolite-repressible element
CRISPRi	clustered regularly interspaced short palindromic repeats interference
CRP	cAMP receptor protein
CS	chondroitin sulfate

Cur	carbohydrate utilization regulator
Cya	adenylate cyclase
DHAP	dihydroxyacetone phosphate
DSS	dextran sodium sulfate
ECF	extracytoplasmic function
EF-G2	elongation factor-G2
EI	Enzyme I
EII	Enzyme II
EMP	Embden-Meyerhof-Parnas Pathway
FBP	fructose 1,6-bisphosphate
FMT	fecal microbiota transplant
Foxp3	forkhead box p3
GD	Graves' disease
gDNA	genomic DNA
GFP	green fluorescent protein
GH	glycosyl hydrolase
Glc	glucose
GLUT	glucose transporter
GT	glycosyltransferase
HA	hemagglutinin
HRP	horseradish peroxidase
HTCS	hybrid two component system
IBD	inflammatory bowel disease
IBS	irritable bowel syndrome
IL	interleukin
IP	immunoprecipitation
IPTG	isopropyl β -D-1-thiogalactopyranoside
LPMO	lytic polysaccharide monooxygenase
LPS	lipopolysaccharide
mRNA	messenger RNA
MUFA	monounsaturated fatty acids
noPPP	non-oxidative PPP
OD	optical density
oPPP	oxidative PPP
ORF	open reading frame
PBP	penicillin binding protein
PCR	polymerase chain reaction

PEP	phosphoenol pyruvate
PL	polysaccharide lyase
PMOG	porcine mucin O-glycan
PPP	pentose phosphate pathway
PRPP	phosphoribosyl diphosphate
PRS	phosphoribosylpyrophosphate synthetase
PSA	surface a polysaccharide
PTS	phosphotransferase
PUFA	polyunsaturated fatty acid
PUL	polysaccharide utilization loci
qPCR	quantitative PCR
RBP	RNA binding protein
Ri5P	ribose-5-phosphate
Roc	regulator of colonization
RPE	ribulose-phosphate 3-epimerase
RPI	ribose-5-phosphate isomerase
rRNA	ribosomal RNA
Ru5P	ribulose-5-phosphate
SCFA	short chain fatty acid
SEM	standard error of the mean
SES	socioeconomic status
SFA	saturated fatty acid
SGBP	surface glycan binding protein
SGLT	sodium-glucose transport protein
SNP	single nucleotide polymorphism
sRNA	small RNA
Sus	starch utilization system
TBDT	TonB-dependent transporter
TKL	transketolase
Treg	regulatory T cell
TYG	tryptone-yeast extract
UC	ulcerative colitis
US	United States

ACKNOWLEDGMENTS

First and foremost, I would like to thank my advisor and mentor, Dr. Guy Townsend for his encouragement and support throughout my time in his lab. He has invested an inordinate amount of time into my training both on and off the bench. I have become a better writer, presenter, and scientist with his help than I ever could have achieved on my own. We have learned together over the past several years as I was the pioneer student of his first laboratory. I am incredibly grateful for his patience and extra push when I need it most.

I have been very fortunate in the support I have received at Penn State. I thank my dissertation committee: Drs. Amanda Nelson, Gregory Yochum, Mauricio Pontes, and Prashant Nighot for their guidance and support through this journey. They have provided wonderful advice and asked important questions to help influence my work as my project took twists and turns over time.

I would be remiss if I didn't thank Jennifer Modesto who actually recruited me to the Townsend lab. Our weekly, turned daily, coffee runs and our ability to talk for hours on end about experiments and life were invaluable to me during this journey. Furthermore, I thank Christopher Kendra who has been my closest friend throughout my graduate career. Being the only two students who mainly focus on bacteria has been a challenge and I am so thankful to have had Chris by my side. From our regular "back lab" vent sessions, grammar checking

important emails, troubleshooting experiments, and late-night lab chats over some fast food, I couldn't have asked for a better bacteria buddy.

I have to thank the friends I have gained over the years who have become an integral part of my support network though I cannot possibly name everyone. Starting with the PhD fam that began day one of orientation, MedNotes, GSA, and especially LTS. My graduate career has brought some truly amazing people into my life who have helped me in more ways than I realize.

I would not be here if it weren't for the support of my family. Thank you to my parents for always being willing to listen to me and read over my documents for grammatical checks even when they give them a headache. Thank you to my sister and her family for always bringing a smile to my face when needed with pictures of my niece and nephews. Thank you to my in-laws for always checking in on me and supporting me. I want to thank each and every one of them for being understanding throughout this journey.

Finally, I want to thank my husband Isaac for his endless support and love. He has been by my side since before even applying to graduate school. Together we have been through a PhD, medical school, the match, residency, a global pandemic, an engagement, and a wedding all during 6 years of long distance between two states. His patience and understanding through all of it has been incomprehensible and I can't wait to finally live under the same roof. Thank you Isaac, I love you.

A portion of this work was supported by National Institutes of Health Grant GM147178 awarded to Guy E. Townsend II. The findings and conclusions do not necessarily reflect the view of the funding agency.

CHAPTER 1: LITERATURE REVIEW

The human microbiota is a critical health determinant

Microbes from all domains of life, Eukarya, Archaea, viruses, and Bacteria begin colonizing the neonate immediately following birth. These domains coexist, competing and collaborating with one another, and inhabit niches in which they are capable of survival in and on the host. The human host supplies these organisms with nutrient rich habitats while the microbes perform numerous functions for the host including digestion, pathogen defense, and immune system training together forming a mutualistic relationship. Microbiomes exist across the human body containing distinct organisms which are spatially constrained and perform functions specific to the environment they occupy. A healthy microbiota is generally diverse and beneficial symbiotic bacteria, known as commensals, are more abundant than potentially harmful bacteria. Perturbations in this balance can lead to a state of dysbiosis where pathogenic organisms colonize or become more abundant ultimately causing disease (1). Here, I will highlight four of the most highly colonized microbiomes including skin, vagina, oral, and gut and describe their roles in human health and development.

Microbes colonize the largest organ of the human body creating an incredibly diverse skin microbiota (2-4). The skin itself provides a physical barrier against the environment and a way to perceive the surrounding world. Skin consists of layers called the hypodermis, dermis, and epidermis. The epidermis is

comprised of stratum basale, stratum spinosum, stratum granulosum, stratum lucidum, and stratum corneum as the outermost layer (5). The stratum corneum is composed of densely packed layers of keratinocytes continuously shedding and allowing new cells to move up and is only broken up by hair follicles, sweat glands, and sebaceous glands. These glands and follicles provide colonizing bacteria niches across the body due to the production of sweat or sebum altering the environment (6). The bacteria comprising the skin microbiota are mostly aerobes, organisms dependent on oxygen for aerobic respiration, and a few facultative anaerobes, microbes that can switch between aerobic respiration and fermentation based on available oxygen as most areas of the skin encounter oxygen constantly (7). These include organisms from the phyla Firmicutes, Actinobacteria, Proteobacteria, and Bacteroidetes. Microbes on the skin are subjected to numerous environmental factors such as clothing, hygiene products, and the elements which change with geographic location. The taxonomic distribution of the skin flora changes based on body location as these organisms require different skin surface topography to thrive. For example, microbes favoring sebaceous areas like the face, include *Propionibacterium* species which are lipophilic and encode lipases which can degrade sebum, whereas *Corynebacterium* species prefer moist, humid environments like the axilla (8, 9). Arm and leg skin is rather desiccated and more exposed than other areas leading to lower microbial load (10). Common cosmetic products such as moisturizer change the hydration level of the skin at points of use across the body. At higher hydration levels, *Propionibacterium acnes*, a major player in acne development,

is significantly more abundant than at low hydration levels demonstrating the importance of the environment and nutrient availability on microbial abundance and the impact of lifestyle choices made by the host (11).

Importantly, the skin microbiota aids in establishing host immune tolerance, allowing the immune system to differentiate symbiont from pathogen. One such example is *Staphylococcus epidermidis* which promotes IL-1 signaling and T cell function to modulate the immune response to pathogenic *Staphylococcus aureus*, the most common cause of cutaneous bacterial infection (12). When the skin is breached through wounding, both commensal skin microbes and environmental microbes are introduced to the site of injury including *S. aureus*, which promotes inflammation. *S. aureus* is a commensal skin microbe colonizing 5-30% of individuals but can cause infection of an open wound (13). An increase in *S. aureus* colonization is also associated with atopic dermatitis (AD). This inflammatory skin lesions causing disease affects about 10-12% of children adults in the United States (US) (14, 15). 75-100% of AD patients have *S. aureus* within lesions and as *S. aureus* is a commensal, the host has an insufficient immune response due to the developed immune tolerance allowing for chronic and recurrent lesions (13). One of the features associated with AD is a reduction of diversity in the microbiome permitting an increase in *S. aureus* abundance (16). Together, the flora comprising the skin microbiota functions to protect from pathogen invasion by defending the physical barrier of the skin and as such are crucial to skin health.

The vaginal microbiota is comprised of an estimated 10^{10} obligate anaerobic bacteria, organisms which perform fermentation and require a strict oxygen free environment (17, 18). Glucose, oxygen, and other nutrients diffuse through submucosal tissues into the vaginal mucosa generating an anaerobic environment in contrast to the oxygen rich environment of the skin (19). Vaginal flora is limited in diversity with *Lactobacillus* species being the most prominent at 90% of organisms, which function to produce antimicrobial compounds like bacteriocins, hydrogen peroxide, and lactic acid to maintain a low pH in the environment and inhibit pathogen invasion (20-26). Temporal changes in the vaginal microbiota are due to hormones of the individual's menstrual cycle and pregnancy status along with sexual activity, stress, hygiene, and other lifestyle choices (27-31).

Disrupting the balance of the vaginal microbiota can lead to bacterial vaginosis (BV) indicated by a drastic loss of *Lactobacillus* upwards of 80% coupled with increasing abundance in facultative or obligate anaerobes (32, 33). This occurs because *Lactobacillus* species produce lactic acid which drives the vaginal pH down to steady-state levels. When *Lactobacillus* abundance drops, there is a subsequent drop in lactic acid production increasing the pH and making the environment more easily inhabitable for other organisms such as *Gardnerella vaginalis*, the most common causative agent of BV (34). Additionally, decreased *Lactobacillus* abundance can also allow for expansion of *Escherichia coli*, the most common cause of urinary tract infection (35). By maintaining

environmental homeostasis, the vaginal flora aims to inhibit potential pathogenic invaders and prevent host infection of the urogenital tract.

The oral cavity contains its own unique microbiota. The flora in the oral cavity is rich in diversity as the tongue, cheek, hard and soft palates, lip, saliva, and teeth are all niches to inhabit (36). The oral microbiota increases in abundance as more teeth erupt in a growing child's mouth due to more surfaces to inhabit. This incredibly well-studied microbiome is comprised of over 700 species falling into 12 phyla including Firmicutes, Fusobacteria, Proteobacteria, Actinobacteria, and Bacteroidetes (37-39). Location plays a key role in colonization as there are only a few sites, such as between the papillae of the tongue, which can harbor anaerobes where otherwise, organisms in the oral cavity are aerobic (38, 40). Together, the bacteria throughout the oral cavity exist in the form of a biofilm, covering all surfaces. The α -diversity, or how diverse the community is, of the oral microbiota is second only to the gut microbiota due to its frequent communication with the external environment. However, β -diversity, or the measure of similarity between communities, in this case different locations within the oral cavity, is incredibly low unlike the gut microbiota (38, 41, 42). Much like the skin microbiota, the oral microbiota defends the physical barrier of the oral epithelium to prevent pathogen invasion and helps to develop immune tolerance so the host immune system can fight off potential pathogens ingested or inhaled (43, 44).

Periodontitis, a progressive and irreversible destruction of the tooth attachment system leads to eventual tooth loss. Poor oral hygiene, tobacco use, and disease comorbidities can aggravate this inflammatory disease. The host inflammatory reaction causing this disease is driven by dysbiosis of the oral microbiota (45). Generally, an increase in already present anaerobic bacteria, such as *Porphyromonas gingivalis* is found to be associated with periodontitis, with this bacterium being found almost 86% of chronic periodontitis patients (46, 47). These anaerobic bacteria present within the gums trigger inflammatory cytokine release initiating the first stage of periodontitis and allowing for prolonged dysbiosis in the subgingival space (48). Thus, oral hygiene is incredibly important to remove disease-causing bacteria and maintain a healthy, balanced oral microbiota.

The gut contains one of the most well-characterized human microbiotas residing primarily in the large intestine, or colon, of the gastrointestinal tract (49). The colon is lined with colonocytes covered in microvilli forming a barrier and aiding in water reabsorption and stool impaction (50-53). Additionally, goblet cells are abundant in the colon and secrete a mucus layer to protect colonocytes and other cells comprising the differentiated epithelium later from luminal material and colonizing gut microbes (54). An estimated 10^{12} anaerobic bacterial cells per milliliter inhabit this environment creating an exceptionally dense ecosystem found in the intestinal lumen, within the mucus lining, and proximal to the intestinal epithelium (55, 56). Overlapping mostly with the oral microbiota, the

phyla found within the gut include mainly Proteobacteria, Firmicutes, and Bacteroidetes with a small percentage belonging to Verrucomicrobia, Fusobacteria, Actinobacteria, and Acidobacteria (57-62). Together the gut flora functions to aid in host digestion and defend the gut from pathogen invasion in addition to the mucus barrier already lining the intestines.

Numerous diseases have known associations with altered or dysbiotic gut microbiota, however, the specific causes are unknown due to confounding variables. One well known disease associated with microbiota alterations is inflammatory bowel disease (IBD) (1, 63). IBD is a chronic inflammatory condition of the gastrointestinal tract comprised of two different clinical presentations: ulcerative colitis (UC) and Crohn's disease (CD) (1). While these illnesses differ in symptoms and etiology, both are chronic, inflammatory, and have depleted Firmicutes and Bacteroidetes phyla in the gut microbiota (64-66). The gut microbiota has an immunomodulatory function in the host, but when in a state of dysbiosis, the microbes are unable to regulate immune responses normally, causing an increase in inflammation such as is observed in IBD (67). Furthermore, dysbiosis of the gut microbiota can lead to a disruption and dysfunction of the intestinal barrier. As resident microbes are the main producers of short chain fatty acids (SCFA), a perturbation in SCFA producers can lead to a reduction in these important products causing further inflammation in the gastrointestinal tract as molecules and microbes can more easily pass through this barrier (68, 69). A fecal microbiota transplantation (FMT) is when fecal

material from a healthy donor is transplanted into an IBD patient's gastrointestinal tract. IBD patients receiving FMT experience a roughly 50% disease remission rate signifying the importance of a healthy and balanced gut microbiota (70).

Obesity is another prominent health concern associated with altered gut flora (71). The relationship between obesity and a perturbed gut microbiota is incredibly intertwined with little understanding as to whether obesity causes changes in microbiota composition or microbial changes could lead to obesity (72). Some organisms in the Bacteroidetes phylum protect against adiposity linking the finding of depleted *Bacteroides* species in the gut and obesity (56, 73). However, *Bacteroides* species are also reduced in high-fat or high-sucrose diets but there is no certainty as to if this compositional alteration leads to or is caused by obesity (74). Unlike IBD when both Bacteroidetes and Firmicutes are depleted, in obesity Firmicutes increase in abundance causing an increase in SCFAs which are known to be higher in obese adolescents (75, 76).

Conversely, decreased SCFAs and a lower abundance of SCFA producing bacteria are found in individuals with type 1 diabetes. Increased intestinal permeability and decreased diversity in gut microbiota are also common findings (77). A study by Maffeis, et al., compared the microbiotas of healthy children and children at risk of developing type 1 diabetes and identified *Dialister invisus*, *Gemella sanguinis*, and *Bifidobacterium longum* in 80, 90, and 60% of at risk children compared to 30, 0, and 0% of healthy controls (78).

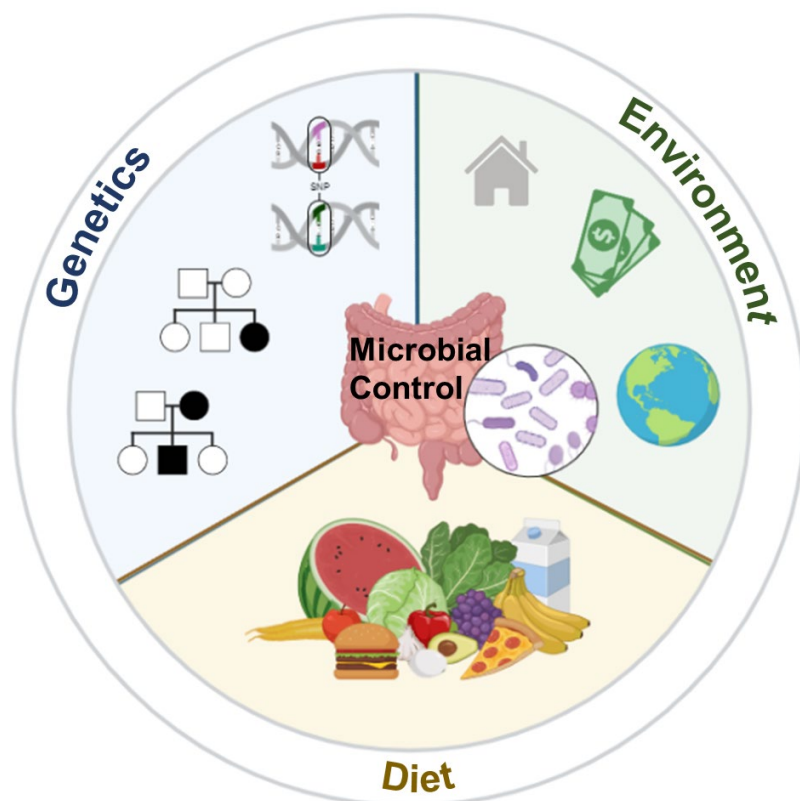


Figure 1-1: Multifactorial control of the microbiota. The microbiota can be manipulated by host genetics including SNPs and heritable or spontaneous genetic diseases (blue) Environmental factors include build environment, socioeconomic status, and geographic location (green). Diet plays one of the largest roles and includes all things consumed by the host which interact with the microbiota (yellow).

Further, there was a significant increase in intestinal permeability likely because the SCFAs produced by these species are acetate and propionate rather than butyrate which stimulates tight junction production and instead the integrity of the gut barrier weakens (78, 79). Therefore, the delicate balance of microbial composition in the gut is crucial for maintaining human health.

Multi-factorial control of the human gut microbiota

Understanding the factors which govern the development and alterations of the microbiota are crucial to fully comprehend its importance to human health. Independent of delivery method, bacteria begin colonizing in numerous locations

within and on an infant's body at birth (58, 80). These pioneer colonizers come from the infant's mother as well as the birthing environment (81, 82). This initial microbiota composition is simple, having some resemblance of the mother's microbiota, but evolves over time, fluctuating in composition and increasing in complexity (60, 83). As an individual ages and comes into contact with more lifestyle and environmental factors, the microbiota will change accordingly (84, 85). The multitude of internal and external factors like genetics, location, and diet create an incredibly individualized microbiota as depicted in Figure 1-1 (62, 86-89).

Host genetics

The host genetic landscape is variable between individuals much like the gut microbiota. While family members often share more similar microbiotas compared to unrelated individuals, it is unclear whether these similarities are due to genetics or external environmental factors (90). Microbial species are capable of forming a persistent colonization within the host for long periods of time suggesting host genetics could play a role in defining the microbiome composition (90). Additionally, associations between bacterial taxa and host single nucleotide polymorphisms (SNP) have been described (91-93). For example, a SNP in *FUT2*, a risk factor for CD, regulates the mucosal barrier and as such could modulate microbial metabolism due to altered availability of mucosal glycans for microbes to consume (91). Historically, testing the interaction between host genetics and the microbiota in humans has used sets of

adult twins to look at individuals with identical or near identical genetics. These studies have shown that monozygotic (identical) twins have significantly more similar microbiotas compared to dizygotic (fraternal) twins suggesting a role for genetics in microbial composition (94-96). However, these studies have been unable to pinpoint heritable elements of the microbiota or genetic effects placed on these microbes from the host and require further investigation (62, 97).

Genetic diseases, heritable or spontaneous, are also associated with dysbiosis of the gut microbiota. Graves' disease (GD) is an autoimmune disorder of the thyroid, also known as hyperthyroidism, where hormone thyroxine is hypersecreted (98, 99). The immune system produces thyroid-stimulating immunoglobulin mimicking thyroid stimulating hormone to trigger this over secretion of thyroxine while simultaneously attacking the thyroid (100). While the etiology of GD is still unclear, it is thought that both genetic and environmental factors could play a role in the development of GD (101). Dietary habits are an increasing focus of study for the increased rate of autoimmune disorders. A study from Tonstad et al. identified a lower rate of hyperthyroidism in individuals who consume vegan and vegetarian diets over an omnivore diet (102). While the relationship between hyperthyroidism and diet is not well understood, the gut microbiota is one potential cause for the development of this autoimmune disorder. As the gut microbiota has an immunomodulatory role in the host, recent studies have sought to identify a link between gut dysbiosis and GD. In fact, Ishaq et al. found an increase in Bacteroidetes (57.55%), Actinobacteria (0.90%)

and Proteobacteria (8.47%) in GD patients compared to non-GD controls (51.47, 0.31, and 7.26%, respectively) while Firmicutes were less prevalent in GD patients (32.89 vs 40.61%) (103). The significant changes at the species level did not cause a drastic impact on overall phyla abundance and exhibit no direct relationship between the gut microbiota and GD. However, these data still demonstrate microbial alterations associated with GD patients compared to non-GD individuals (103-105). Overall, compositional alterations in the microbiota still remain widely unexplored due in part to the inability to acquire samples from before disease onset ruling out any potential for intraindividual studies.

Host environment

Numerous factors comprise an individual's environment and can affect the microbiota without an individual's knowledge. First, the built environment, comprised of man-made structures such as homes, buildings, and vehicles (106). Interactions with the built environment and other individuals inside it can lead to potential microbial exposures via direct contact and inhalation. For example, the pathogen *Clostridium difficile* can be passed through skin or mucus contact or contact with a contaminated surface (107). Further, surfaces and air within the environment can contain microbial metabolites like certain molds which can enter the respiratory system. Not all environmental exposures pose pathogenic threats, however (107). Humans need exposure to microbes in order to form a strong immune system by way of immune tolerance. A lack of exposure to a diverse microbial community, especially at a young age, can lead to development of

autoimmune conditions or an increased likelihood of developing asthma (108, 109). Further, a study by Abrahamsson et al, found children with lower microbiota diversity during their first month of life, were more likely to develop asthma later in life (110). Likewise, children exposed to farming environments, containing an incredibly diverse microbial community, have a drastically reduced risk of asthma development by about 50% showing the importance of the microbiota to human development (111, 112).

Another environmental component to consider is socioeconomic status (SES) of the individual. Low SES is often associated with low or no health insurance leading to reduced access to medical care (113). Additionally, increased engagement in unhealthy behaviors combined with decreases in exercise and healthy eating habits are also associated with low SES (114, 115). For example, Gangrade, et al., identified that adolescents in low SES households consume 10.88g of sugar per 100 calories of a snack item which is significantly more than adolescents in high SES households who consumed 10.21g per 100 calories (116). This increased sugar consumption along with other lifestyle choices culminates in higher incidence rates of obesity, diabetes, and cancer, which plague low SES communities with an overall higher rate of morbidity and mortality (117, 118). Higher SES is associated with increased α -diversity in the gut microbiota compared to low SES in the US which could be an effect of sugar consumption (119). The role the microbiota could play in this situation is currently under investigation with the built environment being an important variable (120).

The vast number of environmental exposures humans encounter on a daily basis complicates the ability to study and directly identify specific microbial changes related to each variable.

Given the multitude of variables in human life, including living environment, culture, and diet, the gut microbiota varies between geographic locations. This microbiota compositional variability often coincides with a variety of factors such as food availability, nutritional needs, ancestry, ethnicity, traditions, and even location elevation (121). The vast majority of studies focusing on geographic alteration in gut microbes have been performed in the US, Europe, or industrialized countries, but there is a need for studies to be conducted in non-Western populations and additional countries outside of the US (122, 123). In effort to identify differences in the microbiota due to geography, Yatsunenکو, et al. examined bacterial species in US metropolitan residents, rural Malawi residents, and Amerindians from the Venezuelan Amazon (97). Unsurprisingly, there was staggering separation in the phylogenetic composition by PCA between each country's microbial communities. The US population was even further separated as the Malawian and Amerindian populations have similar lifestyles and diets (97). This finding highlights the impact diet has on the gut microbiota. It also supports an important role for geography as populations with similar diets still have variations in their microbiomes. Importantly, these differences make defining a "healthy" microbiota challenging as a healthy

microbiota in one country likely will not resemble what is considered a healthy microbiota in another country.

Host diet

The host diet is the primary contributor to determining gut microbiota composition. Food consumed by the host is a significant source of energy for these microbes and as such governs the overall population of organisms able to survive and colonize within the gastrointestinal tract (124, 125). Previous studies reveal that host genetics may account for 12% of changes in the microbiota, but changes in the diet account for up to 57% (126). As such, dietary components are of particular interest to understanding more about gut microbiota composition. Typically, the main three macronutrients are proteins, fats, and carbohydrates and human diets are generally constructed with varying percentages of each macronutrient (127). For example the average US diet is comprised of 15.4% protein, 32.8% fat, and 51.8% carbohydrate (128).

The relationship between diet and microbial changes is best examined using population specific diets. A recent study conducted by Bourdeau-Julien et al. compared a Mediterranean diet to that typical of a Canadian, which is very similar to the diet in the US, with the goal being to understand short term dietary interventions while also highlighting the drastic differences food consumption can make to the gut microbiota (129). Using this strict dietary regimen revealed quick and dramatic alterations in microbes present in the gut (129). Further, pre-study microbiotas with higher α diversity were more resistant to these short-term

alterations suggesting a more stable community of microbes (129). In the same vein, Turnbaugh et al. used humanized mice colonized with healthy human fecal material to assess the effects of a low fat, polysaccharide rich diet compared to a typical high fat, high sugar Western diet (130). Not only did diet switches lead to dramatic and rapid compositional alterations in the microbiota, but these microbes can be transferred to and maintained in offspring (130). Together these data highlight the changes population specific diets can have on the microbiota.

Proteins

Proteins, comprised of amino acids, are fermented in the colon by Proteobacteria, Bacteroidetes, and Firmicutes. Fermentation of proteins produces both SCFAs which are used mostly for intestinal barrier maintenance and branched-chain fatty acids (BCFA) which can be used for energy, modulation of inflammation, and insulin signal transduction (131). Proteins can be animal or plant-based and differ in effect due to structural distinctions. Animal proteins, often red meat or dairy products, lead to increased abundance of *Bacteroides* and *Bilophila* species (132, 133). Additionally, the risk of IBD may be increased with high animal protein consumption due to decreases in Bifidobacterium in turn reducing SCFA production leading to gut inflammation (134, 135). Conversely, plant-based protein fermentation may enhance SCFA production by increasing Bifidobacterium and Lactobacillus phyla abundance (134).

Fats

Dietary fats fall into saturated (SFA), monounsaturated (MUFA), and polyunsaturated fatty acids (PUFA) dependent on structure. SFAs mainly come from animal products, with meat with fat striations throughout, having the highest percentage (136, 137). SFAs have been shown to increase Firmicutes and Proteobacteria while decreasing Bacteroidetes (138, 139). Firmicutes are sulfate-reducing bacteria meaning they can reduce disulfide bonds found in the mucus layer of the intestine and thus upon increase of Firmicutes, the imbalance of microbes can result in mucosal barrier instability (140, 141). Therefore, increased SFA consumption leads to gut inflammation and an increased risk of IBD development.

MUFAs have only one unsaturated carbon bond. Foods enriched with MUFAs include avocados, nuts such as almonds and cashews, and plant-based oils like sesame, canola, and olive oils (142). In general, MUFA-enriched foods are recommended to reduce cardiovascular disease risk, type 2 diabetes incidence, and manage body weight (143-145). Importantly, MUFAs do not alter α or β diversity of the gut, nor adjust the ratio of Firmicutes and Bacteroidetes (146).

PUFAs are not synthesized by the body but can be found in some nuts and seeds as well as soybean and corn oils. PUFAs are divided into omega-3 and omega-6 PUFAs with these two having opposing effects on the body (147). Omega-3 PUFAs are most commonly consumed by way of fatty fish, and these

PUFAs can increase production of anti-inflammatory molecules (148). Omega-3 PUFAs also aid in restoring a healthy ratio of Firmicutes and Bacteroidetes in the gut, in turn ensuring a strong gut barrier with appropriate SCFA production (148-150). In recent years, consumption of omega-6 PUFAs have increased an estimated 10- to 50-fold correlating with elevated cardiovascular and chronic disease diagnoses (151-153). Moreover, high omega-6 PUFA consumption has driven increased gut barrier permeability (151). As such, a balance in PUFA consumption is needed to ensure proper gut health.

Carbohydrates

Carbohydrates can generally be categorized into digestible or indigestible components also known as dietary sugar or dietary fiber, respectively. Most sugars consumed are glucose, fructose, or galactose which humans can degrade and absorb in the small intestine to be released into the bloodstream (154, 155). Though not specifically established and variable between individuals, there is a limit to the absorptive capacity of the small intestine and as such, these dietary components continue on to the large intestine affording an opportunity to interact with the microbiota (156, 157). The average US adult consumes approximately 77 grams of added sugar per day when the daily recommended intake is limited to about 36 grams of added sugar per day (158). Alternative artificial sweeteners have also become increasingly common in the US diet and are poorly metabolized by the body suggesting they also travel to the large intestine (159).

This discrepancy in sugar and sweetener consumption has led to numerous studies to better understand the impact these additives may have on the gut environment in addition to human physiology as a whole.

Dietary fibers can be categorized into fermentable or non-fermentable or based on solubility. Fermentable fibers include pectin, inulin, fructo-oligosaccharides, and galacto-oligosaccharides. Non-fermentable fibers are cellulose, hemicellulose and resistant starch (160). These carbohydrate molecules are comprised of monosaccharides connected with various different glycosidic linkages with occasional acetyl and sulfate groups (161). Fiber is unable to be digested in the small intestine and as such, travels to the large intestine to be digested by gut microbes. One of the main functions of the gut microbiota is to ferment fiber to produce SCFAs. SCFAs can be utilized as an energy source by the host but also function to regulate metabolism, inflammation, balance intestinal pH, and maintain the integrity of the intestinal barrier (74, 162). These organisms rely on dietary fiber and have evolutionarily developed ways to consume particular carbohydrates to ensure their survival and successful colonization (163, 164). As such, saccharide consumption governs microbial abundance and gut microbiota composition (165, 166).

Modulating the gut microbiota can alter disease status

Prebiotics

There are a multitude of ways to modulate the microbiota in addition to the diet with the use of supplements like prebiotics. Some individuals elect to

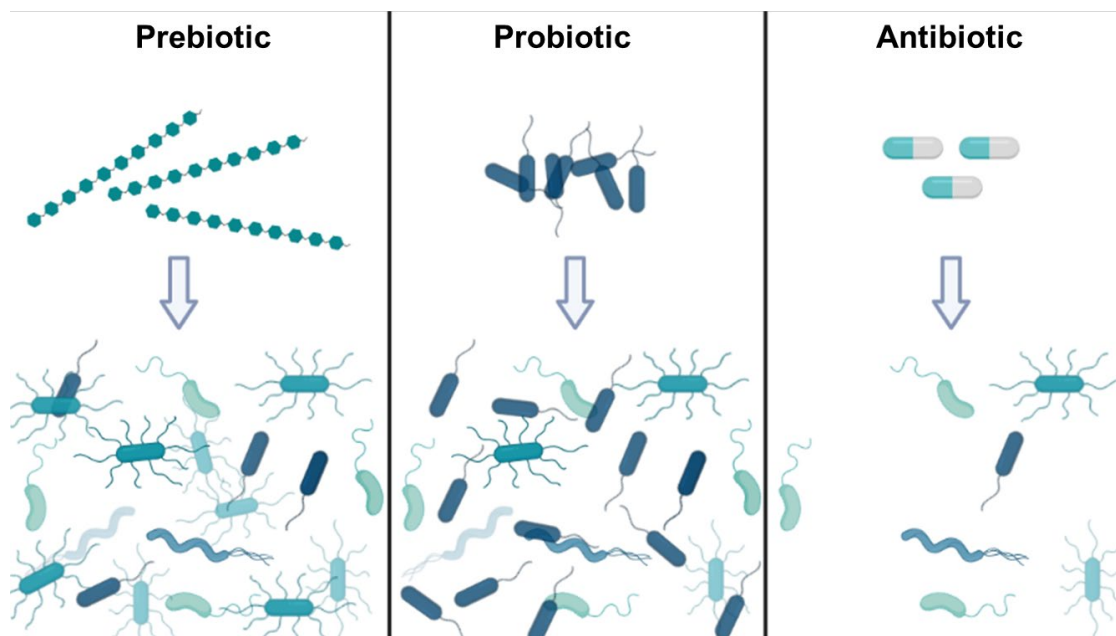


Figure 1-2: Mechanisms of microbial modulation. Microbial abundance can be modulated via prebiotics, probiotics, and antibiotics. Prebiotics are non-host digestible polysaccharides which enrich abundance of microbes which can utilize them. Probiotics are live organisms which enrich the abundance of already colonized microbes or provide new microbes to the environment. Antibiotics kill of organisms in the microbiota which are susceptible in either a narrow or broad-spectrum.

consume prebiotics which are often grouped in with dietary fibers. Prebiotics are a category of dietary components consumed in food or dietary supplements which cannot be metabolized or absorbed by the host, resistant to the gastrointestinal tract pH, can be fermented by intestinal microbes, and can enrich for bacteria based on growth or activity stimulated by the compound (Fig. 1-2). Generally, any nondigestible food ingredient which the host benefits from through altering intestinal bacteria (167). Most prebiotics are oligosaccharide carbohydrates including fructans, galacto-oligosaccharides, starch and oligosaccharides derived from glucose, and other oligosaccharides not specifically falling into these categories. Fructan structure is comprised of linear $\beta(2-1)$ linked fructose such as inulin or $\beta(2-6)$ linked fructose such as levan, both

containing a terminal $\beta(2-1)$ linked glucose (168). Galacto-oligosaccharides are lactose based with galactose at carbons 3, 4, or 6 or lactose which has undergone trans-glycosylation. This generates tri- to pentasaccharides with $\beta(1-6)$, $\beta(1-3)$, and $\beta(1-4)$ linked galactose (167, 169). Resistant starch is unaffected by upper gut digestion allowing for it to reach the microbiota in the lower gastrointestinal tract which in turn increases the production of the SCFA butyrate, benefiting host intestinal health (170). Other oligosaccharides include pectic oligosaccharides, which are often galacturonic acid or rhamnose based and can also contain different sugars linked to side chains (171, 172). Prebiotics serve as energy sources for bacteria housed in the gut (173). However, there is species specificity when it comes to degradation of particular prebiotics (174). For example, resistant starch is degraded by *Ruminococcus bromii* and concomitantly these degradation products serve as agonists or antagonists to neighboring microbes (175). As such, prebiotics serve as a substrate for cross-feeding where they not only modulate the organisms which specifically degrade them, but also have effects on the microbial community at large (176, 177). Similarly, fermentation products generated from prebiotic degradation can modify the pH of the overall environment as most products are acidic (178, 179). This small change can drastically alter the species able to inhabit the environment.

Prebiotics are available as over the counter supplements and come in a variety of formulations. These supplements boast improvements in digestion, regulation of bowel movements, and lower inflammation through modulating the gut microbiota. The clinical impact prebiotics have on already healthy individuals

is unknown as studies are limited. However, a study performed by Silk, et al., focused on the benefits of trans-galactooligosaccharide on irritable bowel syndrome (IBS), a disorder causing abdominal pain, bloating, and changes in bowel movements. There was a dose-dependent effect as the low dose (3.5g/day) significantly improved flatulence and bloating whereas a higher dose (7.0g/day) improved anxiety and overall quality of life for patients (180). Importantly, as with all supplements, benefits vary between individuals due to physiology, diet, and already established microbiota. In addition to supplementation, prebiotics are an emerging therapeutic option as there are some studies suggesting prebiotics aid in disease amelioration. Most studies to date have been performed *in vitro* due to the confounding variables humans introduce. Videla, et al., used a rat colitis model to assess if the addition of inulin, a polyfructan, would protect against induced colitis (181). Inulin is utilized by bacteria which consume butyrate and encourages growth of lactic acid bacteria, Bifidobacterium and Lactobacillus, which prevent intestinal inflammation (182). Inulin consumption in rats already exposed to dextran sodium sulfate (DSS) for 5 days to induce colitis-like inflammation, exhibited significantly lower scores of mucosal damage than rats not consuming inulin and exposed to DSS (181). These data suggest that prebiotics could provide benefits to patients experiencing intestinal diseases such as colitis, but further studies are warranted.

Probiotics

An additional dietary component potentially consumed by the host is probiotics. Probiotics are live microbes which can be administered to a host to confer a health benefit (Fig. 1-2) (183). The most commonly used probiotics are species from the *Lactobacillus*, *Saccharomyces*, *Bifidobacterium*, *Bacillus*, *Escherichia*, *Streptococcus*, and *Propionibacterium* genera (184). Probiotics can be consumed by way of a dietary supplement but more often enter the host through consumption of fermented foods. Historically, fermentation not only preserved foods when resources were sparse, but also provides a unique sensory experience to the consumer (185, 186). Microorganisms may already be present in particular foods such as kimchi, sauerkraut, or miso. Conversely, microbes can be added to initiate fermentation as seen in yogurt and other fermented dairy products (185). While probiotics are unable to drastically modify an already well-established microbiota, the benefit lies in the increase in specific strains being consumed. Not only is consumption of microbes beneficial to the host by introducing beneficial microbes to the ecosystem, but the fermentation of food products can enhance the nutrient content or partially transform the chemical landscape of the food (187, 188). A prime example is sourdough bread, in which the bacteria partially degrade the gluten during fermentation (189). As with all supplements, benefits vary between individuals due to physiology, diet, and already established microbiota.

The overall goal of supplemental probiotics is to modulate the already existing microbiota in the host. In order for probiotics to reach the microbiota,

they must traverse the length of the digestive tract and survive numerous host defense mechanisms of stomach and bile acids, defensins, and the immune system (190). Therefore, not all organisms will successfully reach the gut microbiota and those that do often have short persistence (191). Additionally, once within the gut environment, the probiotic organisms must evade predation and compete with already established organisms for available nutrients. Thus, successful probiotic generation requires a sufficient number of adaptable, diverse, and rapidly growing bacteria that can survive host defense mechanisms and compete or synergistically interact with co-resident microbes (190, 192).

Probiotics have also been of interest as a therapeutic option for individuals suffering from intestinal disease, specifically UC. The gold standard of UC therapy are aminosaliclates, reducing inflammation through a yet unknown mechanism of action (193). However, UC patients also have altered microbiota compositions compared to non-UC individuals. This suggests that supplementing with probiotics could aid disease remission through manipulating the microbiota composition to that of a healthy individual. Zocco, et al., performed a clinical trial assessing the efficacy of supplementing *Lactobacillus rhamnosus* GG (LGG) compared to a standard aminosaliclate, mesalazine, for UC remission and maintenance (194). LGG, one of the most widely utilized probiotics, was used hoping to reduce inflammation experienced in UC due to LGG's ability to downregulate proinflammatory cytokines through proteins Msp1 and Msp2 (195). Patients receiving LGG supplementation had approximately the same rate of remission and relapse compared to mesalazine over a 12-month period (194).

While the equivalent efficacy of therapeutics does not suggest the use of one over the other, this provides UC patients with additional options for therapy should the need arise. This study highlights the potential for probiotics as a more natural approach to treatment, likely with reduced side effects, however longitudinal studies are required as long-term effects have yet to be characterized.

Antibiotics

One of the most common methods to modulate the gut microbiota is the use of antibiotics. Antibiotics are classified by mechanism of action against bacteria including targeting the synthesis of the cell wall, protein, or nucleic acid (Fig. 1-2). One type of antibiotic targeting cell wall synthesis is β -lactams. β -lactams target penicillin binding proteins (PBP), enzymes which cross-link peptides to form the peptidoglycan cell wall (196). This activity blocks the production of the peptidoglycan layer leading to bacterial cell death. Glycopeptides also act to inhibit cell wall synthesis but through binding the peptide portion of peptidoglycan subunits preventing PBP binding to form the peptidoglycan cell wall (197). Inhibiting protein synthesis is achieved by targeting the 30S or 50S subunit which together comprise the 70S ribosome required for translation. Aminoglycosides and tetracyclines are both inhibitors of the 30S subunit (198). These drugs interact with the 16S rRNA, which gives rise to the 30S subunit, by preventing binding of tRNA to the A site causing misreading and premature termination of mRNA translation (198). As such, bacteria can no

longer translate mRNA leading to cell death. Chloramphenicol, macrolides, and oxazolidinones all inhibit the 50S subunit. Chloramphenicol targets 23S rRNA, which gives rise to the 50S subunit, by preventing tRNA binding to the ribosome A site (199). Macrolides instead target translocation by binding to the peptidyl transferase ring of the 23S rRNA blocking nascent peptide elongation (200). Oxazolidinones have two actions, inhibit binding of the 50S subunit to prevent the 70S ribosome from forming or it can bind and block translocation to the A site in an already formed ribosome (201). Finally, quinolones act to inhibit DNA replication. DNA replication requires DNA gyrase in Gram-negative organisms or topoisomerase IV in Gram-positive organisms. This enzyme nicks double-stranded DNA, catalyzes negative supercoil formation to help DNA unwind to be transcribed, and reseals the nicks. DNA gyrase is comprised of two A subunits which nick and reseal DNA and two B subunits which form negative supercoils. Topoisomerase IV is similarly comprised of 4 subunits, two ParC and two ParE, homologous to the A and B subunits of DNA gyrase, respectively. Quinolones inhibit this process by binding to the A subunit or ParC inhibiting the nicking and resealing of DNA in turn blocking DNA replication (202).

Antibiotics have been used since the production of penicillin in 1945 with more being discovered and developed to target new infections and multi-drug resistant or antibiotic resistant pathogens (203). Antibiotics are additionally classified as narrow-spectrum and broad-spectrum referring to the range of bacterial types they act on. One downside to oral antibiotic use is that these drugs progress through the gastrointestinal tract eventually reaching the distal

colon where they can kill off any susceptible bacteria including the commensal microbes in the microbiota. The broader the antibiotic effect, the higher the collateral damage to beneficial bacteria housed in the gut along with the causative agent of infection. In cases of unknown infectious agent, broad spectrum antibiotics would be preferred to increase the chance of killing of the unknown pathogen. However, one common side effect of antibiotic overuse, particularly broad spectrum, is alteration of normal gut flora, the main barrier against intestinal infection. A weakened microbial barrier allows for organisms like *Clostridium difficile* to infect more easily. *C. difficile* forms spores which can live on surfaces for months and is transmitted via fecal-oral route (204). *C. difficile* is resistant to heat, acid, and most antibiotics and is able to consume primary bile acids to support its growth (204, 205). One increasingly prevalent treatment for recurrent or refractory *C. difficile* infection post-antibiotic use is a fecal microbiota transplant (FMT). In an FMT, donor stool is transplanted into the gastrointestinal tract of the patient requiring treatment. As with any type of transplant, screening of donor material is essential to minimize any potential disease transmission. By using healthy donor stool, the healthy and diverse microbiota can take hold and outcompete *C. difficile* providing disease remission. This transplant is generally performed via colonoscopy however, endoscopy and even oral capsules can be used if necessary (206). A clinical trial by Kao, et al. found that 116 adults who underwent FMT by either colonoscopy or oral capsules had prevented recurrence in 96.2% of patients after 12 weeks (207).

Overall, *C. difficile* is the epitome of antibiotic manipulation of the gut microbiota and nutrient access being essential for successful colonization.

Intra-Intestinal Nutrient Utilization Mechanisms

Actinobacteria

In the gut, Actinobacteria often comprise less than 5% of bacteria present (208). While low in number, these organisms are not insignificant and play a key role in overall health. Bacteria in the actinobacteria phyla dedicate a large portion of their genome to carbohydrate metabolism with roughly half of these genes being devoted to uptake of carbohydrates as the primary function of Actinobacteria, chiefly the *Bifidobacterium* genera, is to breakdown carbohydrates (209). They utilize carbohydrate-modifying enzymes including glycosyl hydrolases (GH), ATP binding cassette (ABC) transporters, and phosphoenol pyruvate-phosphotransferase (PEP-PTS) systems (210-214).

GHs function to hydrolyze glycosidic bonds present between two or more carbohydrates. *Bifidobacteria* contain α -galactosidases and β -galactosidases with the latter being incredibly prevalent and well-studied. β -galactosidases have hydrolytic and transglycolytic activity on lactose allowing these organisms to survive on milk-derived substrates (215, 216). ABC transporters use energy from ATP hydrolysis to import molecules via two intracellular nucleotide binding domains (217, 218). Target molecules are captured by extracellular solute binding proteins before being transported across both membranes through a pore (217, 218). PEP-PTS systems are designed to transport and phosphorylate

carbohydrates to be utilized within the cell. PEP is used as a phosphoryl donor and energy source for PTS (219). PTS is comprised of up to four proteins, at least three of which are called enzyme II complexes (EIIs) which have carbohydrate specificity, and each protein carries out a phosphotransferase reaction in succession and move the target carbohydrate into the cell (220).

Each of the carbohydrate consumption mechanisms present in actinobacteria exist in different proportions for each bacterium allowing for species specificity in carbohydrate utilization. For example, *Bifidobacterium longum* contains an estimated 10 ABC transporters systems and a glucose-specific PEP-PTS system whereas *B. breve* contains four PEP-PTS systems, and one is specific to fructose and glucose uptake (221, 222). Conversely another species in this the Bifidobacteria genus, *B. animalis*, contains no PEP-PTS systems but does have two specific ABC transporters (214). Using these nutrient utilization mechanisms, most characterized actinobacteria are able to utilize ribose, fructose, glucose, sucrose, galactose, maltose, raffinose, and melibiose. However, they cannot consume L-arabinose, rhamnose, N-acetylglucosamine, sorbitol, xylitol, or inulin, leaving these carbon sources for neighboring microbes (210, 223).

Verrucomicrobia

Verrucomicrobia, specifically *Akkermansia* species, comprise roughly 3% of the overall bacterial population in the gut (224-227). Similarly, to Actinobacteria, these species contain numerous GHs specific to particular

carbohydrates. These GHs allow for the cleavage of galactose, sialic acid, N-acetyl glucosamine, and fucose of which all can be found in the gut mucin layer (228). *Akkermansia* are known mucin degraders and produce SCFAs such as acetic acid which then encourages more mucin production (229). This positive feedback loop aids in mucus barrier maintenance and consequently limits gut inflammation. But importantly, if *Akkermansia* becomes more abundant, mucus could degrade more rapidly than be produced, in turn driving inflammation due to a weakened gut barrier. As mucus degradation is the core activity of these species these mucolytic GHs are the only mechanism by which nutrients are accessed and utilized (225, 230).

Proteobacteria

Proteobacteria, comprising up to 5% of the microbes found in the gut, predominantly only consume simple sugars, or mono- and disaccharides though a few are able to consume more complex molecules (231, 232). *Escherichia coli* is one of the most well studied bacteria and the epitome of the proteobacteria possessing solute binding proteins, PTS and ABC transporter systems and a few GHs (233-236). The PEP-PTS systems encoded in *E. coli* have slightly different protein nomenclature than those contained in Actinobacteria. These proteins are named enzyme I (EI), histidine-phosphorylatable phosphocarrier protein (HPr), EIIA and EIIB occasionally in complex with EIIC (220, 237-240). EI and HPr proteins are non-specific, and membrane associated whereas EIIIs have carbohydrate specificity and are intracellular (241).

Importantly, some PTS proteins have additional activities when phosphorylated. For example, when phosphorylated, the enzyme specific for glucose uptake, EIIA^{Glc}, activates adenylate cyclase (Cya) which generates cyclic adenosine monophosphate (cAMP) (242, 243). cAMP will then go on to activate numerous transcription factors including cAMP receptor protein (CRP) which regulates a number of catabolic genes (further discussed in the carbon-catabolite repression section) (244-247).

Firmicutes

Firmicutes typically comprise around 30% of the colonized organisms in the gut however this fluctuates often inversely of Bacteroidetes (59). As one of the predominant phyla in the gut, dietary fiber fermentation is the primary role (79, 248). To fulfil this role, Firmicutes encode a large number of carbohydrate-active enzymes (CAZymes) (79, 248). These include GHs, polysaccharide lyases (PLs) which specifically break glycosidic linkages between a carbohydrate and non-carbohydrate moiety, and glycosyltransferases (GTs) which function to biosynthesize varying sizes of saccharides by transferring moieties between donor molecules and sugar molecules (249, 250). Each of these CAZymes have specificity to the carbohydrate which they target. Firmicutes also harbor ABC transporters, PEP-PTS systems, and carbohydrate binding modules like previously mentioned phyla (Table 1-1) (220, 232, 251).

Bacteroidetes

Together, Bacteroidetes and Firmicutes encompass approximately 90% or more of the cells in the gut microbiota with Bacteroidetes often being the most predominant phyla overall (252). *Bacteroides* exhibit incredible adaptability and flexibility when it comes to nutrient consumption in the gut as they are able to utilize host- or dietary-derived glycans as needed (253, 254). Carbohydrate acquisition and utilization in the *Bacteroides* is incredibly unique (Table 1-1) using polysaccharide utilization loci (PUL) (255, 256). PULs are co-ordinately regulated gene clusters which orchestrate detection, binding, depolymerization, and transportation of complex carbohydrates. The aforementioned CAZymes, GHs and PLs are encoded in PULs along with carbohydrate esterases (CE) designed to modify or degrade carbohydrates by releasing ester linked acyl or alkyl groups (257, 258). Additionally, PULs can include TonB-dependent transporters (TBDT) and surface glycan binding proteins (SGBP) which generally fall under the canonical pair, *susC* and *susD*, respectively (255, 259).

Bacteroides thetaiotaomicron for example, dedicates 18% of its genome to encoding 88 different PULs (260). The prototypical PUL is known as the starch utilization system, or Sus locus (259, 261, 262). This locus (*susRABCDEFG*) contains five outer membrane proteins (*SusCDEFG*), glycosidases (*SusAB*), and a regulator protein (*SusR*) (263-266). *SusC* is an outer membrane transporter and associated with *SusD* which binds the target glycan (263, 267). Also found on the outer membrane are *SusE* and *SusF* which bind target glycans, and finally *SusG*, a cell surface associated enzyme for polysaccharide degradation before

transportation (264, 267). SusA and SusB are found in the periplasm and act to further breakdown the target polysaccharide for appropriate utilization (265, 268). Lastly, SusR is a membrane spanning protein with a sensor domain facing the periplasm and the DNA binding domain within the cytoplasm (269).

There are numerous SusR-like and other regulatory systems within the Bacteroidetes. SusR activates expression of the PUL genes after binding the corresponding target glycan (269-271). Hybrid two component systems (HTCS) are chimeric proteins containing a transmembrane sensor histidine kinase and a DNA-binding response regulator all attached to a glycan-sensing domain (271-274). Upon sensing the target carbohydrate, HTCSs autophosphorylate, phosphotransfer, and promote transcriptional regulation via the DNA binding domain. Bacteroidetes also contain extracytoplasmic function (ECF) anti- σ factor/ECF- σ factors which contain a SusC like transport protein coupled with an anti- σ factor transmitting a signal to free the ECF- σ factor in the cytoplasm. The ECF- σ factor then interacts with RNA polymerase to regulate transcription of glycan specific utilization genes (260, 269, 270, 272). Finally, some cytoplasmic regulators have unknown function but have been annotated for monosaccharide sensing and utilization. Importantly, the contents of PULs vary greatly depending on the machinery needed to access and degrade a particular glycan from the environment (275).

Non-intestinal microbial mechanisms

Aside from the gut, bacteria are also incredibly prevalent in the soil and

Table 1-1. Nutrient utilization machinery in gut microbes

Phylum	Machinery	Nutrients Consumed
Actinobacteria	GH	Mono- and disaccharides, lactose
	ABC transporter	
	PEP-PTS	
Verrucomicrobia	GH	Mucosa
Proteobacteria	GH	Monosaccharides
	ABC transporter	
	PEP-PTS	
Firmicutes	GH	Complex carbohydrates, poly- and oligosaccharides, free monosaccharides
	ABC transporter	
	PEP-PTS	
	PL	
	GT	
Bacteroidetes	PUL	Complex carbohydrates, poly- and oligosaccharides, free monosaccharides
	GH	
	PL	
	CE	
	TBDT	
	SGBP	
	HTCS	
	ECF anti- σ /ECF σ	

Nutrient utilization machinery used by gut bacteria broken-down by phylum and the nutrients each are able to consume.

are critical for maintaining soil health as the bacteria degrade organic compounds and liberate nutrients for the plants to utilize (276). Furthermore, they help to keep disease and pests at bay which can destroy the vegetation (277). Interestingly the top phyla comprising the soil bacterial community are identical to that of the human gut microbiota: Firmicutes, Bacteroidetes, and Proteobacteria likely due to shedding by humans and animals. Actinobacteria, Acidobacteria, Verrucomicrobia, and Fusobacteria are present as well. Additional phyla include Chloroflexi, Gemmatimonadetes, and Planctomycetes. Importantly, much like the individualist nature of the human gut microbiota, soil microbial communities vary widely based on the needed and available nutrients in the environment (276).

While gut microbes mainly focus on carbohydrate utilization, soil microbes access different nutrients in the environment such as nitrogen, phosphorus, and metals like iron. However, carbohydrate utilization is still necessary in these organisms and some complex carbohydrates like cellulose and chitin are abundant in the soil (278). As such, soil microbes often contain a number of GHs, carbohydrate binding modules (CBM), and lytic polysaccharide monoxygenases (LPMO) (278). LMPOs, once activated by copper, cleave glycosidic bonds at C1 and C4 using oxidation to disrupt polysaccharides (279, 280).

Importance of nutrient access

Overall, the need for nutrient access is essential to ensure survival of bacteria and provide benefits to the hosts which they form a symbiotic relationship with. The human gut microbiota is able to access nutrients of which a host is incapable to degrade and generate nutrients, signalling molecules, and SCFAs (132, 281, 282). The mechanisms of nutrient acquisition and utilization are specific to phyla, or even individual species within each phylum, for consumption of nutrients available in the surrounding environment. This is incredibly important as these organisms compete against one another to inhabit this nutrient-rich, microbially dense niche. Organisms that are unable to access nutrients from the intestinal milieu (host diet, host glycans, cross feeding on other bacterial products), are at a fitness disadvantage compared to organisms that can readily utilize the available nutrients (283, 284).

Nutrient Prioritization in a Challenging Environment

Carbon catabolite repression (CCR)

An important competitive advantage for bacteria in the gut is utilizing the most favorable accessible carbon sources, or those that provide the fastest growth (285). This selectivity or preferential use of carbon sources is called carbon catabolite repression (CCR) (286). The regulatory mechanism of CCR includes increased expression of proteins which utilize the preferred carbon source. Concurrently, there is a reduction in the activity or presence of enzymes not required for utilization of the preferred carbon source (285). This enzyme repression is caused by the presence of a preferred substrate. Preference for carbon sources arises when numerous utilizable nutrients are present at once in high abundance. This situation is frequent in the gut as the host consumes a meal comprised of many different macronutrients which the microbiota then has access to. Gut microbes are then forced to make a choice as to which nutrients are accessible and most advantageous to ensure their survival in the densely populated environment.

CCR mechanisms in intestinal bacteria

There are several mechanisms of CCR used by the different microbial phyla in the gut. One mechanism of CCR is achieved through Crp. Crp is activated through binding cAMP after generation by Cya (245, 246). When sugars are transported through the PEP-PTS system, metabolism of the sugar eventually results in pyruvate production, and high pyruvate levels indicate that

enough substrate has been consumed compared to low pyruvate levels indicating additional carbon is required. As such the ratio of pyruvate to PEP, the phosphoryl donor to import sugar, governs this overall mechanism. The phosphorylation cascade from PEP ends with a phosphorylated EIIA^{Glc} which can donate a phosphoryl group to EIIB to transport sugar which occurs when pyruvate is low. However, when sugar importation is no longer required, and pyruvate levels are high, EIIA^{Glc} remains dephosphorylated. Phosphorylated EIIA^{Glc} can activate Cya triggering production of cAMP which will then interact with and activate Crp to govern the expression of numerous genes and operons (237). One of which is Fis, a DNA binding protein that in turn regulates transcription of *crp* (287, 288). The ratio of cAMP to Crp indicates what regulation it will impose, and importantly its transcriptional regulation is bifunctional providing activation and repression activity (245, 289).

CCR can also be achieved through catabolite control protein A (CcpA). CcpA is a bifunctional global transcriptional regulator and can interact with HPr, in the PEP-PTS system. When a preferred substrate is present, HPr is phosphorylated at serine 46 forming HPr(Ser-P). CcpA interacts with HPr(Ser-P) increasing the affinity of CcpA to bind catabolite-repressible elements (*cre*) throughout the genome. Generally, binding of the CcpA-HPr(Ser-P) dimer causes promoter repression and as such, overall CCR of enzymes not required for utilization of the preferential substrate present (290, 291).

These CCR mechanisms are crucial to microbial fitness in the ever-fluctuating gut environment to allow for utilization of mixed substrates when

nutrient availability is low or utilize the most preferred substrate to promote fitness in high nutrient availability conditions. The number one goal of gut microbes is survival in the challenging and dense intestinal environment. Selecting the most beneficial carbon source to use first is a life-or-death decision for these organisms as the wrong choice could mean a co-resident microbe overtakes the niche.

CCR influence on host-microbe interactions

A prime example of substrate prioritization driving host-microbe interactions is the evolution of the neonate microbiota to one resembling that of an adult. The initial microbiota of an infant is dominated by Actinobacteria due to the encoded β -galactosidases allowing for microbial expansion with the influx of milk which is a lactose-based substrate that can be broken down by β -galactosidases (292-295). When the infant is weaned, they begin consuming a diet of solid foods leading to an increased variety in nutrients for the organisms in the gut and causing changes in microbiota composition to be dominant in Bacteroidetes and Firmicutes (296, 297). This compositional change occurs due to the reduction in favorable substrates for Actinobacteria concurrent with increased favorable substrates for Bacteroidetes and Firmicutes which subsequently aids in further development of the child's immune system. Some Actinobacteria species, like *Bifidobacterium animalis* and *Lactobacillus rhamnosus* GG, promote development of immunological tolerance, whereby T-cell populations are trained to discriminate against self-antigen reactivity (298).

This process is essential in a developing child as disruption of immune tolerance can lead to development of autoimmunity, inflammatory diseases, and food allergies (299-301). Further, Bacteroidetes and Firmicutes are suggested to program regulatory T cells (Treg) in the intestine. For example, *Bacteroides fragilis* produces a cell-surface polysaccharide (PSA), that induces anti-inflammatory activity in Treg cells by stimulating IL-10 and reducing IL-17 production, overall reducing inflammation (302-305). Additionally, *Bacteroides thetaiotaomicron* for example encodes the gene BT4295 encoding an outer membrane protein which is recognized by host T cells and by regulating the expression of BT4295, T cell responses can be modulated (306). The benefit Bacteroidetes species provide in controlling inflammation make this an ideal phylum to target for rational therapeutic design.

Host Dietary Sugar Consumption Alters the Gut Microbiota

Dietary sugar consumption in human populations

Dietary sugars come from a number of sources within the diet split into naturally occurring and added sugars. As the name suggests, naturally occurring sugars exist in certain foods and are not added. Most commonly this is fructose found in fruit and lactose found in milk. On the other hand, added sugars are added to foods and beverages to increase palatability. This can be anything from white table sugar, sucrose, added to coffee, to the high fructose corn syrup found in many mass-produced foods and beverages in the US (307). The consumption of added sugars has drastically increased since their inception as these are often

tremendously cheaper and sweeter than traditional sugars. The most commonly associated disease with increased added sugar consumption is obesity, plaguing an estimated 68% of adults in the US as of 2018 (308). This is unsurprising as about 58% of calories consumed by Americans are from ultra-processed foods which on average contain 5-fold higher added sugars than unprocessed foods (309). The US daily average added sugar intake is 292.2 calories, roughly 15-20% of an average caloric requirement, which is much higher than the 10% maximum recommended by The US Dietary Guidelines Advisory Committee (309, 310). In terms of caloric intake, all sugars, unless artificial, will provide energy, however how these sugars are metabolised differs.

Microbiota alteration due to high sugar

On the apical side of the small intestine is a glucose transporter known as SGLT-1, an Na⁺ co-transporter, which imports glucose into the cytosol to then be transported basolaterally through the GLUT2 transporter to enter the bloodstream. Fructose, however, is passively transported by GLUT5 on the apical side and can enter the bloodstream through GLUT2 like glucose (Fig. 1-3) (311). There is a point of saturation in the small intestine at high levels of fructose consumption and the absorptive capacity is met (157). Once saturated, the small intestine can no longer import fructose and continues through the gastrointestinal tract to the large intestine where the gut microbiota is housed (312).

The influx of fructose interacting with the microbiota provides an additional nutrient to promote or inhibit growth. Mice fed a high fructose or high glucose diet

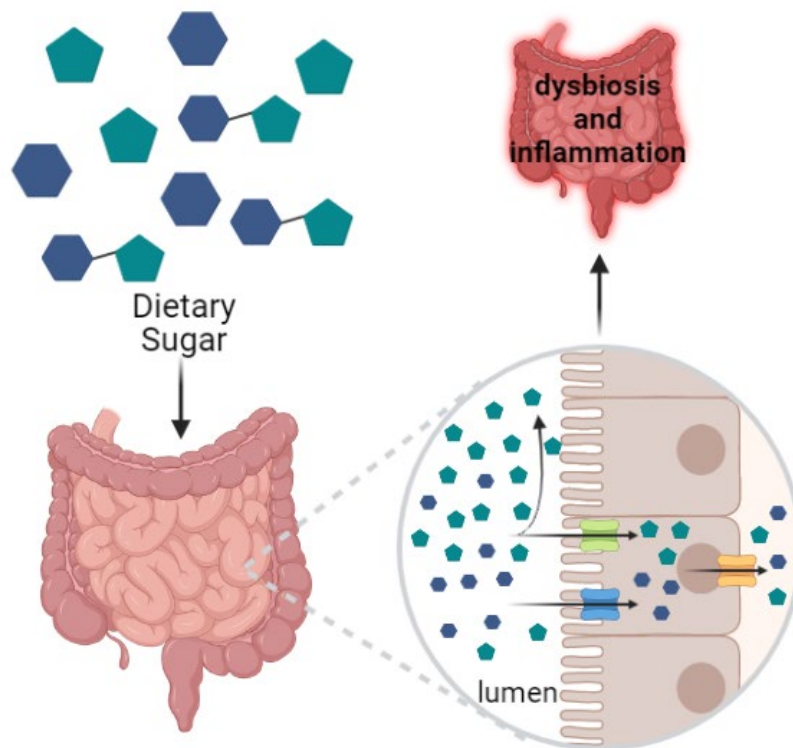


Figure 1-3: High sugar consumption alters microbiota and drives disease. Glucose is imported through SGLT-1 (blue) while fructose is imported through GLUT5 (green) on the apical, lumen side. Both monosaccharides are transported through GLUT2 (yellow) on the basolateral side. When sugar can no longer be absorbed in the small intestine, it continues to the large intestine driving compositional alterations and inflammation.

had significantly lower abundance of Bacteroidetes and Firmicutes coupled with significantly increased Proteobacteria abundance (313). This suggests high dietary sugar consumption favors the expansion of Proteobacteria since they rapidly utilize monosaccharides and disfavors Bacteroidetes and Firmicutes as they are specialized in degrading more complex carbohydrates. Additionally, this occurrence is caused by CCR as each organism is selecting the carbohydrate which they are able to better consume and utilize. With the disproportionate increase in Proteobacteria, there is an increase in pro-inflammatory lipopolysaccharide (LPS) in the gut inducing IL-8 release and gut barrier

breakdown (314). Additionally, LPS-driven inflammation triggers the onset of insulin resistance, obesity, diabetes, and is associated with IBD demonstrating the negative effects of high sugar on the gut microbiota and human health (315, 316). The expression of BT4295, a T cell response regulator in *Bt*, is regulated by the glycans available to the cell. When fed a high-glucose diet, mice had reduced T cell activation demonstrating how dietary components regulate microbial products and in turn, host immune response (306).

Thesis Overview

With the growing prevalence of dietary sugar in the Western diet, individuals are likely to encounter this additive on a daily basis without realizing it and in high quantities, dietary sugar can interact with the microbes housed in the gut. Dietary components can alter microbial composition and potentially drive disease development or exacerbate symptoms. I specifically aimed to identify microbial mechanisms governing this compositional alteration. Here, I explored the detrimental effects of dietary sugar on the colonization of a symbiotic bacteria, *Bacteroides thetaiotaomicron*. Further, I examined the mechanism by which dietary sugar silences a global transcription factor, in turn reducing the production of downstream colonization factors. This transcription factor silencing also extends to other members of this abundant phyla suggesting a phylum-wide mechanism which can be manipulated. Additionally, this work aimed to identify the metabolic mechanism governing this transcription factor activity by identifying specific genetic determinants of transcription factor activation signal production.

My findings set the groundwork for further elucidation of potential CCR mechanisms which can be harnessed to therapeutically target a widely abundant phyla in the gut microbiota.

CHAPTER 2: DIETARY SUGARS SILENCE THE MASTER REGULATOR OF CARBOHYDRATE UTILIZATION IN HUMAN GUT *BACTEROIDES* SPECIES

Abstract

The mammalian gut microbiota is a critical human health determinant with therapeutic potential for remediation of many diseases. The host diet is a key factor governing the gut microbiota composition by altering nutrient availability and supporting the expansion of distinct microbial populations. Diets rich in simple sugars modify the abundance of microbial subsets, enriching microbiotas that elicit pathogenic outcomes. We previously demonstrated that diets rich in fructose and glucose can reduce the fitness and abundance of a human gut symbiont, *Bacteroides thetaiotaomicron*, by silencing the production of a critical intestinal colonization protein, called Roc, via its mRNA leader through an unknown mechanism. We have now determined that dietary sugars silence Roc by reducing the activity of BT4338, a master regulator of carbohydrate utilization. Here, we demonstrate that BT4338 is required for Roc synthesis, and that BT4338 activity is silenced by glucose or fructose. We show that the consequences of glucose and fructose on orthologous transcription factors are conserved across human intestinal *Bacteroides* species. This work identifies a molecular pathway by which a common dietary additive alters microbial gene expression in the gut that could be harnessed to modulate targeted microbial populations for future therapeutic interventions.

Introduction

The gut microbiota compositional changes associated with various human diseases potentiate therapeutic interventions that target distinct microbial populations (1, 64, 67, 317-321). Intriguingly, the abundance of individual microbial taxa can be dramatically altered through corresponding changes in the host diet, which directly supplies nutrients to gut microbes (132, 281, 322). For example, dietary supplementation with arabinoxylan, a hemicellulose, can increase the intestinal abundance of *Bacteroides cellulosilyticus* (*Bc*) (125) and supplementation with the marine polysaccharide porphyran can increase abundance of *Bacteroides ovatus* (*Bo*) strains (283, 323). The advantages exhibited by *Bc* and *Bo* during administration of each respective dietary additive requires glycan utilization machinery that enables bacterial consumption of these structurally distinct substrates (255, 260, 270). Thus, microbial populations that can competitively access the available nutrients are favored and increase in abundance, while populations that cannot are disfavored and consequently decrease in abundance (283, 323).

Dietary components can also influence gut microbial populations by modulating the synthesis of factors necessary for intestinal colonization and host-microbial interactions independently of serving as nutrients (283, 306, 324, 325). For example, the amount of Roc, a gut colonization factor from *Bacteroides thetaiotaomicron* (*Bt*), dramatically decreases upon host consumption of fructose and glucose-rich diets although Roc is dispensable for growth on either substrate

(325). Roc silencing occurs independently of transcription initiation at the *roc* promoter but requires the 54 nucleotide 5' leader region of the *roc* mRNA (325). Similarly, abundant dietary glucose consumption reduces the amount of BT4295, a *Bt* cell-surface protein that elicits beneficial host immune responses but is dispensable for intestinal colonization (306). Roc and BT4295 are each encoded within distinct polysaccharide utilization loci that putatively target unknown host-derived glycans (274, 326). Thus, human dietary components such as glucose and fructose control both gut microbiota composition and behavior by altering gene expression in intestinal microbes. Glucose and fructose are highly abundant in the diets of industrialized populations (327), can reduce the abundance of beneficial microbes such as *Bt* (325), and remodel gut microbial populations into those that elicit pathogenic consequences (322, 328, 329). However, how these sugars mechanistically exert their effects on gut microbes remains largely unknown.

Carbohydrate utilization genes are regulated by various mechanisms in intestinal *Bacteroides* species, including an extensive repertoire of glycan-responsive transcription factors (273, 330-334), an intricate network of sRNAs (335-337), RNA-binding proteins (338, 339), DNA inversions (340, 341), and activation of the master transcriptional regulator of carbohydrate utilization, BT4338 in *Bt* (originally identified as MalR) (342) and is conserved in the *Bacteroides* genus (330, 331). BT4338 binds DNA to control expression of many mono- and polysaccharide utilization genes and several other factors necessary

for successful gut colonization (330, 331). *BT4338*-dependent mRNAs dramatically increase when *Bt* is subjected to carbon limitation for 10 minutes in laboratory media, but only a fraction of the 464 differentially transcribed genes exhibit *BT4338* binding to their putative promoter regions (331). This suggests that *BT4338* controls target gene transcription both directly and indirectly.

Here, we used Roc protein abundance as a reporter to elucidate how glucose and fructose target regulatory pathways in *Bt* and identified *BT4338* as necessary for controlling Roc amounts following carbon limitation and during growth in substrates other than glucose or fructose. We establish that *BT4338* indirectly controls Roc amounts via the *roc* mRNA leader, which is necessary for and sufficient to confer *BT4338*-dependent control to a heterologous gene. Furthermore, we show that *BT4338* governs Roc abundance independently of an alternative translation elongation factor, EF-G2 (343), whose mRNA levels are regulated by *BT4338* and increase dramatically during carbon limitation (331). Finally, we demonstrate that glucose and fructose exert rapid, dramatic, and dominant silencing of *BT4338*-dependent genes *in vitro* and that these effects are consistent across distinct gut *Bacteroides* species. Importantly, *BT4338* protein levels remain stable, indicating that the metabolism of glucose or fructose alters production of an unidentified signal that controls *BT4338* activity. Our findings collectively indicate that abundant dietary sugar consumption by the host silences *BT4338* activity *in vivo*, thereby modulating the production of microbial factors necessary for host interactions and fitness in the mammalian gut.

Results

BT4338 is necessary for Roc synthesis.

We sought to determine how *Bt* controls Roc levels by identifying genes required for its synthesis. We screened 8,000 mutants harboring random transposon insertions for reduced Roc levels *in vitro* using colony blotting from strains cultured on solid media containing 0.25% each of rhamnose and galactose. This condition was selected because Roc levels are readily detectable (Fig. 1A) and mutations that could disable growth on one monosaccharide were unlikely to prevent growth on the other. We identified seven mutants exhibiting reduced Roc levels and subsequent semi-random PCR revealed that these strains contained an insertion in one of three different open reading frames (ORF): *BT1222*, *BT1221*, or the master regulator of carbohydrate utilization, *BT4338* (Fig. 2-1A) (331). On solid media, *BT1222* and *BT1221* mutants exhibited heterogeneous signal intensity within and between colonies, suggesting local differences in Roc abundance, whereas *BT4338* mutants displayed uniform reductions in Roc amounts in all colonies (Fig. 2-1A). We engineered *Bt* strains with in-frame, chromosomal deletions of *BT1222*, *BT1221*, or *BT4338* and measured Roc amounts by western blotting following carbon limitation conditions, which were previously shown to increase Roc levels[19] and *BT4338* binding to target promoters (331).

Roc amounts increased 5.8-fold and 15.6-fold, respectively, in *wild-type Bt* following a 60-minute exposure to carbon limitation conditions following mid-

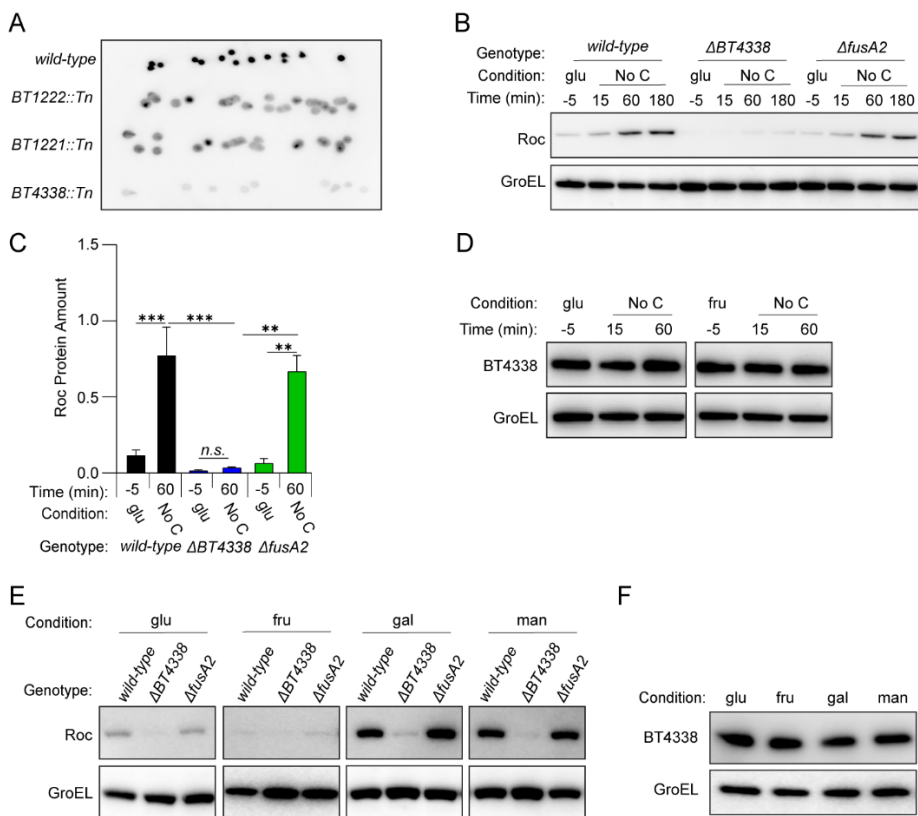


Figure 2-1: BT4338 is required for Roc synthesis(a) Colony blot analysis of selected mutants harboring transposon insertions in BT1222 (GT3148), BT1221 (GT3150), or BT4338 (GT3151) compared to a control strain (GT1663) grown on solid minimal media containing rhamnose and galactose. Each strain is represented by at least 10 different isogenic colonies. (b) Western blot analysis of Roc from wild-type (GT593) or *Bt* strains deficient for BT4338 (GT1234) or *fusA2* (GT1310) during growth in glucose (*glu*; -5) or 15-, 60-, and 180-minutes following exposure to carbon limitation (No C). (c) Quantified western blot analysis of wild-type (GT593; black), or *Bt* strains deficient for BT4338 (GT1234; gray), or *fusA2* (GT1310; green) during growth in glucose (*glu*; -5) and 60-min following exposure to carbon limitation (No C) ($n = 4$ biological samples; error bars represent SEM; P values derived from two-way ANOVA; *n.s.* indicates P -values ≥ 0.05 ; $***P < 0.001$; $****P < 0.0001$). (d) Western blot analysis of BT4338 (GT1481) during mid-exponential growth in glucose (*glu*; -5) or fructose (*fru*; -5) or 15-, and 60-minutes following exposure to carbon limitation. (e) Western blot analysis of Roc from the strains described in (b) following mid-exponential growth in glucose (*glu*), fructose (*fru*), galactose (*gal*), or mannose (*man*). (f) Western blot analysis of BT4338 (GT1481) during mid-exponential growth in glucose (*glu*), fructose (*fru*), galactose (*gal*), or mannose (*man*). Blots were probed using anti-HA and anti-GroEL antibodies.

exponential growth in media containing either glucose (Fig. 2-1B and Fig. 2-1C) or fructose (Fig. C-1A and C-1B) as the sole carbon source. Compared to *wild-type Bt*, an isogenic *BT4338*-deficient strain exhibited similar Roc levels during

growth in glucose (Fig. 2-1B) or fructose (Fig. C-1A), which increased 2.5- and 2.3-fold after 60 minutes in carbon limitation conditions (Fig. 2-1C and Fig. C-1B, respectively). Conversely, strains lacking either *BT1222* or *BT1221*, which putatively mediate two discreet steps in the oxidative pentose phosphate pathway (Fig. C-2A), exhibited 5.6- and 7.3-fold increased Roc amounts after 60 minutes that were significantly lower than wild-type *Bt* under identical conditions (Fig. C-2B and C). Additionally, a strain lacking *BT1220*, which is putatively required for an intermediate metabolic step between *BT1221* and *BT1222* (Fig. C-2A), also exhibited lower Roc amounts than *wild-type Bt* following carbon limitation (Fig. C-2C), indicating that the oxidative pentose phosphate pathway is involved in controlling Roc abundance. However, we focused our investigation on understanding how *BT4338* controls Roc because it elicited the strongest effect across all conditions.

We determined that *BT4338* protein amounts were similar during mid-exponential phase growth in either glucose or fructose, and subsequent exposure to carbon limitation conditions (Fig. 2-1D and Fig. C-3A and C-3B). These results indicate that carbon limitation increases Roc by stimulating *BT4338* activity rather than increasing its protein amount and reciprocally suggest that growth in glucose or fructose reduce *BT4338* activity. Consistent with this notion, relative to *wild-type Bt* cells grown in galactose and mannose, Roc amounts were 12.0- and 6.6-fold lower, respectively, in fructose grown cells and 5.8- and 3.2-fold lower, respectively, in glucose grown cells (Fig. 2-1E and

Fig. C-3C) agreeing with previous results (325). By contrast, a BT4338-deficient strain exhibited similar Roc amounts across *Bt* cells grown in glucose, fructose, galactose, or mannose (Fig. 2-1E and Fig. C-3C), which were 3.8-, 4.0-, 17.2-, and 10.3-fold lower than those from *wild-type Bt* in each respective condition (Fig. C-3C). Finally, increased Roc amounts during growth in each monosaccharide are not the result of altered BT4338 protein abundance, which were identical during growth in all four carbon sources (Fig. 2-1F and Fig. C-3D). Cumulatively, these data demonstrate that *Bt* controls Roc amounts in response to carbon limitation and carbohydrate metabolism by modulating BT4338 activity.

BT4338 indirectly controls Roc via its mRNA leader.

We examined Roc amounts in *BT4338*-deficient strains harboring constructs encoding the *roc* ORF preceded either by its native leader or by the sugar-resistant leader upstream of the heterologous gene, *BT3334*, that enables Roc production even in the presence of fructose or glucose (325). As previously demonstrated, the strain that includes the *BT3334* leader displayed similar Roc amounts when grown in either glucose, fructose, galactose, or mannose (Fig. 2-2A and C-4A) (325). This contrasts a strain encoding the *roc* ORF downstream of the native *roc* leader that exhibits 19.4- and 12.1-fold more Roc in galactose and mannose, respectively, compared to fructose grown cells and 3.8- and 2.4-fold more Roc compared to glucose grown cells (Fig. 2-2A and Fig. C-4B). These results independently demonstrate that the silencing effect of fructose or glucose on Roc protein amounts require its mRNA leader. The *BT4338*-deficient strain

encoding *roc* downstream of its native promoter and leader displayed similar Roc amounts in glucose or fructose grown cells but 44.6- and 9-fold lower abundances in galactose and mannose, respectively, than those from a wild-type strain harboring an identical construct (Fig. 2-2A and Fig. C-4A). Furthermore, a strain encoding the *BT3334* promoter preceding the *roc* leader exhibited 34.9- and 11-fold greater Roc amounts in galactose and mannose, respectively, compared to fructose grown cells and 6.4- and 2-fold more Roc, compared to glucose grown cells (Fig. 2-2A and Fig. C-4C). In this strain, increased Roc protein abundances in galactose or mannose compared to fructose or glucose grown cells required *BT4338* (Fig. 2-2A and Fig. C-4C), demonstrating that the *roc* leader is necessary for *BT4338*-dependent Roc production while the promoter is dispensable.

To determine whether the *roc* leader confers fructose- and glucose-dependent silencing to the heterologous gene, *BT3334*, which is synthesized in the presence of glucose or fructose (325) independently of *BT4338* (Fig. 2-2B and C-4D), we used a strain where the *BT3334* ORF was expressed from its native promoter but preceded by the *roc* leader. This strain exhibited *BT3334* protein amounts that were 11- and 6.7-fold higher when grown in galactose or mannose, respectively, compared to fructose grown cells and 2.3- and 1.4-fold higher compared to glucose grown cells (Fig. 2-2B and C-4E). Increased *BT3334* amounts in this strain required *BT4338* (Fig. 2-2B and C-4E) demonstrating that the *roc* leader confers *BT4338*-dependent control of the downstream ORF,

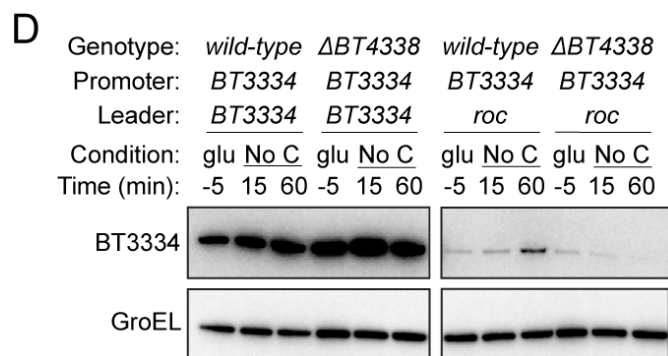
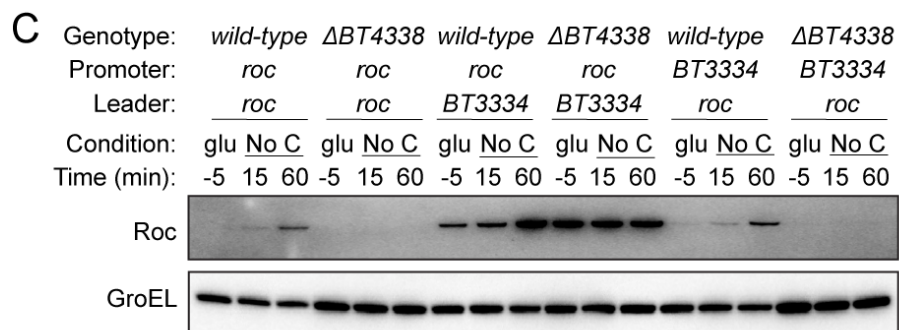
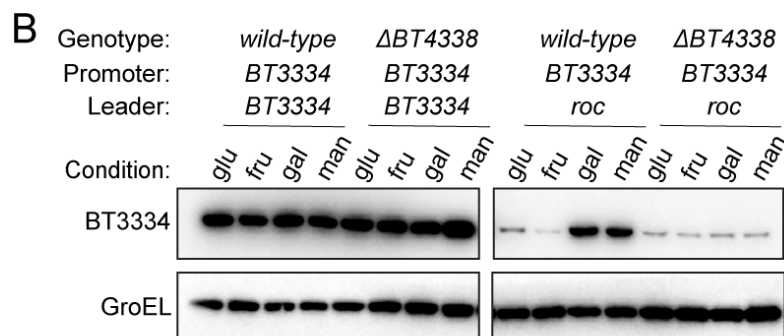
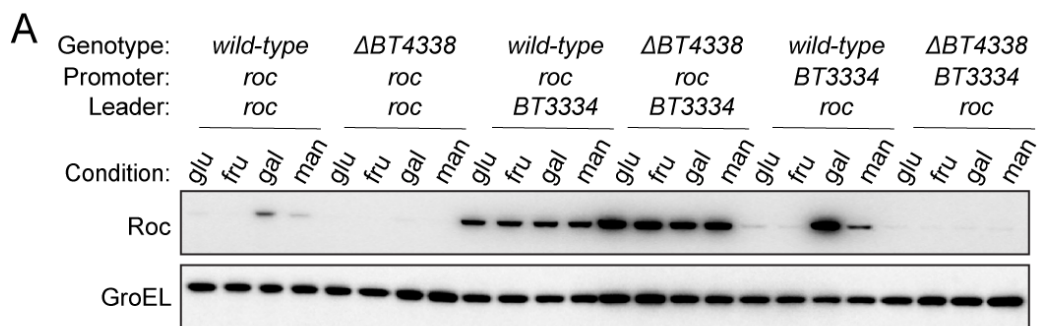


Figure 2-2: *BT4338* governs *Roc* levels via its 5' mRNA leader. (a) Western blot analysis of *Roc* from engineered strains harboring the *roc* leader and ORF positioned downstream of its native (*GT530*) or heterologous (*GT670*) promoters, or strains with the native *roc* promoter upstream of a heterologous 5' leader region (*GT665*) in strains encoding *BT4338* or a *BT4338*-deficient background (*GT3509*, *GT3511*, and *GT3510*, respectively) grown in minimal media containing 0.5% glucose (*glu*), fructose (*fru*), galactose (*gal*), or mannose (*man*) as the sole carbon source. (b) Western blot analysis of *BT3334* from engineered strains harboring the *BT3334* promoter and ORF flanking either the *BT3334* (*GT534*) or *roc* (*GT663*) leaders in isogenic strains encoding *BT4338* or in a *BT4338*-deficient background (*GT3512* and *GT3514*, respectively) grown in minimal media containing 0.5% glucose (*glu*), fructose (*fru*), galactose (*gal*), or mannose (*man*). (c) Western blot analysis of *Roc* from strains described in (a) during mid-exponential growth in glucose (*glu*, -5) or 15-, and 60- minutes following exposure to carbon limitation conditions. (d) Western blot analysis of *BT3334* levels from strains described in (b) during mid-exponential growth in glucose (*glu*, -5) or 15-, and 60- minutes following exposure to carbon limitation conditions. Blots were probed using anti-HA and anti-GroEL antibodies.

suggesting that growth in glucose or fructose reduce the corresponding protein abundances by silencing *BT4338* activity. Accordingly, when either the *roc* or *BT3334* ORFs were encoded immediately downstream of the *roc* leader, removing glucose from the media increased the corresponding protein amounts by 20.2-fold (Fig. 2-2C and Fig. C-4F) and 3.5-fold, respectively (Fig. 2-2D and Fig. C-4G). Increased *Roc* amounts during carbon limitation required *BT4338* when the *roc* ORF was preceded by its native leader regardless of the preceding promoter (Fig. 2-2C and Fig. C-4H). While strains encoding the *BT3334* leader upstream of the *roc* ORF exhibited 2.9-fold increased *Roc* abundance 60 minutes following exposure to carbon limitation, *Roc* amounts were increased in a *BT4338*-deficient background during growth in glucose (Fig. 2-2C and Fig. C-4I), which resembled *BT3334* protein amounts when the *BT3334* ORF was positioned downstream of its leader (Fig. 2-2D and Fig. C-4J). Collectively, these data demonstrate the *roc* mRNA leader is sufficient to confer *BT4338*-dependent

synthesis of the downstream ORF, which is silenced by glucose and fructose independently of the upstream promoter.

Carbon limitation increases Roc abundance (Fig. 2-1B and Fig. 2-2C) (325) and stimulates BT4338 binding to chromosomal regions throughout the *Bt* genome (331). While our previous RNAseq study revealed that *roc* transcript levels were 2.6-fold lower in a *BT4338*-deficient strain 10 minutes following carbon limitation, a corresponding ChIP-seq analysis did not detect BT4338 binding to regions upstream of the *roc* ORF under the same conditions (331). This contrasts targets like *fusA2*, whose promoter occupancy dramatically increased 10-minutes after exposure to carbon limitation conditions, resulting in a *BT4338*-dependent 238-fold increase in the corresponding mRNA levels (331). In agreement with these results, we determined that enrichment of the *fusA2* promoter increased 7.3- and 8.4-fold by 10 minutes following carbon limitation compared to immunoprecipitation of BT4338 from glucose (Fig. 2-3A) or fructose (Fig. 2-3B) grown *Bt*. Although BT4338 levels remain constant throughout carbon limitation following growth in glucose or fructose (Fig. 2-1D), *roc* promoter enrichment was not detected under these conditions (Fig. 2-3A and 2-3B) and the *roc* promoter lacks sequences resembling the BT4338 consensus (271). Thus, BT4338 controls Roc amounts by a mechanism other than directing *roc* transcription initiation.

EF-G2 and other BT4338 regulated products are dispensable for Roc synthesis.

We hypothesized that BT4338 controls Roc amounts by regulating

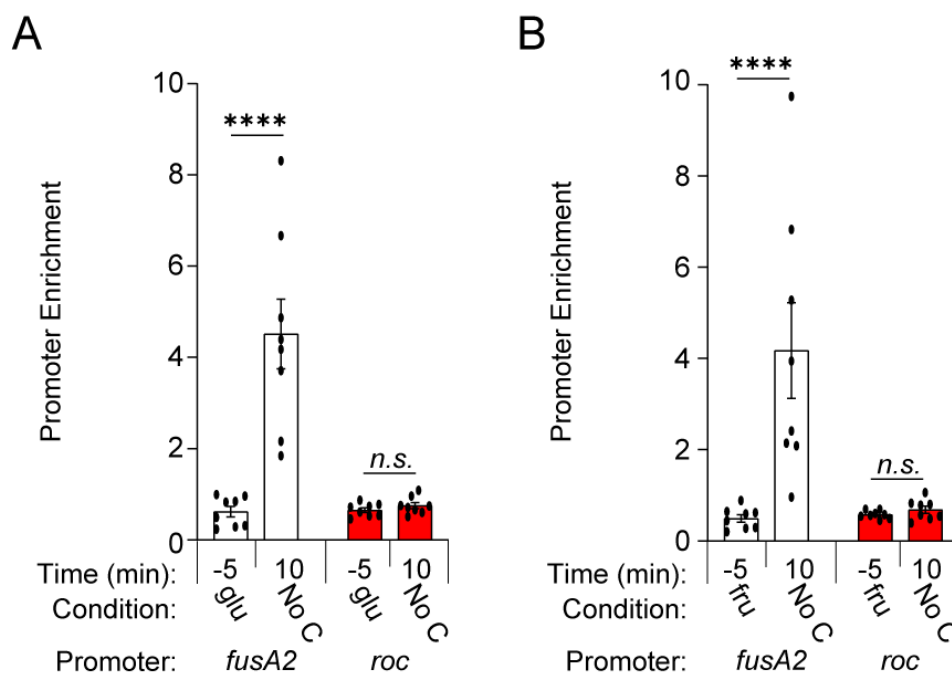


Figure 2-3: *BT4338* DNA binding activity is stimulated during carbon starvation. (a - b) ChIP analysis of the *fusA2* (BT2167; black) and *roc* (BT3172; red) promoter regions from wild-type *Bt* (GT1481) cells grown to mid-exponential phase in minimal media containing (a) glucose (glu; -5) or (b) fructose (fru; -5) and 10 minutes following exposure to carbon limitation conditions ($n = 8$ biological samples; error bars represent SEM; P values derived from two-way ANOVA; n.s. indicates P -values ≥ 0.05 ; **** $P < 0.0001$).

transcription of an unknown factor(s) involved in its synthesis. The most highly induced *BT4338*-dependent gene during carbon limitation conditions is *fusA2* (BT2167), which encodes a non-essential, alternative translation elongation factor G (EF-G2) that enables GTP-independent translation (343) and is critical for mammalian intestinal colonization (331). Because *BT4338* is required for synthesis of both EF-G2 and Roc, and *BT4338*-dependent control of Roc protein is indirect and mediated via the *roc* 5' mRNA leader, we reasoned that *BT4338*-dependent EF-G2 expression may control Roc amounts by governing its translation in a leader-dependent manner. However, a *fusA2*-deficient strain exhibited 10.3- and 9.3-fold increased Roc amounts following a 60-minute

exposure to carbon limitation from glucose or fructose, respectively, which resembled the 7.2- and 11.7-fold increases exhibited by *wild-type Bt* (Fig. 2-1B and 2-1C and Fig. C-1A and C-1B). Furthermore, a *fusA2*-deficient strain displayed similar Roc amounts as *wild-type Bt* in all growth conditions with 15.5- and 10.5-fold increases over fructose in either galactose or mannose, respectively (Fig. 2-1E and Fig. C-3C). Cumulatively, these data demonstrate that EF-G2 is dispensable for Roc synthesis.

To explore the role of additional BT4338 regulated genes in controlling Roc abundance, we examined the consequences of inactivating the *BT4338*-dependent polysaccharide utilization locus (PUL), *BT4299-BT4295*, and putative methylmalonyl-CoA biosynthetic genes, *BT1450-BT1448*. However, both mutants displayed similarly increased Roc amounts compared to *wild-type Bt* after carbon limitation for 60 minutes (Fig. C-5A-C). We also examined Roc levels in strains lacking *BT2131*, which encodes a conserved hypothetical protein, that could putatively silence Roc levels in the absence of *BT4338* because the *BT2131* transcript increases 57.3-fold in a *BT4338*-deficient strain during growth in glucose (331). However, Roc amounts were indistinguishable between a *BT4338* mutant and a strain lacking both *BT4338* and *BT2131* (Fig. C-5A and C-5D), and between *wild-type Bt* and a strain lacking *BT2131* alone (Fig. C-5A and C-5D). Thus, *BT4338* controls Roc abundance by an unidentified gene product(s).

Candidate *Bt* sRNAs are insufficient to control Roc levels.

Bt produces hundreds of small RNAs (sRNA) that have established roles in regulating gene products involved in carbohydrate utilization (335-337). Furthermore, a subset of *Bt* sRNAs increase in abundance following exposure to carbon limitation *in vitro* (337) and are positioned proximally to BT4338 binding sites (331). Computational analysis revealed that three of these sRNAs, *BTnc140*, *BTnc195*, and *BTnc364* exhibit complementarity to the *roc* leader (Fig. C-6A), suggesting a role in controlling Roc amounts. However, *Bt* strains engineered to over-produce either *BTnc140*, *BTnc195*, or *BTnc364* (Fig. C-6B) exhibited indistinguishable Roc amounts compared to those of a control strain during mid-exponential phase growth in glucose (Fig. C-6C and C-6D). These data indicate that increased expression of three candidate sRNAs cannot increase Roc protein amounts.

Glucose and fructose rapidly and dominantly silence BT4338 activity.

Host consumption of abundant dietary glucose and fructose reduce the levels of two *BT4338*-dependent products, Roc (325) and BT4295 *in vivo* (306). Because *BT4338* is a critical determinant of mammalian intestinal colonization (331), we hypothesized that host consumption of sugar-rich chow would silence *BT4338* activity in *wild-type Bt*, thereby reducing the competitive defect exhibited by a *BT4338*-deficient strain. An independently constructed *Bt* strain lacking *BT4338* was 1.3×10^4 -fold lower in abundance than wild-type *Bt* 10 days following introduction into germ-free mice fed a sugar-rich diet (Fig. 2-4A). The introduction

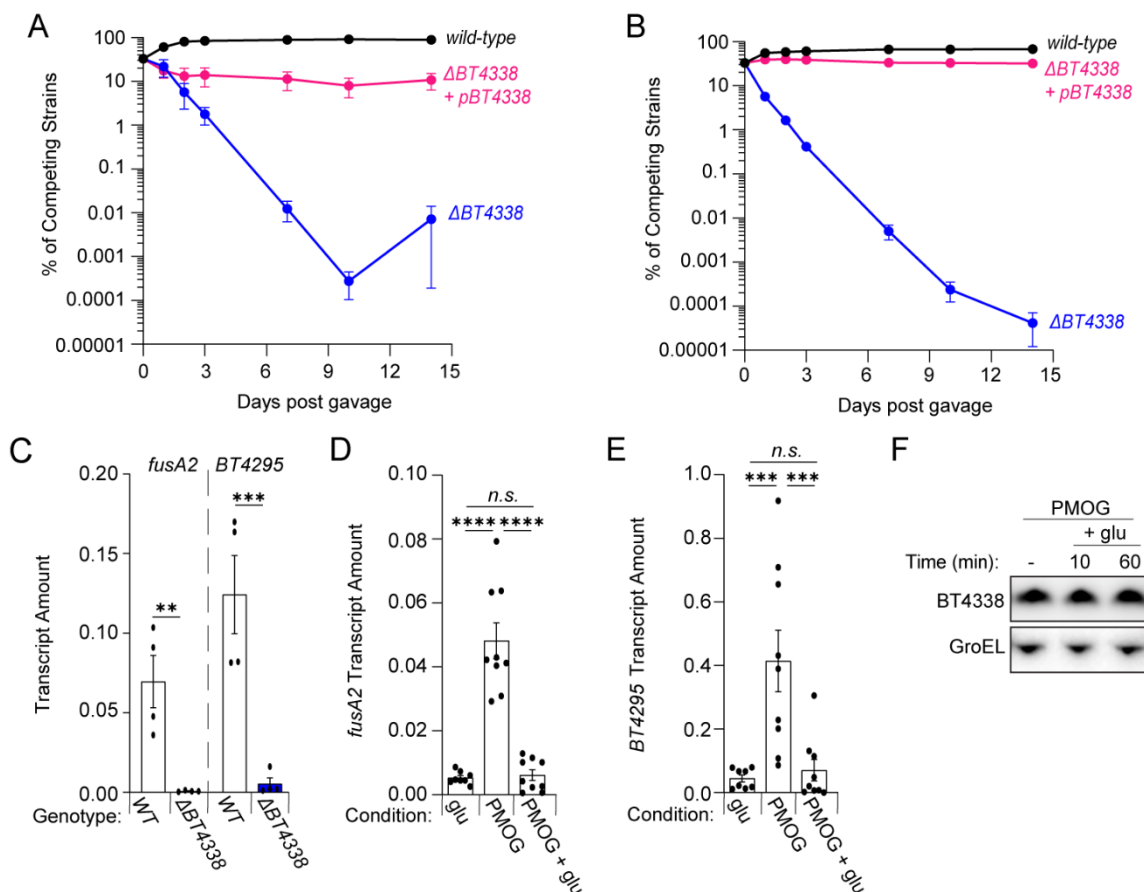


Figure 2-4: Dietary sugars silence BT4338 activity. (a & b) The relative abundances of bar-coded strains wild-type (GT3361; black) or BT4338-deficient Bt strains harboring an empty vector (GT3522; blue) or complementation plasmid (GT3363; pink) at the indicated times following gavage with equal cfus of each strain into germ-free mice fed (a) a sugar-rich diet or (b) a standard diet ($n = 5$; error bars represent SEM). (c) qPCR analysis of *fusA2* (BT2167) or BT4295 transcript levels measured in wild-type (GT593; black) or BT4338 deficient (GT1234; gray) Bt strains during mid-exponential growth in 1% PMOG ($n = 4$ biological samples; error bars represent SEM, P values derived from two-way ANOVA; *n.s.* indicates P values ≥ 0.05 ; ** $P < 0.01$ *** $P < 0.001$). (d - e). qPCR analysis of (d) *fusA2* (BT2167) or (e) BT4295 transcript levels measured in wild-type Bt (GT23) during mid-exponential growth in either 0.5% glucose (glu) or 1% PMOG, and 10-minutes following the addition of 0.2% glucose to the PMOG grown cells. ($n = 9$ biological samples; error bars represent SEM, P -values were calculated using two-way ANOVA; *n.s.* indicates P -values ≥ 0.05 ; *** $P < 0.001$; **** $P < 0.0001$). (f) Western blot analysis measuring BT4338 levels (GT1481) grown in 1% PMOG or 10 and 60-minutes following the addition of glucose to 0.2%. Blot was probed using anti-HA and anti-GroEL antibodies.

of a plasmid-borne copy of BT4338 complemented this mutant, which exhibited 1.5×10^3 -fold greater abundance than the BT4338-deficient strain (Fig. 2-4A). The BT4338-deficient strain exhibited a 1.6×10^6 -fold lower abundance than the wild-

type Bt strain in mice fed a standard, low sugar, high plant polysaccharide diet (Fig. 2-4B), indicating that *BT4338* is required for intestinal colonization regardless of host dietary sugar consumption. These results agree with previous reports demonstrating that *Bt* mutants harboring insertions in *BT4338* exhibit severe competitive defects for murine gut colonization in hosts fed either standard low in sugar or glucose and fructose-rich chows (125, 331). Thus, this transcription factor performs critical regulatory roles in the mammalian gut independently of dietary composition (331). To determine whether fructose or glucose exert dominant silencing effects on *BT4338* activity, thereby reducing target gene transcription, we compared *fusA2* transcript abundances during growth on glucose or a glycan mixture derived from the porcine gastric mucosa (PMOGs). PMOGs support growth of *wild-type* and *BT4338*-deficient *Bt* strains (Fig. C-7A) (260) and elicit 9.3- and 9.1-fold increases in *fusA2* and *BT4295* transcripts, respectively, in a *BT4338*-dependent manner (Fig. 2-4C). Glucose dominantly silences *BT4338* activity because *fusA2* and *BT4295* transcripts decreased by 7.9- and 5.9-fold, respectively, 10 minutes following the introduction of 0.2% glucose to *Bt* cells grown to mid-exponential phase in 1% PMOGs (Fig. 2-4D and 2-4E, respectively). Likewise, the addition of fructose to PMOG-grown *Bt* cells also decreased *fusA2* and *BT4295* transcripts by 5.4- and 14.8-fold, respectively, after 60 minutes although no change was detected by 10 minutes (Fig. C-7B and C-7C, respectively), likely because additional time is necessary for optimal synthesis of gene products necessary for fructose consumption (270, 344). Importantly, *BT4338* protein levels remained constant

after 60 minutes following glucose addition, indicating that transcription factor activity is silenced (Fig. 2-4F and Fig. C-7D). Collectively, these data indicate that available glucose and fructose can rapidly modulate BT4338 activity even in the presence of other growth substrates.

BT4338 orthologs govern a partially conserved regulon.

BT4338 is conserved among numerous *Bacteroides* species (125) including *B. fragilis* (*Bf*, *BF9343_0915*), *B. ovatus* (*BACOVA_05152*), and *B. vulgatus* (*Bv*, *BVU_3580*), which share 84.1, 96.1, and 77.3% amino acid sequence identity with BT4338, respectively. Exposing each species to carbon limitation for 10 minutes elicited 109.9-, 360.9-, and 75.6-fold increased transcription of their corresponding *fusA2* orthologs, *BF9343_3536*, *BACOVA_03178*, and *BVU_0017* (Fig. 2-5A, Fig. 2-5B and 2-5C, respectively), whose products share 89.1, 97.9, and 86.9% amino acid sequence identity to *BT2167*, respectively. *Bf*, *Bo*, and *Bv* strains deficient for their respective BT4338-orthologs are unable to increase *fusA2* transcription in response to carbon limitation conditions (Fig. 2-5A, Fig. 2-5B and 2-5C, respectively) (331). Furthermore, *Bf*, *Bo*, and *Bv* mutants deficient for this transcription factor are unable to grow on fucose or xylose (Fig. 2-5D and 2-5E, respectively) but can grow on glucose or fructose (Fig. C-8A and C-8B, respectively). Together, these data demonstrate a conserved regulon including control of *fusA2* transcription and distinct carbon utilization genes across *Bacteroides* species.

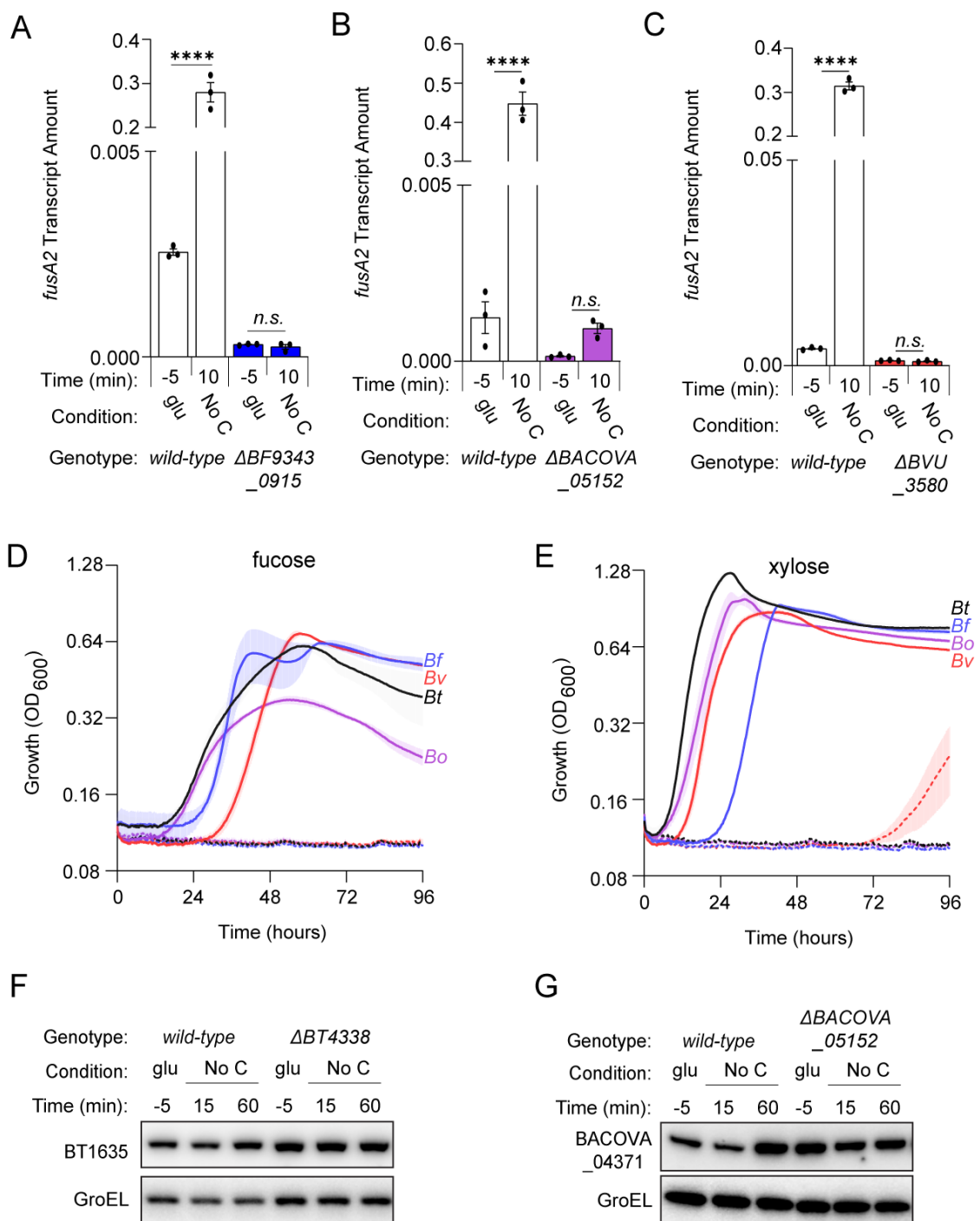


Figure 2-5: BT4338-orthologs govern a conserved regulon among prominent *Bacteroides* species. (a) The transcript level of *B. fragilis* *fusA2* (BF9343_3536) was measured in wild-type (ATCC 25285; black) or a BF9343_0915-deficient (GT2520; blue) *B. fragilis* strain grown in glucose (*glu*; -5) and 10-minutes after exposure to carbon limitation (No C) ($n = 3$ biological samples; error bars represent SEM, P -values was calculated using two-way ANOVA; n.s. indicates P -values ≥ 0.05 ; **** $P < 0.0001$). (b) The transcript level of *B. ovatus* *fusA2* (BACOVA_03178) was measured in wild-type (ATCC 8483; black) or BACOVA_05152-deficient (GT2413; purple) strains grown in glucose (*glu*; -5) or 10-minutes after exposure to carbon limitation (No C) ($n = 3$ biological samples; error bars represent SEM, P values derived from two-way ANOVA; n.s. indicates P values ≥ 0.05 ; **** $P < 0.0001$). (c) The transcript level of *B. vulgatus* *fusA2* (BVU_0017) was measured in wild-type (ATCC 8482; black) or BVU_3580-deficient (GT2399; red) strains grown in glucose (*glu*; -5) or 10-minutes after exposure to carbon limitation (No C) ($n = 3$ biological samples; error bars represent SEM, P values derived from two-way ANOVA; n.s. indicates P values ≥ 0.05 ; **** $P < 0.0001$). (d – e). Growth of bar-coded wild-type (solid lines) *B. thetaiotaomicron* (Bt; GT3361; black), *B. fragilis* (Bf; GT3551; blue), *B. vulgatus* (Bv; GT3367; red), or *B. ovatus* (Bo; GT3364; purple) or bar-coded isogenic BT4338-ortholog-deficient strains (dashed lines; GT3522, GT3555, GT3643, GT3553, respectively) in minimal media containing 0.5% (d) fucose or (e) xylose ($n = 4$ biological samples; error bars represent SEM). (f) Western blot analysis of BT1635 amounts from wild-type (GT4372) or a Bt strain deficient for BT4338 (GT4373) during growth in glucose (*glu*; -5) or 15-, or 60-minutes following exposure to carbon limitation (No C). (g) Western blot analysis of BACOVA_04371 from wild-type Bo (GT4362) or a strain deficient for BACOVA_05152 (GT4369) during growth in glucose (*glu*; -5) or 15-, or 60-minutes following exposure to carbon limitation (No C). Blots were probed using anti-HA and anti-GroEL antibodies.

To determine whether BT4338-orthologs control the abundances of Roc homologs, we examined the amounts of BT1635, which is a putative hybrid two-component system (HTCS) exhibiting 74.1% amino acid sequence identity to Roc. Like Roc, BT1635 regulates the expression of linked PUL genes in response to unknown glycans (274, 345). In contrast to Roc, BT1635 protein amounts are similar during growth in 8 different substrates, including glucose or fructose (325). Both *wild-type* and *BT4338*-deficient strains display indistinguishable BT1635 abundances either during mid-exponential phase growth in glucose or following carbon limitation for 60 minutes (Fig. 2-5F and C-9A), indicating that BT4338 does not control this protein even though it shares high sequence identity to Roc. We also examined the abundance of

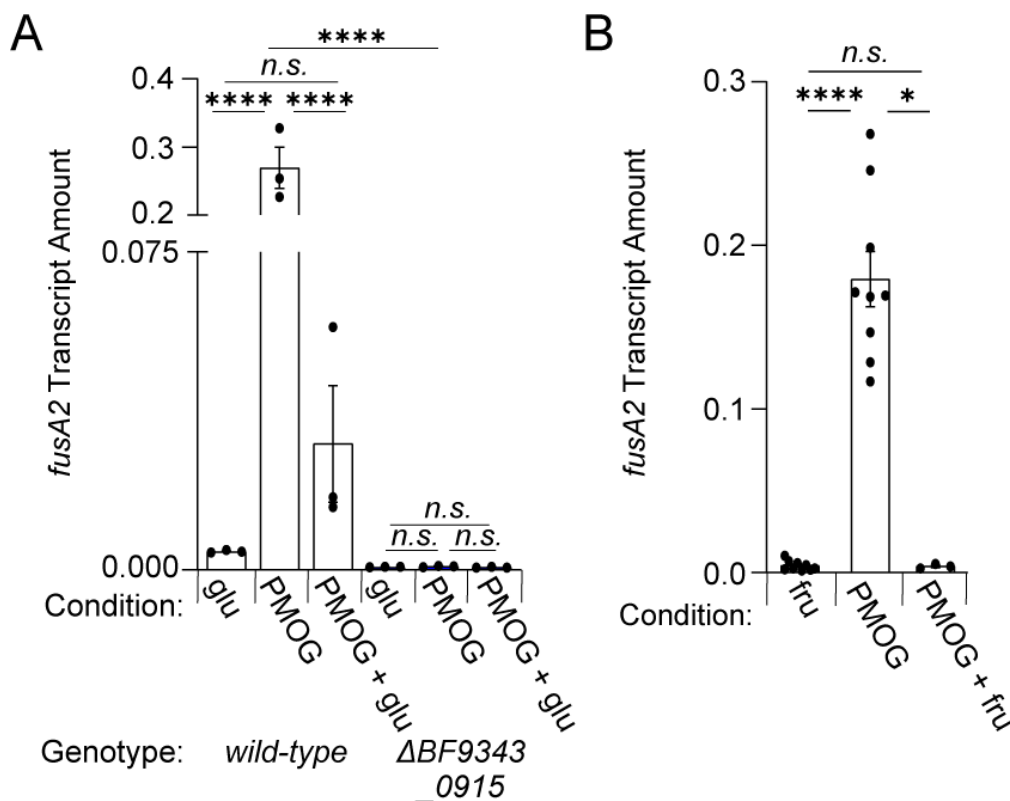


Figure 2-6: A BT4338-ortholog is silenced by dietary sugar addition in *B. fragilis*. (a) *Bf fusA2* (BF9343_3536) transcript levels were measured in wild-type (ATCC 25285; black) or a BF9343_0915-deficient (GT2520; blue) *B. fragilis* strain grown in 0.5% glucose, 1% PMOG, or 1% PMOG 10-minutes after addition of 0.2% glucose ($n = 3$ biological samples; error bars represent SEM, P -values derived from two-way ANOVA; n.s. indicates P values ≥ 0.05 ; **** $P < 0.0001$). (b) The transcript level of *B. fragilis fusA2* (BF9343_3536) was measured in wild-type (ATCC 25285) or a BF9343_0915-deficient (GT2520) strain during mid-exponential growth in either 0.5% fructose (fru) or 1% PMOG, and 60-minutes following the addition of fructose to 0.2% ($n = 9$ biological samples for fru and PMOG; $n = 3$ for PMOG + fru; error bars represent SEM, P values derived from one way ANOVA; n.s. indicates P values ≥ 0.05 ; * $P < 0.05$ **** $P < 0.0001$).

BACOVA_04371, a HTCS in *Bo* that shares 73.3% identity to Roc and 80.6% identity to BT1635. In contrast to both BT1635 and Roc, BACOVA_04371 is not predicted to control PUL gene expression and its abundance increased 3-fold in a BACOVA_05152-deficient strain compared to wild-type *Bo* grown in glucose (Fig. 2-5G and C-9B). BACOVA_04371 levels remained 2-5G and C-9B). This indicates that control of Roc-like protein amounts by BT4338-orthologs is

unpredictable based on sequence identity across Bt and Bo, and the regulatory outcomes can differ between species.

Dietary sugar silences BT4338-ortholog activity across prominent *Bacteroides* species.

To determine if glucose and fructose dominantly silence the activity of BT4338 orthologs, we examined *fusA2* transcript levels in *Bf* during mid-exponential phase growth in either glucose or PMOGs, which both support growth of *wild-type* and *BF9343_0915*-deficient strains (Fig. C-10). We determined that *fusA2* transcript levels in *wild-type Bf* are 42.2- and 44.9-fold lower during growth in glucose (Fig. 2-6A) or fructose (Fig. 2-6B), respectively, compared to PMOGs as a sole carbon source. Additionally, the *BF9343_0915*-deficient strain exhibited indistinguishable *fusA2* levels during growth in either glucose or PMOGs, which were 6.4- and 335-fold lower than *wild-type Bf* in each respective condition (Fig. 2-6A). The addition of 0.2% glucose to *Bf* cells growing on 1% PMOGs as a sole carbon source reduced *fusA2* transcript levels 24.5-fold after 10 minutes (Fig. 2-6A), and 44.9-fold after 60 minutes following fructose addition (Fig. 2-6B). Together, these results demonstrate that the introduction of glucose and fructose rapidly silence BT4338 ortholog activity and reduce target gene transcription in abundant intestinal *Bacteroides* species.

Discussion

We have established that a widely distributed transcription factor in human gut bacteria governs carbohydrate utilization (Fig. 2-5D and 2-5E) and

transcription of the alternative translation elongation factor, EF-G2 (Fig. 2-4C). Moreover, introduction of the abundant human dietary sugars, glucose and fructose, reduce the levels of *BT4338*-dependent transcripts and proteins including *Bt* gene products, Roc (Fig. 2-1B), *fusA2* (Fig. 2-4D and Fig. C-7B) and *BT4295* (Fig. 2-4E and Fig. C-7C), that mediate host-microbial interactions and are silenced in vivo by host consumption of dietary sugars (306, 325). Furthermore, the addition of glucose or fructose rapidly and dominantly exert these effects on cultured cells consuming host-derived glycans (Fig. 2-4D and 2-4E and Fig. C-7B and C-7C), and conversely, removing fructose or glucose from the growth media dramatically increase target promoter binding (Fig. 2-3A and 2-3B) and gene transcription (331) without altering transcription factor levels (Fig. 2-1D and Fig. C-3A and C-3B). Collectively, these data indicate that glucose and fructose modulate the activity of this transcription factor, which we propose to rename Cur (Carbohydrate utilization regulator), distinguishing this protein from analogous regulators in Proteobacteria and Firmicutes (346). This work identifies a conserved mechanism governing gene expression in dominant human gut bacteria in response to abundant dietary additives, and highlights this pathway as a potential mediator of intestinal disease observed in animals fed a sugar-rich diet (322).

Cur is an important component of carbon catabolite repression (CCR) in the Bacteroidetes because Cur binds to *Bt* carbon utilization gene promoters (331), is required for controlling transcription of downstream genes (331), and

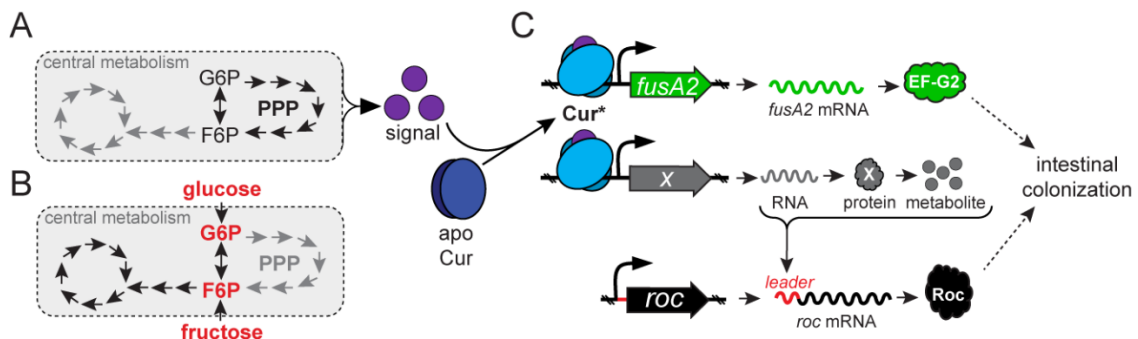


Figure 2-7: Model depicting the consequences of glucose and fructose on *Cur* activity. a) an unknown signal(s) (purple) is putatively synthesized in response to metabolic cues derived from the PPP pathway that converts apo-*Cur* (dark blue) to *Cur** (light blue). (b) Introduction of fructose or glucose modulate central metabolism to reduce *Cur* signal(s), thereby hindering products necessary for intestinal colonization. (c) *Cur** increases transcription of *fusA2* (green) and an unidentified gene (gray), whose product(s) govern *Roc* abundance by interacting with the *roc* mRNA leader region (red).

growth on distinct monosaccharides across four representative *Bacteroides* species (Fig. 2-5D and 2-5E) (330). In other gut bacterial phyla, CCR is mediated by similar transcription factors such as Crp (also called CAP) in the Enterobacteriaceae and CcpA in Firmicutes, which recognize intracellular signaling molecules that modulate their target promoter binding activities and direct transcription of genes required for “less-preferred” substrates (347). For example, Crp binds cyclic-adenosine monophosphate (cAMP) and CcpA binds a phosphorylated form of HPr, which are differentially synthesized in response to metabolic cues resulting in increased catabolic gene expression (347). The activation of Crp and CcpA require components of the phosphoenolpyruvate: sugar transferase system (PTS), which couple monosaccharide transport and phosphorylation to serve as an intracellular indicator of preferred substrate availability (220). Thus, the transport of preferred growth substrates reduces

transcription of genes mediating utilization of “less-preferred” substrates present in the environment by decreasing the activation of Crp and CcpA (347).

Bacteroides species impose CCR by a distinct mechanism(s) because: 1.) all sequenced *Bacteroides* species lack HPr, CcpA, and PTS orthologs, and 2.) although *Bacteroides* Cur is classified as a Crp/Fnr-like regulator, these transcription factors exhibit only 18% amino acid sequence identity (331). Furthermore, neither cAMP nor its biosynthetic enzyme, adenylate cyclase, have been detected in the Bacteroidetes (348, 349) indicating that Cur activity is controlled by unique signal(s) in this phylum. We hypothesize that perturbations in pentose phosphate pathway (PPP) intermediates modulate this signal (Fig. 2-7A) because *cur* is required for growth on pentose sugars (Fig. 2-5E) (330), Roc levels increase during growth on pentose sugars (325, 330), and many PPP genes are dispensable for *in vitro* growth but critical for intestinal colonization, which is similar to the *cur* gene (125, 350, 351). Additionally, two independent genetic screens identified oxidative PPP genes as necessary for synthesis of Cur-dependent products (Fig. 2-1A) (306), although a third screen identified PPP genes as regulators of Cur-independent gene expression (352). We hypothesize that dietary sugars exert CCR by modulating cellular carbon metabolism, thereby reducing production of the putative Cur signal (Fig. 2-7B), which consequently lowers the synthesis of factors mediating host interactions including those that function independently of carbohydrate utilization (Fig. 2-7C). Thus, identifying the signal(s) that governs Cur activity in *Bacteroides* species is imperative to

understand how CCR is imposed *in vivo* and to identify strategies to exploit this regulatory system for manipulation of intra-intestinal microbial abundance and metabolism.

Intestinally isolated *Bacteroides* species can harvest monosaccharides from various complex polysaccharides using expansive repertoires of coordinately regulated glycan detection, importation, and degradation enzymes encoded within PULs (260, 333, 344, 353-355). PUL gene transcripts can also be silenced by glucose or fructose and exhibit prioritized expression by a myriad of mechanisms (284, 330). Here, we demonstrate that in *Bt*, Cur indirectly controls the amount of the PUL-encoded sensor protein, Roc (Fig. 2-2A), and that glucose and fructose silencing of Roc is mediated by a corresponding reduction in Cur activity (Fig. 2-1E and 2-1F and Fig. 2-3A). Additionally, Cur is required for increased transcript levels of another PUL-encoded gene, *BT4295*, following exposure to carbon limitation conditions even though Cur does not bind to the putative promoter regions upstream of either *roc* (Fig. 2-3A and 2-3B) or *BT4299*, the gene initially transcribed in the PUL containing *BT4295* (331). Thus, Cur likely regulates many more genes than previously estimated, including those facilitating polysaccharide utilization, permitting dynamic carbon source prioritization as conditions change within the host (271, 331). We predict that Cur controls Roc synthesis indirectly by governing transcription of an unknown target gene(s) whose product interacts with the *roc* leader independently of transcription initiation (Fig. 2-7C). In the Bacteroidetes phylum, mRNA leaders

can control downstream gene product synthesis by functioning as riboswitches (356-358), sRNA targets (337, 359-361), and interacting with RNA binding proteins (338, 339). Although the *roc* mRNA leader could function as a riboswitch (362), we hypothesize that Cur is more likely to regulate an unknown RNA-binding protein or sRNA that controls Roc production via its leader. Future investigations are necessary to identify species-specific Cur regulons and determine how the abundance of distinct intestinal *Bacteroides* species are differentially altered in hosts fed glucose and fructose-rich diets (322).

Materials and Methods

Bacterial culture conditions.

Bacterial strains and plasmids used in this study are listed in Table S1. *Escherichia coli* strains were cultured on Luria-Bertani (BD). *Bt* strains were cultured on solid brain heart infusion agar (Sigma) containing 5% defibrinated horse blood (Hardy), tryptone-yeast extract-glucose (TYG), or *Bacteroides* minimal medium, plus individual carbon sources (0.5% weight/volume unless otherwise noted) as previously described (328). All bacterial strains included the following antibiotics where appropriate: 100 µg/mL ampicillin (Sigma), 200 µg/mL gentamicin (Sigma), 2 µg/mL tetracycline (Sigma), or 25 µg/mL erythromycin (Sigma).

Construction of strains.

pNBU2 plasmids were introduced by di-parental mating and att-1 site integration was verified by PCR as previously described (325). Strains harboring

chromosomal deletions of *BT4338*, *BACOVA_05152*, or *BVU_3580* were constructed by allelic exchange as previously described (363). A strain lacking *BF9343_0915* was constructed by allelic exchange as previously described (364). Strains harboring chromosomal deletions of *BT1450-BT1448* or *BT2131* were constructed by allelic exchange as previously described (365) Epitope tagging of *BACOVA_04371* and inactivation of *BT4299* genes was performed using the pKNOCK-tetQ vector as described (366) Overexpression of candidate sRNAs was achieved using the multicopy plasmid pLYL01 as described (274) Primers used in this study are listed in Table S2.

Generation of Bt transposon insertion library.

E. coli donor S17-1 strain harboring pSAM-*Bt* (GT671) and recipient *Bt* strain containing a multi-copy plasmid encoding epitope-tagged Roc (GT1663) were cultured overnight to stationary phase in LB and TYG, respectively, containing the appropriate antibiotics (351) The *E. coli* strain was diluted 2000-fold into LB media containing ampicillin and the recipient *Bt* strain was diluted 250-fold into 10 ml pre-reduced TYG containing tetracycline. Upon reaching early exponential phase ($OD_{600} \sim 0.3$), 1 mL of donor was combined with 10 mL recipient, centrifuged at 7,200 x g for 2 minutes, and washed with 10 mL of PBS. The pellet was resuspended in the residual volume, spread onto solid BHI-B, incubated aerobically for 3 hours, and then anaerobically overnight. 1.0 mL 1X PBS was added and the confluent growth was dislodged from the plate using a cell spreader. The suspension was increased to with 1X PBS to a final volume of

5.0 mL, homogenized by vortex, and 1.0 mL of the resulting cell suspension was spread onto five 245 mm square BioAssay dishes (Nunc) containing solid BHI-B containing 0.2% galactose and the appropriate antibiotics before 48 hours of anaerobic incubation. The resulting colonies were collected using a plastic spreader and 12 mL 1X PBS containing 20% glycerol. All re-suspended cells were homogenized by vortex and stored at -80°C as 0.25 mL aliquots prior to colony blotting.

Colony Blotting.

One aliquot of the *Bt* library described above was thawed, diluted, and spread onto 150 mm petri dishes containing solid minimal media containing 0.25% galactose and 0.25% rhamnose such that each plate contained approximately 1,000 colonies. Plates were incubated anaerobically for 48 to 72 hours until colonies were readily visible by eye, transferred to nitrocellulose membranes, and immunoblotted as previously described.⁽³²⁵⁾ Selected colonies were isolated on solid BHI-B prior to cryo-preservation.

Western Blotting.

Cell pellets were re-suspended in 375 µl 1x Tris-buffered saline (TBS) containing 1 mM EDTA and 0.5 mg/ml chicken egg lysozyme (Sigma). Cell suspensions were transferred to a 2.0 mL tube containing 0.1 mm Zirconia/Silica beads (BioSpec) and subject to disruption using a Mini-Beadbeater (BioSpec, Bartlesville, OK, USA) at 2,800 rpm for 5 cycles of 40 seconds with 5-minute incubations at 4°C between each cycle. Samples were centrifuged for 2 minutes

at 15,294 x g at 4°C to remove cell debris and the supernatant was reserved. Protein concentration was estimated by measuring absorbance at 280 nanometers using a NanoQuant plate in a Spark plate reader (Tecan, Männedorf, Switzerland). A volume corresponding to 30 µg of protein from each sample was combined with 3 µl 4x LDS buffer (ThermoFisher) containing 100 mM dithiothreitol and subject to heating at 95°C for 5 minutes. A modified protocol was used for PMOG grown cells to reduce reagent consumption. For this, equivalent 0.75 ODs were calculated from mid-exponential grown cells, pelleted, decanted, and flash frozen. Cell pellets were resuspended in 75 µl lysis buffer containing 50mM Tris, 1% SDS, and 2x protease inhibitor (P8849, Sigma) before being boiled at 95°C for 5 minutes. After cooling samples on ice, 25 µl 4x LDS buffer (ThermoFisher) containing 100 mM dithiothreitol was added and samples were incubated at 75°C for 10 minutes. 15 µl of each sample were loaded onto a 4-12% Bis-tris NuPAGE gel (ThermoFisher) and fractionated for 60 minutes at 180V in 1X MOPS running buffer (ThermoFisher) before transfer to a nitrocellulose membrane using an iBlot2 (Invitrogen, Waltham, Massachusetts, USA). The resulting membrane was cut below the 100 kD marker and both portions blocked for 1 hour in 1x TBS with 3% skim milk (BD). The top portion of the membrane was incubated with a 1 to 5,000 dilution of a rabbit anti-HA antibody (Sigma) followed by a 1 to 5,000 dilution of an HRP-conjugated anti-rabbit antibody (GE). GroEL was detected on the bottom portion of the membrane using a 1 to 5,000 dilution of a rabbit anti-GroEL antibody (Sigma) followed by a 1 to 5,000 dilution of an HRP-conjugated anti-rabbit antibody (GE).

Membranes were washed before and after addition of secondary antibody with TBS containing 0.05% Tween-20 (Sigma) and rinsed with 1x TBS prior to detection with ECL Prime Western Blotting Detection Reagent Substrate (Cytiva). Blots were quantified using Image Studio Lite (LI-COR Biosciences, Lincoln, Nebraska, USA).

Quantitative PCR (qPCR).

mRNA was prepared from 1.0 mL of *Bt* cell culture pre-treated with RNA protect (Qiagen) using the RNeasy kit (Qiagen) according to the manufacturer's instructions. Contaminating DNA was removed using on-column DNase treatment (Qiagen) during purification according to the manufacturer's instructions. cDNA was synthesized from 1.0 µg of RNA using Superscript VILO IV master mix (ThermoFisher) according to the manufacturer's instructions. mRNA levels were measured by quantification of cDNA using Fast SYBR Green PCR Master Mix (Applied Biosystems) and primers listed in Table S2 using a QuantStudio 12K Flex Real-Time PCR System (Applied Biosystems, Waltham, Massachusetts, USA). Data were normalized to 16s ribosomal RNA from 1,000-fold diluted cDNA as previously described (330). qPCR primers are listed in Table S2.

Monitoring growth of bacterial strains in vitro.

Bacteroides strains were grown in TYG medium anaerobically overnight before being diluted 1 to 200 into 100ul of *Bacteroides* minimal medium containing 0.5% of the carbon source of interest. For PMOG growth curves, 1.0% PMOG was

used. Growth was monitored for 96 hours following dilution using an Infinite M Nano plate reader (Tecan, Männedorf, Switzerland) maintained anaerobically. Absorbance at OD₆₀₀ was measured every 15 minutes after 5 seconds of orbital shaking.

Chromatin Immunoprecipitation.

ChIP was carried out as previously described (331). The abundance of *rpoD*, *fusA2*, and *roc* promoters were measured in 50-fold-diluted input DNA and 2-fold-diluted IP or control samples by qPCR using primers listed in Table S2. The fold enrichment was calculated as previously described (367).

Carbon limitation experiments.

Bt or *Bo* strains were grown in TYG medium anaerobically overnight before being diluted 1 to 400 into 2.0 mL of *Bacteroides* minimal medium containing 0.5% glucose. After reaching stationary phase, the resulting culture was diluted 1 to 50 into pre-reduced medium containing 0.5% glucose or 0.5% fructose and grown to mid-exponential phase (OD₆₀₀ = 0.45 to 0.6), at which time an aliquot was collected by centrifugation, decanted, and immediately placed on dry ice representing the “-5” time points in carbon limitation experiments. The remaining culture was centrifuged at 7,200 x g at room temperature for 3 minutes in sealed tubes and reintroduced into the anaerobic chamber where the tubes were unsealed, and the supernatant was decanted. Cell pellets were resuspended in an equivalent volume of pre-warmed, pre-reduced minimal medium lacking a carbon source and incubated at 37°C anaerobically. Aliquots

were collected by centrifugation at indicated time points following incubation and the supernatant was decanted before the pellet was placed on dry ice and stored at -80°C.

Examining bacterial abundance in the murine gut.

Germ-free C57BL/6J (JAX # 000664) mice were bred and maintained in gnotobiotic isolators with a 12-hr light/dark cycle at Penn State University. All experiments were carried out using, 8–12-week-old mice with males and females at similar ratios. Experimental groups contained 5 mice and each group was provided with autoclaved standard mouse chow (5021, Lab Diet) or an irradiated glucose-sucrose chow (S4944, Bio-Serv) *ad libitum*. Diet information is available in supplemental tables S3 and S4, respectively. Animal gavage, fresh fecal sample collection, and relative strain abundance measurements were carried out as previously described.⁽²⁶⁰⁾ All experiments using mice were performed using protocols approved by the Penn State Institutional Animal Care and Use Committee.

Measuring BT4338 ortholog silencing by dietary sugar addition.

Bt and *Bf* were grown as described above in 0.5% glucose, 0.5% fructose or 1.0% PMOG. Once mid-exponential phase growth was reached, a 1 ml sample was collected for downstream RNA preparation and a 20% glucose or fructose solution was added to PMOG grown cells to 0.2% final weight/volume and incubated for the indicated times. Subsequently, 1 ml samples were collected 10 and 60-minutes after the addition of either sugar solution, mRNA

was harvested as described above, and transcript abundance was measured by qPCR using primers 1050 and 1051 to measure *Bt fusA2*, 1958 and 1959 to measure *Bf fusA2*, and 1956 and 1957 to measure universal 16s to normalize both genes.

sRNA binding prediction using IntaRNA.

In-silico analysis of putative sRNA interactions with the Roc mRNA leader was achieved using ThetaBase v2 to identify sRNAs upregulated during carbon limitation (368). Upregulated sRNAs were compared to BT4338 binding as predicted by ChIP-seq (331). Candidate sRNA binding analysis was performed using IntaRNA (v3.3.1) at default settings using the Vienna RNA package (2.5.0) (369).

Statistical analysis.

All data analysis was performed using Prism v9.3.1 (GraphPad, San Diego, California, USA). Western blot, ChIP, and qPCR experiments were conducted independently in at least biological triplicate. Data were expressed as mean \pm standard error of the mean (SEM) and analyzed by one- or two-way ANOVA with Fisher's Least Significant Difference test, or paired, two-tailed Student's t-test where indicated and *P* values < 0.05 were statistically significant. Growth curves and *in vivo* bacterial abundance experiments were expressed as mean \pm SEM with no additional statistical analysis conducted. Specific statistical tests, significance, and *n* are indicated in each figure legend.

CHAPTER 3: CARBON UTILIZATION PATHWAYS DIRECT CUR ACTIVITY IN HUMAN GUT *BACTEROIDES*

Abstract

Manipulating the gut microbiota is an attractive therapeutic avenue requiring identification of gut microbial pathways that can be pharmacologically targeted. Members of the dominant gut bacterial phylum, Bacteroidetes, encode a conserved transcription factor called Cur required for intestinal colonization and carbohydrate utilization that responds to an unknown differentially synthesized intracellular signal. Cur activity is silenced by host intake of abundant dietary sugars, glucose and fructose, reducing the amounts of Cur-dependent products. We sought to elucidate the mechanism controlling Cur activation in *Bacteroides thetaiotaomicron* (*Bt*) using genetic and metabolomic approaches to identify the molecular pathways that control this transcription factor. We now report that *Bacteroides* metabolism of glucose and fructose is necessary for Cur silencing and this effect is mediated by one of four putative phosphofructokinase genes that stimulates high levels of fructose-1,6,-bisphosphate. Furthermore, increased Cur activity in this *pfkA* mutant requires a bi-directional ribose 5-phosphate isomerase in the pentose phosphate pathway, implicating that discreet metabolic steps control transcription factor activity. Intriguingly, these enzymes work to coordinate Cur activity during steady state growth but are dispensable for increased activity in response to carbon limitation. Our work defines the metabolic cues

governing the activity of a critical signalling pathway in the mammalian gut and identifies a key metabolic space for pharmacological manipulation of the human gut microbiota.

Introduction

Identifying mechanisms that control microbial colonization of the mammalian intestine and synthesis of host-absorbed metabolites is critical to leveraging the gut microbiota as a therapeutic target. A key barrier to manipulating gut microbial activities is identifying phyla-specific enzymes that can be exploited to control microbial abundance, overcome colonization resistance, and direct metabolism. Microbial intestinal colonization requires efficient extraction of the dynamic and differentially available nutrients present in the mammalian intestine. Furthermore, gut microbial nutrient utilization requires distinct metabolic processes and results in the synthesis of host absorbed metabolites, indicating that elucidating nutrient utilization processes could be exploited to manipulate both microbiota composition and metabolic output.

The abundant human intestinal phyla, Bacteroidetes, dominate in this densely populated environment by exhibiting unique mechanisms to persist in this space. For example, *Bacteroides* species include an intrinsically disordered domain within the essential transcriptional termination factor Rho, which facilitates lipid-lipid phase separation and forms intracellular condensates that regulate transcription by arresting translation, condensing transcription factors with RNA, and storing untranslated mRNAs (339). Additionally, *Bacteroides*

species employ a specialized translation elongation factor, EF-G2, that is dispensable for *in vitro* growth but facilitates GTP-independent translation in the intestine (370). Furthermore, these organisms encode specialized glycan sensors to detect and utilize glycans harvested from the host diet, mucosa, and other co-resident microbes (325, 333, 344, 371). Finally, *Bacteroides* species frequently encode a master regulator, called Cur, that regulates the expression of distinct carbohydrate utilization genes (330), *fusA2* (331), and the abundance of glycan utilization proteins. Because Cur controls numerous processes critical for gut colonization and nutrient utilization by an unknown interconvertible mechanism, elucidating the signals that govern this transcription factor's activity could allow for precision control of bacterial abundance and metabolism in the intestine.

Cur is an attractive target to manipulate gut microbial composition and metabolism because this transcription factor is differentially activated by an unknown signal, is conserved among some of the most abundant members of the gut microbiota (Fig. 2-5 and Fig. 2-6) and is critical for intestinal colonization and conversion of environmentally available glycans into host-absorbed metabolites (271). Interestingly, abundant human dietary additives, fructose and glucose, silence Cur activity by an unknown mechanism, indicating that these monosaccharides control intracellular signals that govern Cur. Therefore, we hypothesize that elucidating how fructose and glucose control Cur activity could identify novel strategies to manipulate gut microbial composition and metabolism. In contrast to the well-defined mechanisms of glucose and fructose utilization in

Proteobacteria and Firmicutes, *Bacteroides* species transport these monosaccharides independently of phosphosugar transport systems (PTS). While the cellular machinery necessary for glucose utilization is unknown in *Bacteroides* species (372), fructose activates a transmembrane transcription factor that regulates expression of a genetically linked polysaccharide utilization locus (344, 373), suggesting that these sugars could differentially regulate transcription of products that directly control Cur activity. Alternatively, Cur activity could be controlled by intracellular metabolites generated during the utilization of either monosaccharide independently of controlling transcription because mutations disrupting central metabolic genes alter expression of Cur-dependent products.

Here, we demonstrate that glucose and fructose regulate Cur activity by distinct metabolic pathways rather than serving as extra-cytoplasmic signals. Fructose and glucose silence Cur activity by increasing glycolytic metabolites and disabling a single phosphofructokinase (pfkA) is sufficient to increase synthesis of Cur-dependent products. The increased Cur activity observed in a pfkA-deficient strain requires a bi-directional ribose-5-phosphate isomerase (RpiB). RpiB is non-essential and dispensable for Cur activation during carbon starvation. Finally, disrupting essential metabolic steps with a newly developed inducible-CRISPRi system demonstrates that Cur activation during carbon limitation requires the synthesis of ribulose-5-phosphate. Together, these data suggest that Cur activity is controlled by distinct Ru5P-derived metabolites because genetically reducing EMP metabolites increases Cur activity whereas

disrupting PPP metabolites reciprocally reduce Cur activity. Elucidating the activating mechanism of Cur provides a target for metabolic manipulation in *Bacteroides*.

Results

Fructose and glucose metabolism is required for Cur silencing.

The addition of glucose or fructose silences Cur activity in *Bacteroides* species. However, fructose can serve as a signal independently of its metabolism by activating a transmembrane transcription factor, called BT1754, in the *Bt* periplasm (344). Thus, fructose could silence Cur via this compartmentalized signaling machinery independently of its metabolism. To differentiate whether fructose silences Cur by serving as signal or growth substrate, we measured *fusA2* transcript levels in a *Bt* mutant lacking *BT1758*, an inner membrane fructose transporter, that can transport fructose across the outer but not the inner membrane, thereby trapping fructose in the periplasm, eliciting increased signaling through BT1754, but preventing fructose utilization (344). We grew strains in PMOG as this induces high Cur activity and the *BT1758* mutant is able to grow unlike the growth defect exhibited during growth in fructose (Fig. 3-1A and 3-1B). The addition of fructose for 60 minutes to cells growing exponentially in PMOGs was unable to reduce the Cur target *fusA2* mRNA amounts in *BT1758*-deficient cells (Fig. 3-1C). Previous data demonstrates a decrease in *fusA2* mRNA amounts in wild-type after the addition of fructose for 60-minutes (Fig. C-7B). Thus, fructose importation into the cytoplasm is required for silencing

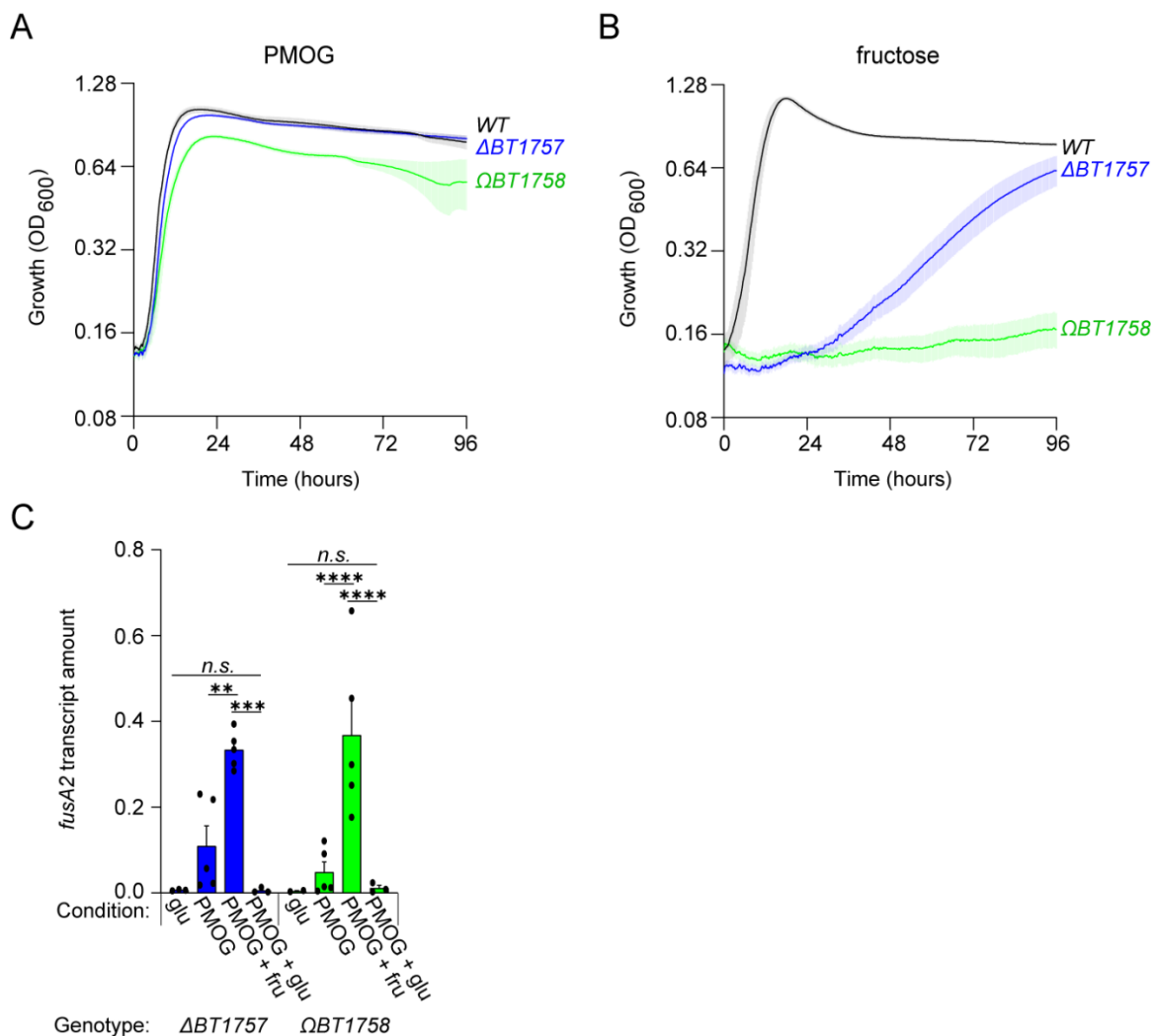


Figure 3-1: Fructose importation is required for Cur silencing. a-b. Growth of wild-type (GT593; black) or *Bt* strains deficient for BT1757 (GT955; blue) or a BT1758 inactivation (GT3495; green) in minimal media containing 1% PMOG (a), or 0.5% fructose (b). (Values are the mean of 4 biological replicates, error bars represent SEM.) c. The transcript level of *fusA2* measured in strains described in (a) during mid log growth in 0.5% glucose (glu), fructose (fru), or 1% PMOG, and 10-minutes following the addition of 0.5% fructose or glucose to PMOG growth cells. (Values are the mean of 3 to 5 independent measurements, error bars represent SEM, *P* values derived from one way ANOVA; n.s. indicates *P* values ≥ 0.05 ; ** *P* < 0.01 *****P* < 0.0001)

of Cur activity. To determine whether Cur silencing required fructose-derived metabolites, we measured *fusA2* levels in a mutant lacking BT1757, which is a fructokinase required for converting fructose to fructose-6-phosphate, an essential step for fructose utilization. As expected, disabling Cur silencing in the

BT1758 or *BT1757* mutants was specific to fructose because these strains exhibited a similar reduction of *fusA2* transcripts 10 minutes following addition of glucose compared to *wild-type* cells (Fig. 3-1C). Together, these data suggest both the importation and metabolism of fructose are required for silencing of Cur activity.

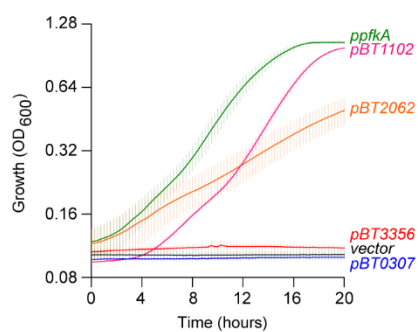
Disrupting the Embden-Meyerhof-Parnas Pathway increases Cur activity in glucose and fructose.

To determine whether metabolism through the EMP is governing Cur activity, we genetically disabled the first step in fructose catabolism, the production of fructose-1,6-bisphosphate (FBP) from fructose 6-phosphate through PfkA. If FBP production can be interrupted by engineering strains deficient in *pfkA*, we can measure Cur activity when the EMP is disrupted, and glucose and fructose cannot be metabolized by this pathway. If metabolism through the EMP is required for silencing, then genetically blocking carbon metabolism by disabling *pfkA* will alleviate Cur silencing exhibited in glucose or fructose containing conditions. *Bt* encodes 4 ORFs annotated as *pfkA*, however *E. coli* only encodes 2 annotated PfkAs and closely related *Bo* and *Bf* each encode 3 ORFs annotated as PfkAs (Fig. 3-2A). To determine if the PfkAs in *Bt* function to produce FBP, we engineered inducible plasmids containing an individual *pfkA* and introducing these plasmids into a *pfkA* deficient *E. coli* strain, we found that only *BT1102* and *BT2062* can complement growth suggesting they are bona fide PfkAs and further their sequence homology is 53.0 and 33.3% similar to *E. coli* *pfkA* and *pfkB*, respectively. (Fig. 3-2B). *BT0307* and *BT3356*

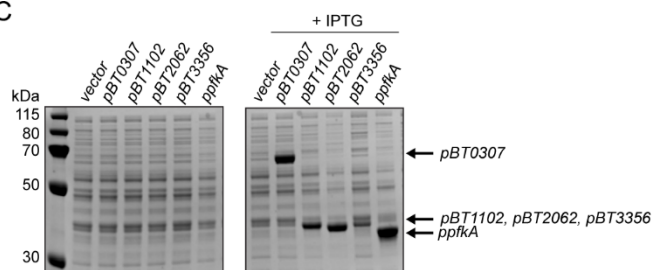
A

		Percent Identity												
Divergence		Ec pfkA	Ec pfkB	BT_0307	BT_1102	BT_2062	BT_3356	BO_00152	BO_02100	BO_03488	BF_0174	BF_2852	BF_3444	
Ec pfkA				32.3	53.0	32.6	31.3	32.6	31.9	31.9	31.5	41.5	31.6	Ec pfkA
Ec pfkB		152.3		30.8	31.4	33.3	30.9	30.7	32.7	31.6	31.7	31.9	32.8	Ec pfkB
BT_0307		200.2	240.3		30.9	41.1	42.0	90.9	42.3	42.0	42.6	31.6	41.3	BT_0307
BT_1102		74.7	204.3	211.2		31.1	31.4	31.1	30.7	32.3	31.2	41.4	30.8	BT_1102
BT_2062		179.5	186.8	118.9	200.7		52.4	41.5	86.3	50.6	51.7	29.0	82.8	BT_2062
BT_3356		199.1	199.1	114.3	199.5	76.5		42.2	51.6	82.5	78.6	29.6	51.0	BT_3356
BO_00152		202.1	240.9	9.8	205.8	117.4	113.9		42.5	41.8	42.8	30.8	41.9	BO_00152
BO_02100		185.7	209.6	112.1	203.0	15.3	78.8	111.7		50.6	52.9	29.9	82.8	BO_02100
BO_03488		205.4	192.5	114.3	189.3	82.3	20.3	115.5	81.9		77.3	29.6	50.7	BO_03488
BF_0174		212.7	185.1	112.6	209.7	78.7	25.5	112.6	75.4	27.2		29.1	51.0	BF_0174
BF_2852		114.0	190.1	182.6	118.0	262.4	215.8	193.1	225.6	218.8	218.7		31.3	BF_2852
BF_3444		187.6	201.8	117.7	196.7	19.8	80.5	114.0	19.9	81.7	80.9	201.6		BF_3444
		Ec pfkA	Ec pfkB	BT_0307	BT_1102	BT_2062	BT_3356	BO_00152	BO_02100	BO_03488	BF_0174	BF_2852	BF_3444	

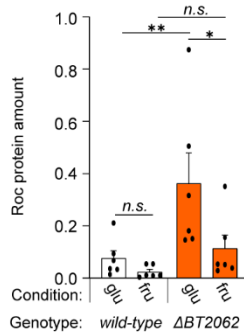
B



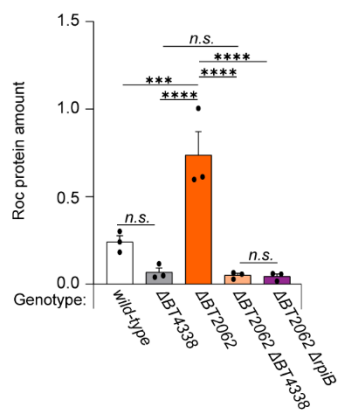
C



D



E



F

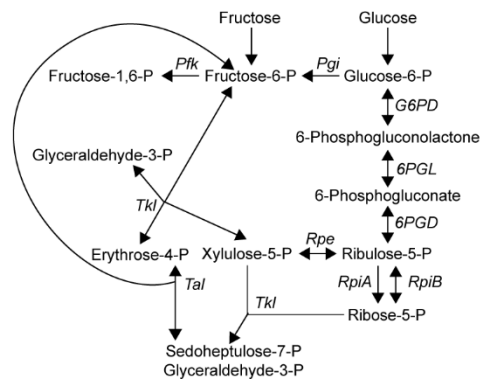


Figure 3-2: EMP disruption increases Cur activity. a. Percent identity and divergence of annotated *pfk* enzyme sequences from *Bt*, *Ec*, *Bo*, and *Bf* aligned with ClustalW. b. Growth of *Ec* strains harboring plasmids containing empty vector (GT3382; black), BT0307 (GT3383; blue), BT1102 (GT3384; pink), BT2062 (GT3385; orange), BT3356 (GT3386; red) or *Ec pfkA* (GT4231; green) in MOPS minimal media containing 0.5% glucose and 100uM IPTG (Values are the mean of 4 biological replicates, error bars represent SEM). c. Representative coomassie stained gel of strains described in (b) grown in rich medium (left) or supplemented with 100uM IPTG (right). d. Quantified western blot analysis of wild-type (GT593; white), or *Bt* strain deficient for BT2062 (GT762; orange) during growth in glucose (*glu*) or fructose (*fru*) (Values are the mean of 6 biological replicates, error bars represent SEM; *P* values derived from two way ANOVA; n.s. indicates *P* values ≥ 0.05 ; * *P* < 0.05 ***P* < 0.01). e. Quantified western blot analysis of wild type (GT593; white), or *Bt* strains deficient for BT4338 (GT1234; gray), BT2062 (GT762; orange), both BT2062 and BT4338 (GT1314; light orange), or both BT2062 and BT0346 (GT2735; purple) (Values are the mean of 3 biological replicates, error bars represent SEM, *P* values derived from one way ANOVA; n.s. indicates *P* values ≥ 0.05 ; *** *P* < 0.001 *****P* < 0.0001). f. Metabolic map depicting the connections between the EMP and PPP.

share less than 33% identity with either *E. coli pfkA* and *pfkB* and both failed to rescue growth despite being inducibly expressed (Fig. 3-2B and 3-2C). Further, by engineering strains deficient for individual *pfkAs*, we discovered that BT0307 is essential whereas BT1102, BT2062, and BT3356 are non-essential and can easily be deleted. Further, we determined that elimination of just BT2062 increases Cur activity as indicated by a 4.5-fold increase in Roc expression over wild-type in either glucose or fructose containing media (Fig. 3-2D). The increase in Roc expression is Cur dependent as a strain lacking both *cur* and BT2062 resembles that of a *cur* deletion strain alone (Fig. 3-2E). Together these data indicate that glucose and fructose metabolism silence Cur activity by increasing FBP levels and thus, carbon flow through the EMP (Fig. 3-2F).

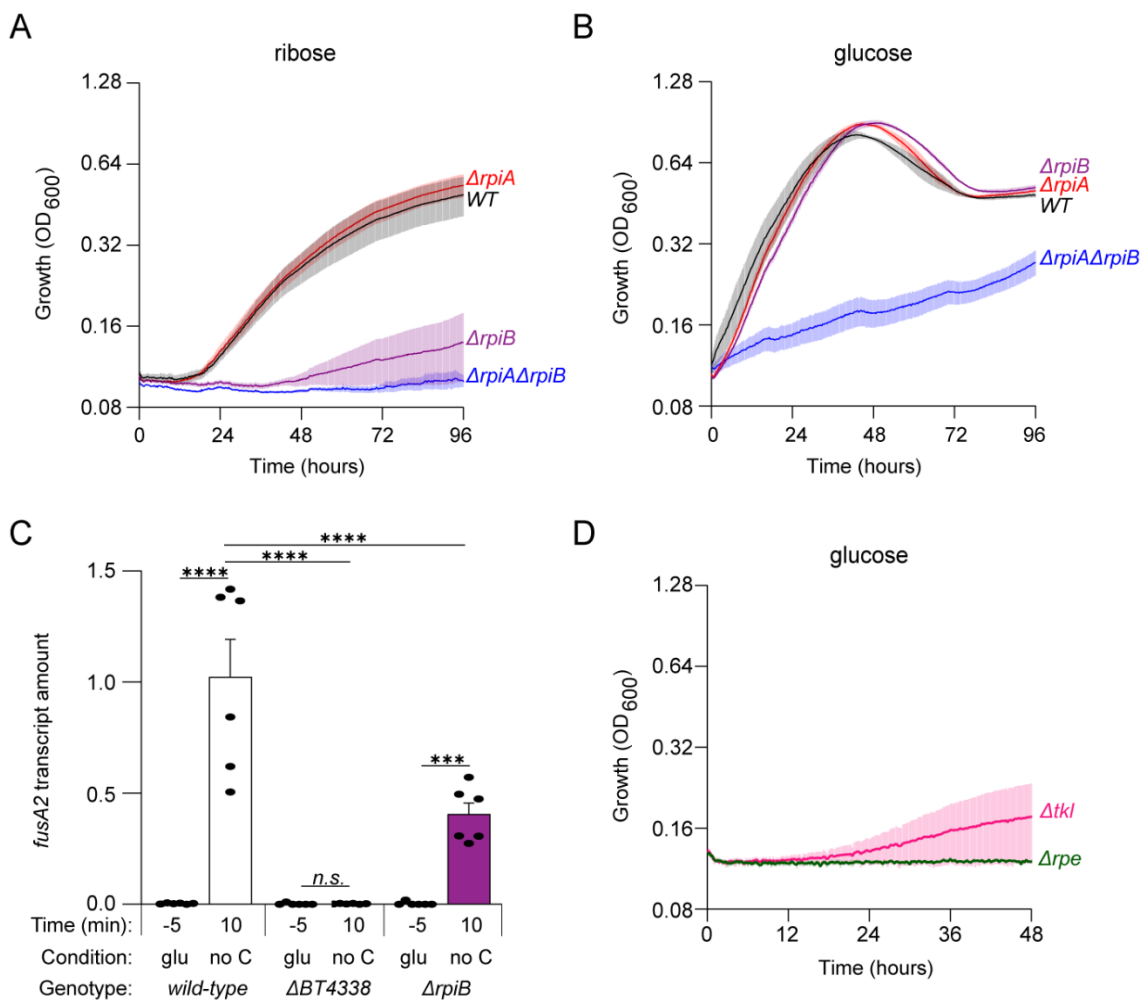


Figure 3-3: Cur activity is differentially stimulated during carbon starvation. a-b. Growth of wild-type (GT23; black) or Bt strains deficient for *rpiA* (GT2385; red), *rpiB* (GT2284; purple) or both *rpiA* and *rpiB* (GT2437; blue) in minimal media containing 0.5% ribose (a), or 0.5% glucose (b) (Values are the mean of 4 biological replicates, error bars represent SEM). c. The transcript level of *fusA2* measured in wild-type (GT593; black) or Bt strains deficient for *cur* (GT1234; gray), *rpiB* (GT2829; purple) during mid log growth in 0.5% glucose (glu; -5), and 10-minutes following carbon starvation (10). (Values are the mean of 6 biological replicates, error bars represent SEM, *P* values derived from two way ANOVA; n.s. indicates *P* values ≥ 0.05 ; *** *P* < 0.001 *****P* < 0.0001) d. Growth of Bt strains deficient for *rpe* (GT2381; green) or *tkl* (GT2387; pink) in minimal media containing 0.5% glucose (Values are the mean of 4 biological replicates, error bars represent SEM).

Removing specific steps in non-oxidative pentose phosphate pathway reduces Cur activation during carbon starvation.

I hypothesized that disabling *pfkA*s increases Cur activity by re-routing carbon metabolism through alternative metabolic pathways. Because we

previously identified mutations in the oxidative PPP (oPPP) that reduce, but do not abolish Cur activity (Fig. C-2), we reasoned that downstream steps in the non-oxidative PPP (noPPP) are involved in Cur activation. To identify steps in the noPPP required for Cur activation during carbon starvation, each enzyme was assessed independently. Only one enzyme, ribose-5-phosphate isomerase (Rpi) is putatively encoded by more than one ORF (Fig. 3-2F). Genetically disabling *rpi* activity can be achieved due to this redundancy. Therefore, we started with determining the requirement of either Rpi for Cur activation. We first identified that RpiA is a monodirectional isomerase whereas RpiB is a bidirectional isomerase as an *rpiB* deletion exhibits a growth defect in minimal media containing ribose but no defect in minimal media containing glucose (Fig. 3-3A and 3-3B, respectively). Conversely, a deletion of *rpiA* exhibits no defect in either condition indicating that only RpiB is responsible for interconverting ribulose-5-P (Ru5P) and ribose-5-P (Ri5P) (Fig. 3-3A and 3-3B). Further, an *rpiB* mutation relieves the increase of Cur activity exhibited by a *BT2062* mutant suggesting Ru5P plays an important role in activity as this strain encourages carbon flow through *rpiA* to produce Ri5P. (Fig. 3-2D). Additionally, an *rpiB* mutation exhibits an 107-fold increase in *fusA2* transcript amounts after 10-minutes of carbon starvation whereas a 257-fold increase is exhibited by wild-type (Fig. 3-3C). Together, these data suggests that Cur activity is differentially stimulated by genetically redirecting carbon metabolism during carbon starvation. When carbon flow through the EMP is blocked, Cur activity is increased, and

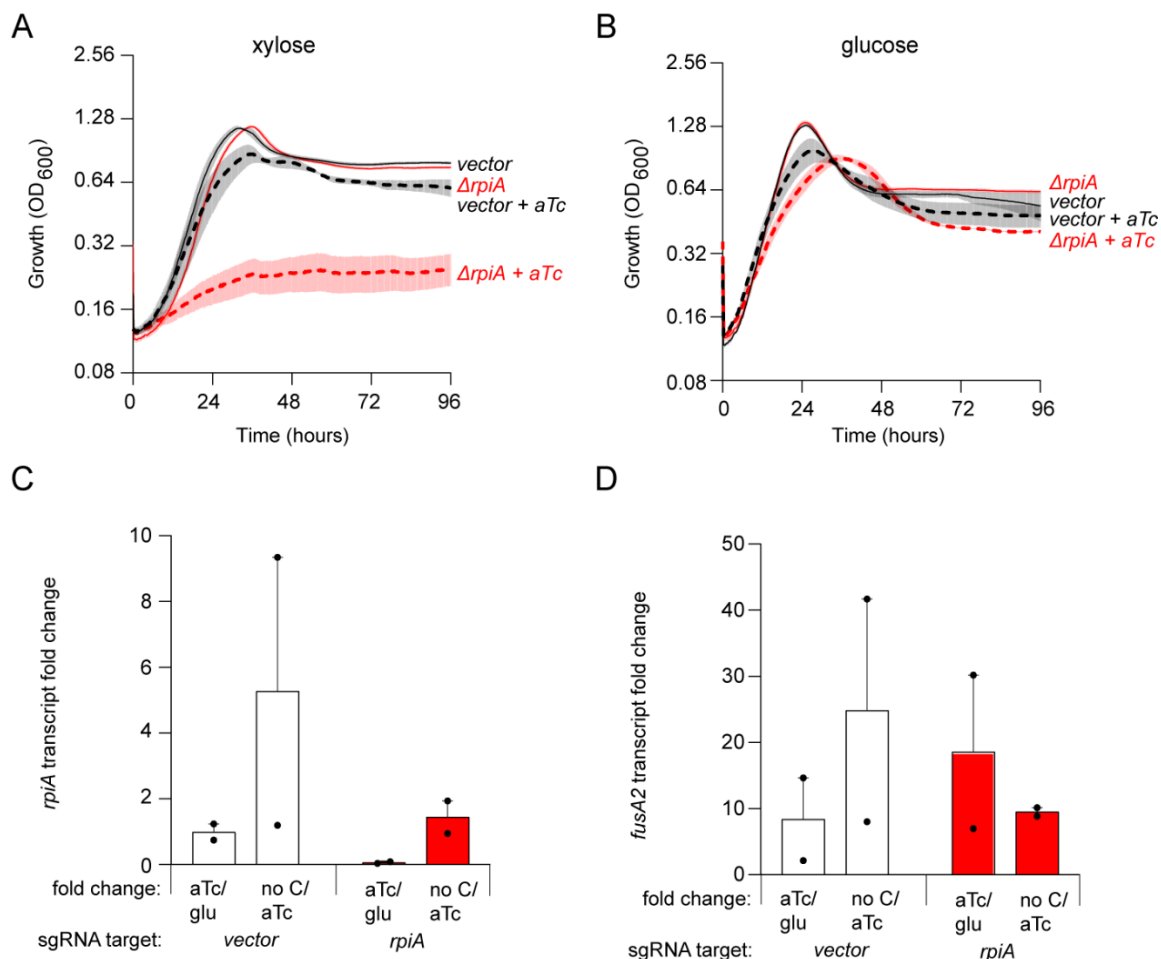


Figure 3-4: CRISPRi interferes with *rpiA* transcription. a-b. Growth of *rpiB* deletion *Bt* strains harboring either a vector control plasmid (GT4051; black) or an sgRNA targeting *rpiA* (GT4053; red) in minimal media containing 0.5% xylose (a), or 0.5% glucose (b) and aTc induction indicated by dotted lines (Values are the mean of 4 biological replicates, error bars represent SEM). c-d. The fold change in the transcript level of *rpiA* (c) or *fusA2* (d) measured in vector control (GT4051; white) or a strain harboring an sgRNA targeting *rpiA* (GT4053; red) during early log growth in 0.5% glucose (glu), addition of aTc (aTc) and 10-minutes following carbon starvation (no C; 10) (Values are the mean of 2 biological replicates, error bars represent SEM).

when *rpiB* is inactivated, Cur activity is reduced suggesting the importance of Ru5P in Cur activation. We propose that this could be mediated by Ru5P, or a derived product synthesized during carbon starvation.

Genetically disabling downstream genes posed a challenge as they are essential for growth in minimal media. Therefore, disabling these genes using

loss-of-function mutations cannot be utilized to assess the role of these enzymes in Cur activation through carbon starvation. Genetically eliminating ribulose-phosphate 3-epimerase (Rpe) or transketolase (Tkl), exhibits a severe growth defect when grown in glucose containing media, preventing further examination with either of these mutants (Fig. 3-3D). To genetically examine downstream genes, we adapted a CRISPRi system induced by the addition of aTc, genetically interfering with transcription of target genes when cells are already rapidly growing, removing this concern. We started with an sgRNA specific for *rpiA* in an *rpiB* mutant to validate our methodology. Induction of CRISPRi caused a severe growth defect when cells were grown in xylose, but this was not exhibited in glucose suggesting the noPPP has been blocked through removal of both *rpi*s (Fig. 3-4A and 3-4B, respectively). Upon introduction of aTc, *rpiA* transcript levels decreased 18.4-fold compared to glucose grown cells alone and remained unchanged in the vector control (Fig. 3-4C). Furthermore, 10-minutes post carbon starvation, *fusA2* levels increased 28.3-fold in the control strain compared to the *rpiA* CRISPRi strain exhibiting a 9.4-fold increase (Fig. 3-4D) meaning that removal of *rpiA* in addition to *rpiB* does not completely abolish Cur activity in carbon starvation. These data suggest that neither *rpi* alone nor in combination are solely responsible for Cur activity during carbon starvation, though additional experiments are required as preliminary results are based on 2 replicates. However, these data suggest that a reduction in carbon flow to downstream noPPP steps lead to reduced Cur activity (Fig 3-2F). We expect that the reduction of a metabolite produced in a later step in the noPPP will abolish Cur

activation following carbon starvation and as such be a crucial component in Cur activation.

Discussion

We have determined that Cur, a global transcription factor encoded in many *Bacteroides* species within the human gut has interconvertible activity governed by genetically redirecting carbon metabolism based on the available environmental nutrients. We have elucidated that the Cur silencing by fructose requires importation and metabolism (Fig. 3-1) indicating fructose itself cannot act as an intracellular signal to govern Cur, but a metabolite could. When provided glucose and fructose, Cur activity is silenced, but reducing carbon metabolism through the EMP alleviates this silencing (Fig. 3-2). Consistent with this, reducing carbon flow through the oPPP through genetically inactivating any one of the three steps reduces Cur activity (Appendix C; Figure C-2). We have additionally established the directionality of two encoded ribose-5-phosphate isomerases in *Bt* (Fig. 3-3A and 3-3B). Blocking the bi-directional RpiB and a highly active pfkA (BT2062) results in reduced Cur activity indicating Cur activation requires carbon flow through the PPP, specifically Ru5P production (Fig. 3-2D). Finally, we have generated an inducible CRISPRi system to address the essentiality of genes within central metabolism where loss-of-function mutations cannot be utilized. Using this system, we have identified that neither *rpi* is solely responsible for Cur activation in carbon starvation as removal or

blocking both together reduce Cur activation suggesting the importance of Ru5P for carbon starvation-dependent activation. (Fig. 3-3C and 3-4).

Bacteroidetes encode specific coordinately regulated gene clusters for sensing, de-polymerizing, importing, and utilizing complex carbohydrates, called PULs. These systems include specific nutrient sensors encoded both within and outside of these PULs required for utilization of target nutrients (284, 326, 330, 374). Co-resident Proteobacteria are more adept at utilizing monosaccharides and prefer glucose over other carbon sources. When glucose is present and recognized, cAMP is differentially synthesized in response and results in increased gene expression by activating Crp, a Proteobacterial global transcription regulator. Firmicutes use a similar mechanism in which CcpA is activated by phosphorylated HPr in response to intracellular metabolic cues to govern gene expression. In the presence of less preferred carbon sources, cAMP production is halted thereby preventing activation of Crp resulting in no increased in gene expression (375). In Firmicutes, less preferred substrates lead to phosphorylated HPr instead enhancing activity of transcriptional activators to utilize the less preferred carbon sources rather than activating CcpA (376). These CCR mechanisms reduce transcription of genes required for metabolizing less preferred carbon sources when more preferred carbon sources are available in the environment. We find that Cur also exhibits differing activity, which is carbon source dependent, consistent with the notion that Cur serves as an important component of *Bacteroides* CCR however the mechanism differs from

Proteobacteria and Firmicutes because *Bacteroides* specialize in consuming more complex carbohydrates.

As *Bacteroides* do not encode either of these mechanisms and *Bacteroides* CCR is not well understood, we propose that Cur is an important component in CCR in these species. Further, *Bacteroides* must prioritize consumption of complex glycans and their constituents suggesting *Bacteroides* species exert CCR in the opposite manner of Proteobacteria of Firmicutes and to repress genes responsible for utilizing simple sugars since Bacteroidetes are more adept at metabolizing complex carbohydrates compared to other phyla. Therefore, the preferred carbon source which would provide Bacteroidetes a fitness advantage would be the available complex carbohydrates. Importantly, our experiments examine *Bt* in isolation, but in the context of the gut, millions of organisms are competing for the available nutrients so currently, *Bacteroides* preferred carbon sources remain unknown in monoculture. Because Cur is required for gut colonization and its activity is necessary for transcription of a multitude of carbohydrate utilization genes, host-microbial interaction proteins, and translation factors, the silencing exhibited by glucose and fructose suggest these to be less preferred carbon sources as their consumption leads to reduction in these genes required for intestinal colonization.

Our work suggests that Cur activity relies on a metabolite generated by consumption of a more favorable carbohydrate and when consuming less favorable substrates, Cur activity is silenced (Chapter 2). Further investigation is

required to identify the signal to activate Cur by we hypothesize this signal is Ru5P or a derivative due to the importance of RpiB to Cur activity as RpiB can convert Ri5P back to Ru5P. The PUL responsible for ribose consumption encodes two kinases which function to generate Ri5P from free ribose and ribose-1,5-P from Ri5P or ribose-1-P. These two kinases are required for *in vivo* colonization together, but individually dispensable and are not transcribed when cells are switched from glucose containing media to ribose containing media (332). Further, Cur is essential for growth in ribose as it is required for ribose utilization suggesting that metabolites derived directly from ribose are unlikely metabolites to activate Cur (330, 332). Because disrupting divergent central metabolic pathways produces opposing effects on Cur activity, we hypothesize that molecules derived from these metabolites differentially govern Cur DNA binding activity to target promoters. One of the main roadblocks to the reverse genetics employed is the essentiality of these metabolic steps to allow for growth. The development of the CRISPRi system is incredibly beneficial as genes can be knocked down in a targeted manner in cells which are already growing. This allows for investigation of more enzymes within central metabolism which otherwise are unable to be inactivated. This preliminary work suggests that removal of *rpiA* in an *rpiB* deletion strain does reduce the activity of Cur as measured by reduced *fusA2* transcription. While this still does not identify the key step required for Cur activity, it provides a more specific area within central metabolism to focus, Ru5P and derivatives. Therefore, future experiments should explore reducing the expression of Rpe, Tkl, and Prs, downstream noPPP

enzymes which are essential and cannot be inactivated. Genetically disrupting these pathways may be impossible because of genetic essentiality and therefore this CRISPRi system could be utilized to determine the role of these metabolites in governing Cur activity. Identifying the regulatory signal to govern Cur in *Bacteroides*, will provide a better understanding of a previously unknown CCR mechanism which can be exploited for manipulating microbial abundance.

Material and Methods

Bacterial culture conditions.

Bacterial strains and plasmids used in this study are listed in Table 3-1. *Escherichia coli* strains were cultured on Luria-Bertani (BD), or MOPS media plus 0.5% weight/volume glucose. *Bt* strains were cultured on solid brain heart infusion agar (Sigma) containing 5% defibrinated horse blood (Hardy), tryptone-yeast extract-glucose (TYG), or *Bacteroides* minimal medium, plus individual carbon sources (0.5% weight/volume unless otherwise noted) as previously described (328). All bacterial strains included the following antibiotics where appropriate: 100 µg/mL ampicillin (Sigma), 200 µg/mL gentamicin (Sigma), 2 µg/mL tetracycline (Sigma), or 25 µg/mL erythromycin (Sigma).

Construction of strains.

pNBU2 plasmids were introduced by di-parental mating and att-1 site integration was verified by PCR as previously described (325). Strains harboring chromosomal deletions of *BT4338*, *rpiA*, *rpiB*, *rpe*, or *pfk* were constructed by allelic exchange as previously described (363). pUHE21-lacIQ plasmids

containing *pfk* genes were constructed by PCR amplifying from *wild-type Bt* using primers listed in Table 3-2, followed by NEBuilder with pUHE21-lacQ digested with BamHI and HindIII.

Inducible system (CRISPRi).

dcas9 was amplified from pMM763 (Addgene #68900, (377)) using primers 2352 and 2353 and introduced into pNBU2-ermG-TetR-P1T_DP-GH023 digested with NcoI and PstI (378) using NEBuilder. The resulting plasmid was digested with PstI and Sall and combined with amplicons harboring 1.) the *Bt 16s rrs* promoter, amplified from *Bt* gDNA with primers 2354 and 2355, and 2.) the *S. pyogenes* sgRNA scaffold, amplified from pMM763 with primers 2356 and 2357. We determined that the resulting plasmid, pGT3920, contained 2 point mutations within the *dcas9* ORF that were also found in the template plasmid, pMM763. Therefore, we ligated a 2117 bp fragment from *pdcas9*-bacteria (Addgene #44249, (379)) digested with BamHI and SphI and with an 8062 bp fragment from pGT3920 digested with the same enzymes. The resulting plasmid, pGT3945, harbored *dcas9* under control of an aTc-inducible promoter followed by a constitutively expressed sgRNA scaffold with a SpeI restriction site for convenient introduction of sgRNA target sequences.

Western Blotting.

Cell pellets were re-suspended in 375 μ l 1x Tris-buffered saline (TBS) containing 1 mM EDTA and 0.5 mg/ml chicken egg lysozyme (Sigma). Cell suspensions were transferred to a 2.0 mL tube containing 0.1 mm Zirconia/Silica

beads (BioSpec) and subject to disruption using a Mini-Beadbeater (BioSpec, Bartlesville, OK, USA) at 2,800 rpm for 5 cycles of 40 seconds with 5-minute incubations at 4°C between each cycle. Samples were centrifuged for 2 minutes at 15,294 x g at 4°C to remove cell debris and the supernatant was reserved. Protein concentration was estimated by measuring absorbance at 280 nanometers using a NanoQuant plate in a Spark plate reader (Tecan, Männedorf, Switzerland). A volume corresponding to 30 µg of protein from each sample was combined with 3 µl 4x LDS buffer (ThermoFisher) containing 100 mM dithiothreitol and subject to heating at 95°C for 5 minutes. Each sample was loaded onto a 4-12% Bis-tris NuPAGE gel (ThermoFisher) and fractionated for 60 minutes at 180V in 1X MOPS running buffer (ThermoFisher) before transfer to a nitrocellulose membrane using an iBlot2 (Invitrogen, Waltham, Massachusetts, USA). The resulting membrane was cut below the 100 kD marker and both portions blocked for 1 hour in 1x TBS with 3% skim milk (BD). The top portion of the membrane was incubated with a 1 to 5,000 dilution of a rabbit anti-HA antibody (Sigma) followed by a 1 to 5,000 dilution of an HRP-conjugated anti-rabbit antibody (GE). GroEL was detected on the bottom portion of the membrane using a 1 to 5,000 dilution of a rabbit anti-GroEL antibody (Sigma) followed by a 1 to 5,000 dilution of an HRP-conjugated anti-rabbit antibody (GE). Membranes were washed before and after addition of secondary antibody with TBS containing 0.05% Tween-20 (Sigma) and rinsed with 1x TBS prior to detection with ECL Prime Western Blotting Detection Reagent Substrate (Cytiva).

Blots were quantified using Image Studio Lite (LI-COR Biosciences, Lincoln, Nebraska, USA).

Quantitative PCR (qPCR).

mRNA was prepared from 1.0 mL of *Bt* cell culture pre-treated with RNA protect (Qiagen) using the RNeasy kit (Qiagen) according to the manufacturer's instructions. Contaminating DNA was removed using on-column DNase treatment (Qiagen) during purification according to the manufacturer's instructions. cDNA was synthesized from 1.0 µg of RNA using Superscript VILO IV master mix (ThermoFisher) according to the manufacturer's instructions. mRNA levels were measured by quantification of cDNA using Fast SYBR Green PCR Master Mix (Applied Biosystems) and primers listed in Table 3-2 using a QuantStudio 12K Flex Real-Time PCR System (Applied Biosystems, Waltham, Massachusetts, USA). Data were normalized to 16s ribosomal RNA from 1,000-fold diluted cDNA as previously described (330). qPCR primers are listed in Table 3-2.

CRISPRi carbon limitation experiments.

Bt strains were grown in TYG medium anaerobically overnight before being diluted 1 to 400 into 2.0 mL of *Bacteroides* minimal medium containing 0.5% glucose. After reaching stationary phase, the resulting culture was diluted 1 to 50 into pre-reduced medium containing 0.5% glucose or 0.5% fructose and grown to early-exponential phase ($OD_{600} \sim 0.1$) at which time an aliquot was collected by centrifugation, decanted, and immediately placed on dry ice before

adding aTc to 100ng/mL. The remaining culture was then grown to mid-exponential phase ($OD_{600} = 0.45$ to 0.6), at which time an aliquot was collected by centrifugation, decanted, and immediately placed on dry ice representing the “-5” time points in carbon limitation experiments. The remaining culture was centrifuged at $7,200 \times g$ at room temperature for 3 minutes in sealed tubes and reintroduced into the anaerobic chamber where the tubes were unsealed, and the supernatant was decanted. Cell pellets were resuspended in an equivalent volume of pre-warmed, pre-reduced minimal medium lacking a carbon source and incubated at 37°C anaerobically. Aliquots were collected by centrifugation at indicated time points following incubation and the supernatant was decanted before the pellet was placed on dry ice and stored at -80°C .

Monitoring growth of bacterial strains *in vitro*.

Escherichia strains were grown in LB medium overnight before being diluted 1 to 200 into 200ul of MOPS minimal medium containing 0.5% glucose plus 100uM IPTG where indicated. *Ec* growth was monitored for 24 hours following dilution using a Spark plate reader (Tecan, Männedorf, Switzerland). *Bacteroides* strains were grown in TYG medium anaerobically overnight before being diluted 1 to 200 into 100ul of *Bacteroides* minimal medium containing 0.5% of the carbon source of interest. For PMOG growth curves, 1.0% PMOG was used. Growth was monitored for 96 hours following dilution using an Infinite M Nano plate reader (Tecan, Männedorf, Switzerland) maintained anaerobically.

Absorbance at OD600 was measured every 15 minutes after 5 seconds of orbital shaking.

Coomassie staining of IPTG induced strains.

Ec strains harboring plasmids expressing pfkAs were grown overnight in LB media with or without 100uM IPTG. 25ul of the resulting culture was combined with 5 μ l 4x LDS buffer (ThermoFisher) containing 100 mM dithiothreitol and subject to heating at 95°C for 5 minutes. Each sample was loaded onto a 10% Bis-tris NuPAGE gel (ThermoFisher) and fractionated for 45 minutes at 180V in 1X MES running buffer (ThermoFisher). The gel was placed in Coomassie stain and microwaved for 40 seconds before incubating at room-temperature for 5 minutes. The gel was rinsed with deionized water before being placed in destain solution and microwaved for another 40 seconds. The gel was then incubated at room temperature with Kim-wipes in the container until the stain reduced and protein bands were visible.

Statistical analysis.

All data analysis was performed using Prism v9.3.1 (GraphPad, San Diego, California, USA). Western blot, ChIP, and qPCR experiments were conducted independently in at least biological triplicate. Data were expressed as mean \pm standard error of the mean (SEM) and analyzed by one- or two-way ANOVA with Fisher's Least Significant Difference test, or paired, two-tailed Student's t-test where indicated and *P* values < 0.05 were statistically significant. Growth curves and *in vivo* bacterial abundance experiments were expressed as

mean \pm SEM with no additional statistical analysis conducted. Specific statistical tests, significance, and *n* are indicated in each figure legend.

Supplemental Tables

Table 3-1. Strains and plasmids used in this study

Name	Genotype	Plasmid	Reference
<i>E. coli</i>			
MG1655	<i>F</i> ⁻ , <i>lambda</i> ⁻ , <i>rph</i> -1		ATCC 700926
GT1	λ <i>pir</i>		(380)
GT3172	<i>F</i> ⁻ , [<i>araD</i> 139] <i>B/r</i> , <i>lacI</i> p-4000(<i>lacI</i> Q), <i>e14</i> ⁻ , <i>pfk</i> B205(<i>del-ins</i>):: <i>FRT</i> , <i>flhD</i> 5301, Δ (<i>fruK</i> - <i>yeiR</i>)725(<i>fruA</i> 25), <i>relA</i> 1, <i>rpsL</i> 150(<i>strR</i>), <i>rbsR</i> 22, <i>pfkA</i> 203(<i>del-ins</i>):: <i>FRT</i> , Δ (<i>fimB</i> - <i>fimE</i>)632:: <i>IS1</i> , <i>deoC</i> 1		Yale CGSC
GT3382	<i>F</i> ⁻ , [<i>araD</i> 139] <i>B/r</i> , <i>lacI</i> p-	<i>pUHE21-lacI</i> Q	This study
GT3383	4000(<i>lacI</i> Q), <i>e14</i> ⁻ , <i>pfk</i> B205(<i>del-</i>	<i>pUHE21-lacI</i> Q:: <i>BT0307</i>	This study
GT3384	<i>ins</i>):: <i>FRT</i> , <i>flhD</i> 5301, Δ (<i>fruK</i> -	<i>pUHE21-lacI</i> Q:: <i>BT1102</i>	This study
GT3385	<i>yeiR</i>)725(<i>fruA</i> 25), <i>relA</i> 1,	<i>pUHE21-lacI</i> Q:: <i>BT2062</i>	This study
GT3386	<i>rpsL</i> 150(<i>strR</i>), <i>rbsR</i> 22,	<i>pUHE21-lacI</i> Q:: <i>BT3356</i>	This study
GT4231	<i>pfkA</i> 203(<i>del-ins</i>):: <i>FRT</i> , Δ (<i>fimB</i> - <i>fimE</i>)632:: <i>IS1</i> , <i>deoC</i> 1	<i>pUHE21-lacI</i> Q:: <i>pfkA</i>	This study
<i>B. thetaiotaomicron</i>			
GT22			ATCC 29148
GT23	Δ <i>tdk</i>		(267)
GT593	Δ <i>tdk</i> <i>BT3172HACLEAN</i>		(381)
GT762	Δ <i>tdk</i> <i>BT3172HACLEAN</i> Δ <i>BT2062</i>		This study
GT955	Δ <i>tdk</i> <i>BT3172HACLEAN</i> Δ <i>BT1757</i>		This study
GT1234	Δ <i>tdk</i> <i>BT3172HACLEAN</i> Δ <i>BT4338</i>		This study
GT1314	Δ <i>tdk</i> <i>BT3172HACLEAN</i> Δ <i>BT4338</i> Δ <i>BT2062</i>		This study
GT2284	Δ <i>tdk</i> Δ <i>BT0346</i>		This study
GT2381	Δ <i>tdk</i> Δ <i>BT0347</i>		This study
GT2385	Δ <i>tdk</i> Δ <i>BT1986</i>		This study
GT2387	Δ <i>tdk</i> Δ <i>BT3946</i>		This study
GT2437	Δ <i>tdk</i> Δ <i>BT0346</i> Δ <i>BT1986</i>		This study
GT2735	Δ <i>tdk</i> <i>BT3172-HACLEAN</i> Δ <i>BT2062</i> Δ <i>BT0346</i>		This study
GT2829	Δ <i>tdk</i> <i>BT3172-HACLEAN</i> Δ <i>BT0346</i>		This study
GT3495	Δ <i>tdk</i> <i>BT3172HACLEAN</i> <i>BT1758</i> :: <i>pKNOCK-ermGb</i> :: <i>BT1758KO</i>		This study

GT4051	<i>Δtdk ΔBT0346 att-1::pNBU2-ermG-TetR-P1T_DP-GH023-dCas9-PBt16s-sgRNA-SpeI</i>		This study
GT4053	<i>Δtdk ΔBT0346 att-1::pNBU2-ermG-TetR-P1T_DP-GH023-dCas9-PBt16s-sgRNA-BT1986-2</i>		This study

Table 3-2. Oligonucleotides used in this study

Identifier	Name	Sequence (5' → 3')	Purpose
1987	pUHE-BT0307f	AATTA ACTATGAGAGGATCC ATGACTAAAAGTGCATTGCA AATCGC	Constructing a plasmid to inducibly express <i>BT0307</i> in <i>E. coli</i>
1988	pUHE-BT0307r	TCCAAGCTCAGCTAATTAAG CTTATTTAGCTTGTTCCAATT GCAAAGTC	
1989	pUHE-BT3356f	AATTA ACTATGAGAGGATCC ATGAGAATTGGAATCCTGAC TTCCG	Constructing a plasmid to inducibly express <i>BT3356</i> in <i>E. coli</i>
1990	pUHE-BT3356r	TCCAAGCTCAGCTAATTAAG CTTAACCGAAACAAATCCCC ATGC	
1991	pUHE-BT1102f	AATTA ACTATGAGAGGATCC ATGGATAACAAGTATATTGG AATTCTGACTTC	Constructing a plasmid to inducibly express <i>BT1102</i> in <i>E. coli</i>
1992	pUHE-BT1102r	TCCAAGCTCAGCTAATTAAG CTTAGATCGATAATTCGTTA AGGACCCG	
1993	pUHE-BT2062f	AATTA ACTATGAGAGGATCC ATGGGAACAGTTAAATGTAT CGGTATT	Constructing a plasmid to inducibly express <i>BT2062</i> in <i>E. coli</i>
1994	pUHE-BT2062r	TCCAAGCTCAGCTAATTAAG CTTATATAGAAAGTTCTTTCA ATACATTGACCAGATC	
2511	pUHE-MG1655-pfkAf	AATTA ACTATGAGAGGATCC ATGATTAAGAAAATCGGTGT GTTGACAAGC	Constructing a plasmid to inducibly express <i>Ec pfkA</i> in <i>E. coli</i>
2512	pUHE-MG1655-pfkAr	TCCAAGCTCAGCTAATTAAG CTTAATACAGTTTTTTTCGCG CAGTCC	
1044	qBt16sF	GGTAGTCCACACAGTAAAC GATGAA	Measuring 16s rRNA transcript levels from <i>Bt</i> by qPCR
1045	qBt16sR	CCCGTCAAATTCCTTTGAGT TTC	
1050	qBT2167f	AAAACGTCGCGGATCTGTT G	Measuring <i>fusA2</i> transcript levels from <i>Bt</i> by qPCR
1051	qBT2167r	TGGAGAACGGTAGAGAAAA CGG	
1876	qBT1986f	AAAGCGGATTCACGAAGAG C	Measuring <i>rpiA</i> transcript levels from <i>Bt</i> harboring a CRISPRi plasmid by qPCR
1877	qBT1986r	TGCCAGTTGTATGCAAGTC	
1479	dBT0346_5f	GCTCTAGAACTAGTGGATCC TCACTTCACGGTGGTGTGAT C	Generating a deletion of <i>BT0346</i> in its chromosomal locus in <i>Bt</i> .
1480	dBT0346_5r	TTAAATCATTGCTTTTACCTG ATTATATACGTTCTC	
1481	dBT0346_3f	AAAGCAATGATTTAATGCCT	

		GAAAATCTATAAAAATAAGG TGGAA	
1482	dBT0346_3r	AAGATAACATTCGAGTCGAC GATGTCCGGTTAGGGATTG GT	
1483	dBT0346_UP	CAAGAAGGGCGATTTTCAGC G	
1484	dBT0346_DOWN	CAAATGCCTGCTAGTGGGA TT	
1592	pEXC:dBT1986_5f	CTCTAGAACTAGTGGATCCT TGTCTTTCCGGTTACTCCAA TGG	Generating a deletion of <i>BT1986</i> in its chromosomal locus in <i>Bt</i> .
1593	pEXC:dBT1986_5r	GGTTCTTGCAGTTTTAGAGT CTCTATTTAT	
1594	pEXC:dBT1986_3f	CTCTAAAACGCAAGAACCA AACCAAGCATAGCACATAG GAAAATC	
1595	pEXC:dBT1986_3r	AGATAACATTCGAGTCGACG GGATTGTAGTAGGCGTCGG	
1596	dBT1986_UP	CGTGCTATCCTCAGCGCAA	
1597	dBT1986_DOWN	TCCTTGATCAGGTTGGTCAA CG	
1598	pEXC:dBT3946_5f	CTCTAGAACTAGTGGATCCC TTTTCGTATGTTGCCGGAGG	
1599	pEXC:dBT3946_5r	CATTCTATTGTTTTAAGTTCT AAGTTAGCTTGACC	
1600	pEXC:dBT3946_3f	AACTTAAAACAATAGAATGC GGACACATTGAATACTGCCT C	
1601	pEXC:dBT3946_3r	AGATAACATTCGAGTCGACT TAAATCGGTCTTCTCACCCA CG	
1602	dBT3946_UP	TGTGCAGGCACTTCGTGAG	
1603	dBT3946_DOWN	CGGATAGAGCCAAGACATG ACT	
2077	pKO-BT1758f	CGCTCTAGAACTAGTGGATC CAGAAAACCGTGTTACTCAG TTTGATCG	Generating an inactivation of <i>BT1758</i> in its chromosomal locus in <i>Bt</i> .
2078	pKO-BT1758r	GGGCCCCCCTCGAGGTCG ACAAATAACAGAGAACACAT TCGAGTTACC	
2378	sgRNA-BT1986_2f	GCTAAAAGTTCTTATCTTTG CAGTATAATCTCATTGGACC ATTG	Generating an sgRNA of <i>BT1986</i> to insert into CRISPRi plasmid.
2379	sgRNA-BT1986_2r	ACTTGCTATTTCTAGCTCTA AAACCAATGGTCCAATGAGA TTAT	
2354	P16s_f	AATCCTAGCACCTGCAGC AGTACTGCTTGACCATAAGA AC	Generating the <i>16s rrs</i> promoter from <i>Bt</i> for CRISPRi plasmid
2355	P16s_r	GCTATTTCTAGCTCTAAAAC ACTAGTACTGCAAAGATAAG	

		AACTTTTAGCTT	
2356	sgRNAscaf_f	GTTCTTATCTTTGCAGTACT AGTGTTTTAGAGCTAGAAAT AGCAAGT	Generating the sgRNA scaffold from <i>S. pyogenes</i> for CRISPRi plasmid.
2357	sgRNAscaf_r	CACTGGAAGATAGGCAATTA GTCGACAAAAAAGCACCGA CTCGGTG	

CHAPTER 4: RESEARCH SUMMARY AND DISCUSSION

Summary

The work detailed in this dissertation has established the foundation of CCR in *Bacteroides* species by identifying key players in this mechanism. A global transcription factor, widely distributed throughout *Bacteroidetes* governs carbohydrate utilization factors and translation elongation factor, EF-G2. Using genetics, we identified that Cur also regulates synthesis of colonization factor, Roc albeit indirect. Dietary sugars silence the production of Roc, EF-G2, and a host-microbial interaction mediator protein, BT4295 (Fig. 2-1B, 2-4D and C-7B) (306, 325). We now know this is achieved via silencing of Cur activity by dietary sugar consumption. *Bacteroidetes* do not encode CcpA, HPr, or PTS systems by which co-resident Proteobacteria and Firmicute species use to achieve CCR and preferential nutrient utilization. However, *Bacteroidetes* do exhibit preferential carbohydrate utilization in mixtures suggesting a mechanism of CCR exists but is the components remain unknown. Cur shares many of the same intracellular functions with that of Crp which governs CCR in Proteobacteria suggests that Cur is a critical component in *Bacteroides* CCR. Further, mutants identified in the PPP reduce Roc synthesis indicative of reduced Cur activity. As such, we hypothesize that perturbations in PPP intermediates through dietary sugar modulating carbon metabolism and exerting CCR modulate the production of a Cur activating signal.

To elucidate the Cur activating signal, I employed reverse genetics to elucidate steps within central carbon metabolism that are required for Cur activity and potentially producing the activating signal. I identified that the metabolism of fructose is important to governing Cur silencing and as such hypothesized that the activating signal likely originates from metabolism. My initial investigation down the EMP revealed that one specific PfkA, when inactivated, increased Cur activity (Fig. 3-1) suggesting that carbon flow through the PPP rather than the EMP drives activity. Consistent with this notion, inactivation of individual oPPP steps reduce Cur activity highlighting the importance of the PPP in Cur activation (Fig. C-2). Further investigation into the PPP revealed two Rpi enzymes, of which the bi-directional RpiB coordinates with PfkA to modulate Cur as inactivating both genes decreases Cur activity (Fig. 3-2). Overall, these data are consistent with the notion that carbon flow through the PPP drives the production of an activating signal to govern Cur activity.

Limitations and future perspectives

My work in Chapter 2 identified that Roc synthesis is governed by Cur however the regulation occurs indirectly because Cur does not directly bind to the *roc* promoter region (Fig. 2-3). Further, regulation of Roc synthesis by dietary sugar, which also silences Cur, requires the *roc* mRNA leader. While we were unable to determine the identity of what lies between active Cur and Roc synthesis, we identified EF-G2, the number one target of active Cur and a logical intermediate due to its regulation of translation, is not required for Roc synthesis

leading to further investigation of Cur regulated targets. Additional Cur regulated PUL genes *BT4299-4295*, putative methylmalonyl-CoA biosynthetic genes *BT1450-1448*, and a conserved hypothetical protein *BT2131* are all dispensable for Roc synthesis. Further, Cur dependent sRNAs, *BTnc140*, *BTns195*, and *BTnc364* were assessed for a potential role in Roc synthesis. These three sRNAs were selected due to their increased transcription in carbon limitation, a Cur activation condition, proximity to Cur binding sites, and complementarity to the *roc* leader. All three sRNAs were dispensable for Roc synthesis. Overall, I identified that active Cur is required for Roc expression and that this is achieved indirectly.

Our approach is biased in assuming there is only one unknown factor in this mechanism. One important limitation in identifying the intermediate factor is that multiple factors could be required for this mechanism to take place. For example, Cur could be driving transcription of another transcription factor which then produces the intermediate factor required for Roc synthesis. To address this, it would be beneficial to scour ChIP-seq data for Cur-bound known transcription factors and assess their requirement for Roc synthesis. Though, the factor(s) we aim to identify could be uncharacterized at this time requiring further investigation into putative proteins. Additionally, we have only looked at Cur-dependent proteins and sRNAs sharing complementarity to the *roc* leader sequence. One avenue yet to be explored is the *roc* mRNA leader interacting with an RNA binding protein (RBP) which are also an emerging concept of CCR in *Bacteroides*. RBPs could regulate translation by inducing conformational

changes of mRNA or possibly facilitate sRNA binding (338). Both mechanisms have the potential to block ribosomal access or alter mRNA stability. Currently, these proposed mechanisms both aim to inhibit translation and we are seeking a mechanism which activates translation of *roc* mRNA making this avenue less attractive.

My work in Chapter 3 highlights the importance of elucidating discreet metabolic steps to identify the mechanism by which Cur activity is modulated. I have demonstrated that importation and metabolism of fructose are required for silencing of Cur, however these two steps have not been addressed for glucose. Since the mechanism in which *Bt* imports glucose into the cell is unknown, reverse genetics cannot be employed to inactivate specific genes required for importation or metabolism of glucose. However, this could be partially addressed biochemically rather than genetically by using 2-deoxyglucose (2-DG), which in *Bacteroides*, can be phosphorylated but cannot be metabolized (382, 383). By introducing 2-DG to cells rapidly growing in a Cur-activating carbon source like PMOG, the requirement of glucose metabolism can be assessed. I hypothesize that fructose and glucose act through similar mechanisms to silence Cur, achieved through the EMP. If glucose is required to be metabolized to silence Cur activity, then Cur will remain active even when 2-DG is added whereas the addition of glucose silences Cur.

If an Rpe knockdown also reduces Cur activity, then Ru5P should be further investigated for any direct effect on Cur or other potential unannotated destinations for this metabolite. Prs generates PRPP from Ri5P and due to the

role of RpiA and RpiB on Cur activity, the signal could be derived from Ri5P, however this is less likely due to the requirement of *rpiB* in carbon starved Cur activation. Tkl is more challenging to elucidate as it performs two metabolic steps. Thus, if a Tkl knockdown reduces Cur activity, then several metabolites would need to be investigated including xylulose-5-P, sedoheptulose-7-P, erythrose-4-P, and glyceraldehyde-3-P. In addition, transcription of transaldolase, converting sedoheptulose-7-P and glyceraldehyde-3-P to erythrose-4-P and fructose-6-P, is increased 3.4-fold in carbon starvation compared to glucose-grown cells indicating an increase in activity is required during carbon starvation (331). Importantly, increases in these metabolites also lead to increases in amino acid biosynthesis which would be required for bacteria to maintain colonization or even expanding abundance in the gut. Therefore, I hypothesize that a Tkl knockdown will reduce Cur activity by reducing downstream metabolites solidifying that Ru5P derivatives are likely serving as the activating signal. Silencing of Cur activity can also be further investigated through the EMP by using CRISPRi to target aldolase which converts FBP to glyceraldehyde-3-P and DHAP. If Cur activity increases, then this suggests that carbon flow through the EMP exerts silencing of Cur. However, a decrease of Cur activity suggests FBP could act as an inhibitory signal for Cur. Together, the flow of carbon through central metabolism governs the activity of Cur via through directly generating a signal or modulating the ratio of metabolites governing additional factors. It is necessary to elucidate how this mechanism works to better understand how Bacteroidetes survey the environment for nutrients and select the more preferred

substrates which provide them with a fitness advantage over neighboring microbes. Further studies are required to identify key factors in this mechanism to provide targets for future therapeutic approaches to manipulate microbial abundance in the gut.

One major question that still remains is what portions of Cur are required for function and if binding is even necessary for activity in all cases. Currently, Cur is annotated as having an N-terminal DNA binding domain and a C-terminal putative ligand binding domain. However, little work has been done to characterize these regions, and furthermore, to determine essentiality of these regions for function on downstream genes. To address this, the regions of Cur should be swapped out with that of another transcription factor. Once either region is swapped, Cur activity can be measured. If one or both regions are required for Cur activity, then Cur will no longer be active with the required region swapped. This will determine if ligand binding and/or binding to target DNA is needed for Cur-target transcription. Additionally, scanning mutagenesis can be used to pinpoint which amino acids are essential for Cur activity. This will provide insight into not only the regions essential for activation but could also provide insight into how to make a constitutively active Cur to be used in future experiments.

The ideal goal of manipulating the Cur mechanism is to develop a novel probiotic-type therapeutic in which *Bacteroides* can colonize in an environment where Cur would generally be inactive causing a loss of fitness for *Bacteroides*. To reach this point, many *in vivo* studies need to be performed to ensure this

constant expression of Cur is 1) not lethal to the bacteria, 2) not lethal to the host, 3) provides the increase in fitness I hypothesize based on the data I have generated, and 4) has a lasting effect on the microbiota. I hypothesize that increasing Cur activity will allow *Bt* to produce a persistent relationship with the host and by doing so, lead to increased microbial diversity in microbiotas with otherwise lower diversity such as microbiotas associated with both UC and CD (64-66). Furthermore, immunomodulatory activities performed by *Bacteroides* species would benefit the host by providing reduced inflammatory responses (67). Moreover, Cur modulation may allow *Bacteroides* to outcompete other organisms such as the increase of Firmicutes often associated with obesity to better balance bacterial abundance and metabolically produced products in the gut (75, 76).

To address the studies needed to understand the use of a constitutively active Cur, cells could be grown in both Cur-activating (rhamnose or galactose) and Cur-silencing conditions (glucose or fructose) and measure cell growth *in vitro* to ensure a constitutively active Cur is not lethal to the bacteria. This strain could then be monitored in monoculture in germ-free mice fed either a standard diet or high sugar diet to ensure successful gut colonization on its own. It should then be competed against a wild-type strain *in vivo* using both a standard diet and high sugar diet to measure the anticipated increase in fitness as I hypothesize the constitutively active Cur strain would outcompete the wild-type *Bt* strain in both diets. This should further be tested in germ-free mice using a synthetic bacterial community that includes the constitutively active Cur strain

and monitor this microbiota over time in both a standard and high sugar diet. I hypothesize that the Cur strain will remain relatively stable over time in both diet cohorts. Importantly, a Cur strain must not outcompete other strains such that it becomes the sole organism in the gut as diversity is incredibly important for gut microbiota health. These studies will establish the function of *Bt* with a constitutively active Cur *in vivo*, with further implications for use in the phylum as a whole.

The current studies linking microbiota dysbiosis to disease states are all based on association rather than causation as there are an incredibly number of factors which govern the state of the microbiota as well as human health, most of which overlap (diet, environment, genetics, and age to name a few). Furthermore, what is deemed a “healthy” gut microbiota varies between individuals making a one-size-fits-all therapeutic approach unlikely. However, by generating synthetic bacterial communities that mimic those seen in specific intestinal conditions, the effects of constitutively active Cur can be addressed. For example, while CD and UC present differently in the gut, both have been associated with depleted Firmicutes and Bacteroides species (64). By generating synthetic bacterial communities with lower abundance of these notable members of the microbiota along with constitutively active Cur, the microbiota can be monitored for alterations from a dysbiotic state back to a healthier, homeostatic, and diverse microbiota. Importantly, if restoration of the gut occurs, this does not necessarily mean disease resolution. Since it is not currently known whether gut dysbiosis is a cause of disease or an unfortunate effect of disease development,

this therapeutic is not likely to be a cure-all but to be used alongside other disease modulators providing two points of therapy. If dysbiosis is caused by disease, then modulation of the microbiota would likely not last due to the constant pressure placed on it by the disease. Conversely, if dysbiosis causes disease, restoration of a more balanced gut microbiota may not address damage already caused by disease which may continue to produce symptoms. Given the ethical impact of providing potentially dangerous biological materials to humans, and the lack of animal models that natively develop human diseases, there are currently no models to definitively determine whether disease or dysbiosis is the causative agent.

In conclusion, the research described here will contribute to the advancement of novel therapeutics targeting the gut microbiota. Moreover, understanding how sugars are metabolised and effect gut microbes will allow for further studies on how nutrients impact healthy microbiotas. Overall, these data provide insight into how beneficial organisms colonize, establish a persistent relationship, and can potentially be manipulated within a human host.

APPENDIX A: HARNESSING GUT MICROBES FOR GLYCAN DETECTION AND QUANTIFICATION

Appendix A highlights my contributions to a previously published paper (Modesto et al., 2023, Nature Communications). The text has been reformatted for this dissertation.

Introduction

Microbes comprising the gut microbiota have evolved systems of machinery specific to the degradation of glycans present in the gut (384). These unique gene clusters are known as polysaccharide utilization loci (PULs) in the abundant bacterial group *Bacteroides* (260, 333, 385). PULs encode proteins required for binding, transportation, and depolymerization of glycans with both glycan and species specificity. For example, *Bacteroides thetaiotaomicron* (*Bt*) encodes 88 different PULs to facilitate glycan consumption (260, 333). One *Bt* PUL is designated to degrade levan, a β 2,6-linked polyfructan which is inaccessible to a closely related species *Bacteroides ovatus* (*Bo*) (270, 386). However, one of 112 *Bo* encoded PULs can access inulin, a β 2,1-linked fructan, whereas *Bt* is incapable of degrading this glycan showcasing the specificity of these co-ordinately regulated genes (270, 386).

Glycan detection has numerous challenges including cost, sensitivity, and specificity. Since PULs contain specific sensor proteins, expressed constitutively

at low levels, we hypothesized that *Bacteroides* sensor proteins could be harnessed for glycan detection by way of transcriptional response upon glycan sensing. Traditional transcription measurements rely on assays like microarrays, RNAseq, and qPCR or reporters like luciferase and GFP which require oxygen to fold properly and report accurately (260, 270, 273, 284, 330, 377, 378, 387). As such, we developed a luciferase reporter which can be utilized in *Bacteroides* during anaerobic conditions which accurately reflects transcription based on specific glycan sensing. Here, I report my contributions to the development of this anaerobic luminescence reporter, *pBolux*.

Results

PUL reporters confer dose-dependent *susC* transcription

PULs encode a *susCD*-like gene pair required for translocation of target glycans through the membrane(260, 333, 345, 386, 388). When the target glycan is present, the transcription of these genes quickly increases (270, 332, 354). To determine whether *susC* transcripts increase in a concentration-dependent manner, defined quantities of glycan were supplied to *wild-type Bt* and the resulting *susC* expression was measured. Utilization of chondroitin sulfate (CS) requires *BT3332* whereas levan utilization requires the *BT1763* (270, 354). When CS was supplied in ten-fold dilutions for 2 hours, *BT3332* expression correspondingly decreased (Fig. A-1A). This same concentration-dependent response was exhibited by *BT1763* when supplied ten-fold dilutions of levan for 2

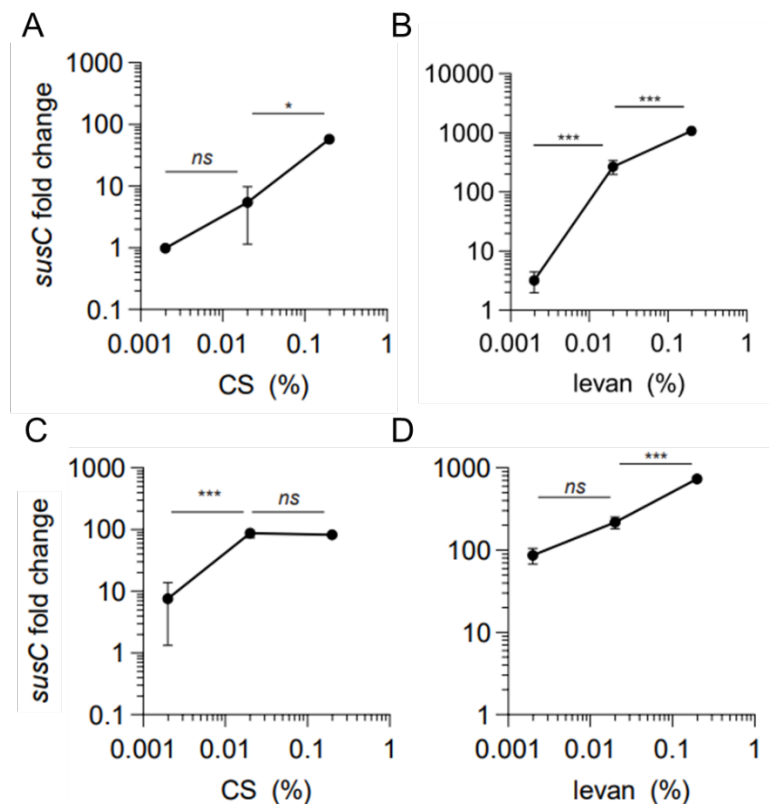


Figure A-1: PULs exhibit dose-dependent transcriptional responses. a-d The fold increase of (a&c) BT3332 or (b&d) BT1763 mRNA levels in wild-type *Bt* following the introduction of mixtures containing either 0.2%, 0.02%, or 0.002% (a&c) CS or (b&d) levan supplemented with galactose to 0.5% total carbohydrate. The fold increase was calculated as the change in transcript levels between cultures before and after (a&b) 2 hours or (c&d) 1 hour following induction of glycan mixtures. Values are the mean of 6 independent measurements, error bars represent SEM, and P-values were calculated by 2-way ANOVA with Tukey's honest significance test and *** represents values < 0.001, * < 0.05, and ns indicates values > 0.05.

hours (Fig A-1B). Importantly, this response is also time dependent as addition of either glycan for only 1-hour exhibits differing expression levels of either *susC* (Fig A-1C and A-1D). These data demonstrate that not only is PUL transcription dose-dependent, but it is also time dependent demonstrating the need for a real-time transcriptional reporter.

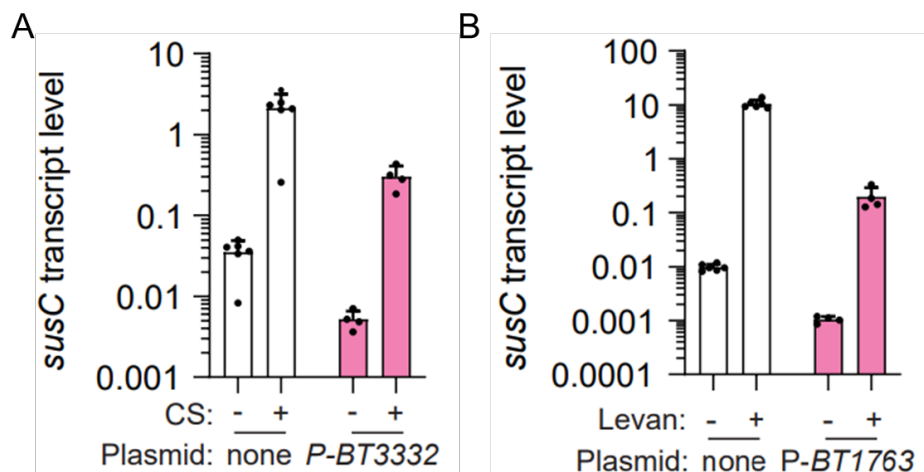


Figure A-2: *pBolux* reporter does not inhibit transcription. a&b. *susC* transcript levels of BT3332 (a) or BT1763 (b) in wild-type *Bt* strains without a plasmid (open bars) or harboring P-BT3332 (a) or P-BT1763 (b) grown in galactose or a mixture of galactose and target glycan. Values are the mean of 6 (no plasmid) or 4 (P-BT3332 or P-BT1763) measurements and error bars are standard deviation.

***pBolux* reporter does not inhibit typical glycan-responsive transcription**

The *pBolux* reporter utilizes the promoter region upstream of *susC* to drive transcription of luminescence genes upon target glycan detection. To determine whether *pBolux*, which is a multi-copy plasmid does not interfere with native transcription upon glycan introduction, *susC* expression was measured in strains harboring the *pBolux* compared to a strain with no plasmid. We measured *susC* transcription in the presence of absence of CS when the BT3332 promoter is present in *pBolux* (P-BT3332). While *susC* expression is overall reduced in the strain harboring P-BT3332, the same dramatic increase in transcription is present when grown in CS (Fig. A-2A). When *pBolux* includes the BT1763 promoter (P-BT1763), there is an overall reduction in *susC* transcript but an identical increase in transcript level is demonstrated when grown in levan (Fig. A-2B). Further, there was no growth deficit exhibited by these plasmid-harboring strains.

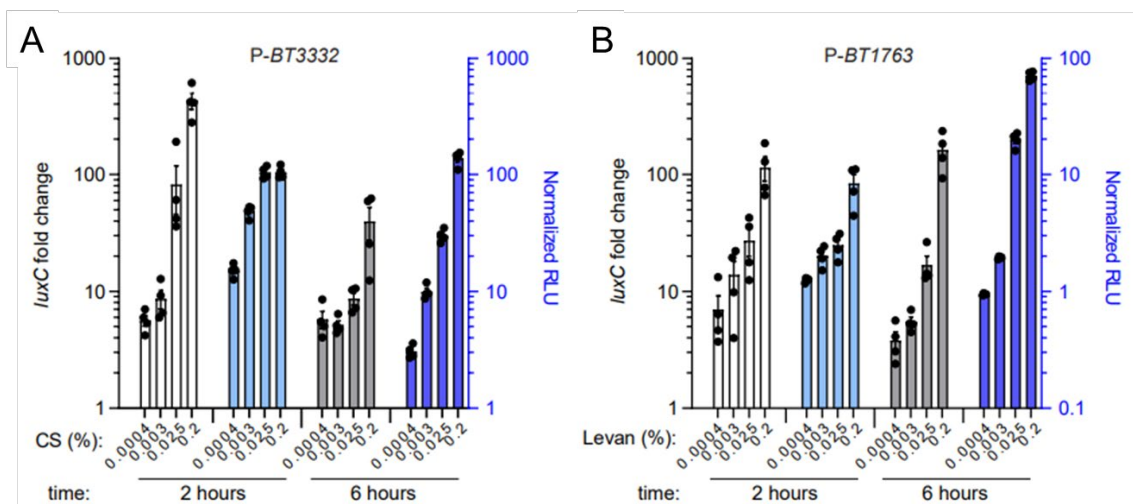


Figure A-3: PUL reporters confer dose-dependent *lux* transcription and activity. a&b. The fold increase in *luxC* transcript levels (open and gray bars, left Y-axis) and corresponding luminescence (blue bars, right Y-axis) from wild-type *Bt* strains harboring (a) P-BT3332 or (b) P-BT1763 after 2 and 6 hours following the introduction of decreasing concentrations of either (a) CS or (b) levan containing galactose to a total carbohydrate content of 0.5% and normalized by identical cultures supplied galactose alone. Values are the mean of 4 independent measurements and error bars are SEM. Luminescence measurements and RLU normalization performed by J.L.M.

These data establish that the p*Bolux* plasmid reduces transcription of the native locus but does not inhibit glycan utilization.

PUL reporters confer dose-dependent *lux* transcription

To determine if *lux* gene expression is governed by the PUL promoter is dose dependent like PUL transcription itself, we measured *luxC* transcript levels when strains harboring p*Bolux* reporters were supplied CS or levan in decreasing concentrations. *luxC* levels were compared to the corresponding luminescence from the p*Bolux* when grown in identical conditions. Furthermore, measurements were taken at 2 and 6 hours after glycan addition as we have established transcriptional responses are time dependent. Luminescence and *luxC* expression both exhibited dose-dependent changes when supplied the

respective target glycan (Fig. A-3) demonstrating that luminescence is a reliable measurement of intracellular transcriptional activity based on glycan quantity.

Discussion

This work establishes a novel reporter system optimized for anaerobic bacteria, specifically *Bacteroides*. We demonstrate that PUL promoters exhibit dose-dependent transcription of downstream genes based on target glycan presence and abundance. Further, we establish *pBolux* reporter plasmids exhibits no off-target effects and allows for reliable native transcription in the cell. Finally, we demonstrate that luminescence expressed by cells harboring *pBolux* recapitulates *luxC* transcript abundance in both a dose- and time-dependent manner.

The generation of this unique reporter allows for quick and accurate detection and quantification of glycans. This also removes the necessity of kinetically sampling bacteria as reporter luminescence can be read during anaerobic growth over time. Further, these measurements require less materials than typical transcriptomics approaches such as qPCR. As such, the *pBolux* reporter is an incredibly beneficial tool for glycomics and gut microbial substrate analysis.

Materials and Methods

Bacterial culture

All *E. coli* strains were cultured on LB agar (BD) aerobically at 37 °C and inoculated from single colonies into LB media (BD) with agitation at 275 rpm. All

Bacteroides strains were cultured as previously described (325, 331) on brain-heart infusion agar (70138, Millipore Sigma) containing 5% horse blood (Hardy) anaerobically and inoculated from single colonies into TYG incubated under identical conditions. *Bacteroides* strains were sub-cultured at the indicated dilutions from stationary phase growth in TYG into minimal media containing the indicated carbon sources described in the corresponding figure legends. All strains were cultured in the presence of antibiotic selection where appropriate at the following concentrations: 100 µg/mL ampicillin, 2 µg/mL tetracycline, 25 µg/mL erythromycin.

Transcript quantification

mRNA was prepared from 1.0 mL of pelleted *Bt* cell culture treated with RNA protect (Qiagen) using the RNeasy kit (Qiagen) according to the manufacturer's directions. cDNA was subsequently synthesized from 500 ng of isolated RNA using Superscript VILO IV master mix (ThermoFisher) according to the manufacturer's directions. Transcript levels were measured by qPCR using PowerUp SYBR Green PCR Master Mix (Applied Biosystems) and primers 1060 and 1061 (*BT3332*), 1056 and 1057 (*BT1763*), or 2208 and 2209 (*luxC*) were monitored using a QuantStudio 12 K Flex instrument (Applied Biosystems). All mRNA transcripts were normalized as previously described (330) to 16 s rRNA measured from 1000-fold diluted cDNA using primers 1044 and 1045.

Statistics and reproducibility

No statistical method was used to predetermine sample size. Sample sizes were chosen based on the limits of the instrumentation to simultaneously measure multiple reactions in 384-well plates. No data were excluded from the analyses. The experiments were not randomized. The Investigators were not blinded to allocation during experiments and outcome assessment. All experiments were independently repeated at least twice. Microsoft Excel 365 was used to collect and compute gene expression data. Repeated measurements were analyzed by paired, two tailed student's t-test, 1-way, or 2-way ANOVA using GraphPad Prism 9.3.1 where appropriate as indicated in each figure legend.

Supplemental Tables

Table A-1. Strains used in this study

Name	Genotype	Plasmid	Reference
GT1867	Δtdk	<i>pBolux</i>	(344)
GT1893	Δtdk	<i>P-BT1763</i>	
GT1934	Δtdk	<i>P-BT3332</i>	

Table A-2. Oligonucleotides used in this study

Identifier	Name	Sequence (5' → 3')	Purpose
1044	qBT16s_f	GGTAGTCCACACAGTAAACGATGAA	Measure 16s rRNA levels using qPCR
1045	qBT16s_r	CCCGTCAAATTCCTTTGAGTTTC	
1060	qBT3332_f	TGGTTGTCGGCTATCAGGAAGT	Measure <i>BT3332</i> mRNA levels using qPCR
1061	qBT3332_r	ACATCTGCCATGTTGGCTTTC	
1056	qBT1763_f	AGCGTAAAGCCGACCTGACA	Measure <i>BT1763</i> mRNA levels using qPCR
1057	qBT1763_r	TCACCTTGCTTCTGGATTTTCG	
2208	qluxC_f	TGCGCCATCTTATGCTGATG	Measure <i>luxC</i> mRNA levels using qPCR
2209	qluxC_r	TGCGGACGTCAAATCAACAG	

Table A-3. Plasmids used in this study

Name	Description	Reference
<i>pBolux</i>	pLYL01 multi-copy vector harboring BamHI and SpeI sites upstream of the <i>Bacteroides</i> optimized lux cassette	(344)
<i>P-BT3332</i>	300 bp upstream of BT3332 were cloned into pBolux	
<i>P-BT1763</i>	300 bp upstream of BT1763 were cloned into pBolux	

APPENDIX B: GENERATION OF A GDNA LIBRARY IN *BACTEROIDES* *THETAOTAOMICRON*

Introduction

Our previous studies have identified loss-of-function mutants which exhibit lower Roc levels. One of the mutants identified was Cur but the regulation of Roc by Cur is indirect as Cur does not directly bind to the Roc promoter. Further, the additional mutations identified in the pentose phosphate pathway did not alleviate Roc synthesis entirely leading us to further investigate the PPP. In tandem, we have developed a novel gain-of-function genomic DNA library in *B. thetaiotaomicron* to identify genes that, when overexpressed, can modulate expression of target proteins. This complements the loss-of-function screen which cannot adequately address redundancy or essentiality of genes responsible for Roc expression.

Previous approaches to constructing a library in *Bacteroides* utilize fosmid vectors (389), cosmid vectors (390-392), and in general requiring an additional mobilizer strain, which is unnecessary with our design. A more recent approach uses sheared genomic DNA to generate a library and screens individual colonies in liquid culture requiring maintenance of a large number of strains at a given time (393). Our library was generated by whole genome amplification instead of sheared DNA allowing for a smaller starting genomic DNA sample. Furthermore, our library allows for screening on solid media before isolating strains of interest

rather than maintaining individual strains to be screened in liquid culture. This approach provided a way to screen for strains harboring fragments of *B. thetaiotaomicron* DNA to identify plasmids containing fragments of interest for further characterization.

Generation of the gDNA library

1. Establish the fragmentation method

First, we needed to identify the size of DNA fragments needed. *Bt* contains roughly 4800 annotated genes in 6.2 Mb and as such, we aimed for fragments of ≥ 5 kb to capture at least one gene in each fragment. To fragment the DNA, we first started by partially digesting wild-type genomic DNA with Sau3A1. This is a common digestion method as the 4-mer Sau3A1 sites are incredibly common throughout most genomic DNA and the sites are compatible with the 6-mer BamHI, a common site used to clone into plasmids. As Sau3A1 has 16,900 sites in the *Bt* genome, we started with short incubation times ranging between 30-seconds and 1 hour. Size selection after gel electrophoresis was employed to ensure only the appropriately sized fragments were included in the pool of DNA. Sau3A1 was combined with either Aval, SmaI, or StyI and partially digested in an attempt to produce more uniform fragments at the specified size. After identifying that the amount of DNA wasn't adequate in these reactions we employed GenomiPhi, which amplifies the entire genome using multiple strand displacement amplification.

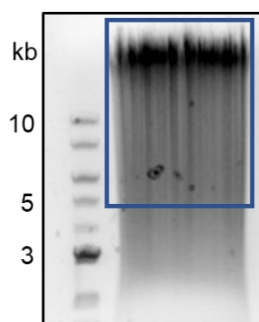


Figure B-1: Fragmentation of gDNA using GenomiPhi. Agarose gel containing GenomiPhi amplified gDNA which was size selected. Gel extraction boundaries indicated with the blue box containing fragments $\geq 5\text{kb}$.

After GenomiPhi, we attempted several different methods of fragmentation. First, Sau3A1 was used with partial digestion. Secondly, we mechanically sheared the DNA using Covaris g-TUBEs. The resulting DNA was subjected to gel electrophoresis and size selection. However, GenomiPhi already generates varying sizes of fragments and as such we electrophoresed the GenomiPhi material, followed up by size selection, and generated fragments of DNA which would ligate into our ideal vector (Fig. B-1).

2. Determine the appropriate plasmid

Plasmids can be single or multi-copy and since our goal was to overexpress the gene(s) of interest, we elected to use a multi-copy plasmid, pLYL01. Initially, pLYL01 was simply cut with BamHI to accommodate DNA fragments digested with Sau3A1. When other restriction enzymes were introduced, pLYL01 was then cut with BamHI and Xba or Sall according to the cut site overlap. However, once identified that GenomiPhi material alone would be ideal for gDNA fragmentation and size selection, we needed to identify a way for pLYL01 to accept these fragments which have non-specific ends.

We used a Blunt II-TOPO vector in which topoisomerase I is covalently bound to the 3' end of the linearized vector and allows for blunt fragments to be cloned in. Since the TOPO vector cannot be maintained in *Bt*, we still needed to move the fragments into pLYL01. As such, the fragments of interest were cloned from the TOPO vector using NotI and FseI and ligated into a modified pLYL01 cut with the same enzymes using NEBuilder.

3. Moving the library into appropriate *Bt* background

The final step in library generation is identifying the background in which to introduce the library to adequately answer our main question. We initially introduced the library into *wild-type Bt* with a chromosomal HA-tagged *roc*. While this background worked well with the library, colony selection was clouded by the low level of Roc production in all strains due to Cur activation (Fig B-2A). To overcome this, we introduced the library into *Bt* with a deletion of *cur*, an HA-tagged *roc*, FLAG-tagged *fusA2* which could be used as an alternate screening protein. This background then enhanced the contrast between colonies which produce high levels of Roc and those which do not (Fig. B-2B).

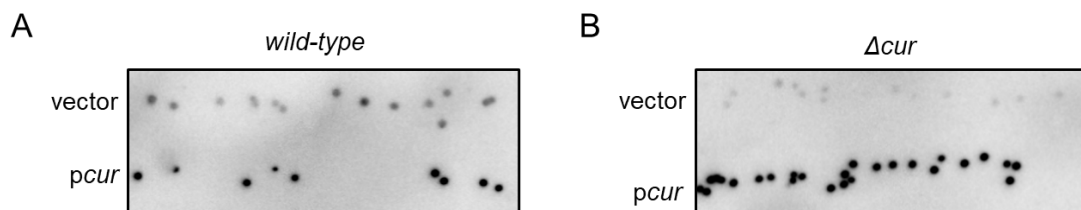


Figure B-2: Identifying appropriate *Bt* background. (a & b) colony blots of wild-type (a) or Δcur (b) harboring either a vector control plasmid or pLYL01 plasmid containing *cur*. Blots were probed with anti-HA antibody.

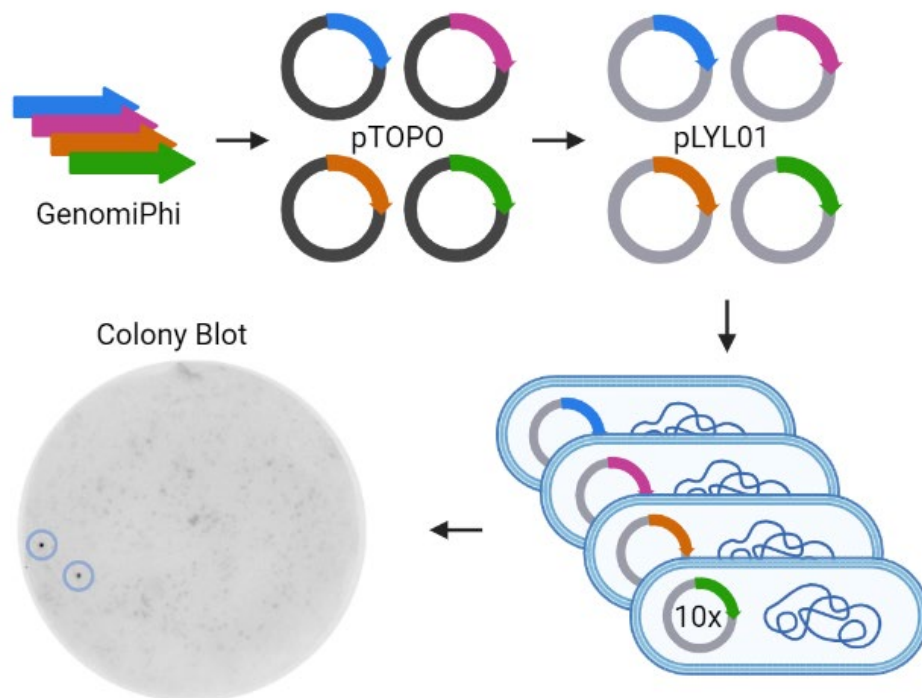


Figure B-3: Model for gDNA library generation. DNA was first amplified using GenomiPhi before size selection of ≥ 5 kb fragments. Fragments were inserted into Blunt II-TOPO. After digestion with FseI and NotI, fragments were maintained in pLYL01. After library introduction into Bt with a *cur* deletion, HA-tagged Roc and FLAG-tagged *fusA2*, colony blotting was performed on rhamnose and galactose containing media. Representative colony blot with two selected colonies indicated with blue circles. Figure generated using BioRender.

4. Identify fragments expressing increased Roc

Once the final gDNA library had been constructed and introduced into the *cur* deletion background, we screened 40,000 colonies using colony blotting on rhamnose and galactose containing media which typically generates high Roc levels when *cur* is present (Fig. B-3). After colony blotting, selected colonies were isolated and secondarily screened (Fig B-4A). First, plasmids were purified from the selected colonies and then were digested using FseI and NotI to verify a fragment had been indeed inserted into the plasmid. Interestingly, very

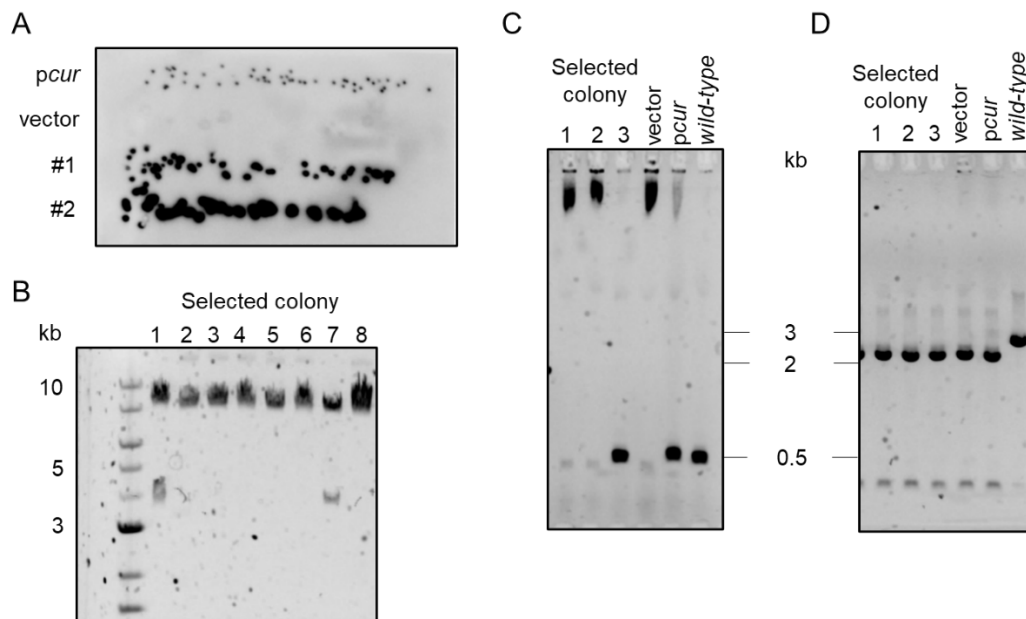


Figure B-4: Identify fragments expressing increased Roc. (a) Representative colony blot with 2 selected strains expressing increased Roc compared to vector control or a plasmid containing *cur*. (b) Representative gel of plasmids isolated from selected strains digested with *FseI* and *NotI* with only colonies 1 and 7 containing fragments. (c) Representative gel of PCR to amplify *cur* ORF run on selected colonies using primers 1941 and 1432. (d) Representative gel of PCR to amplify across Δcur chromosomal locus using primers 1423 and 1424.

few showed visible inserts after electrophoresis (Fig B-4B). However, we determined via PCR that two selected colonies contained *cur*, but it seemingly was not contained within the plasmid nor within the *cur* chromosomal locus (Fig B-4C & B-4D).

Other selected colonies also exhibited the same conundrum where there was a noticeable difference in Roc production, a plasmid contained within the cell, yet no sizeable or identifiable insert within the plasmid. To further investigate these colonies of interest, we obtained PacBio sequencing on them to determine if gDNA fragments somehow inserted into the genome rather than being maintained on the plasmid. Unfortunately, these sequences did not help us to

identify any insertions as any reads containing gDNA fragments mapped to the chromosomal locus of the genome or were excluded clouding any differentiation as to an alternate location.

This led us to send colonies of interest for RNAseq to identify if there are any alternatively regulated RNAs which could be driving Roc expression. We have identified increased transcription in two conserved hypothetical proteins, *BT3886* and *BT1784* which correspond with increased binding by Cur when active in ChIP-seq (331). Further, these have undergone whole genome sequencing to assess any potential insertions or mutations generating high Roc production.

Discussion and Future Directions

The goal of this gDNA library is to identify the gene or genes responsible for Roc synthesis after Cur activation. We have identified 3 strains which consistently express Roc in the absence of *cur* suggesting they contain the gene(s) necessary for this production. Further analysis of the RNAseq and whole genome sequencing data will lead to gene targets to inducibly express and determine Roc production. We hypothesize that one of these genes of interest will be the intermediate factor between active Cur and Roc synthesis. As two conserved hypothetical proteins identified also have increased Cur binding during carbon starvation, these two are ideal starting candidates. Importantly, sRNAs were not enriched for in the RNA-seq protocol and as such bias this approach which may be overcome with whole genome sequencing. Preliminary inducible

expression experiments with these two genes in a *cur* deletion background are inconclusive as the single copy plasmid used does not express enough Roc even when containing the complimentary *cur* ORF. As such, further experiments should include inducible overexpression of candidates in inducible multicopy plasmids.

Materials and Methods

Final construction of *B. thetaiotaomicron* genomic DNA library.

Wild-type *B. thetaiotaomicron* was subjected to whole genome amplification using GenomiPhi (Cytiva) according to the manufacturer's instructions. The amplified DNA was fractionated by agarose gel electrophoresis and fragments >6kb were purified from the gel using a QIAquick Gel Purification Kit (Qiagen). DNA fragments were then cloned into Blunt II-TOPO using the Zero Blunt TOPO PCR Cloning Kit for sequencing (Invitrogen) and maintained in competent *E. coli* cells. The resulting plasmid was purified and digested using FseI and NotI and the gDNA fragment was subsequently cloned into a modified pLYL01 containing FseI and NotI sites using NEBuilder HiFi DNA Assembly (NEB) and maintained in competent *E. coli* cells. A di-parental mating was carried out with gDNA library and *B. thetaiotaomicron* with an HA-tagged roc, FLAG-tagged fusA2 and a deletion of BT4338 (GT2873).

Colony Blotting

One aliquot of the *Bt* library described above was thawed, diluted, and spread onto 150 mm petri dishes containing solid minimal media containing

0.25% galactose and 0.25% rhamnose such that each plate contained approximately 1,000 colonies. Plates were incubated anaerobically for 48 to 72 hours until colonies were readily visible by eye, transferred to nitrocellulose membranes, and immunoblotted as previously described.⁽³²⁵⁾ Selected colonies were isolated on solid BHI-B prior to cryo-preservation.

RNA-seq

Five milliliters of bacterial culture were collected from triplicate cultures growing exponentially in minimal medium containing glucose ($OD_{600} = 0.45$ to 0.6). Cell pellets were immediately frozen on dry ice and stored at -80°C . The mRNA was stabilized by treatment with 5 mL of RNAprotect (Qiagen) diluted 2 to 1 prior to extraction using the RNeasy minikit (Qiagen) with on-column DNase I treatment. The eluates were treated with Turbo DNase (Invitrogen) for 30 minutes before a subsequent round of purification using the RNeasy minikit. RNA-seq was performed by Azenta and included an rRNA depletion step.

Supplemental Tables

Table B-1. Strains and plasmids used in this study

Name	Genotype	Plasmid
GT22	<i>Wild-type Bt</i>	-
GT2873	<i>Δtdk BT3172-HACLEAN ΔBT4338 BT2167- FLAG::pKNOCK-ermGb</i>	-
gDNA library	-	pLYL01 [FseI+NotI] + gDNA fragments

Table B-2. Oligonucleotides used in this study

Identifier	Name	Sequence (5' → 3')	Purpose
1423	dBT4338f	GCCAGGTAGGAAATGAGAAAATGAC	Amplify across Δcur chromosomal locus
1424	dBT4338r	CCACGTAGGTGATACTTTATATGTCTGT G	
1941	pT7- BT4338_D10 f	AGAAGGAGATATACATATGGATATTT CGGAACCATTATCCGATTTGTTA	amplify <i>cur</i> ORF
1432	BT4338mut_r	TCAGCGATTCTGCCAGACG	

APPENDIX C: SUPPLEMENTAL INFORMATION FOR CHAPTER 2

Supplemental Figures

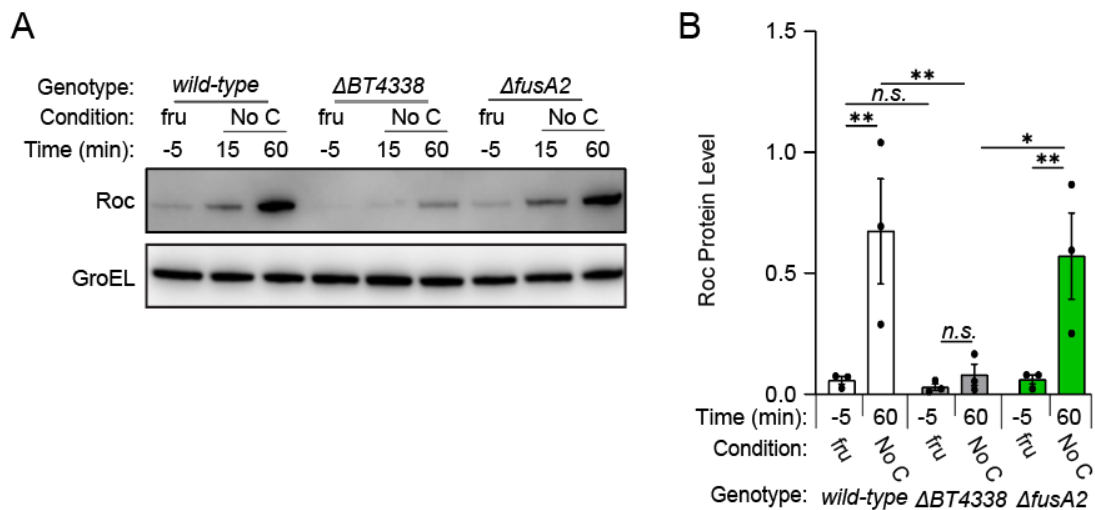


Figure C-1: *BT4338* is required for Roc synthesis through carbon limitation. (a) Western blot analysis of Roc amounts from wild-type (GT593) or *Bt* strains deficient for *BT4338* (GT1234) or *fusA2* (GT1310) during growth in glucose (*glu*; -5) or 15-, and 60-minutes following exposure to carbon limitation (No C). Blot probed for anti-HA and anti-GroEL. (b) Quantified western blot analysis of Roc from strains described in (a) during growth in fructose (*fru*; -5) or 60-minutes following exposure to carbon limitation (No C) ($n = 3$ biological samples; error bars represent SEM, P values derived from two-way ANOVA; *n.s.* indicates P values ≥ 0.05 ; ** < 0.01).

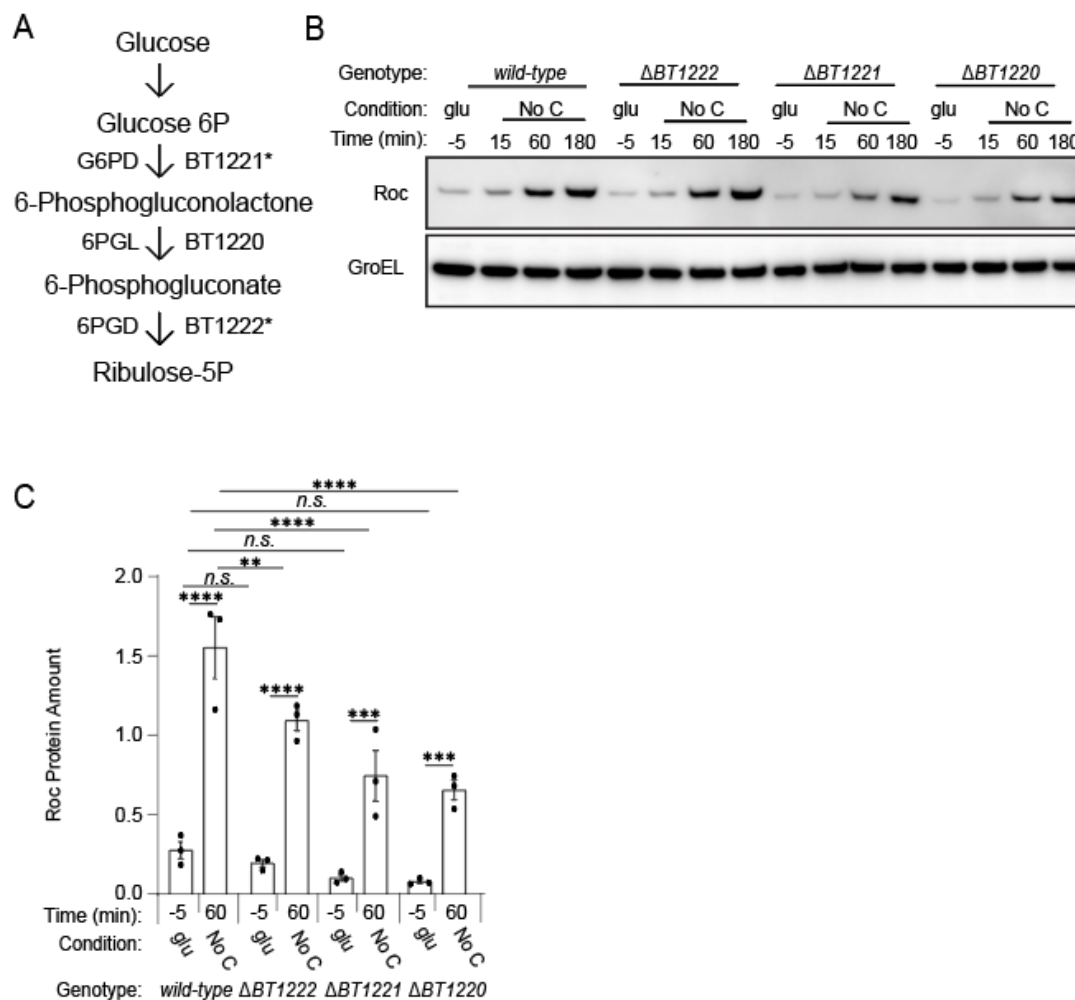


Figure C-2: Pentose phosphate pathway mutants exhibit reduced Roc amounts following carbon limitation. (a) Schematic of the oxidative pentose phosphate pathway with recovered loss-of-function mutants indicated with *. (b) Western blot analysis of Roc from wild-type *Bt* (GT426) or strains deficient for BT1222 (GT2727), BT1221 (GT2728), or BT1220 (GT2729) during mid-exponential growth in glucose (glu; -5) or 15, 60, and 180-minutes following exposure to carbon limitation (No C). Blots were probed with anti-HA and anti-GroEL antibodies. (c) Quantified western blot analysis of strains described in (b) during mid-exponential growth in glucose (glu; -5) or 60-min following exposure to carbon limitation (No C) ($n = 3$ biological samples error; bars represent SEM, P values derived from two-way ANOVA; n.s. indicates P values ≥ 0.05 ; ** $P < 0.01$; *** $P < 0.001$; **** $P < 0.0001$).

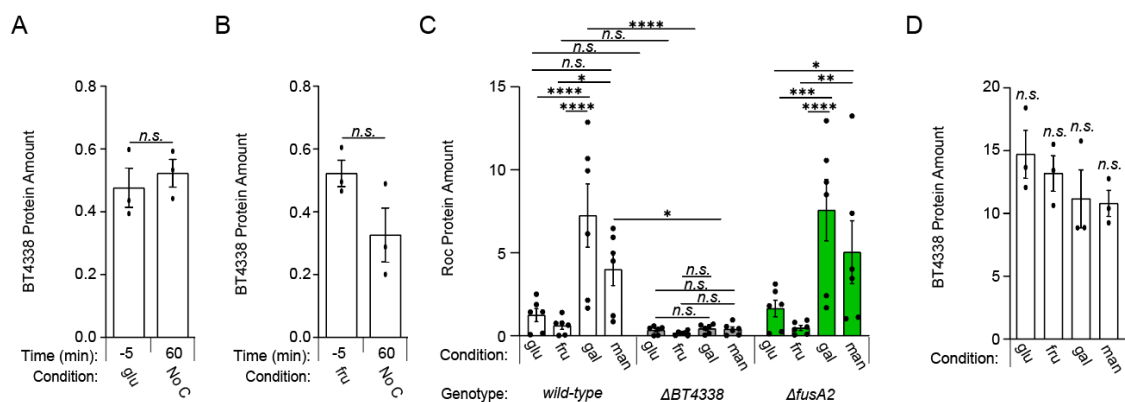


Figure C-3: Carbon limitation and various carbon sources change BT4338 activity independent of protein amount. (a & b) Quantified western blot analysis of BT4338 from *Bt* strains expressing an epitope-tagged BT4338 (GT1481) during mid-exponential growth in (a) glucose (glu; -5) or (b) fructose (fru, -5) and after 60 minutes following exposure to carbon limitation (No C) from each condition ($n = 3$ biological samples; error bars represent SEM, P values derived from one-way ANOVA; n.s. indicates P values ≥ 0.05). (c) Quantified western blot analysis of wild-type *Bt* (GT593; white) or strains deficient for BT4338 (GT1234; gray) or *fusA2* (GT1310; green) during mid-exponential growth in 0.5% glucose (glu), 0.5% fructose (fru), 0.5% galactose (gal), or 0.5% mannose (man) ($n = 6$ biological samples; error bars represent SEM, P values derived from two-way ANOVA; n.s. indicates P values ≥ 0.05 ; * $P < 0.05$; ** $P < 0.01$; *** $P < 0.001$; **** $P < 0.0001$). (d) Quantified western blot analysis of BT4338 from a *Bt* strain expressing an epitope-tagged BT4338 (GT1481) during mid-exponential growth during growth in 0.5% glucose (glu), 0.5% fructose (fru), 0.5% galactose (gal), or 0.5% mannose (man) ($n = 3$ biological samples; error bars represent SEM, P values derived from one-way ANOVA; n.s. indicates P values ≥ 0.05).

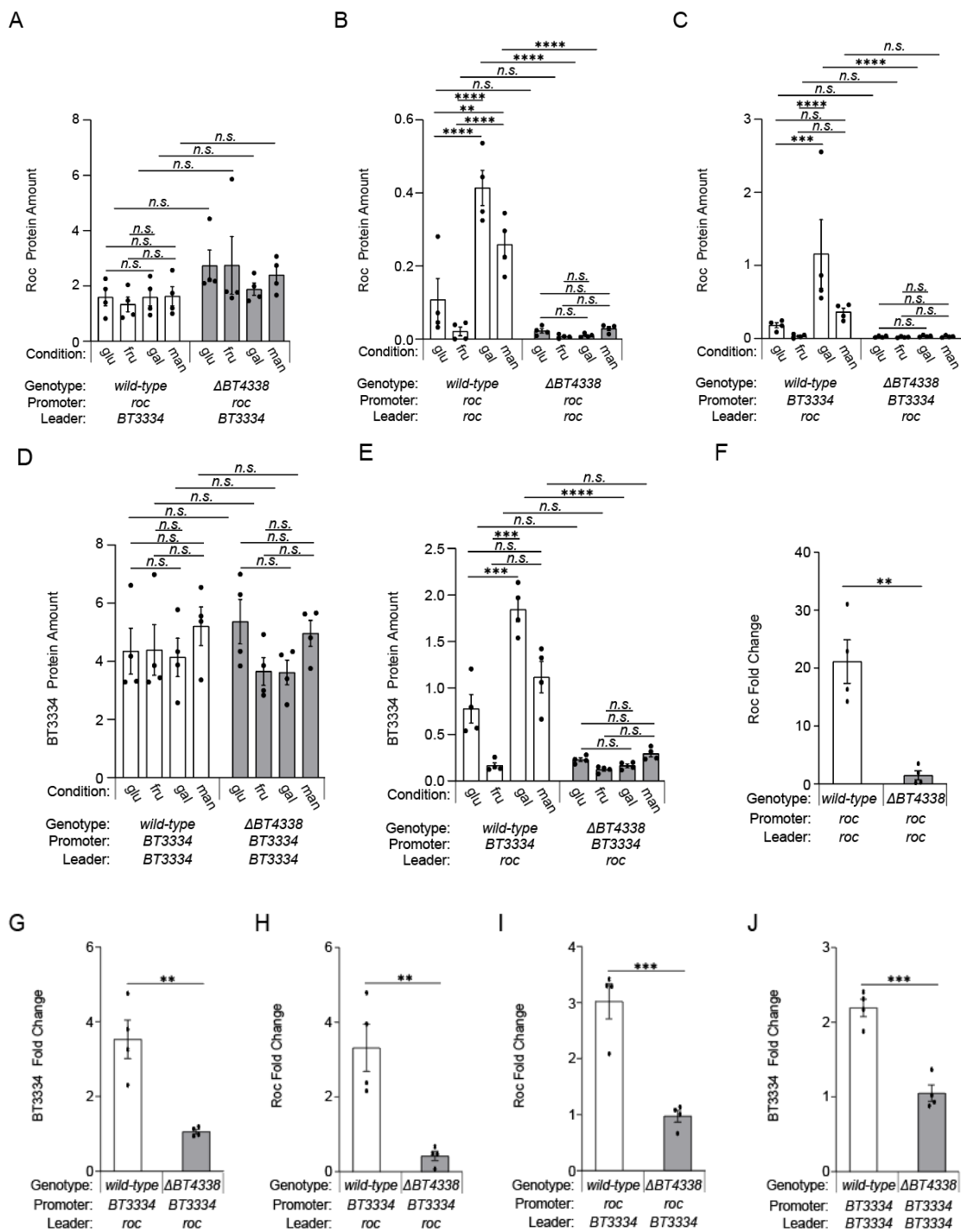


Figure C-4: The roc mRNA leader is necessary and sufficient for BT4338-dependent control of the downstream ORF. (a - c) Quantified western blot analysis of Roc from engineered strains expressing the roc ORF positioned downstream of (a) the roc promoter and BT3334 leader in backgrounds either encoding BT4338 (GT665; white) or lacking BT4338 (GT3510; gray), (b) the roc promoter and leader in backgrounds either encoding BT4338 (GT530; white) or lacking BT4338 (GT3509; gray), or (c) the BT3334 promoter and the roc leader in backgrounds either encoding BT4338 (GT670; white) or lacking BT4338 (GT3511; gray) during mid-exponential growth in 0.5% glucose (glu), 0.5% fructose (fru), 0.5% galactose (gal), or 0.5% mannose (man) (n = 4 biological samples; error bars represent SEM; P values derived from two-way ANOVA; n.s. indicates P values \geq 0.05; *P < 0.05; **P < 0.01; ***P < 0.001; ****P < 0.0001). (d & e) Quantified western blot analysis of BT3334 from engineered strains expressing the BT3334 ORF positioned downstream of (d) the BT3334 promoter and leader in backgrounds either encoding BT4338 (GT663; white) or lacking BT4338 (GT3514; gray) or (e) the BT3334 promoter and roc leader in backgrounds either encoding BT4338 (GT534; white) or lacking BT4338 (GT3512; gray) during mid-exponential growth in 0.5% glucose (glu), 0.5% fructose (fru), 0.5% galactose (gal), or 0.5% mannose (man) (n = 4 biological samples; error bars represent SEM; P values derived from two-way ANOVA; n.s. indicates P values \geq 0.05; *P < 0.05; **P < 0.01; ***P < 0.001; ****P < 0.0001). (f) Quantified western blot analysis depicting fold increase in Roc amounts from strains described in (b) following exposure to carbon limitation for 60-minutes (n = 4 biological samples; error bars represent SEM; P values derived from two-tailed t-test; **P < 0.01). (g) Quantified western blot analysis depicting the fold increase in BT3334 amounts from strains described in (e) following exposure to carbon limitation for 60-minutes. (h) Quantified western blot analysis depicting the fold increase in Roc amounts from strains described in (c) following exposure to carbon limitation for 60-minutes. (i) Quantified western blot analysis depicting the fold increase in Roc amounts from strains described in (a) following exposure to carbon limitation for 60-minutes. (j) Quantified western blot analysis depicting the fold increase in BT3334 amounts from strains described in (d) following exposure to carbon limitation for 60-minutes (for panels (f – j), n = 4 biological samples; error bars represent SEM; P values derived from two-tailed t-test; **P < 0.01; ***P < 0.001).

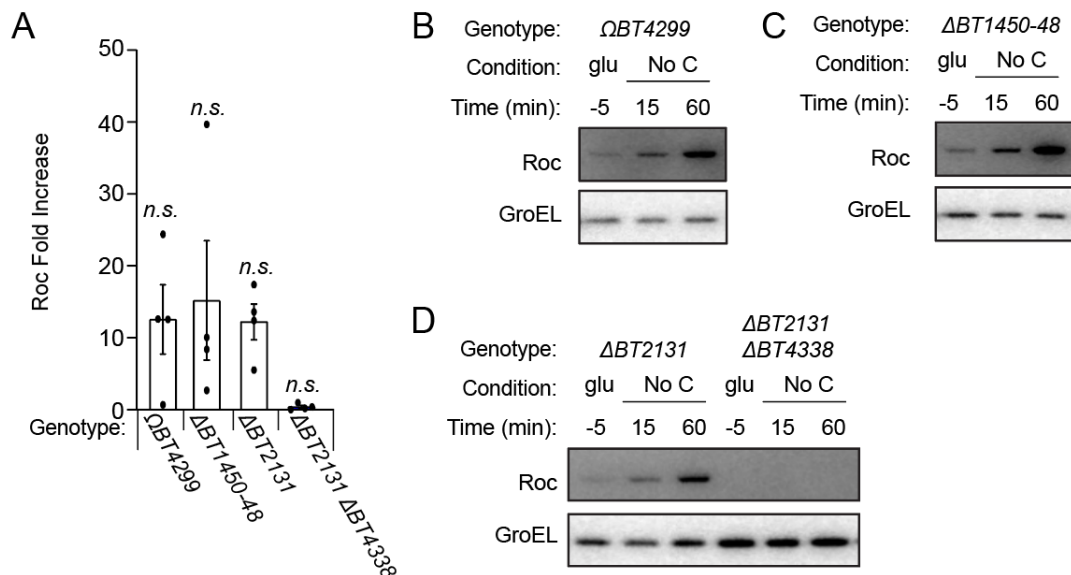


Figure C-5: Candidate BT4338 regulated products are not required for Roc synthesis. (a) Quantified western blot analysis of strains deficient for BT4299 (GT1459), BT1450-48 (GT1427), or BT2131 (GT1372), or both BT2131 and BT4338 (GT4361). Bars represent the fold increase between (glu; -5) and 60-minute time points ($n = 4$ biological samples; error bars represent SEM; P values derived from one-way ANOVA calculated against isogenic wild-type GT593 or GT1234 for the BT4338 deficient strain; n.s. indicates P values ≥ 0.05). (b - d) Western blot analysis of Roc levels from strains deficient for (b) BT4299 (GT1459), (c) BT1450-48 (GT1427), or (d) BT2131 (GT1372) and both BT2131 and BT4338 (GT1374). Blots were probed using anti-HA and anti-GroEL antibodies.

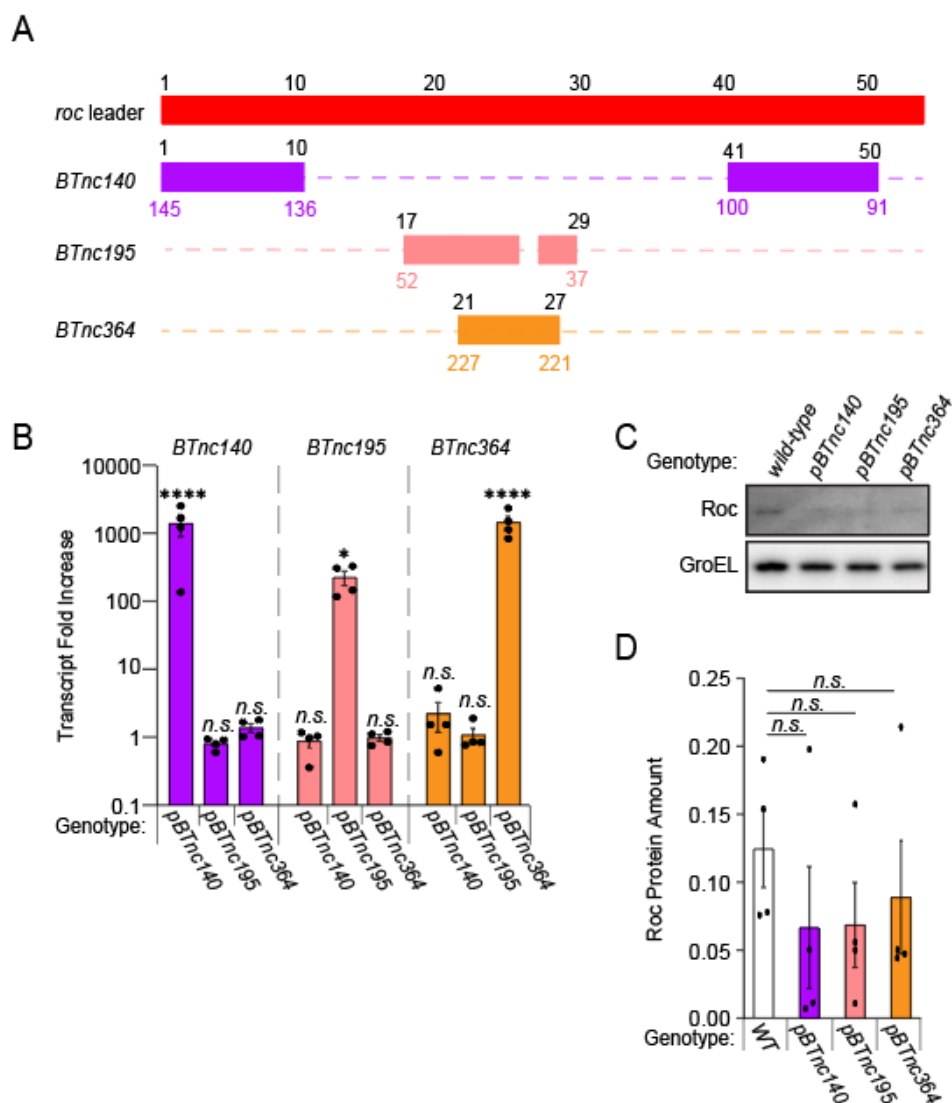


Figure C-6: Expression of candidate sRNAs are insufficient to increase Roc amounts. (a) Schematic of selected sRNAs BTnc140 (purple), BTnc195 (pink), BTnc364 (orange) complementarity to the roc leader (red). (b) The transcript amounts of BTnc140 (purple), BTnc195 (pink), or BTnc364 (orange) were measured in strains overexpressing each of these sRNAs during mid-exponential growth in 0.5% glucose compared to wild-type Bt (GT593) ($n = 4$ biological replicates; error bars represent SEM; P values derived from two-way ANOVA; n.s. indicates P values ≥ 0.05 ; * $P < 0.05$; **** $P < 0.0001$). (c) Western blot analysis of Roc amounts from wild-type Bt (GT593) or strains heterologously expressing BTnc140 (GT4340), BTnc195 (GT4344), or BTnc364 (GT4381) during mid-exponential growth in glucose. Blots were probed using anti-HA and anti-GroEL antibodies. (d) Quantified western blot analysis of strains described in (c) ($n = 4$ biological samples; error bars represent SEM; P values derived from one-way ANOVA; n.s. indicates P values ≥ 0.05).

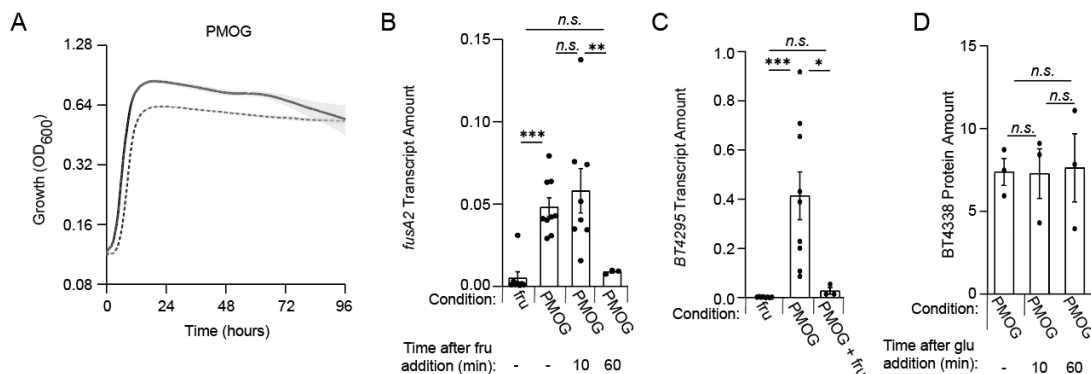


Figure C-7: BT4338 is dispensable for growth in PMOG and necessary for *fusA2* and BT4295 expression. (a) Growth of wild-type (ATCC 29148; solid line) or isogenic BT4338-deficient (GT2623; dotted line) Bt strains in minimal media containing 1% PMOG ($n = 4$ biological samples; error bars represent SEM). (b) qPCR analysis of *fusA2* (BT2167) transcript amounts measured in wild-type Bt (ATCC 29148) during mid-exponential growth in either 0.5% fructose (*fru*) or 1% PMOG, and 10 and 60-minutes following the addition of fructose to 0.2% ($n = 9$ biological samples for *fru*, PMOG, and PMOG + *fru* 10m; $n = 3$ for PMOG + *fru* 60m; error bars represent SEM, P values derived from one way ANOVA; *n.s.* indicates P values ≥ 0.05 ; $**P < 0.01$; $***P < 0.001$). (c) qPCR analysis of BT4295 transcript amounts measured in wild-type Bt (ATCC 29148) during mid-exponential growth in either 0.5% fructose (*fru*) or 1% PMOG, and 60-minutes following the addition of fructose to 0.2% ($n = 9$ biological samples for *fru* and PMOG; $n = 3$ for PMOG + *fru*; error bars represent SEM, P values derived from one way ANOVA; *n.s.* indicates P values ≥ 0.05 ; $*P < 0.05$; $***P < 0.001$). (d) Quantified western blot analysis of BT4338 protein amounts from a Bt strain expressing epitope-tagged BT4338 (GT1481) during mid-exponential growth in 1% PMOG, and 10 and 60-minutes following the addition of glucose to 0.2% ($n = 3$ biological samples; error bars represent SEM, P values derived from two-way ANOVA; *n.s.* indicates P values ≥ 0.05).

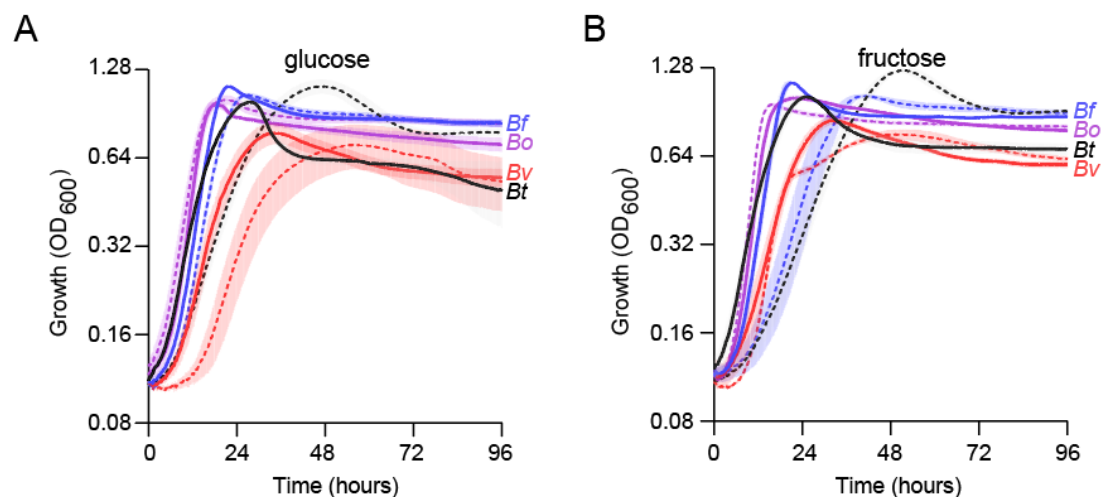


Figure C-8: BT4338 orthologs are dispensable for growth in glucose and fructose across *Bacteroides* species. (a – b) Growth of bar-coded wild-type (solid lines) *B. thetaiotaomicron* (Bt; GT3361; black), *B. fragilis* (Bf; GT3551; blue), *B. vulgatus* (Bv; GT3367; red), or *B. ovatus* (Bo; GT3364; purple) or bar-coded isogenic BT4338-ortholog-deficient strains (dashed lines; GT3522, GT3555, GT3643, GT3553, respectively) in minimal media containing 0.5% (a) glucose or (b) fructose as the sole carbon source ($n = 4$ biological replicates; error bars represent SEM).

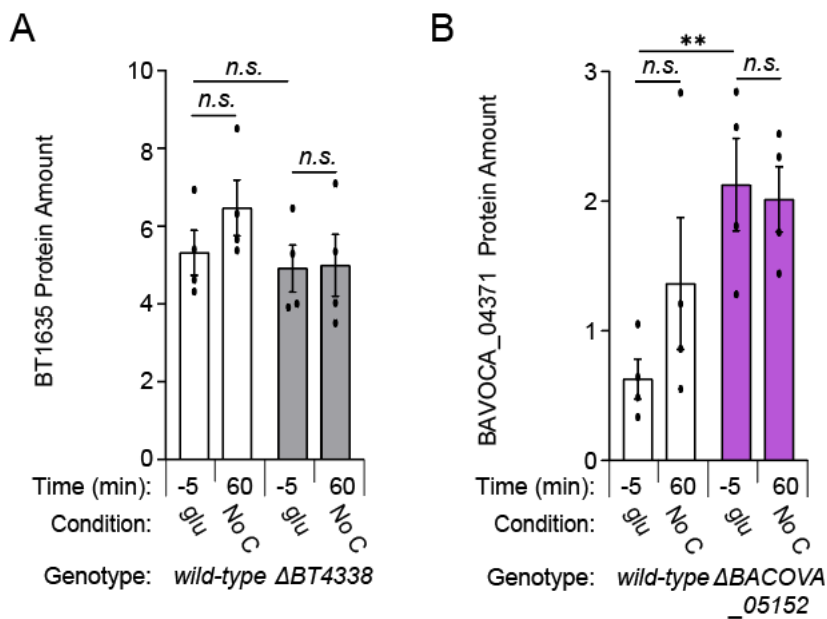


Figure C-9: Roc homologs are differentially regulated by BT4338 orthologs. (a) Quantified western blot analysis of BT1635 protein amounts from wild-type *Bt* (GT4372; white) or a strain deficient for BT4338 (GT4373; gray) ($n = 4$ biological samples; error bars represent SEM; P values derived from one-way ANOVA; n.s. indicates P values ≥ 0.05). (b) Quantified western blot analysis of BACOVA_04371 amounts from wild-type *Bo* (GT4362; white) or a strain deficient for BACOVA_05152 (GT4369; purple) ($n = 4$ biological samples; error bars represent SEM; P values derived from one-way ANOVA; n.s. indicates P values ≥ 0.05 ; ** $P < 0.01$).

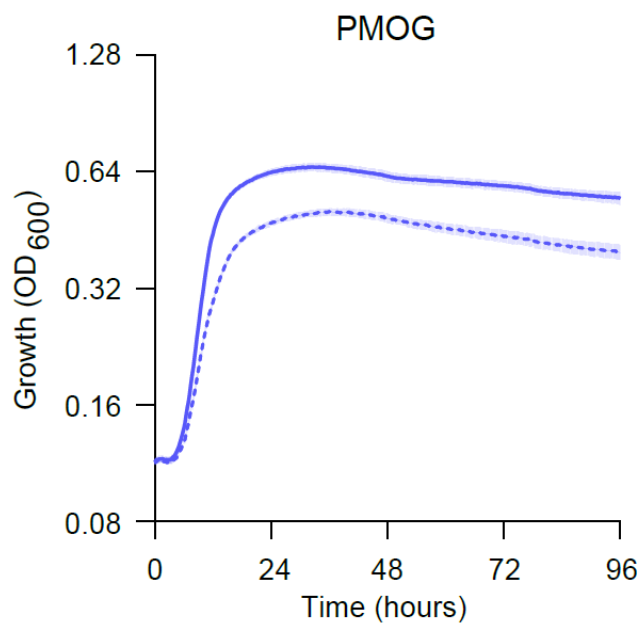


Figure C-10: PMOGs support *B. fragilis* growth. Growth of wild-type *B. fragilis* (ATCC 25285; solid line) or an isogenic BT4338-ortholog-deficient strain (GT2520; dashed line) in minimal media containing 1% PMOG ($n = 4$ biological replicates; error bars represent SEM).

Supplemental Tables

Table C-1. Strains and plasmids used in this study

Identifier	Description	Genotype	Source
<i>B. thetaiotaomicron</i>			
ATCC 29148	<i>wild-type Bt</i>		ATCC
GT23	<i>A tdk-deficient strain</i>	Δtdk	(365)
GT593	<i>A strain harboring an in-frame C-terminally HA-tagged roc</i>	Δtdk BT3172-HA	(381)
GT1234	<i>A cur-deficient strain harboring an in-frame C-terminally HA-tagged roc</i>	Δtdk BT3172-HA $\Delta BT4338$	This study
GT1310	<i>A fusA2-deficient strain harboring an in-frame C-terminally HA-tagged roc</i>	Δtdk BT3172-HA $\Delta BT2167$	This study
GT1663	<i>A strain harboring a chromosomal roc deletion and a multi-copy plasmid encoding C-terminally HA-tagged roc</i>	Δtdk $\Delta BT3172$ + pLYL01::BT3172-HA	This study
GT3148	<i>A GT1663-derived strain harboring a transposon insertion in BT1222</i>	Δtdk $\Delta BT3172$ BT1222::Tn + pLYL01::BT3172-HA	This study
GT3150	<i>A GT1663-derived strain harboring a transposon insertion in BT1221</i>	Δtdk $\Delta BT3172$ BT1221::Tn + pLYL01::BT3172-HA	This study
GT3151	<i>A GT1663-derived strain harboring a transposon insertion in BT4338</i>	Δtdk $\Delta BT3172$ BT4338::Tn + pLYL01::BT3172-HA	This study
GT1481	<i>A strain expressing a C-terminally HA-tagged BT4338 gene</i>	Δtdk $\Delta BT4338$ att- 1::pNBU2-tetQ- PBT4338-4xG-HA	(331)
GT426	<i>A strain expressing a C-terminally HA-tagged roc gene</i>	Δtdk pKNOCK- tetQ::BT3172-HA	(381)
GT530	<i>A strain harboring chromosomal deletions of roc and BT3334 complemented with a single-copy plasmid encoding C-terminally HA-tagged roc expressed from its native promoter and leader</i>	Δtdk $\Delta BT3334$ $\Delta BT3172$ att- 1::pNBU2-tetQ- BT3172-HA	(381)
GT534	<i>A strain harboring chromosomal deletions of roc and BT3334 complemented with a single-copy plasmid encoding C-terminally HA-tagged BT3334 expressed from its native promoter and leader</i>	Δtdk $\Delta BT3334$ $\Delta BT3172$ att- 1::pNBU2-tetQ- BT3334-HA	(381)
GT640	<i>A strain harboring chromosomal deletions of roc and BT3334 complemented with a single-copy plasmid encoding C-terminally HA-tagged BT3334 expressed from the roc promoter and native leader</i>	Δtdk $\Delta BT3334$ $\Delta BT3172$ att- 1::pNBU2-tetQ- P _{BT3172} - BT3334LEADER- BT3334-HA	(381)
GT663	<i>A strain harboring chromosomal deletions of roc and BT3334 complemented with a single-copy plasmid encoding C-terminally HA-tagged BT3334 expressed from its native promoter and the roc leader</i>	Δtdk $\Delta BT3334$ $\Delta BT3172$ att- 1::pNBU2-tetQ- P _{BT3334} - BT3172LEADER- BT3334-HA	(394)

GT665	<i>A strain harboring chromosomal deletions of roc and BT3334 complemented with a single-copy plasmid encoding C-terminally HA-tagged roc expressed from its native promoter and the BT3334 leader</i>	$\Delta tdk \Delta BT3334 \Delta BT3172$ att-1::pNBU2-tetQ- P_{BT3172} -BT3334LEADER-BT3172-HA	(394)
GT670	<i>A strain harboring chromosomal deletions of roc and BT3334 complemented with a single-copy plasmid encoding C-terminally HA-tagged roc expressed from the BT3334 promoter and its native leader</i>	$\Delta tdk \Delta BT3334 \Delta BT3172$ att-1::pNBU2-tetQ- P_{BT3334} -BT3172LEADER-BT3172-HA	(394)
GT2623	<i>A cur-deficient strain</i>	$\Delta BT4338$	This study
GT2727	<i>a strain lacking BT1222 expressing a C-terminally HA-tagged roc gene</i>	$\Delta tdk \Delta BT1222$ pKNOCK-tetQ::BT3172-HA	This study
GT2728	<i>a strain lacking BT1221 expressing a C-terminally HA-tagged roc gene</i>	$\Delta tdk \Delta BT1221$ pKNOCK-tetQ::BT3172-HA	This study
GT2729	<i>a strain lacking BT1220 expressing a C-terminally HA-tagged roc gene</i>	$\Delta tdk \Delta BT1220$ pKNOCK-tetQ::BT3172-HA	This study
GT3509	<i>A strain harboring chromosomal deletions of roc, BT3334, and cur complemented with a single-copy plasmid encoding C-terminally HA-tagged roc expressed from its native promoter and leader</i>	$\Delta tdk \Delta BT3172 \Delta BT3334 \Delta BT4338$ att-1::pNBU2-tetQ-BT3172-HA	This study
GT3510	<i>A strain harboring chromosomal deletions of roc, BT3334, and cur complemented with a single-copy plasmid encoding C-terminally HA-tagged roc expressed from its native promoter and the BT3334 leader</i>	$\Delta tdk \Delta BT3172 \Delta BT3334 \Delta BT4338$ att-1::pNBU2-tetQ- P_{BT3172} -BT3334LEADER-BT3172-HA	This study
GT3511	<i>A strain harboring chromosomal deletions of roc, BT3334, and cur complemented with a single-copy plasmid encoding C-terminally HA-tagged roc expressed from the BT3334 promoter and its native leader</i>	$\Delta tdk \Delta BT3172 \Delta BT3334 \Delta BT4338$ att-1::pNBU2-tetQ- P_{BT3334} -BT3172LEADER-BT3172-HA	This study
GT3512	<i>A strain harboring chromosomal deletions of roc, BT3334, and cur complemented with a single-copy plasmid encoding C-terminally HA-tagged BT3334 expressed from its native promoter and leader</i>	$\Delta tdk \Delta BT3172 \Delta BT3334 \Delta BT4338$ att-1::pNBU2-tetQ-BT3334-HA	This study
GT3513	<i>A strain harboring chromosomal deletions of roc, BT3334, and cur complemented with a single-copy plasmid encoding C-terminally HA-tagged BT3334 expressed from the roc promoter and its native leader</i>	$\Delta tdk \Delta BT3172 \Delta BT3334 \Delta BT4338$ att-1::pNBU2-tetQ- P_{BT3172} -BT3334LEADER-BT3334-HA	This study
GT3514	<i>A strain harboring chromosomal deletions of roc, BT3334, and cur complemented with a single-copy plasmid encoding C-</i>	$\Delta tdk \Delta BT3172 \Delta BT3334 \Delta BT4338$ att-1::pNBU2-tetQ-	This study

	<i>terminally HA-tagged BT3334 expressed from its native promoter and the roc leader</i>	P_{BT3334} - <i>BT3172LEADER-</i> <i>BT3334-HA</i>	
GT3361	<i>a bar-coded wild-type Bt strain</i>	<i>att-1::pNBU2-tetQ-</i> <i>BC01</i>	This study
GT3522	<i>a bar-coded cur-deficient strain</i>	Δ <i>BT4338 att-</i> <i>1::pNBU2-tetQ-BC06</i>	This study
GT3363	<i>a bar-coded strain lacking the native cur gene complemented with cur</i>	Δ <i>BT4338 att-</i> <i>1::pNBU2-tetQ-</i> <i>BC04-BT4338</i>	This study
GT1372	<i>A strain harboring a chromosomal deletion of BT2131 and an in-frame C-terminally HA-tagged roc</i>	Δ <i>tdk BT3172-HA</i> Δ <i>BT2131</i>	This study
GT1374	<i>A strain harboring a chromosomal deletion of BT2131 and cur with an in-frame C-terminally HA-tagged roc</i>	Δ <i>tdk BT3172-HA</i> Δ <i>BT2131</i> Δ <i>BT4338</i>	This study
GT1427	<i>A strain harboring a chromosomal deletion of BT1450-48 and an in-frame C-terminally HA-tagged roc</i>	Δ <i>tdk BT3172-HA</i> Δ <i>BT1450-48</i>	This study
GT1459	<i>A strain harboring a BT4299 insertion and an in-frame C-terminally HA-tagged roc</i>	Δ <i>tdk BT3172-HA</i> <i>pKNOCK-</i> <i>tetQ::BT4299</i>	This study
GT4358	<i>A strain harboring an in-frame C-terminally HA-tagged roc</i>	<i>pKNOCK-</i> <i>tetQ::BT3172-HA</i>	This study
GT4359	<i>A strain harboring a chromosomal deletion of cur and an in-frame C-terminally HA-tagged roc</i>	<i>pKNOCK-</i> <i>tetQ::BT3172-HA</i> Δ <i>BT4338</i>	This study
GT4372	<i>A strain harboring an in-frame C-terminally HA-tagged BT1635</i>	<i>pKNOCK-</i> <i>tetQ::BT1635-HA</i>	This study
GT4373	<i>A strain harboring a chromosomal deletion of cur and an in-frame C-terminally HA-tagged BT1635</i>	<i>pKNOCK-</i> <i>tetQ::BT1635-HA</i> Δ <i>BT4338</i>	This study
GT4340	<i>A strain harboring an in-frame C-terminally HA-tagged roc and a multi-copy plasmid encoding BTnc140 following the 16S promoter</i>	Δ <i>tdk BT3172-HA</i> <i>pLYL01-tet::P-16S-</i> <i>nc140</i>	This study
GT4344	<i>A strain harboring an in-frame C-terminally HA-tagged roc and a multi-copy plasmid encoding BTnc195 following the 16S promoter</i>	Δ <i>tdk BT3172-HA</i> <i>pLYL01-tet::P-16S-</i> <i>nc195</i>	This study
GT4381	<i>A strain harboring an in-frame C-terminally HA-tagged roc and a multi-copy plasmid encoding BTnc364 following the 16S promoter</i>	Δ <i>tdk BT3172-HA</i> <i>pLYL01-tet::P-16S-</i> <i>nc364</i>	This study
<i>B. fragilis</i>			
ATCC 25285	<i>Wild-type Bf</i>		ATCC
GT2520	<i>a cur-deficient strain</i>	Δ <i>BF9343_0915</i>	This study
GT3551	<i>a bar-coded wild-type Bf strain</i>	<i>att-1::pNBU2-tetQ-</i> <i>BC01</i>	This study
GT3555	<i>a bar-coded cur-deficient strain</i>	Δ <i>BF9343_0915 att-</i> <i>1::pNBU2-tetR-BC06</i>	This study
<i>B. ovatus</i>			

ATCC 8483	<i>Wild-type Bo</i>		ATCC
GT2413	<i>a cur-deficient strain</i>	Δ BACOVA_05152	This study
GT3364	<i>a bar-coded wild-type Bo strain</i>	<i>att-1::pNBU2-tetQ-BC01</i>	This study
GT3553	<i>a bar-coded cur-deficient strain</i>	Δ BACOVA_05152 <i>att-1::pNBU2-tetQ-BC06</i>	This study
GT4362	<i>A strain harboring an in-frame C-terminally HA-tagged BACOVA_04371</i>	<i>pKNOCK-tetQ::BACOVA_04371-HA</i>	This study
GT4369	<i>A strain harboring a chromosomal deletion of cur and an in-frame C-terminally HA-tagged BACOVA_04371</i>	<i>pKNOCK-tetQ::BACOVA_04371-HA</i> Δ BACOVA_05152	This study
<i>B. vulgatus</i>			
ATCC 8482	<i>Wild-type Bv</i>		ATCC
GT2399	<i>a cur-deficient strain</i>	Δ BVU_3580	This study
GT3367	<i>a bar-coded wild-type Bv strain</i>	<i>att-1::pNBU2-tetQ-BC01</i>	This study
GT3643	<i>a bar-coded cur-deficient strain</i>	Δ BVU_3580 <i>att-1::pNBU2-tetQ-BC06</i>	This study
<i>E. coli</i>			
GT1	<i>S17-1</i>	λ pir	(380)
Plasmids			
Identifier	Description	Source	
pSAM-Bt	A plasmid-borne mariner transposon	(351)	
pEXCHANGE-tdk	A plasmid for engineering chromosomal gene deletions in <i>tdk</i> -deficient <i>Bt</i> strains	(365)	
pEXCHANGE-tdk- Δ BT1222	A plasmid used to delete <i>BT1222</i>	This study	
pEXCHANGE-tdk- Δ BT1221	A plasmid used to delete <i>BT1221</i>	This study	
pEXCHANGE-tdk- Δ BT1220	A plasmid used to delete <i>BT1220</i>	This study	
pSIE1	A plasmid for engineering chromosomal deletion in <i>Bacteroides</i> species	(395)	
pSIE1- Δ BT4338	A plasmid used to delete <i>cur</i> from the <i>Bt</i> chromosome	This study	
pSIE1- Δ Bvu_3580	A plasmid used to delete <i>cur</i> from the <i>Bv</i> chromosome	This study	
pSIE1- Δ BACOVA_05152	A plasmid used to delete <i>cur</i> from the <i>Bo</i> chromosome	This study	
pLGB13	A plasmid for engineering chromosomal deletion in <i>Bacteroides</i> species	(396)	
pLGB13- Δ BF9343_0915	A plasmid used to delete <i>cur</i> from the <i>Bf</i> chromosome	This study	
pRK231	A helper plasmid for conjugation into <i>Bf</i>	(397)	
pNBU2-tetQ-BC01	A plasmid bearing a unique molecular barcode	(381)	
pNBU2-tetQ-BC04	A plasmid bearing a unique molecular barcode	(381)	
pNBU2-tetQ-	A plasmid bearing a unique molecular bar-	(381)	

BC06	code	
pLYL01-BT3172-HA	A multi-copy plasmid expressing a C-terminally HA-tagged <i>roc</i> gene from its native promoter and leader	(381)
pNBU2-tetQ-BT3172-HA	A single-copy plasmid expressing a C-terminally HA-tagged <i>roc</i> gene from its native promoter and leader	(381)
pNBU2-tetQ-PBT3172-BT3334LEADER-BT3172-HA	A single-copy plasmid expressing a C-terminally HA-tagged <i>roc</i> gene from its native promoter and the <i>BT3334</i> leader	(381)
pNBU2-tetQ-PBT3334-BT3172LEADER-BT3172-HA	A single-copy plasmid expressing a C-terminally HA-tagged <i>roc</i> gene from the <i>BT3334</i> promoter and its native leader	(381)
pNBU2-tetQ-BT3334-HA	A single-copy plasmid expressing a C-terminally HA-tagged <i>BT3334</i> gene from its native promoter and leader	(381)
pNBU2-tetQ-PBT3172-BT3334LEADER-BT3334-HA	A single-copy plasmid expressing a C-terminally HA-tagged <i>BT3334</i> gene from the <i>roc</i> promoter and its native leader	(381)
pNBU2-tetQ-PBT3334-BT3172LEADER-BT3334-HA	A single-copy plasmid expressing a C-terminally HA-tagged <i>BT3334</i> gene from its native promoter and the <i>roc</i> leader	(381)
pKNOCK-tetQ-BT3172-HA	A plasmid that C-terminally HA-tags <i>roc</i> in its chromosomal locus	(381)
pKNOCK-tetQ::BT4299	A plasmid that inactivates <i>BT4299</i> and downstream genes.	This study
pKNOCK-tetQ::BACOVA_04371-HA	A plasmid that C-terminally HA-tags <i>BACOVA_04371</i> in its chromosomal locus	This study
pKNOCK-tetQ::BT1635-HA	A plasmid that C-terminally HA-tags <i>BT1635</i> in its chromosomal locus	(381)
pLYL01-tet::P-16S-nc140	A multi-copy plasmid expressing <i>BTnc140</i> from the <i>Bt</i> 16s promoter.	This study
pLYL01-tet::P-16S-nc195	A multi-copy plasmid expressing <i>BTnc195</i> from the <i>Bt</i> 16s promoter.	This study
pLYL01-tet::P-16S-nc364	A multi-copy plasmid expressing <i>BTnc364</i> from the 16s promoter.	This study

Table C-2. Oligonucleotides used in this study

ID	Name	Sequence	Purpose	Source
qPCR				
1044	qBt16sF	GGTAGTCCACACAGT AAACGATGAA	Measuring 16s rRNA transcript levels from <i>Bt</i> by qPCR	(381)
1045	qBt16sR	CCCGTCAAATTCCTTT GAGTTTC		(381)
1050	qBT2167f	AAAACGTCGCGGATC TGTTG	Measuring <i>fusA2</i> transcript levels from <i>Bt</i> by qPCR	(331)
1051	qBT2167r	TGGAGAACGGTAGAG AAAACGG		(331)
1995	ChIP_roc_f	AGAAGGGCAACTGGA CAAAG	Measuring roc promoter levels by qPCR following ChIP	This study
1996	ChIP_roc_r	CCTTTCACGGTGCTG AATGAG		This study
1997	ChIP_fusA2_f	ATAAGTCTGGCCTGTC TGCTAC	Measuring <i>fusA2</i> promoter levels by qPCR following ChIP	(331)
1998	ChIP_fusA2_r	AGGGATTTATTGGGG GAAAAGC		(331)
1999	ChIP_rpoD_f	GTCAGTGATCTGGAA GAAGCAATG	measuring <i>rpoD</i> promoter levels by qPCR following ChIP	(331)
2000	ChIP_rpoD_r	GGGAATACACCTGTC AGGAACAA		(331)
1956	qBacteroides_ 16Sf	TGAAAGTTTGCGGCT CAACC	Measuring 16s rRNA transcript levels from <i>Bacteroides</i> species by qPCR	This study
1957	qBacteroides_ 16Sr	AAGCATTTACCGCTA CACC		This study
1958	qBF9343_fus A2f	AGAAGACGAAATGCG CGAAG	measuring <i>fusA2</i> transcript levels from <i>Bf</i> by qPCR	This study
1959	qBF9343_fus A2r	ATCTTTGCCTGCACAT ACGC		This study
1962	qBACOVA_fu sA2r	TGGAGAACGGTGGAG AAAACG	measuring <i>fusA2</i> transcript levels from <i>Bo</i> by qPCR	This study
1965	qBVU_fusA2f	AATGTGCTCGAACAGT TGCG	Measuring <i>fusA2</i> transcript levels from <i>Bf</i> by qPCR	This study
1966	qBVU_fusA2r	AGGTCCCCTTTCAAG AGGATAC		This study
2028	pNBU2_tet_B C01	ATGTCGCCAATTGTCA CTTTCTCA	Measuring relative strain abundance from mouse fecal pellets	(381)
2030	pNBU2_tet_B C04	CTCCATAAAGGCGCA TACCGACTA		(381)
2031	pNBU2_tet_B C06	GATTACGGCGTGATA GATTGGTGT		(381)
2033	UNIV-R	CACAATATGAGCAACA AGGAATCC		(381)
2676	qBTnc140f	AGCAGGTTTGTACCCT CTAAGG	Measuring <i>BTnc140</i> rRNA transcript levels from <i>Bt</i> by qPCR	This study
2677	qBTnc140r	TTTCGGTTAGGCTCTG GTAAGC		This study
2678	qBTnc195f	ACCACAGGTTACACA GTTTTGC	Measuring <i>BTnc195</i> rRNA transcript levels from <i>Bt</i> by qPCR	This study
2679	qBTnc195r	CTCGTCAGCATGGAT		This study

		ATTCACC		
2680	qBTnc364f	TCTGATACTCGGCAC CAGAAAG	Measuring <i>BTnc364</i> rRNA transcript levels from <i>Bt</i> by qPCR	This study
2681	qBTnc364r	AGATAGAAGCCATCC AGTGCAG		This study
<i>Tn insertion site identification</i>				
1064	AR1A	GGCCACGCGTCGACT AGTACNNNNNNNNNN GTAAT	Semi-random PCR for determining sites of transposon insertion	(351)
1065	AR1B	GGCCACGCGTCGACT AGTACNNNNNNNNNN GATGC		(351)
1066	AR1C	GGCCACGCGTCGACT AGTACNNNNNNNNNN GGCCG		(351)
1067	AR1D	GGCCACGCGTCGACT AGTACNWNWNWNWN WCTTAA		(351)
1068	AR2	GGCCACGCGTCGACT AGTAC		(351)
1069	PATseq1	ACGTAATCATGGTTCA TCCCGATA		(351)
1070	PATseq2	GCGTATCGGTCTGTAT ATCAGCAA		(351)
<i>Plasmid construction</i>				
1459	pEXCHANGE-dBT1222_5f	GCTCTAGAAGTAGTG GATCCAGGAAGATAT GCAACAGAAAGATAA CTC	Constructing a plasmid to delete <i>BT1222</i> from the <i>Bt</i> genome	This study
1460	dBT1222_5r	ATCTTATATATTTTAA ATATTGTTTATGTAAG AAACAC		This study
1461	dBT1222_3f	TAAAATATATAAGATG TACTTTTCTTTTGCCTT GATGCAAAAG		This study
1462	pEXCHANGE-dBT1222_3r	AGATAACATTTCGAGTC GACGCCCGGCCGCTT TCAAAT		This study
1463	pEXCHANGE-dBT1221_5f	GCTCTAGAAGTAGTG GATCCATGGAATCTG GATTTGGCTTCCA	Constructing a plasmid to delete <i>BT1221</i> from the <i>Bt</i> genome	This study
1464	dBT1221_5r	CGTCGTATTTTAACT TTTTACCTTTTATCC		This study
1465	dBT1221_3f	GTTAAAAATACGACGA TGGAGACAGCCCGTT CGTTG		This study
1466	pEXCHANGE-dBT1221_3r	AGATAACATTTCGAGTC GACCCAATGTTACTCT CTCTTCTTATATATAAT		This study
1467	pEXCHANGE-dBT1220_5f	GCTCTAGAAGTAGTG GATCCGGATAATTTCC GGAATGAGGTAGTG		Constructing a plasmid to delete <i>BT1220</i> from the <i>Bt</i> genome

1468	dBT1220_5r	ATTGTCTCTCTCTTTA GACGACGGGAAAACA GATAGTT		This study
1469	dBT1220_3f	AAAGAGAGAGACAAT ATAAAGACAAAGTATA TTATA		This study
1470	pEXCHANGE- dBT1220_3r	AGATAACATTTCGAGTC GACACAAACACATAAC TGCCTCCTGC		This study
1612	pLGB13- dBF9343_091 5_5f	GATTAGCATTATGAGG ATCCAGCTATCTAACA GAAAGCCCTTAGAAAT TACTAC	Constructing a plasmid to delete <i>cur</i> from the <i>Bf</i> genome	This study
1613	dBF9343_091 5_5r	ATCTGTTGCAAACTG TGTTATAAAGCACA		This study
1691	dBF9343_091 5_3f:	ACACAGTTTTGCAACA GATAAGCGCTTTGTC GCCATTCA		This study
1617	pLGB13- dBF9343_091 5_3r	TCCACCGCGGTGGCG GCCGCTGATGTGGTC GTTAATATACTTCTATT TCGTC		This study
1618	pSIE1- dBvu_3580_5f	GATTAGCATTATGAGG ATCCTGAAGGTGACG GCTACTCG	Constructing a plasmid to delete <i>cur</i> from the <i>Bv</i> genome	This study
1619	dBvu_3580_5r	TATGAATTGATATTAG ATTAAACGTGCTATAA AACCGTGTTATAGAGC		This study
1620	dBvu_3580_3f	AATCTAATATCAATTC ATACTTCACACACACA GG		This study
1623	pSIE1- dBvu_3580_3r	TCCACCGCGGTGGCG GCCGCTCTTCTGCCA TAATATGTTTGCCA		This study
1624	pSIE1- dBACOVA_05 152_5f	GATTAGCATTATGAGG ATCCAACAATTATCGC CTCCGAACC	Constructing a plasmid to delete <i>cur</i> from the <i>Bo</i> genome	This study
1625	dBACOVA_05 152_5r	ATTCATTTTTACCATG AGTGCTACAAAACCTG		This study
1626	dBACOVA_05 152_3f	ACTCATGGTAAAAATG AATGAGAGTTTCTGCA CCAATCGTTC		This study
1627	pSIE1- dBACOVA_05 152_3r	TCCACCGCGGTGGCG GCCGCCACGATAGTT CTTTTCCTCTTCGG		This study
2624	pKO_BACOV A_04371f	GCTCTAGAACTAGTG GATCCGATTTGACGG ATTTTCTGAAAAAGTC AC	Constructing a plasmid to C-terminally HA tag <i>BACOVA_04371</i>	This study
2625	pKO_BACOV A_04371-HAr	CCCCCTCGAGGTCTGA CTTAAGCGTAGTCTG GGACGTCGTATGGGT		This study

		ACTCTTTTTTCCGTTCTGTTTTCTC		
2664	lyl-BT16Sf	GTGAATTCGAGCTCGGTACCCAGTACTGCTTGACCATAAGAAC	Constructing a multi-copy plasmid incorporating the 16s promoter upstream of a MCS	This study
2665	lyl-BT16Sr	AGGTCGACTCTAGAGGATCCACTGCAAAGATAAGAACTTTTAGC		This study
2666	16S-BTnc140f	GCTAAAAGTTCTTATCTTTGCAGTATAACAGTCTGCGATATATCTTATCG	Constructing a multicopy plasmid to express <i>BTnc140</i> from the 16s promoter	This study
2667	lyl-BTnc140r	TTGCATGCCTGCAGGTGCACAAAAAGAAAAAGGACGCAACACTATC		This study
2670	16S-BTnc195f	GCTAAAAGTTCTTATCTTTGCAGTGTTGAACTTAAAGCTAACATTATGGG	Constructing a multicopy plasmid to express <i>BTnc195</i> from the 16s promoter	This study
2671	lyl-BTnc195r	TTGCATGCCTGCAGGTGCACACAAAAAGAAATTCACCACGGACTACCC		This study
2674	16S-BTnc364f	GCTAAAAGTTCTTATCTTTGCAGTTAACCATAGCGAAAAAGTATAAAATGAAGTC	Constructing a multicopy plasmid to express <i>BTnc364</i> from the 16s promoter	This study
2675	lyl-BTnc364r	TTGCATGCCTGCAGGTGCACAATAGGAATAGCTGGCAGGAAG		This study
W359 5	dBT2131_5f	GCTCTAGAAGTAGTGATCCTGAGCAAGGAGTATTATTGCTCAAC	Constructing a plasmid to delete <i>BT2131</i> from the <i>Bt</i> chromosome	This study
W359 6	dBT2131_5r	TTACTTTTTGGTTTAAAGGTTGATAATTTT		This study
W359 7	dBT2131_3f	ACCTTTAAACCAAAGTAAAGTTAACAATTACTTTTCTTACAGAGAGAGTGTG		This study
W359 8	dBT2131_3r	AAGATAACATTCGAGTCGACTATCTCTGCTAAATTTGATTTGAGACAGA		This study
W370 2	dBT1450_5f	GCTCTAGAAGTAGTGATCCCGTCACCGCGGGCATATTTA	Constructing a plasmid to delete <i>BT1450-BT1448</i> from the <i>Bt</i> chromosome	This study
W370 3	dBT1450_5r	AGGCTGTTTGTATTAAATGTTATGTGTAATA		This study
W370 4	dBT1448_3f	AACATTAATACAAACAGCCTTTCTCAAAAAAATAAAGGTGTTTTACG		This study

		TA		
W370 5	dBT1448_3r	AAGATAACATTCGAGT CGACAACCTCCGGCGT GCGCATAGA		This study
W382 9	BT4299KOf	GCTCTAGAACTAGTG GATCCGCACCAGACC AATTCCTATAACAAGA	Constructing a plasmid to disrupt <i>BT4299</i> .	This study
W383 0	BT4299KOr	GGCCCCCCTCGAGG TCGACAGTGTCTTTAT CTCCGGAGTGATC		This study

REFERENCES

1. Matijašić M, Meštrović T, Perić M, Paljetak H, Panek M, Bender DV, Kelečić DL, Krznarić, Verbanac D. 2016. Modulating composition and metabolic activity of the gut microbiota in IBD patients. *International Journal of Molecular Sciences* 17:1-22. PMID: 15790.
2. Yao Y, Cai X, Ye Y, Wang F, Chen F, Zheng C. 2021. The Role of Microbiota in Infant Health: From Early Life to Adulthood. *Front Immunol* 12:708472. PMC8529064.
3. Dominguez-Bello MG, Costello EK, Contreras M, Magris M, Hidalgo G, Fierer N, Knight R. 2010. Delivery mode shapes the acquisition and structure of the initial microbiota across multiple body habitats in newborns. *Proc Natl Acad Sci U S A* 107:11971-5. PMC2900693.
4. Coelho GDP, Ayres LFA, Barreto DS, Henriques BD, Prado M, Passos CMD. 2021. Acquisition of microbiota according to the type of birth: an integrative review. *Rev Lat Am Enfermagem* 29:e3446. PMC8294792.
5. Proksch E, Brandner JM, Jensen JM. 2008. The skin: an indispensable barrier. *Exp Dermatol* 17:1063-72.
6. Leeming JPH, K. T.; and Cunliffe, W. J. 1984. The Microbial Ecology of Pilosebaceous Units Isolated from Human Skin. *Journal of General Microbiology* 130:803-807.
7. Lomholt HB, Scholz CFP, Bruggemann H, Tettelin H, Kilian M. 2017. A comparative study of *Cutibacterium* (*Propionibacterium*) *acnes* clones from acne patients and healthy controls. *Anaerobe* 47:57-63.
8. Byrd AL, Belkaid Y, Segre JA. 2018. The human skin microbiome. *Nat Rev Microbiol* 16:143-155.
9. Rudolf R, Roth WDJ. 1988. Microbial ecology of the skin. *Annual Review of Microbiology* 42:441-64.
10. Grice EA, Segre JA. 2011. The skin microbiome. *Nat Rev Microbiol* 9:244-53. PMC3535073.
11. Lee HJ, Jeong SE, Lee S, Kim S, Han H, Jeon CO. 2018. Effects of cosmetics on the skin microbiome of facial cheeks with different hydration levels. *Microbiologyopen* 7:e00557. PMC5911989.

12. Scharschmidt TC, Vasquez KS, Truong HA, Gearty SV, Pauli ML, Nosbaum A, Gratz IK, Otto M, Moon JJ, Liese J, Abbas AK, Fischbach MA, Rosenblum MD. 2015. A Wave of Regulatory T Cells into Neonatal Skin Mediates Tolerance to Commensal Microbes. *Immunity* 43:1011-21. PMC4654993.
13. Park HY, Kim CR, Huh IS, Jung MY, Seo EY, Park JH, Lee DY, Yang JM. 2013. *Staphylococcus aureus* Colonization in Acute and Chronic Skin Lesions of Patients with Atopic Dermatitis. *Ann Dermatol* 25:410-6. PMC3870207.
14. Deckers IA, McLean S, Linssen S, Mommers M, van Schayck CP, Sheikh A. 2012. Investigating international time trends in the incidence and prevalence of atopic eczema 1990-2010: a systematic review of epidemiological studies. *PLoS One* 7:e39803. PMC3394782.
15. Silverberg JI. 2017. Public Health Burden and Epidemiology of Atopic Dermatitis. *Dermatol Clin* 35:283-289.
16. Weidinger S, Novak N. 2016. Atopic dermatitis. *Lancet* 387:1109-1122.
17. Chen X, Lu Y, Chen T, Li R. 2021. The Female Vaginal Microbiome in Health and Bacterial Vaginosis. *Front Cell Infect Microbiol* 11:631972. PMC8058480.
18. Chen C, Song X, Wei W, Zhong H, Dai J, Lan Z, Li F, Yu X, Feng Q, Wang Z, Xie H, Chen X, Zeng C, Wen B, Zeng L, Du H, Tang H, Xu C, Xia Y, Xia H, Yang H, Wang J, Wang J, Madsen L, Brix S, Kristiansen K, Xu X, Li J, Wu R, Jia H. 2017. The microbiota continuum along the female reproductive tract and its relation to uterine-related diseases. *Nat Commun* 8:875. PMC5645390.
19. Linhares IM, Summers PR, Larsen B, Giraldo PC, Witkin SS. 2011. Contemporary perspectives on vaginal pH and lactobacilli. *Am J Obstet Gynecol* 204:120 e1-5.
20. Witkin SS, Linhares IM. 2017. Why do lactobacilli dominate the human vaginal microbiota? *BJOG* 124:606-611.
21. Witkin SS, Mendes-Soares H, Linhares IM, Jayaram A, Ledger WJ, Forney LJ. 2013. Influence of vaginal bacteria and D- and L-lactic acid isomers on vaginal extracellular matrix metalloproteinase inducer: implications for protection against upper genital tract infections. *mBio* 4. PMC3735189.
22. A VS, E AK. 2015. Vaginal Protection by H₂O₂-Producing Lactobacilli. *Jundishapur J Microbiol* 8:e22913. PMC4644264.
23. Atassi F, Servin AL. 2010. Individual and co-operative roles of lactic acid and hydrogen peroxide in the killing activity of enteric strain *Lactobacillus johnsonii* NCC933 and vaginal strain *Lactobacillus gasseri* KS120.1 against enteric, uropathogenic and vaginosis-associated pathogens. *FEMS Microbiol Lett* 304:29-38.

24. Pararas MV, Skevaki CL, Kafetzis DA. 2006. Preterm birth due to maternal infection: Causative pathogens and modes of prevention. *Eur J Clin Microbiol Infect Dis* 25:562-9.
25. Lewis FMT, Bernstein KT, Aral SO. 2017. Vaginal Microbiome and Its Relationship to Behavior, Sexual Health, and Sexually Transmitted Diseases. *Obstet Gynecol* 129:643-654. PMC6743080.
26. Antonio MADH, Stephen E; Hillier, Sharon L. 1999. The Identification of Vaginal Lactobacillus Species and the Demographic and Microbiologic Characteristics of Women Colonized by these Species. *The Journal of Infectious Diseases* 180:1950-6.
27. Aagaard K, Riehle K, Ma J, Segata N, Mistretta TA, Coarfa C, Raza S, Rosenbaum S, Van den Veyver I, Milosavljevic A, Gevers D, Huttenhower C, Petrosino J, Versalovic J. 2012. A metagenomic approach to characterization of the vaginal microbiome signature in pregnancy. *PLoS One* 7:e36466. PMC3374618.
28. Hickey RJ, Zhou X, Pierson JD, Ravel J, Forney LJ. 2012. Understanding vaginal microbiome complexity from an ecological perspective. *Transl Res* 160:267-82. PMC3444549.
29. Noyes N, Cho KC, Ravel J, Forney LJ, Abdo Z. 2018. Associations between sexual habits, menstrual hygiene practices, demographics and the vaginal microbiome as revealed by Bayesian network analysis. *PLoS One* 13:e0191625. PMC5783405.
30. Culhane JF, Rauh V, McCollum KF, Elo IT, Hogan V. 2002. Exposure to chronic stress and ethnic differences in rates of bacterial vaginosis among pregnant women. *Am J Obstet Gynecol* 187:1272-6.
31. Nelson TM, Borgogna JC, Michalek RD, Roberts DW, Rath JM, Glover ED, Ravel J, Shardell MD, Yeoman CJ, Brotman RM. 2018. Cigarette smoking is associated with an altered vaginal tract metabolomic profile. *Sci Rep* 8:852. PMC5770521.
32. David N. Fredricks MD, Tina L. Fiedler, B.S., and Jeanne M. Mrazek, M.D., M.P.H. 2005. Molecular Identification of Bacteria Associated with Bacterial Vaginosis. *New England Journal of Medicine* 353.
33. Ling Z, Kong J, Liu F, Zhu H, Chen X, Wang Y, Li L, Nelson KE, Xia Y, Xiang C. 2010. Molecular analysis of the diversity of vaginal microbiota associated with bacterial vaginosis. *BMC Genomics* 11:488. PMC2996984.
34. Morrill S, Gilbert NM, Lewis AL. 2020. Gardnerella vaginalis as a Cause of Bacterial Vaginosis: Appraisal of the Evidence From in vivo Models. *Front Cell Infect Microbiol* 10:168. PMC7193744.

35. Stapleton AE. 2016. The Vaginal Microbiota and Urinary Tract Infection. *Microbiol Spectr* 4. PMC5746606.
36. Dewhirst FE, Chen T, Izard J, Paster BJ, Tanner AC, Yu WH, Lakshmanan A, Wade WG. 2010. The human oral microbiome. *J Bacteriol* 192:5002-17. PMC2944498.
37. Zhao H, Chu M, Huang Z, Yang X, Ran S, Hu B, Zhang C, Liang J. 2017. Variations in oral microbiota associated with oral cancer. *Sci Rep* 7:11773. PMC5603520.
38. Deo PN, Deshmukh R. 2019. Oral microbiome: Unveiling the fundamentals. *J Oral Maxillofac Pathol* 23:122-128. PMC6503789.
39. Perera M, Al-Hebshi NN, Speicher DJ, Perera I, Johnson NW. 2016. Emerging role of bacteria in oral carcinogenesis: a review with special reference to periopathogenic bacteria. *J Oral Microbiol* 8:32762. PMC5039235.
40. Sultan AS, Kong EF, Rizk AM, Jabra-Rizk MA. 2018. The oral microbiome: A Lesson in coexistence. *PLoS Pathog* 14:e1006719. PMC5784999.
41. Moon JH, Lee JH. 2016. Probing the diversity of healthy oral microbiome with bioinformatics approaches. *BMB Rep* 49:662-670. PMC5346311.
42. Caselli E, Fabbri C, D'Accolti M, Soffritti I, Bassi C, Mazzacane S, Franchi M. 2020. Defining the oral microbiome by whole-genome sequencing and resistome analysis: the complexity of the healthy picture. *BMC Microbiol* 20:120. PMC7236360.
43. Bäckhed F, Ding H, Wang T, Hooper LV, Gou YK, Nagy A, Semenkovich CF, Gordon JI. 2004. The gut microbiota as an environmental factor that regulates fat storage. *Proceedings of the National Academy of Sciences of the United States of America* 101:15718-15723. PMCID: PMC524219.
44. Backhed F, Fraser CM, Ringel Y, Sanders ME, Sartor RB, Sherman PM, Versalovic J, Young V, Finlay BB. 2012. Defining a healthy human gut microbiome: current concepts, future directions, and clinical applications. *Cell Host Microbe* 12:611-22.
45. Hathaway-Schrader JD, Novince CM. 2021. Maintaining homeostatic control of periodontal bone tissue. *Periodontol 2000* 86:157-187. PMC8294452.
46. Abusleme L, Dupuy AK, Dutzan N, Silva N, Burleson JA, Strausbaugh LD, Gamonal J, Diaz PI. 2013. The subgingival microbiome in health and periodontitis and its relationship with community biomass and inflammation. *ISME J* 7:1016-25. PMC3635234.
47. Datta HK, Ng WF, Walker JA, Tuck SP, Varanasi SS. 2008. The cell biology of bone metabolism. *J Clin Pathol* 61:577-87.

48. Loos BGC, Jeroen; Hoek, Frans J.; Wertheim-van Dillen, Paulien M. E.; van der Velden, Ubele. 2000. Elevation of Systemic Markers Related to Cardiovascular Diseases in the Peripheral Blood of Periodontitis Patients. *Journal of Periodontology* 71:1528-34.
49. Dieterich W, Schink M, Zopf Y. 2018. Microbiota in the Gastrointestinal Tract. *Med Sci (Basel)* 6. PMC6313343.
50. Barker N. 2014. Adult intestinal stem cells: critical drivers of epithelial homeostasis and regeneration. *Nat Rev Mol Cell Biol* 15:19-33.
51. Helander HF, Fandriks L. 2014. Surface area of the digestive tract - revisited. *Scand J Gastroenterol* 49:681-9.
52. Snoeck V, Goddeeris B, Cox E. 2005. The role of enterocytes in the intestinal barrier function and antigen uptake. *Microbes Infect* 7:997-1004.
53. Miron N, Cristea V. 2012. Enterocytes: active cells in tolerance to food and microbial antigens in the gut. *Clin Exp Immunol* 167:405-12. PMC3374272.
54. Allaire JM, Morampudi V, Crowley SM, Stahl M, Yu H, Bhullar K, Knodler LA, Bressler B, Jacobson K, Vallance BA. 2018. Frontline defenders: goblet cell mediators dictate host-microbe interactions in the intestinal tract during health and disease. *Am J Physiol Gastrointest Liver Physiol* 314:G360-G377. PMC5899238.
55. Swidsinski AL-B, Vera; Lochs, Herbert; Hale, Laura P. 2005. Spatial organization of bacterial flora in normal and inflamed intestine: A fluorescence in situ hybridization study in mice. *World Journal of Gastroenterology* 11:1131-1140.
56. Ley RE, Turnbaugh PJ, Klein S, Gordon JI. 2006. Human gut microbes associated with obesity. *Nature* 444:1022-1023.
57. Arumugam M, Raes J, Pelletier E, Le Paslier D, Yamada T, Mende DR, Fernandes GR, Tap J, Bruls T, Batto JM, Bertalan M, Borruel N, Casellas F, Fernandez L, Gautier L, Hansen T, Hattori M, Hayashi T, Kleerebezem M, Kurokawa K, Leclerc M, Levenez F, Manichanh C, Nielsen HB, Nielsen T, Pons N, Poulain J, Qin J, Sicheritz-Ponten T, Tims S, Torrents D, Ugarte E, Zoetendal EG, Wang J, Guarner F, Pedersen O, de Vos WM, Brunak S, Dore J, Meta HITC, Antolin M, Artiguenave F, Blottiere HM, Almeida M, Brechot C, Cara C, Chervaux C, Cultrone A, Delorme C, Denariáz G, et al. 2011. Enterotypes of the human gut microbiome. *Nature* 473:174-80. PMC3728647.
58. Rodriguez JM, Murphy K, Stanton C, Ross RP, Kober OI, Juge N, Avershina E, Rudi K, Narbad A, Jenmalm MC, Marchesi JR, Collado MC. 2015. The composition of the gut microbiota throughout life, with an emphasis on early life. *Microb Ecol Health Dis* 26:26050. PMC4315782.
59. King CH, Desai H, Sylvetsky AC, Lotempio Id J, Ayanyan S, Carrie J, Crandallid KA, Fochtman BC, Gasparyan L, Gulzar N, Howell P, Issa N, Krampis K, Mishra

- L, Morizono H, Pisegna JR, Rao S, Renid Y, Simonyan V, Smith K, Vedbrat S, Yao MD, Mazumderid R. 2019. Baseline human gut microbiota profile in healthy people and standard reporting template. doi:10.1371/journal.pone.0206484.
60. Peroni DG, Nuzzi G, Trambusti I, Di Cicco ME, Comberiati P. 2020. Microbiome Composition and Its Impact on the Development of Allergic Diseases. *Frontiers in Immunology* 11.
 61. O'Malley MA, Skillings DJ. 2018. Methodological Strategies in Microbiome Research and their Explanatory Implications. *Perspectives on Science* 26:239-265.
 62. Turnbaugh PJ, Hamady M, Yatsunencko T, Cantarel BL, Duncan A, Ley RE, Sogin ML, Jones WJ, Roe BA, Affourtit JP, Egholm M, Henrissat B, Heath AC, Knight R, Gordon JI. 2009. A core gut microbiome in obese and lean twins. *Nature* 457:480-484.
 63. Matthew J. Bull NTP. 2014. Part 1: The Human Gut Microbiome in Health and Disease. *Integrative Medicine* 13.
 64. Frank DN, St. Amand AL, Feldman RA, Boedeker EC, Harpaz N, Pace NR. 2007. Molecular-phylogenetic characterization of microbial community imbalances in human inflammatory bowel diseases. *Proceedings of the National Academy of Sciences of the United States of America* 104:13780-13785. PMID: PMC1959459.
 65. Baumgart DC, Sandborn WJ. 2007. Inflammatory bowel disease: clinical aspects and established and evolving therapies. *Lancet* 369:1641-57.
 66. Nagalingam NA, Lynch SV. 2012. Role of the microbiota in inflammatory bowel diseases. *Inflamm Bowel Dis* 18:968-84.
 67. Ott SJ, Musfeldt M, Wenderoth DF, Hampe J, Brant O, Fölsch UR, Timmis KN, Schreiber S. 2004. Reduction in diversity of the colonic mucosa associated bacterial microflora in patients with active inflammatory bowel disease. *Gut* 53:685-693. PMID: PMC1774050.
 68. Zhang Z, Zhang H, Chen T, Shi L, Wang D, Tang D. 2022. Regulatory role of short-chain fatty acids in inflammatory bowel disease. *Cell Commun Signal* 20:64. PMID: PMC9097439.
 69. Vinolo MA, Rodrigues HG, Nachbar RT, Curi R. 2011. Regulation of inflammation by short chain fatty acids. *Nutrients* 3:858-76. PMID: PMC3257741.
 70. Colman RJ, Rubin DT. 2014. Fecal microbiota transplantation as therapy for inflammatory bowel disease: a systematic review and meta-analysis. *J Crohns Colitis* 8:1569-81. PMID: PMC4296742.
 71. Kasai C, Sugimoto K, Moritani I, Tanaka J, Oya Y, Inoue H, Tameda M, Shiraki K, Ito M, Takei Y, Takase K. 2015. Comparison of the gut microbiota composition

- between obese and non-obese individuals in a Japanese population, as analyzed by terminal restriction fragment length polymorphism and next-generation sequencing. *BMC Gastroenterol* 15:100. PMC4531509.
72. Guirro M, Costa A, Gual-Grau A, Herrero P, Torrell H, Canela N, Arola L. 2019. Effects from diet-induced gut microbiota dysbiosis and obesity can be ameliorated by fecal microbiota transplantation: A multiomics approach. *PLoS One* 14:e0218143. PMC6756520.
 73. John GK, Mullin GE. 2016. The Gut Microbiome and Obesity. *Curr Oncol Rep* 18:45.
 74. Aoun A, Darwish F, Hamod N. 2020. The Influence of the Gut Microbiome on Obesity in Adults and the Role of Probiotics, Prebiotics, and Synbiotics for Weight Loss. *Prev Nutr Food Sci* 25:113-123. PMC7333005.
 75. Riva A, Borgo F, Lassandro C, Verduci E, Morace G, Borghi E, Berry D. 2017. Pediatric obesity is associated with an altered gut microbiota and discordant shifts in Firmicutes populations. *Environ Microbiol* 19:95-105. PMC5516186.
 76. McNabney SM, Henagan TM. 2017. Short Chain Fatty Acids in the Colon and Peripheral Tissues: A Focus on Butyrate, Colon Cancer, Obesity and Insulin Resistance. *Nutrients* 9. PMC5748798.
 77. Vijay A, Valdes AM. 2022. Role of the gut microbiome in chronic diseases: a narrative review. *Eur J Clin Nutr* 76:489-501. PMC8477631.
 78. Maffei C, Martina A, Corradi M, Quarella S, Nori N, Torriani S, Plebani M, Contreas G, Felis GE. 2016. Association between intestinal permeability and faecal microbiota composition in Italian children with beta cell autoimmunity at risk for type 1 diabetes. *Diabetes Metab Res Rev* 32:700-709.
 79. Flint HJ, Scott KP, Duncan SH, Louis P, Forano E. 2012. Microbial degradation of complex carbohydrates in the gut. *Gut Microbes* 3:289-306. PMC3463488.
 80. Sommer F, Backhed F. 2013. The gut microbiota--masters of host development and physiology. *Nat Rev Microbiol* 11:227-38.
 81. Roderick I Mackie AS, H Rex Gaskins. 1999. Developmental microbial ecology of the neonatal gastrointestinal tract. *Am J Clin Nutr* 69:1035S-45S.
 82. Reet Mandar MM. 1996. Transmission of Mother's Microflora to the Newborn at Birth. *Biology of the Neonate* 69:30-35.
 83. Bokulich NA, Chung J, Battaglia T, Henderson N, Jay M, Li H, A DL, Wu F, Perez-Perez GI, Chen Y, Schweizer W, Zheng X, Contreras M, Dominguez-Bello MG, Blaser MJ. 2016. Antibiotics, birth mode, and diet shape microbiome maturation during early life. *Sci Transl Med* 8:343ra82. PMC5308924.

84. Xu CZ, Huaiqiu; Qui, Peng. 2019. Aging progression of human gut microbiota. *BMC Microbiology* 19. PMC6824049.
85. An R, Wilms E, Masclee AAM, Smidt H, Zoetendal EG, Jonkers D. 2018. Age-dependent changes in GI physiology and microbiota: time to reconsider? *Gut* 67:2213-2222.
86. Rashidi A, Ebadi M, Rehman TU, Elhousseini H, Nalluri H, Kaiser T, Holtan SG, Khoruts A, Weisdorf DJ, Staley C. 2021. Gut microbiota response to antibiotics is personalized and depends on baseline microbiota. *Microbiome* 9:211. PMC8549152.
87. Leshem A, Segal E, Elinav E. 2020. The Gut Microbiome and Individual-Specific Responses to Diet. *mSystems* 5. PMC7527138.
88. Schupack DA, Mars RAT, Voelker DH, Abeykoon JP, Kashyap PC. 2021. The promise of the gut microbiome as part of individualized treatment strategies. *Nature Reviews Gastroenterology & Hepatology* 19:7-25.
89. Dethlefsen L, Relman DA. 2011. Incomplete recovery and individualized responses of the human distal gut microbiota to repeated antibiotic perturbation. *Proc Natl Acad Sci U S A* 108 Suppl 1:4554-61. PMC3063582.
90. Faith JJ, Guruge JL, Charbonneau M, Subramanian S, Seedorf H, Goodman AL, Clemente JC, Knight R, Heath AC, Leibel RL, Rosenbaum M, Gordon JI. 2013. The long-term stability of the human gut microbiota. *Science* 341:1237439. PMC3791589.
91. Tong M, McHardy I, Ruegger P, Goudarzi M, Kashyap PC, Haritunians T, Li X, Graeber TG, Schwager E, Huttenhower C, Fornace AJ, Jr., Sonnenburg JL, McGovern DP, Borneman J, Braun J. 2014. Reprogramming of gut microbiome energy metabolism by the FUT2 Crohn's disease risk polymorphism. *ISME J* 8:2193-206. PMC4992076.
92. Bonder MJ, Kurilshikov A, Tigchelaar EF, Mujagic Z, Imhann F, Vila AV, Deelen P, Vatanen T, Schirmer M, Smeekens SP, Zhernakova DV, Jankipersadsing SA, Jaeger M, Oosting M, Cenit MC, Masclee AA, Swertz MA, Li Y, Kumar V, Joosten L, Harmsen H, Weersma RK, Franke L, Hofker MH, Xavier RJ, Jonkers D, Netea MG, Wijmenga C, Fu J, Zhernakova A. 2016. The effect of host genetics on the gut microbiome. *Nat Genet* 48:1407-1412.
93. Wang J, Thingholm LB, Skieceviciene J, Rausch P, Kummen M, Hov JR, Degenhardt F, Heinsen FA, Ruhlemann MC, Szymczak S, Holm K, Esko T, Sun J, Pricop-Jeckstadt M, Al-Dury S, Bohov P, Bethune J, Sommer F, Ellinghaus D, Berge RK, Hubenthal M, Koch M, Schwarz K, Rimbach G, Hubbe P, Pan WH, Sheibani-Tezerji R, Hasler R, Rosenstiel P, D'Amato M, Cloppenburg-Schmidt K, Kunzel S, Laudes M, Marschall HU, Lieb W, Nothlings U, Karlsen TH, Baines JF, Franke A. 2016. Genome-wide association analysis identifies variation in vitamin

- D receptor and other host factors influencing the gut microbiota. *Nat Genet* 48:1396-1406. PMC5626933.
94. Goodrich JK, Davenport ER, Beaumont M, Jackson MA, Knight R, Ober C, Spector TD, Bell JT, Clark AG, Ley RE. 2016. Genetic Determinants of the Gut Microbiome in UK Twins. *Cell Host Microbe* 19:731-43. PMC4915943.
 95. Goodrich JK, Waters JL, Poole AC, Sutter JL, Koren O, Blekhman R, Beaumont M, Van Treuren W, Knight R, Bell JT, Spector TD, Clark A, Ley RE. 2014. Human genetics shape the gut microbiome. *Cell* 159:789-799. PubMed Commons.
 96. Xie H, Guo R, Zhong H, Feng Q, Lan Z, Qin B, Ward KJ, Jackson MA, Xia Y, Chen X, Chen B, Xia H, Xu C, Li F, Xu X, Al-Aama JY, Yang H, Wang J, Kristiansen K, Wang J, Steves CJ, Bell JT, Li J, Spector TD, Jia H. 2016. Shotgun Metagenomics of 250 Adult Twins Reveals Genetic and Environmental Impacts on the Gut Microbiome. *Cell Syst* 3:572-584 e3. PMC6309625.
 97. Yatsunenkov T, Rey FE, Manary MJ, Trehan I, Dominguez-Bello MG, Contreras M, Magris M, Hidalgo G, Baldassano RN, Anokhin AP, Heath AC, Warner B, Reeder J, Kuczynski J, Caporaso JG, Lozupone CA, Lauber C, Clemente JC, Knights D, Knight R, Gordon JI. 2012. Human gut microbiome viewed across age and geography, vol 486, p 222-227. *Nature*.
 98. Krassas GE, Poppe K, Glinoeer D. 2010. Thyroid function and human reproductive health. *Endocr Rev* 31:702-55.
 99. Smith TJ, Hegedus L. 2016. Graves' Disease. *N Engl J Med* 375:1552-1565.
 100. Chistiakov DA. 2003. Thyroid-stimulating hormone receptor and its role in Graves' disease. *Mol Genet Metab* 80:377-88.
 101. McIver BM, John C. 1998. The Pathogenesis of Graves' Disease. *Endocrinology and Metabolism Clinics of North America* 27:73-89.
 102. Tonstad S, Nathan E, Oda K, Fraser GE. 2015. Prevalence of hyperthyroidism according to type of vegetarian diet. *Public Health Nutr* 18:1482-7. PMC4377303.
 103. Ishaq HM, Mohammad IS, Shahzad M, Ma C, Raza MA, Wu X, Guo H, Shi P, Xu J. 2018. Molecular Alteration Analysis of Human Gut Microbial Composition in Graves' disease Patients. *Int J Biol Sci* 14:1558-1570. PMC6158725.
 104. Kohling HL, Plummer SF, Marchesi JR, Davidge KS, Ludgate M. 2017. The microbiota and autoimmunity: Their role in thyroid autoimmune diseases. *Clin Immunol* 183:63-74.
 105. Covelli D, Ludgate M. 2017. The thyroid, the eyes and the gut: a possible connection. *J Endocrinol Invest* 40:567-576.

106. Gilbert JA, Stephens B. 2018. Microbiology of the built environment. *Nat Rev Microbiol* 16:661-670.
107. Ahn J, Hayes RB. 2021. Environmental Influences on the Human Microbiome and Implications for Noncommunicable Disease. *Annu Rev Public Health* 42:277-292. PMC8641399.
108. Lax S, Smith DP, Hampton-Marcell J, Owens SM, Handley KM, Scott NM, Gibbons SM, Larsen P, Shogan BD, Weiss S, Metcalf JL, Ursell LK, Vazquez-Baeza Y, Van Treuren W, Hasan NA, Gibson MK, Colwell R, Dantas G, Knight R, Gilbert JA. 2014. Longitudinal analysis of microbial interaction between humans and the indoor environment. *Science* 345:1048-52. PMC4337996.
109. Eder WvM, Erika. 2004. Hygiene hypothesis and endotoxin: what is the evidence? *Current Opinion in Allergy and Clinical Immunology* 4:113-117.
110. Abrahamsson TR, Jakobsson HE, Andersson AF, Bjorksten B, Engstrand L, Jenmalm MC. 2014. Low gut microbiota diversity in early infancy precedes asthma at school age. *Clin Exp Allergy* 44:842-50.
111. Markus J Ege MD, Melanie Mayer, Ph.D., Anne-Cecile Normand, Ph.D., Jon Genuneit, M.D., William O.C.M. Cookson, M.D., D.Phil., Charlotte Braun - Fahrlander, M.D., Dick Heederik, Ph.D., Renaud Piarroux, M.D., Ph.D., and Erika von Mutius, M.D. 2011. Exposure to Environmental Microorganisms and Childhood Asthma. *New England Journal of Medicine* 364:701-709.
112. Stein MM, Hrusch CL, Gozdz J, Igartua C, Pivniouk V, Murray SE, Ledford JG, Marques Dos Santos M, Anderson RL, Metwali N, Neilson JW, Maier RM, Gilbert JA, Holbreich M, Thorne PS, Martinez FD, von Mutius E, Vercelli D, Ober C, Sperling AI. 2016. Innate Immunity and Asthma Risk in Amish and Hutterite Farm Children. *N Engl J Med* 375:411-421. PMC5137793.
113. McMaughan DJ, Oloruntoba O, Smith ML. 2020. Socioeconomic Status and Access to Healthcare: Interrelated Drivers for Healthy Aging. *Front Public Health* 8:231. PMC7314918.
114. Marmot M. 2006. Smoking and inequalities. *Lancet* 368:341-2.
115. Diez Roux AV, Mair C. 2010. Neighborhoods and health. *Ann N Y Acad Sci* 1186:125-45.
116. Gangrade N, Figueroa J, Leak TM. 2021. Socioeconomic Disparities in Foods/Beverages and Nutrients Consumed by U.S. Adolescents When Snacking: National Health and Nutrition Examination Survey 2005-2018. *Nutrients* 13. PMC8399168.
117. Signorello LB, Cohen SS, Williams DR, Munro HM, Hargreaves MK, Blot WJ. 2014. Socioeconomic status, race, and mortality: a prospective cohort study. *Am J Public Health* 104:e98-e107. PMC4232159.

118. Ekblom AA, Hans-Olov; Helmick, Charles G; Jonzon, Anders; Zach, Matthew M. 1990. Perinatal risk factors for inflammatory bowel disease: A case-control study. *American Journal of Epidemiology* 132:1111-1119.
119. Miller GE, Engen PA, Gillevet PM, Shaikh M, Sikaroodi M, Forsyth CB, Mutlu E, Keshavarzian A. 2016. Lower Neighborhood Socioeconomic Status Associated with Reduced Diversity of the Colonic Microbiota in Healthy Adults. *PLoS One* 11:e0148952. PMC4747579.
120. Rook GA, Raison CL, Lowry CA. 2014. Microbial 'old friends', immunoregulation and socioeconomic status. *Clin Exp Immunol* 177:1-12. PMC4089149.
121. De Filippo C, Cavalieri D, Di Paola M, Ramazzotti M, Poullet JB, Massart S, Collini S, Pieraccini G, Lionetti P. 2010. Impact of diet in shaping gut microbiota revealed by a comparative study in children from Europe and rural Africa. *Proceedings of the National Academy of Sciences of the United States of America* 107:14691-14696.
122. Morton ER, Lynch J, Froment A, Lafosse S, Heyer E, Przeworski M, Blekhman R, Segurel L. 2015. Variation in Rural African Gut Microbiota Is Strongly Correlated with Colonization by *Entamoeba* and Subsistence. *PLoS Genet* 11:e1005658. PMC4664238.
123. Gupta VK, Paul S, Dutta C. 2017. Geography, Ethnicity or Subsistence-Specific Variations in Human Microbiome Composition and Diversity. *Front Microbiol* 8:1162. PMC5481955.
124. McKenney PT, Pamer EG. 2015. From Hype to Hope: The Gut Microbiota in Enteric Infectious Disease. *Cell* 163:1326-32. PMC4672394.
125. Wu M, McNulty NP, Rodionov DA, Khoroshkin MS, Griffin NW, Cheng J, Latreille P, Kerstetter RA, Terrapon N, Henrissat B, Osterman AL, Gordon JI. 2015. Genetic determinants of in vivo fitness and diet responsiveness in multiple human gut *Bacteroides*. *Science* 350.
126. Zhang C, Zhang M, Wang S, Han R, Cao Y, Hua W, Mao Y, Zhang X, Pang X, Wei C, Zhao G, Chen Y, Zhao L. 2010. Interactions between gut microbiota, host genetics and diet relevant to development of metabolic syndromes in mice. *ISME J* 4:232-41.
127. Venn BJ. 2020. Macronutrients and Human Health for the 21st Century. *Nutrients* 12. PMC7468865.
128. Tippet KSC, Linda E. 2001. Results FROM USDA's 1994-96 Diet and Health Knowledge Survey. United States Department of Agriculture, Beltsville, Maryland.
129. Bourdeau-Julien I, Castonguay-Paradis S, Rochefort G, Perron J, Lamarche B, Flamand N, Di Marzo V, Veilleux A, Raymond F. 2023. The diet rapidly and

- differentially affects the gut microbiota and host lipid mediators in a healthy population. *Microbiome* 11:26. PMC9921707.
130. Turnbaugh PJ, Ridaura VK, Faith JJ, Rey FE, Knight R, Gordon JI. 2009. The effect of diet on the human gut microbiome: A metagenomic analysis in humanized gnotobiotic mice. *Science Translational Medicine* 1.
 131. Ye Z, Wang S, Zhang C, Zhao Y. 2020. Coordinated Modulation of Energy Metabolism and Inflammation by Branched-Chain Amino Acids and Fatty Acids. *Front Endocrinol (Lausanne)* 11:617. PMC7506139.
 132. David LA, Maurice CF, Carmody RN, Gootenberg DB, Button JE, Wolfe BE, Ling AV, Devlin AS, Varma Y, Fischbach MA, Biddinger SB, Dutton RJ, Turnbaugh PJ. 2014. Diet rapidly and reproducibly alters the human gut microbiome. *Nature* 505:559-63. PMC3957428.
 133. Reddy BSW, John H; Wynder, Ernst L. 1974. Effects of High Risk and Low Risk Diets for Colon Carcinogenesis on Fecal Microflora and Steroids in Man. *The Journal of Nutrition* 105:878-884.
 134. Singh RK, Chang HW, Yan D, Lee KM, Ucmak D, Wong K, Abrouk M, Farahnik B, Nakamura M, Zhu TH, Bhutani T, Liao W. 2017. Influence of diet on the gut microbiome and implications for human health. *J Transl Med* 15:73. PMC5385025.
 135. Jantchou P, Morois S, Clavel-Chapelon F, Boutron-Ruault MC, Carbonnel F. 2010. Animal protein intake and risk of inflammatory bowel disease: The E3N prospective study. *Am J Gastroenterol* 105:2195-201.
 136. Rule DCB, K. S.; Shellito, S. M.; Maiorano, G. 2002. Comparison of muscle fatty acid profiles and cholesterol concentrations of bison, beef cattle, elk, and chicken. *Journal of Animal Science* 80:1202-1211.
 137. Cordain LW, BA; Florant, GL; Kelher, M; Rogers, L; Li, Y. 2002. Fatty acid analysis of wild ruminant tissues: evolutionary implications for reducing diet-related chronic disease. *European Journal of Clinical Nutrition* 56:181-191.
 138. Wu GD, Chen J, Hoffmann C, Bittinger K, Chen YY, Keilbaugh SA, Bewtra M, Knights D, Walters WA, Knight R, Sinha R, Gilroy E, Gupta K, Baldassano R, Nessel L, Li H, Bushman FD, Lewis JD. 2011. Linking long-term dietary patterns with gut microbial enterotypes. *Science* 334:105-108.
 139. Hildebrandt MA, Hoffmann C, Sherrill-Mix SA, Keilbaugh SA, Hamady M, Chen YY, Knight R, Ahima RS, Bushman F, Wu GD. 2009. High-fat diet determines the composition of the murine gut microbiome independently of obesity. *Gastroenterology* 137:1716-24 e1-2. PMC2770164.
 140. Fichtel K, Mathes F, Konneke M, Cypionka H, Engelen B. 2012. Isolation of sulfate-reducing bacteria from sediments above the deep-subseafloor aquifer. *Front Microbiol* 3:65. PMC3282481.

141. Ijssennagger N, van der Meer R, van Mil SWC. 2016. Sulfide as a Mucus Barrier-Breaker in Inflammatory Bowel Disease? *Trends Mol Med* 22:190-199.
142. Mashek DG, Wu C. 2015. MUFAs. *Adv Nutr* 6:276-7. PMC4424766.
143. Colica C, Di Renzo L, Trombetta D, Smeriglio A, Bernardini S, Cioccoloni G, Costa de Miranda R, Gualtieri P, Sinibaldi Salimei P, De Lorenzo A. 2017. Antioxidant Effects of a Hydroxytyrosol-Based Pharmaceutical Formulation on Body Composition, Metabolic State, and Gene Expression: A Randomized Double-Blinded, Placebo-Controlled Crossover Trial. *Oxid Med Cell Longev* 2017:2473495. PMC5569630.
144. Babio NT, Estafania; Estruch, Ramon; Ros, Emilio; Martinez-Gonzalez, Miguel A; Castaner, Olga; Bullo, Monica; Corella, Dolores; Aros, Fernando; Gomez-Gracia, Enrique; Ruis-Gutierrez, Valentina; Fiol, Miquel; Lapetra, Jose; Lamuela-Raventos, Rosa M.; Serra-Majem, Lluís; Pinto, Xavier; Basora, Josep; Sorli, Jose V.; Salad-Salvado, Jordi. 2014. Mediterranean diets and metabolic syndrome status in the PREDIMED randomized trial. *Canadian Medical Association Journal* 186:E649-E657.
145. Estruch R, Ros E, Salas-Salvado J, Covas MI, Corella D, Aros F, Gomez-Gracia E, Ruiz-Gutierrez V, Fiol M, Lapetra J, Lamuela-Raventos RM, Serra-Majem L, Pinto X, Basora J, Munoz MA, Sorli JV, Martinez JA, Fito M, Gea A, Hernan MA, Martinez-Gonzalez MA, Investigators PS. 2018. Primary Prevention of Cardiovascular Disease with a Mediterranean Diet Supplemented with Extra-Virgin Olive Oil or Nuts. *N Engl J Med* 378:e34.
146. Wolters M, Ahrens J, Romani-Perez M, Watkins C, Sanz Y, Benitez-Paez A, Stanton C, Gunther K. 2019. Dietary fat, the gut microbiota, and metabolic health - A systematic review conducted within the MyNewGut project. *Clin Nutr* 38:2504-2520.
147. Rinninella E, Cintoni M, Raoul P, Lopetuso LR, Scaldaferri F, Pulcini G, Miggiano GAD, Gasbarrini A, Mele MC. 2019. Food Components and Dietary Habits: Keys for a Healthy Gut Microbiota Composition. *Nutrients* 11. PMC6835969.
148. Noriega BS, Sanchez-Gonzalez MA, Salyakina D, Coffman J. 2016. Understanding the Impact of Omega-3 Rich Diet on the Gut Microbiota. *Case Rep Med* 2016:3089303. PMC4808672.
149. Menni C, Zierer J, Pallister T, Jackson MA, Long T, Mhoney RP, Steves CJ, Spector TD, Valdes AM. 2017. Omega-3 fatty acids correlate with gut microbiome diversity and production of N-carbamylglutamate in middle aged and elderly women. *Sci Rep* 7:11079. PMC5593975.
150. Watson H, Mitra S, Croden FC, Taylor M, Wood HM, Perry SL, Spencer JA, Quirke P, Toogood GJ, Lawton CL, Dye L, Loadman PM, Hull MA. 2018. A randomised trial of the effect of omega-3 polyunsaturated fatty acid supplements on the human intestinal microbiota. *Gut* 67:1974-1983.

151. Kaliannan K, Wang B, Li XY, Kim KJ, Kang JX. 2015. A host-microbiome interaction mediates the opposing effects of omega-6 and omega-3 fatty acids on metabolic endotoxemia. *Sci Rep* 5:11276. PMC4650612.
152. Simopoulos AP. 2008. The importance of the omega-6/omega-3 fatty acid ratio in cardiovascular disease and other chronic diseases. *Exp Biol Med (Maywood)* 233:674-88.
153. Kang JX. 2011. The Omega-6/Omega-3 Fatty Acid Ratio in Chronic Diseases: Animal Models and Molecular Aspects, p 22-29. *In* Simopoulos AP (ed), *Healthy Agriculture, Healthy Nutrition, Healthy People*, vol 102. Karger, Basel, Switzerland.
154. Stumpel FB, Remy; Jungermann, Kurt; Thorens, Bernard. 2001. Normal kinetics of intestinal glucose absorption in the absence of GLUT2: Evidence for a transport pathway requiring glucose phosphorylation and transfer into the endoplasmic reticulum. *PNAS* 98:11330-11335.
155. Chen L, Tuo B, Dong H. 2016. Regulation of Intestinal Glucose Absorption by Ion Channels and Transporters. *Nutrients* 8. PMC4728656.
156. Gromova LV, Fetisov SO, Gruzdkov AA. 2021. Mechanisms of Glucose Absorption in the Small Intestine in Health and Metabolic Diseases and Their Role in Appetite Regulation. *Nutrients* 13. PMC8308647.
157. Rao SSCA, Ashok; Anderson, Leslie; Stumbo, Phyllis. 2007. The Ability of the Normal Human Small Intestine to Absorb Fructose: Evaluation by Breath Testing. *Clinical Gastroenterology and Hepatology* 5:959-963.
158. Staff AHAE. 2023. How much sugar is too much?, *on* American Heart Association. Accessed
159. Di Rienzi SC, Britton RA. 2020. Adaptation of the Gut Microbiota to Modern Dietary Sugars and Sweeteners. *Adv Nutr* 11:616-629. PMC7231582.
160. Anonymous. 2019. *Dietary Fiber: Properties, Recovery, and Applications*, 1 ed. Academic Press, Cambridge, Massachusetts.
161. Zhang N, Ju Z, Zuo T. 2018. Time for food: The impact of diet on gut microbiota and human health. *Nutrition* 51-52:80-85.
162. Chakaroun RM, Massier L, Kovacs P. 2020. Gut Microbiome, Intestinal Permeability, and Tissue Bacteria in Metabolic Disease: Perpetrators or Bystanders? *Nutrients* 12. PMC7230435.
163. Sonnenburg ED, Sonnenburg JL. 2014. Starving our microbial self: the deleterious consequences of a diet deficient in microbiota-accessible carbohydrates. *Cell Metab* 20:779-786. PMC4896489.

164. Tan J, McKenzie C, Vuillermin PJ, Goverse G, Vinuesa CG, Mebius RE, Macia L, Mackay CR. 2016. Dietary Fiber and Bacterial SCFA Enhance Oral Tolerance and Protect against Food Allergy through Diverse Cellular Pathways. *Cell Rep* 15:2809-24.
165. Kovatcheva-Datchary P, Nilsson A, Akrami R, Lee YS, De Vadder F, Arora T, Hallen A, Martens E, Bjorck I, Backhed F. 2015. Dietary Fiber-Induced Improvement in Glucose Metabolism Is Associated with Increased Abundance of *Prevotella*. *Cell Metab* 22:971-82.
166. Li X, Guo J, Ji K, Zhang P. 2016. Bamboo shoot fiber prevents obesity in mice by modulating the gut microbiota. *Sci Rep* 6:32953. PMC5013436.
167. Gibson GR, Scott KP, Rastall RA, Tuohy KM, Hotchkiss A, Dubert-Ferrandon A, Gareau M, Murphy EF, Saulnier D, Loh G, Macfarlane S, Delzenne N, Ringel Y, Kozianowski G, Dickmann R, Lenoir-Wijnkoop I, Walker C, Buddington R. 2010. Dietary prebiotics: current status and new definition. *Food Science & Technology Bulletin: Functional Foods* 7:1-19.
168. Louis P, Flint HJ, Michel C. 2016. How to Manipulate the Microbiota: Prebiotics. *Adv Exp Med Biol* 902:119-42.
169. Macfarlane GT, Macfarlane S. 2012. Bacteria, colonic fermentation, and gastrointestinal health. *Journal of AOAC International* 95:50-60. PMID: 22468341.
170. Fuentes-Zaragoza E, Sánchez-Zapata E, Sendra E, Sayas E, Navarro C, Fernández-López J, Pérez-Alvarez JA. 2011. Resistant starch as prebiotic: A review. *Starch - Stärke* 63:406-415.
171. Gullón B, Gómez B, Martínez-Sabajanes M, Yáñez R, Parajó JC, Alonso JL. 2013. Pectic oligosaccharides: Manufacture and functional properties. *Trends in Food Science & Technology* 30:153-161.
172. Yoo HD, Kim D, Paek SH. 2012. Plant cell wall polysaccharides as potential resources for the development of novel prebiotics. *Biomol Ther (Seoul)* 20:371-9. PMC3762269.
173. Flint HJ, Duncan SH, Scott KP, Louis P. 2007. Interactions and competition within the microbial community of the human colon: links between diet and health. *Environ Microbiol* 9:1101-11.
174. Scott KP, Gratz SW, Sheridan PO, Flint HJ, Duncan SH. 2013. The influence of diet on the gut microbiota. *Pharmacol Res* 69:52-60.
175. Ze X, Duncan SH, Louis P, Flint HJ. 2012. *Ruminococcus bromii* is a keystone species for the degradation of resistant starch in the human colon. *ISME J* 6:1535-43. PMC3400402.

176. Belenguer A, Duncan SH, Calder AG, Holtrop G, Louis P, Lobley GE, Flint HJ. 2006. Two routes of metabolic cross-feeding between *Bifidobacterium adolescentis* and butyrate-producing anaerobes from the human gut. *Appl Environ Microbiol* 72:3593-9. PMC1472403.
177. Falony G, Vlachou A, Verbrugghe K, De Vuyst L. 2006. Cross-feeding between *Bifidobacterium longum* BB536 and acetate-converting, butyrate-producing colon bacteria during growth on oligofructose. *Appl Environ Microbiol* 72:7835-41. PMC1694233.
178. Duncan SH, Louis P, Thomson JM, Flint HJ. 2009. The role of pH in determining the species composition of the human colonic microbiota. *Environ Microbiol* 11:2112-22.
179. Walker AW, Duncan SH, McWilliam Leitch EC, Child MW, Flint HJ. 2005. pH and peptide supply can radically alter bacterial populations and short-chain fatty acid ratios within microbial communities from the human colon. *Appl Environ Microbiol* 71:3692-700. PMC1169066.
180. Silk DB, Davis A, Vulevic J, Tzortzis G, Gibson GR. 2009. Clinical trial: the effects of a trans-galactooligosaccharide prebiotic on faecal microbiota and symptoms in irritable bowel syndrome. *Aliment Pharmacol Ther* 29:508-18.
181. Videla SV, Jaime; Antolin, Maria; Garcia-Lafuente, Ana; Guarner, Francisco; Crespo, Ernesto; Casalots, Jaume; Salad, Antonio; Malagelada, Juan R. 2001. Dietary Inulin Improves Distal Colitis Induced by Dextran Sodium Sulfate in the Rat. *The American Journal of Gastroenterology* 96.
182. De Preter V, Vanhoutte T, Huys G, Swings J, De Vuyst L, Rutgeerts P, Verbeke K. 2007. Effects of *Lactobacillus casei* Shirota, *Bifidobacterium breve*, and oligofructose-enriched inulin on colonic nitrogen-protein metabolism in healthy humans. *Am J Physiol Gastrointest Liver Physiol* 292:G358-68.
183. FAO/WHO. 2002. Joint FAO/Who Working Group Report on Drafting Guidelines for the *Evaluation of Probiotics in Food*. London, Ontario, Canada.
184. O'Toole PW, Marchesi JR, Hill C. 2017. Next-generation probiotics: the spectrum from probiotics to live biotherapeutics. *Nat Microbiol* 2:17057.
185. Sanders ME, Merenstein D, Merrifield CA, Hutkins R. 2018. Probiotics for human use. *Nutrition Bulletin* 43:212-225.
186. Marco ML, Heeney D, Binda S, Cifelli CJ, Cotter PD, Foligne B, Ganzle M, Kort R, Pasin G, Pihlanto A, Smid EJ, Hutkins R. 2017. Health benefits of fermented foods: microbiota and beyond. *Curr Opin Biotechnol* 44:94-102.
187. LeBlanc JG, Laino JE, del Valle MJ, Vannini V, van Sinderen D, Taranto MP, de Valdez GF, de Giori GS, Sesma F. 2011. B-group vitamin production by lactic acid bacteria--current knowledge and potential applications. *J Appl Microbiol* 111:1297-309.

188. Chamlagain B, Sugito TA, Deptula P, Edelmann M, Kariluoto S, Varmanen P, Piironen V. 2018. In situ production of active vitamin B12 in cereal matrices using *Propionibacterium freudenreichii*. *Food Sci Nutr* 6:67-76. PMC5778212.
189. Gerez CL, Rollan GC, de Valdez GF. 2006. Gluten breakdown by lactobacilli and pediococci strains isolated from sourdough. *Lett Appl Microbiol* 42:459-64.
190. Walter J, Maldonado-Gomez MX, Martinez I. 2018. To engraft or not to engraft: an ecological framework for gut microbiome modulation with live microbes. *Curr Opin Biotechnol* 49:129-139. PMC5808858.
191. Jacobsen CNRN, V.; Hayford, A. E.; Moller, P. L.; Michaelsen, K. F.; Paerregaard, A.; Sandstrom, B.; Tvede, M.; Jakobsen, M. 1999. Screening of Probiotics Activities of Forty-Seven Strains of *Lactobacillus* spp. by In Vitro Techniques and Evaluation of the Colonization Ability of Five Selected Strains in Humans. *Applied and Environmental Microbiology* 65:4949-4956.
192. Catford JA, Jansson R, Nilsson C. 2009. Reducing redundancy in invasion ecology by integrating hypotheses into a single theoretical framework. *Diversity and Distributions* 15:22-40.
193. Mowat C, Cole A, Windsor A, Ahmad T, Arnott I, Driscoll R, Mitton S, Orchard T, Rutter M, Younge L, Lees C, Ho GT, Satsangi J, Bloom S, Gastroenterology IBDSoTBSO. 2011. Guidelines for the management of inflammatory bowel disease in adults. *Gut* 60:571-607.
194. Zocco MA, dal Verme LZ, Cremonini F, Piscaglia AC, Nista EC, Candelli M, Novi M, Rigante D, Cazzato IA, Ojetti V, Armuzzi A, Gasbarrini G, Gasbarrini A. 2006. Efficacy of *Lactobacillus* GG in maintaining remission of ulcerative colitis. *Aliment Pharmacol Ther* 23:1567-74.
195. Claes IJ, Schoofs G, Regulski K, Courtin P, Chapot-Chartier MP, Rolain T, Hols P, von Ossowski I, Reunanen J, de Vos WM, Palva A, Vanderleyden J, De Keersmaecker SC, Lebeer S. 2012. Genetic and biochemical characterization of the cell wall hydrolase activity of the major secreted protein of *Lactobacillus rhamnosus* GG. *PLoS One* 7:e31588. PMC3281093.
196. Bush K, Bradford PA. 2016. beta-Lactams and beta-Lactamase Inhibitors: An Overview. *Cold Spring Harb Perspect Med* 6. PMC4968164.
197. Zeng D, Debatov D, Hartsell TL, Cano RJ, Adams S, Schuyler JA, McMillan R, Pace JL. 2016. Approved Glycopeptide Antibacterial Drugs: Mechanism of Action and Resistance. *Cold Spring Harb Perspect Med* 6. PMC5131748.
198. Kapoor G, Saigal S, Elongavan A. 2017. Action and resistance mechanisms of antibiotics: A guide for clinicians. *J Anaesthesiol Clin Pharmacol* 33:300-305. PMC5672523.

199. Yoneyama HK, Ryoichi. 2006. Antibiotic Resistance in Bacteria and Its Future for Novel Antibiotic Development. *Bioscience Biotechnology & Biochemistry* 70:1060-1075.
200. Schlunzen FZ, Raz; Harms, Jorg; Bashan, Anat; Tocilj, Ante; Albrecht, Renate; Yonath, Ada; Franceschi, Francois. 2001. Structural basis for the interaction of antibiotics with the peptidyl transferase centre in eubacteria. *Nature* 413:814-821.
201. Bozdogan B, Appelbaum PC. 2004. Oxazolidinones: activity, mode of action, and mechanism of resistance. *Int J Antimicrob Agents* 23:113-9.
202. Higgins PGF, A.C.; Schmitz, F-J. 2003. Fluoroquinolones: Structure and Target Sites. *Current Drug Targets* 4:181-190.
203. Aminov RI. 2010. A brief history of the antibiotic era: lessons learned and challenges for the future. *Front Microbiol* 1:134. PMC3109405.
204. Czepiel J, Drozd M, Pituch H, Kuijper EJ, Perucki W, Mielimonka A, Goldman S, Wultanska D, Garlicki A, Biesiada G. 2019. Clostridium difficile infection: review. *Eur J Clin Microbiol Infect Dis* 38:1211-1221. PMC6570665.
205. Francis MB, Allen CA, Shrestha R, Sorg JA. 2013. Bile acid recognition by the Clostridium difficile germinant receptor, CspC, is important for establishing infection. *PLoS Pathog* 9:e1003356. PMC3649964.
206. Tauxe WM, Dhere T, Ward A, Racska LD, Varkey JB, Kraft CS. 2015. Fecal microbiota transplant protocol for clostridium difficile infection. *Lab Med* 46:e19-23. PMC4795811.
207. Kao D, Roach B, Silva M, Beck P, Rioux K, Kaplan GG, Chang HJ, Coward S, Goodman KJ, Xu H, Madsen K, Mason A, Wong GK, Jovel J, Patterson J, Louie T. 2017. Effect of Oral Capsule- vs Colonoscopy-Delivered Fecal Microbiota Transplantation on Recurrent Clostridium difficile Infection: A Randomized Clinical Trial. *JAMA* 318:1985-1993. PMC5820695.
208. Tap J, Mondot S, Levenez F, Pelletier E, Caron C, Furet JP, Ugarte E, Munoz-Tamayo R, Paslier DL, Nalin R, Dore J, Leclerc M. 2009. Towards the human intestinal microbiota phylogenetic core. *Environ Microbiol* 11:2574-84.
209. Ventura M, O'Flaherty S, Claesson MJ, Turrone F, Klaenhammer TR, van Sinderen D, O'Toole PW. 2009. Genome-scale analyses of health-promoting bacteria: probiogenomics. *Nat Rev Microbiol* 7:61-71.
210. Pokusaeva K, Fitzgerald GF, van Sinderen D. 2011. Carbohydrate metabolism in Bifidobacteria. *Genes Nutr* 6:285-306. PMC3145055.
211. Schell MAK, Maria; Snel, Berend; Vilanova, David; Berger, Bernard; Pessi, Gabriella; Zwahlen, Marie-Camille; Desiere, Frank; Bork, Peer; Delley, Michele; Pridmore, R David; Arigoni, Fabrizio. 2002. The genome sequence of

- Bifidobacterium longum* reflects its adaptation to the human gastrointestinal tract. PNAS 99:14422-14427.
212. Lee JH, Karamychev VN, Kozyavkin SA, Mills D, Pavlov AR, Pavlova NV, Polouchine NN, Richardson PM, Shakhova VV, Slesarev AI, Weimer B, O'Sullivan DJ. 2008. Comparative genomic analysis of the gut bacterium *Bifidobacterium longum* reveals loci susceptible to deletion during pure culture growth. BMC Genomics 9:247. PMC2430713.
 213. Kim JF, Jeong H, Yu DS, Choi SH, Hur CG, Park MS, Yoon SH, Kim DW, Ji GE, Park HS, Oh TK. 2009. Genome sequence of the probiotic bacterium *Bifidobacterium animalis* subsp. *lactis* AD011. J Bacteriol 191:678-9. PMC2620821.
 214. Barrangou R, Briczinski EP, Traeger LL, Loquasto JR, Richards M, Horvath P, Coute-Monvoisin AC, Leyer G, Rendulic S, Steele JL, Broadbent JR, Oberg T, Dudley EG, Schuster S, Romero DA, Roberts RF. 2009. Comparison of the complete genome sequences of *Bifidobacterium animalis* subsp. *lactis* DSM 10140 and BI-04. J Bacteriol 191:4144-51. PMC2698493.
 215. Rabiou BA, Jay AJ, Gibson GR, Rastall RA. 2001. Synthesis and fermentation properties of novel galacto-oligosaccharides by beta-galactosidases from *Bifidobacterium* species. Appl Environ Microbiol 67:2526-30. PMC92903.
 216. van den Broek LA, Hinz SW, Beldman G, Vincken JP, Voragen AG. 2008. *Bifidobacterium* carbohydrases-their role in breakdown and synthesis of (potential) prebiotics. Mol Nutr Food Res 52:146-63.
 217. Ejby M, Fredslund F, Andersen JM, Vujcic Zagar A, Henriksen JR, Andersen TL, Svensson B, Slotboom DJ, Abou Hachem M. 2016. An ATP Binding Cassette Transporter Mediates the Uptake of alpha-(1,6)-Linked Dietary Oligosaccharides in *Bifidobacterium* and Correlates with Competitive Growth on These Substrates. J Biol Chem 291:20220-31. PMC5025704.
 218. ter Beek J, Guskov A, Slotboom DJ. 2014. Structural diversity of ABC transporters. J Gen Physiol 143:419-35. PMC3971661.
 219. Long CP, Au J, Sandoval NR, Gebreselassie NA, Antoniewicz MR. 2017. Enzyme I facilitates reverse flux from pyruvate to phosphoenolpyruvate in *Escherichia coli*. Nat Commun 8:14316. PMC5290146.
 220. Deutscher J, Francke C, Postma PW. 2006. How phosphotransferase system-related protein phosphorylation regulates carbohydrate metabolism in bacteria. Microbiol Mol Biol Rev 70:939-1031. PMC1698508.
 221. Lorca GL, Barabote RD, Zlotopolski V, Tran C, Winnen B, Hvorup RN, Stonestrom AJ, Nguyen E, Huang LW, Kim DS, Saier MH, Jr. 2007. Transport capabilities of eleven gram-positive bacteria: comparative genomic analyses. Biochim Biophys Acta 1768:1342-66. PMC2592090.

222. Maze A, O'Connell-Motherway M, Fitzgerald GF, Deutscher J, van Sinderen D. 2007. Identification and characterization of a fructose phosphotransferase system in *Bifidobacterium breve* UCC2003. *Appl Environ Microbiol* 73:545-53. PMC1796965.
223. Scorbati BB, B; Palenzona, D. 1995. *The genus Bifidobacterium*. Springer, Berlin.
224. de Vos WM. 2017. Microbe Profile: *Akkermansia muciniphila*: a conserved intestinal symbiont that acts as the gatekeeper of our mucosa. *Microbiology (Reading)* 163:646-648.
225. Png CW, Linden SK, Gilshenan KS, Zoetendal EG, McSweeney CS, Sly LI, McGuckin MA, Florin TH. 2010. Mucolytic bacteria with increased prevalence in IBD mucosa augment in vitro utilization of mucin by other bacteria. *Am J Gastroenterol* 105:2420-8.
226. Belzer C, de Vos WM. 2012. Microbes inside--from diversity to function: the case of *Akkermansia*. *ISME J* 6:1449-58. PMC3401025.
227. Derrien M, Vaughan EE, Plugge CM, de Vos WM. 2004. *Akkermansia muciniphila* gen. nov., sp. nov., a human intestinal mucin-degrading bacterium. *Int J Syst Evol Microbiol* 54:1469-1476.
228. Glover JS, Ticer TD, Engevik MA. 2022. Characterizing the mucin-degrading capacity of the human gut microbiota. *Sci Rep* 12:8456. PMC9120202.
229. Chelakkot C, Choi Y, Kim DK, Park HT, Ghim J, Kwon Y, Jeon J, Kim MS, Jee YK, Gho YS, Park HS, Kim YK, Ryu SH. 2018. *Akkermansia muciniphila*-derived extracellular vesicles influence gut permeability through the regulation of tight junctions. *Exp Mol Med* 50:e450. PMC5903829.
230. van Passel MW, Kant R, Zoetendal EG, Plugge CM, Derrien M, Malfatti SA, Chain PS, Woyke T, Palva A, de Vos WM, Smidt H. 2011. The genome of *Akkermansia muciniphila*, a dedicated intestinal mucin degrader, and its use in exploring intestinal metagenomes. *PLoS One* 6:e16876. PMC3048395.
231. Shin NR, Whon TW, Bae JW. 2015. Proteobacteria: microbial signature of dysbiosis in gut microbiota. *Trends Biotechnol* 33:496-503.
232. Glowacki RWP, Martens EC. 2020. If you eat it, or secrete it, they will grow: the expanding list of nutrients utilized by human gut bacteria. *J Bacteriol* 203. PMC8092160.
233. Maltby R, Leatham-Jensen MP, Gibson T, Cohen PS, Conway T. 2013. Nutritional basis for colonization resistance by human commensal *Escherichia coli* strains HS and Nissle 1917 against *E. coli* O157:H7 in the mouse intestine. *PLoS One* 8:e53957. PMC3547972.

234. Lombard V, Golaconda Ramulu H, Drula E, Coutinho PM, Henrissat B. 2014. The carbohydrate-active enzymes database (CAZy) in 2013. *Nucleic Acids Res* 42:D490-5. PMC3965031.
235. Steinsiek S, Bettenbrock K. 2012. Glucose transport in *Escherichia coli* mutant strains with defects in sugar transport systems. *J Bacteriol* 194:5897-908. PMC3486086.
236. Conway T, Cohen PS. 2015. Commensal and Pathogenic *Escherichia coli* Metabolism in the Gut. *Microbiol Spectr* 3. PMC4510460.
237. Postma PWL, J. W.; Jacobson, G. R. 1993. Phosphoenolpyruvate: Carbohydrate Phosphotransferase Systems in Bacteria. *Microbiology and Molecular Biology Reviews* 57.
238. Saier MH, Jr.; Reizer, Jonathan. 1992. Proposed Uniform Nomenclature for the Proteins and Protein Domains of the Bacterial Phosphoenolpyruvate: Sugar Phosphotransferase System. *Journal of Bacteriology* 174:1433-1438.
239. Lengler JWJ, K; Wehmeier, U. F. 1994. Enzymes II of the phosphoenolpyruvate-dependent phosphotransferase systems: their structure and function in carbohydrate transport. *Biochimica et Biophysica Acta - Bioenergetics* 1188:1-28.
240. Robillard GTB, J. 1999. Structure/function studies on the bacterial carbohydrate transporters, enzymes II, of the phosphoenolpyruvate-dependent phosphotransferase system. *Biochimica et Biophysica Acta - Biomembranes* 1422:73-104.
241. Saier MH, Jr.; Cox, David F; Feucht, Bridgette U; Novotny, Michael J. 1982. Evidence for the Functional Association of Enzyme I and HPr of the Phosphoenolpyruvate-Sugar Phosphotransferase System With the Membrane in Sealed Vesicles of *Escherichia coli*. *Journal of Cellular Biochemistry* 18.
242. Epstein WR-D, Lucia B; Hesse, Joanne. 1975. Adenosine 3':5'-Cyclic Monophosphate as Mediator of Catabolite Repression in *Escherichia coli*. *PNAS* 72:2300-2304.
243. Hogema BM, Arents JC, Inada T, Aiba H, van Dam K, Postma PW. 1997. Catabolite repression by glucose 6-phosphate, gluconate and lactose in *Escherichia coli*. *Mol Microbiol* 24:857-67.
244. Botsford JLH, James G. 1992. Cyclic AMP in Prokaryotes. *Microbiological Reviews* 56:100-122.
245. Harman JG. 2001. Allosteric regulation of the cAMP receptor protein. *Biochimica et Biophysica Acta* 1547:1-17.
246. Li JC, Xiaodong; Lee, J. Ching. 2002. Structure and Dynamics of the Modular Halves of *Escherichia coli* Cyclic AMP Receptor Protein. *Biochemistry* 41:14771-14778.

247. Polit A, Blaszczyk U, Wasylewski Z. 2003. Steady-state and time-resolved fluorescence studies of conformational changes induced by cyclic AMP and DNA binding to cyclic AMP receptor protein from *Escherichia coli*. *Eur J Biochem* 270:1413-23.
248. Sheridan PO, Martin JC, Lawley TD, Browne HP, Harris HMB, Bernalier-Donadille A, Duncan SH, O'Toole PW, K PS, H JF. 2016. Polysaccharide utilization loci and nutritional specialization in a dominant group of butyrate-producing human colonic Firmicutes. *Microb Genom* 2:e000043. PMC5320581.
249. Schmid J, Heider D, Wendel NJ, Sperl N, Sieber V. 2016. Bacterial Glycosyltransferases: Challenges and Opportunities of a Highly Diverse Enzyme Class Toward Tailoring Natural Products. *Front Microbiol* 7:182. PMC4757703.
250. Onyango SO, Juma J, De Paepe K, Van de Wiele T. 2021. Oral and Gut Microbial Carbohydrate-Active Enzymes Landscape in Health and Disease. *Front Microbiol* 12:653448. PMC8702856.
251. Dintner S, Staron A, Berchtold E, Petri T, Mascher T, Gebhard S. 2011. Coevolution of ABC transporters and two-component regulatory systems as resistance modules against antimicrobial peptides in Firmicutes Bacteria. *J Bacteriol* 193:3851-62. PMC3147537.
252. Dethlefsen L, Huse S, Sogin ML, Relman DA. 2008. The Pervasive Effects of an Antibiotic on the Human Gut Microbiota, as Revealed by Deep 16S rRNA Sequencing. *PLoS Biology* 6:e280-e280.
253. Comstock LE, Coyne MJ. 2003. *Bacteroides thetaiotaomicron*: a dynamic, niche-adapted human symbiont. *BioEssays* 25:926-929. PMID: 14505359.
254. Sonnenburg JL, Xu J, Leip DD, Chen CH, Westover BP, Weatherford J, Buhler JD, Gordon JI. 2005. Glycan foraging in vivo by an intestine-adapted bacterial symbiont. *Science* 307:1955-1959. PMID: 15790854.
255. Bjursell MK, Martens EC, Gordon JI. 2006. Functional genomic and metabolic studies of the adaptations of a prominent adult human gut symbiont, *Bacteroides thetaiotaomicron*, to the suckling period. *Journal of Biological Chemistry* 281:36269-36279.
256. Reeves AR, D'Elia JN, Frias J, Salyers AA. 1996. A *Bacteroides thetaiotaomicron* outer membrane protein that is essential for utilization of maltooligosaccharides and starch. *Journal of Bacteriology* 178:823-830. PMCID: PMC177731.
257. Armendariz-Ruiz M, Rodriguez-Gonzalez JA, Camacho-Ruiz RM, Mateos-Diaz JC. 2018. Carbohydrate Esterases: An Overview. *Methods Mol Biol* 1835:39-68.
258. Grondin JM, Tamura K, Déjean G, Abbott DW, Brumer H. 2017. Polysaccharide Utilization Loci: Fueling Microbial Communities. *Journal of Bacteriology* 199:1-15.

259. Martens EC, Koropatkin NM, Smith TJ, Gordon JI. 2009. Complex Glycan Catabolism by the Human Gut Microbiota: The Bacteroidete Sus-like Paradigm. *The Journal of Biological Chemistry* 284:24673-24677.
260. Martens EC, Chiang HC, Gordon JI. 2008. Mucosal glycan foraging enhances fitness and transmission of a saccharolytic human gut bacterial symbiont. *Cell Host Microbe* 4:447-57. 2605320.
261. Tancula EF, Michael J.; Bedzyk, Laura A; Abigail A. Salyers. 1992. Location and Characterization of Genes Involved in Binding of Starch to the Surface of *Bacteroides thetaiotaomicron*. *Journal of Bacteriology* 174:5609-5616.
262. Foley MH, Cockburn DW, Koropatkin NM. 2016. The Sus operon: a model system for starch uptake by the human gut Bacteroidetes. *Cell Mol Life Sci* 73:2603-17. PMC4924478.
263. Tuson HH, Foley MH, Koropatkin NM, Biteen JS. 2018. The Starch Utilization System Assembles around Stationary Starch-Binding Proteins. *Biophys J* 115:242-250. PMC6051301.
264. Koropatkin NM, Smith TJ. 2010. SusG: a unique cell-membrane-associated alpha-amylase from a prominent human gut symbiont targets complex starch molecules. *Structure* 18:200-15.
265. Kitamura M, Okuyama M, Tanzawa F, Mori H, Kitago Y, Watanabe N, Kimura A, Tanaka I, Yao M. 2008. Structural and functional analysis of a glycoside hydrolase family 97 enzyme from *Bacteroides thetaiotaomicron*. *J Biol Chem* 283:36328-37. PMC2662298.
266. Foley MH, Martens EC, Koropatkin NM. 2018. SusE facilitates starch uptake independent of starch binding in *B. thetaiotaomicron*. *Molecular Microbiology* 108:551-566.
267. Koropatkin NM, Martens EC, Gordon JI, Smith TJ. 2008. Starch Catabolism by a Prominent Human Gut Symbiont Is Directed by the Recognition of Amylose Helices. *Structure* 16:1105-1115. PMCID: PMC2563962.
268. D'Elia JNS, Abigail A. 1996. Contribution of a Neopullulanase, a Pullulanase, and an alpha-Glucosidase to Growth of *Bacteroides thetaiotaomicron* on Starch. *Journal of Bacteriology* 178:7173-7179.
269. John N. D'Elia AAS. 1996. Effect of Regulatory Protein Levels on Utilization of Starch by *Bacteroides thetaiotaomicron*. *J Bacteriol* 178:7180-7186.
270. Sonnenburg ED, Zheng H, Joglekar P, Higginbottom SK, Firbank SJ, Bolam DN, Sonnenburg JL. 2010. Specificity of polysaccharide use in intestinal bacteroides species determines diet-induced microbiota alterations. *Cell* 141:1241-1252.
271. Ravcheev DA, Godzik A, Osterman AL, Rodionov DA. 2013. Polysaccharides utilization in human gut bacterium *Bacteroides thetaiotaomicron*: Comparative

- genomics reconstruction of metabolic and regulatory networks. *BMC Genomics* 14:1-17. PMID: PMC3878776.
272. Martens EC, Roth R, Heuser JE, Gordon JI. 2009. Coordinate regulation of glycan degradation and polysaccharide capsule biosynthesis by a prominent human gut symbiont. *J Biol Chem* 284:18445-57. PMID: PMC2709373.
273. Schwalm ND, Townsend GE, Groisman EA. 2017. Prioritization of polysaccharide utilization and control of regulator activation in *Bacteroides thetaiotaomicron*. *Molecular Microbiology* 104:32-45.
274. Townsend GE, Raghavan V, Zwir I, Groisman EA. 2013. Intramolecular arrangement of sensor and regulator overcomes relaxed specificity in hybrid two-component systems. *Proceedings of the National Academy of Sciences of the United States of America* 110:E161-E169. PMID: PMC3545799.
275. Xu J, Mahowald MA, Ley RE, Lozupone CA, Hamady M, Martens EC, Henrissat B, Coutinho PM, Minx P, Latreille P, Cordum H, Van Brunt A, Kim K, Fulton RS, Fulton LA, Clifton SW, Wilson RK, Knight RD, Gordon JI. 2007. Evolution of symbiotic bacteria in the distal human intestine. *PLoS Biol* 5:e156. PMID: PMC1892571.
276. Wongkiew S, Chaikaew P, Takrattanasaran N, Khamkajorn T. 2022. Evaluation of nutrient characteristics and bacterial community in agricultural soil groups for sustainable land management. *Sci Rep* 12:7368. PMID: PMC9072534.
277. Zhang M, Liang Y, Song A, Yu B, Zeng X, Chen M-S, Yin H, Zhang X, Sun B, Fan F. 2017. Loss of soil microbial diversity may increase insecticide uptake by crop. *Agriculture, Ecosystems & Environment* 240:84-91.
278. Berlemont R, Martiny AC. 2016. Glycoside Hydrolases across Environmental Microbial Communities. *PLoS Comput Biol* 12:e1005300. PMID: PMC5218504.
279. Loose JS, Forsberg Z, Kracher D, Scheiblbrandner S, Ludwig R, Eijsink VG, Vaaje-Kolstad G. 2016. Activation of bacterial lytic polysaccharide monoxygenases with cellobiose dehydrogenase. *Protein Sci* 25:2175-2186. PMID: PMC5119556.
280. Tamburrini KC, Terrapon N, Lombard V, Bissaro B, Longhi S, Berrin JG. 2021. Bioinformatic Analysis of Lytic Polysaccharide Monoxygenases Reveals the Pan-Families Occurrence of Intrinsically Disordered C-Terminal Extensions. *Biomolecules* 11. PMID: PMC8615602.
281. Desai MS, Seekatz AM, Koropatkin NM, Kamada N, Hickey CA, Wolter M, Pudlo NA, Kitamoto S, Terrapon N, Muller A, Young VB, Henrissat B, Wilmes P, Stappenbeck TS, Núñez G, Martens EC. 2016. A Dietary Fiber-Deprived Gut Microbiota Degrades the Colonic Mucus Barrier and Enhances Pathogen Susceptibility. *Cell* 167:1339-1353.e21.
282. Shahanshah Khan SW, Victoria Godfrey, Md Abdul Wadud Khan, Rajalaksmy A. Ramachandran, Brandi L. Cantarel, Cassie Behrendt, Lan Peng, Lora V.

- Hooper, Hasan Zaki. 2020. Dietary simple sugars alter microbial ecology in the gut and promote colitis in mice. *Science Translational Medicine*.
283. Shepherd ES, DeLoache WC, Pruss KM, Whitaker WR, Sonnenburg JL. 2018. An exclusive metabolic niche enables strain engraftment in the gut microbiota. *Nature* 557:434-438. PMC6126907.
284. Pudlo NA, Urs K, Kumar SS, German JB, Mills DA, Martens EC. 2015. Symbiotic human gut bacteria with variable metabolic priorities for host mucosal glycans. *mBio* 6:e01282-15. PMCID: PMC4659458.
285. Gorke B, Stulke J. 2008. Carbon catabolite repression in bacteria: many ways to make the most out of nutrients. *Nat Rev Microbiol* 6:613-24.
286. Magasanik B. 1961. Catabolite repression. *Cold Spring Harb Symp Quant Biol* 26:249-56.
287. Gonzalez-Gil GK, Regine; Muskhelishvili, Georgi. 1998. Regulation of *crp* transcription by oscillation between distinct nucleoprotein complexes. *EMBO J* 17:2877-2885.
288. Nasser W, Schneider R, Travers A, Muskhelishvili G. 2001. CRP modulates *fis* transcription by alternate formation of activating and repressing nucleoprotein complexes. *J Biol Chem* 276:17878-86.
289. Dai JL, Shwu-Hwa; Kemmis, Carly; Chin, Anita J.; Lee, J. Ching. 2004. Interplay between Site-Specific Mutations and Cyclic Nucleotides in Modulating DNA Recognition by *Escherichia coli* Cyclic AMP Receptor Protein. *Biochemistry* 43:8901-8910.
290. Nessler S, Fieulaine S, Poncet S, Galinier A, Deutscher J, Janin J. 2003. HPr kinase/phosphorylase, the sensor enzyme of catabolite repression in Gram-positive bacteria: structural aspects of the enzyme and the complex with its protein substrate. *J Bacteriol* 185:4003-10. PMC164879.
291. Galinier AK, Melanie; Engelmann, Roswitha; Hengstenberg, Wolfgang; Kilhoffer, Marie-Claude; Deutscher, Josef; Haiech, Jacques. 1998. New protein kinase and protein phosphate families mediate signal transduction in bacterial catabolite repression. *PNAS* 95:1823-1828.
292. Aires J, Thouverez M, Allano S, Butel MJ. 2011. Longitudinal analysis and genotyping of infant dominant bifidobacterial populations. *Syst Appl Microbiol* 34:536-41.
293. Turrone F, Peano C, Pass DA, Foroni E, Severgnini M, Claesson MJ, Kerr C, Hourihane J, Murray D, Fuligni F, Gueimonde M, Margolles A, De Bellis G, O'Toole PW, van Sinderen D, Marchesi JR, Ventura M. 2012. Diversity of bifidobacteria within the infant gut microbiota. *PLoS One* 7:e36957. PMC3350489.

294. Lozupone CA, Stombaugh J, Gonzalez A, Ackermann G, Wendel D, Vazquez-Baeza Y, Jansson JK, Gordon JI, Knight R. 2013. Meta-analyses of studies of the human microbiota. *Genome Res* 23:1704-14. PMC3787266.
295. Lahtinen SJB, Robert J.; Kivivuori, Satu; Oppedisano, Frances; Smith, Katherine R.; Robins-Browne, Roy; Salminen, Seppo; Tang, Mimi L.K. 2009. Prenatal probiotic administration can influence *Bifidobacterium* microbiota development in infants at high risk of allergy. *J Allergy Clin Immunol* 123:P499-501.E8.
296. Koenig JE, Spor A, Scalfone N, Fricker AD, Stombaugh J, Knight R, Angenent LT, Ley RE. 2011. Succession of microbial consortia in the developing infant gut microbiome. *Proceedings of the National Academy of Sciences of the United States of America* 108:4578-4585.
297. Fallani M, Amarri S, Uusijarvi A, Adam R, Khanna S, Aguilera M, Gil A, Vieites JM, Norin E, Young D, Scott JA, Dore J, Edwards CA, The Infabio T. 2011. Determinants of the human infant intestinal microbiota after the introduction of first complementary foods in infant samples from five European centres. *Microbiology (Reading)* 157:1385-1392.
298. Finamore A, Roselli M, Britti MS, Merendino N, Mengheri E. 2012. *Lactobacillus rhamnosus* GG and *Bifidobacterium animalis* MB5 induce intestinal but not systemic antigen-specific hyporesponsiveness in ovalbumin-immunized rats. *J Nutr* 142:375-81.
299. Round JL, O'Connell RM, Mazmanian SK. 2010. Coordination of tolerogenic immune responses by the commensal microbiota. *J Autoimmun* 34:J220-5. PMC3155383.
300. Strober W, Fuss IJ, Blumberg RS. 2002. The immunology of mucosal models of inflammation. *Annu Rev Immunol* 20:495-549.
301. Abraham C, Medzhitov R. 2011. Interactions between the host innate immune system and microbes in inflammatory bowel disease. *Gastroenterology* 140:1729-37. PMC4007055.
302. Jiang F, Meng D, Weng M, Zhu W, Wu W, Kasper D, Walker WA. 2017. The symbiotic bacterial surface factor polysaccharide A on *Bacteroides fragilis* inhibits IL-1 β -induced inflammation in human fetal enterocytes via toll receptors 2 and 4. *PLoS One* 12:e0172738. PMC5344356.
303. Mazmanian SK, Kasper DL. 2006. The love-hate relationship between bacterial polysaccharides and the host immune system. *Nat Rev Immunol* 6:849-58.
304. Mazmanian SK, Round JL, Kasper DL. 2008. A microbial symbiosis factor prevents intestinal inflammatory disease. *Nature* 453:620-5.
305. Round JL, Lee SM, Li J, Tran G, Jabri B, Chatila TA, Mazmanian SK. 2011. The Toll-like receptor 2 pathway establishes colonization by a commensal of the human microbiota. *Science* 332:974-7. PMC3164325.

306. Wegorzewska MM, Glowacki RWP, Hsieh SA, Donermeyer DL, Hickey CA, Horvath SC, Martens EC, Stappenbeck TS, Allen PM. 2019. Diet modulates colonic T cell responses by regulating the expression of a *Bacteroides thetaiotaomicron* antigen. *Science Immunology* 4:1-13. PMID: PMC6550999.
307. Duffey KJ, Popkin BM. 2008. High-fructose corn syrup: is this what's for dinner? *The American journal of clinical nutrition* 88:1722S-1732S.
308. Popkin BM, Gordon-Larsen P. 2004. The nutrition transition: worldwide obesity dynamics and their determinants. *Int J Obes Relat Metab Disord* 28 Suppl 3:S2-9.
309. Martinez Steele E, Baraldi LG, Louzada ML, Moubarac JC, Mozaffarian D, Monteiro CA. 2016. Ultra-processed foods and added sugars in the US diet: evidence from a nationally representative cross-sectional study. *BMJ Open* 6:e009892. PMID:4785287.
310. of USDoAaUSD, Services HaH. 2020. *Dietary Guidelines for Americans, 2020-2025.*, 9 ed.
311. Ferraris RP, Choe JY, Patel CR. 2018. Intestinal Absorption of Fructose. *Annu Rev Nutr* 38:41-67. PMID:6457363.
312. Jang C, Hui S, Lu W, Cowan AJ, Morscher RJ, Lee G, Liu W, Tesz GJ, Birnbaum MJ, Rabinowitz JD. 2018. The Small Intestine Converts Dietary Fructose into Glucose and Organic Acids. *Cell metabolism* 27:351-361.e3.
313. Do MH, Lee E, Oh MJ, Kim Y, Park HY. 2018. High-Glucose or -Fructose Diet Cause Changes of the Gut Microbiota and Metabolic Disorders in Mice without Body Weight Change. *Nutrients* 10. PMID:6024874.
314. Teghanemt A, Zhang D, Levis EN, Weiss JP, Gioannini TL. 2005. Molecular basis of reduced potency of underacylated endotoxins. *J Immunol* 175:4669-76.
315. Cani PD, Amar J, Iglesias MA, Poggi M, Knauf C, Bastelica D, Neyrinck AM, Fava F, Tuohy KM, Chabo C, Waget A, Delmee E, Cousin B, Sulpice T, Chamontin B, Ferrieres J, Tanti JF, Gibson GR, Casteilla L, Delzenne NM, Alessi MC, Burcelin R. 2007. Metabolic endotoxemia initiates obesity and insulin resistance. *Diabetes* 56:1761-72.
316. Mukhopadhyay I, Hansen R, El-Omar EM, Hold GL. 2012. IBD-what role do Proteobacteria play? *Nat Rev Gastroenterol Hepatol* 9:219-30.
317. Kowalska-Duplaga K, Gosiewski T, Kapusta P, Sroka-Oleksiak A, Wędrychowicz A, Pieczarkowski S, Ludwig-Słomczyńska AH, Wołkow PP, Fyderek K. 2019. Differences in the intestinal microbiome of healthy children and patients with newly diagnosed Crohn's disease. *Scientific Reports* 9:1-11. PMID: PMC6906406.

318. Liu W, Zhang R, Shu R, Yu J, Li H, Long H, Jin S, Li S, Hu Q, Yao F, Zhou C, Huang Q, Hu X, Chen M, Hu W, Wang Q, Fang S, Wu Q. 2020. Study of the Relationship between Microbiome and Colorectal Cancer Susceptibility Using 16SrRNA Sequencing. *Hindawi BioMed Research International* 2020:17-17. PMID: PMC7011317.
319. Milani C, Ticinesi A, Gerritsen J, Nouvenne A, Andrea Lugli G, Mancabelli L, Turrone F, Duranti S, Mangifesta M, Viappiani A, Ferrario C, Maggio M, Lauretani F, De Vos W, Van Sinderen D, Meschi T, Ventura M. 2016. Gut microbiota composition and *Clostridium difficile* infection in hospitalized elderly individuals: A metagenomic study. *Scientific Reports* 6:1-12. PMID: PMC4863157.
320. Mathew S, Smatti MK, Al Ansari K, Nasrallah GK, Al Thani AA, Yassine HM. 2019. Mixed Viral-Bacterial Infections and Their Effects on Gut Microbiota and Clinical Illnesses in Children. *Scientific Reports* 9:1-12. PMID: PMC6351549.
321. Rao SSC, Rehman A, Yu S, De Andino NM. 2018. Brain fogginess, gas and bloating: A link between SIBO, probiotics and metabolic acidosis. *Clinical and Translational Gastroenterology* 9:1-9. PMID: PMC6006167.
322. Shahanshah Khan1* SW, Victoria Godfrey1, Md Abdul Wadud Khan2,, Rajalaksmy A. Ramachandran1 BLC, Cassie Behrendt4, Lan Peng1, Lora V. Hooper4,5, Hasan Zaki1†. 2020. Dietary simple sugars alter microbial ecology in the gut and promote colitis in mice. *Science Translational Medicine* 12.
323. Pudlo NAU, Karthik; Crawford, Ryan; Pirani, Ali; Atherly, Todd; Jimenez, Roberto; Terrapon, Nicolas; Henrissat, Bernard; Peterson, Daniel; Ziemer, Cherie; Snitkin, Evan; Martens, Eric C. 2022. Phenotypic and Genomic Diversification in Complex Carbohydrate-Degrading Human Gut Bacteria. *mSystems* 7.
324. Zmora N, Suez J, Elinav E. 2019. You are what you eat: diet, health and the gut microbiota. *Nat Rev Gastroenterol Hepatol* 16:35-56.
325. Townsend GE, Han W, Schwalm ND, Raghavan V, Barry NA, Goodman AL, Groisman EA. 2018. Dietary sugar silences a colonization factor in a mammalian gut symbiont. *Proceedings of the National Academy of Sciences* 116:233-238. PMID: PMC6320540.
326. Sonnenburg ED, Sonnenburg JL, Manchester JK, Hansen EE, Chiang HC, Gordon JI. 2006. A hybrid two-component system protein of a prominent human gut symbiont couples glycan sensing in vivo to carbohydrate metabolism. *Proceedings of the National Academy of Sciences of the United States of America* 103:8834-8839. PMID: PMC1472243.
327. Cordain LE, S Boyd; Sebastian, Anthony; Mann, Neil; Lindeberg, Staffan; Watkins, Bruce A; O'Keefe, James H; Brand-Miller, Janette. 2005. Origins and evolution of the Western diet: health implications for the 21st century. *American Journal of Clinical Nutrition* 81:341-354.

328. Fajstova A, Galanova N, Coufal S, Malkova J, Kostovcik M, Cermakova M, Pelantova H, Kuzma M, Sediva B, Hudcovic T, Hrcir T, Tlaskalova-Hogenova H, Kverka M, Kostovcikova K. 2020. Diet Rich in Simple Sugars Promotes Pro-Inflammatory Response via Gut Microbiota Alteration and TLR4 Signaling. *Cells* 9. PMC7766268.
329. Kawano Y, Edwards M, Huang Y, Bilate AM, Araujo LP, Tanoue T, Atarashi K, Ladinsky MS, Reiner SL, Wang HH, Mucida D, Honda K, Ivanov, II. 2022. Microbiota imbalance induced by dietary sugar disrupts immune-mediated protection from metabolic syndrome. *Cell* 185:3501-3519 e20. PMC9556172.
330. Schwalm ND, Townsend GE, Groisman EA. 2016. Multiple Signals Govern Utilization of a Polysaccharide in the Gut Bacterium *Bacteroides thetaiotaomicron*. *mBio* 7:1-9. PMID: PMC5061871.
331. Townsend GE, Han W, Schwalm ND, Hong X, Bencivenga-barry NA, Goodman AL, Groisman EA. 2020. A Master Regulator of *Bacteroides thetaiotaomicron* Gut Colonization Controls Carbohydrate Utilization and an Alternative Protein Synthesis Factor. *mBio* 11:1-14. PMID: PMC6989115.
332. Glowacki RWP, Pudlo NA, Tuncil Y, Luis AS, Sajjakulnukit P, Terekhov AI, Lyssiotis CA, Hamaker BR, Martens EC. 2020. A Ribose-Scavenging System Confers Colonization Fitness on the Human Gut Symbiont *Bacteroides thetaiotaomicron* in a Diet-Specific Manner. *Cell Host and Microbe* 27:79-92.e9. PMID: PMC7031954.
333. Martens EC, Lowe EC, Chiang H, Pudlo NA, Wu M, McNulty NP, Abbott DW, Henrissat B, Gilbert HJ, Bolam DN, Gordon JI. 2011. Recognition and degradation of plant cell wall polysaccharides by two human gut symbionts. *PLoS Biology* 9.
334. Lowe EC, Basle A, Czjzek M, Firbank SJ, Bolam DN. 2012. A scissor blade-like closing mechanism implicated in transmembrane signaling in a *Bacteroides* hybrid two-component system. *Proc Natl Acad Sci U S A* 109:7298-303. PMC3358863.
335. Ryan D, Jenniches L, Reichardt S, Barquist L, Westermann AJ. 2020. A high-resolution transcriptome map identifies small RNA regulation of metabolism in the gut microbe *Bacteroides thetaiotaomicron*. *Nature Communications* 11. PMID: PMC7366714.
336. Cao Y, Förstner KU, Vogel J, Jeffrey Smith C. 2016. cis-encoded small RNAs, a conserved mechanism for repression of polysaccharide utilization in *Bacteroides*. *Journal of Bacteriology* 198:2410-2418.
337. Ryan DB, Elise; Prezza, Gianluca; Alampalli, Shuba Varshini; de Carvalho, Tais Franco; Felchle, Hannah; Ebbecke, Titus; Hayward, Regan; Deutschbauer, Adam M; Berquist, Lars; Westermann, Alexander J. 2023. An integrated transcriptomics-functional genomics approach reveals a small RNA that

- modulates *Bacteroides thetaiotaomicron* sensitivity to tetracyclines. *bioRxiv*. PMC9949090.
338. Adams AND, Azam MS, Costliow ZA, Ma X, Degnan PH, Vanderpool CK. 2021. A Novel Family of RNA-Binding Proteins Regulate Polysaccharide Metabolism in *Bacteroides thetaiotaomicron*. *J Bacteriol* 203:e0021721. PMC8508124.
 339. Kryptou E, Townsend GE, Gao X, Tachiyama S, Liu J, Pokorzynski ND, Goodman AL, Groisman EA. 2023. Bacteria require phase separation for fitness in the mammalian gut. *Science* 379:1149-1156.
 340. Krinos CMC, Michael J; Weinacht, Katja G; Tzianabos, Arthur O; Kasper, Dennis L; Comstock, Laurie E. 2001. Extensive surface diversity of a commensal microorganism by multiple DNA inversions. *Nature* 414.
 341. Cerdeno-Tarraga AM, Patrick S, Crossman LC, Blakely G, Abratt V, Lennard N, Poxton I, Duerden B, Harris B, Quail MA, Barron A, Clark L, Corton C, Doggett J, Holden MT, Larke N, Line A, Lord A, Norbertczak H, Ormond D, Price C, Rabbinowitsch E, Woodward J, Barrell B, Parkhill J. 2005. Extensive DNA inversions in the *B. fragilis* genome control variable gene expression. *Science* 307:1463-5.
 342. Cho KH, Cho D, Wang GR, Salyers AA. 2001. New regulatory gene that contributes to control of *Bacteroides thetaiotaomicron* starch utilization genes. *J Bacteriol* 183:7198-205. PMC95569.
 343. Han W, Peng BZ, Wang C, Townsend GE, 2nd, Barry NA, Peske F, Goodman AL, Liu J, Rodnina MV, Groisman EA. 2022. Gut colonization by *Bacteroides* requires translation by an EF-G paralog lacking GTPase activity. *EMBO J* doi:10.15252/embj.2022112372:e112372.
 344. Modesto JL, Pearce VH, Townsend GE, 2nd. 2023. Harnessing gut microbes for glycan detection and quantification. *Nat Commun* 14:275. PMC9845299.
 345. Terrapon N, Lombard V, Drula E, Lapebie P, Al-Masaudi S, Gilbert HJ, Henrissat B. 2018. PULDB: the expanded database of Polysaccharide Utilization Loci. *Nucleic Acids Res* 46:D677-D683. PMC5753385.
 346. Busby SE, Richard H. 1999. Transcription Activation by Catabolite Activator Protein (CAP). *Journal of Molecular Biology* 293:199-213.
 347. Iyer R, Baliga NS, Camilli A. 2005. Catabolite control protein A (CcpA) contributes to virulence and regulation of sugar metabolism in *Streptococcus pneumoniae*. *J Bacteriol* 187:8340-9. PMC1317011.
 348. Siegel LS, Hylemon PB, Phibbs PV. 1977. Cyclic Adenosine 3',5'-Monophosphate Levels and Activities of Adenylate Cyclase and Cyclic Adenosine 3',5'-Monophosphate Phosphodiesterase in *Pseudomonas* and *Bacteroides*. *Journal of Bacteriology* 129:87-96. PMCID: PMC234899.

349. Han S, Van Treuren W, Fischer CR, Merrill BD, DeFelice BC, Sanchez JM, Higginbottom SK, Guthrie L, Fall LA, Dodd D, Fischbach MA, Sonnenburg JL. 2021. A metabolomics pipeline for the mechanistic interrogation of the gut microbiome. *Nature* 595:415-420. PMC8939302.
350. Liu H, Shiver AL, Price MN, Carlson HK, Trotter VV, Chen Y, Escalante V, Ray J, Hern KE, Petzold CJ, Turnbaugh PJ, Huang KC, Arkin AP, Deutschbauer AM. 2021. Functional genetics of human gut commensal *Bacteroides thetaiotaomicron* reveals metabolic requirements for growth across environments. *Cell Rep* 34:108789. PMC8121099.
351. Goodman AL, McNulty NP, Zhao Y, Leip D, Mitra RD, Lozupone CA, Knight R, Gordon JI. 2009. Identifying genetic determinants needed to establish a human gut symbiont in its habitat. *Cell Host Microbe* 6:279-89. PMC2895552.
352. Liou CS, Sirk SJ, Diaz CAC, Klein AP, Fischer CR, Higginbottom SK, Erez A, Donia MS, Sonnenburg JL, Sattely ES. 2020. A Metabolic Pathway for Activation of Dietary Glucosinolates by a Human Gut Symbiont. *Cell* 180:717-728.e19.
353. Wexler AG, Goodman AL. 2017. An insider's perspective: *Bacteroides* as a window into the microbiome. *Nature Microbiology* 2:1-11.
354. Raghavan V, Lowe EC, Townsend GE, Bolam DN, Groisman EA. 2014. Tuning transcription of nutrient utilization genes to catabolic rate promotes growth in a gut bacterium. *Molecular Microbiology* 93:1010-1025.
355. Crouch LI, Liberato MV, Urbanowicz PA, Basle A, Lamb CA, Stewart CJ, Cooke K, Doona M, Needham S, Brady RR, Berrington JE, Madunic K, Wuhler M, Chater P, Pearson JP, Glowacki R, Martens EC, Zhang F, Linhardt RJ, Spencer DIR, Bolam DN. 2020. Prominent members of the human gut microbiota express endo-acting O-glycanases to initiate mucin breakdown. *Nat Commun* 11:4017. PMC7419316.
356. Degnan PH, Barry NA, Mok KC, Taga ME, Goodman AL. 2014. Human gut microbes use multiple transporters to distinguish vitamin B12 analogs and compete in the gut. *Cell Host Microbe* 15:47-57. PMC3923405.
357. Costliow ZA, Degnan PH, Vanderpool CK. 2019. Thiamine pyrophosphate riboswitches in *Bacteroides* species regulate retranscription or translation of thiamine transport and biosynthesis genes. *bioRxiv* doi:10.1101/867226.
358. Costliow ZA, Degnan PH. 2017. Thiamine Acquisition Strategies Impact Metabolism and Competition in the Gut Microbe *Bacteroides thetaiotaomicron*. *mSystems* 2.
359. King AM, Vanderpool CK, Degnan PH. 2019. sRNA Target Prediction Organizing Tool (SPOT) Integrates Computational and Experimental Data To Facilitate Functional Characterization of Bacterial Small RNAs. *mSphere* 4. PMC6354806.

360. Donaldson GP, Chou WC, Manson AL, Rogov P, Abeel T, Bochicchio J, Ciulla D, Melnikov A, Ernst PB, Chu H, Giannoukos G, Earl AM, Mazmanian SK. 2020. Spatially distinct physiology of *Bacteroides fragilis* within the proximal colon of gnotobiotic mice. *Nature Microbiology* doi:10.1038/s41564-020-0683-3.
361. Comstock LE. 2016. Small RNAs Repress Expression of Polysaccharide Utilization Loci of Gut *Bacteroides* Species. *Journal of Bacteriology* 198:2396-2398.
362. McCown PJ, Corbino KA, Stav S, Sherlock ME, Breaker RR. 2017. Riboswitch diversity and distribution. *RNA* 23:995-1011. PMC5473149.
363. Bencivenga-Barry NA, Lim B, Herrera CM, Stephen Trent M, Goodman AL. 2020. Genetic manipulation of wild human gut bacteroides. *Journal of Bacteriology* 202.
364. García-Bayona L, Comstock LE. 2019. Streamlined genetic manipulation of diverse bacteroides and parabacteroides isolates from the human gut microbiota. *mBio* 10.
365. Koropatkin NM, Martens EC, Gordon JI, Smith TJ. 2008. Starch catabolism by a prominent human gut symbiont is directed by the recognition of amylose helices. *Structure* 16:1105-15. 2563962.
366. Raghavan V, Lowe EC, Townsend GE, 2nd, Bolam DN, Groisman EA. 2014. Tuning transcription of nutrient utilization genes to catabolic rate promotes growth in a gut bacterium. *Mol Microbiol* 93:1010-25.
367. Perez JC, Shin D, Zwir I, Latifi T, Hadley TJ, Groisman EA. 2009. Evolution of a bacterial regulon controlling virulence and Mg(2+) homeostasis. *PLoS Genet* 5:e1000428. PMC2650801.
368. Ryan D, Bornet E, Prezza G, Alampalli SV, de Carvalho TF, Felchle H, Ebbecke T, Hayward R, Deutschbauer AM, Barquist L, Westermann AJ. 2023. An integrated transcriptomics-functional genomics approach reveals a small RNA that modulates *Bacteroides thetaiotaomicron* sensitivity to tetracyclines. *bioRxiv* doi:10.1101/2023.02.16.528795. 9949090.
369. Mann M, Wright PR, Backofen R. 2017. IntaRNA 2.0: enhanced and customizable prediction of RNA-RNA interactions. *Nucleic Acids Res* 45:W435-W439. PMC5570192.
370. Han W, Peng BZ, Wang C, Townsend GE, 2nd, Barry NA, Peske F, Goodman AL, Liu J, Rodnina MV, Groisman EA. 2023. Gut colonization by *Bacteroides* requires translation by an EF-G paralog lacking GTPase activity. *EMBO J* 42:e112372. 9841332.
371. Luis AS, Briggs J, Zhang X, Farnell B, Ndeh D, Labourel A, Baslé A, Cartmell A, Terrapon N, Stott K, Lowe EC, McLean R, Shearer K, Schückel J, Venditto I, Ralet MC, Henrissat B, Martens EC, Mosimann SC, Abbott DW, Gilbert HJ.

2018. Dietary pectic glycans are degraded by coordinated enzyme pathways in human colonic *Bacteroides*. *Nature Microbiology* 3:210-219.
372. Rogers TE, Pudlo NA, Koropatkin NM, Bell JS, Moya Balasch M, Jasker K, Martens EC. 2013. Dynamic responses of *Bacteroides thetaiotaomicron* during growth on glycan mixtures. *Mol Microbiol* 88:876-90. PMC3700664.
373. Sonnenburg ED, Zheng H, Joglekar P, Higginbottom SK, Firbank SJ, Bolam DN, Sonnenburg JL. 2010. Specificity of polysaccharide use in intestinal *Bacteroides* species determines diet-induced microbiota alterations. *Cell* 141:1241-52. PMC2900928.
374. Cameron EA, Kwiatkowski KJ, Lee B-H, Hamaker BR, Koropatkin NM, Martens EC. 2014. Multifunctional Nutrient-Binding Proteins Adapt Human Symbiotic Bacteria for Glycan Competition in the Gut by Separately Promoting Enhanced Sensing and Catalysis. doi:10.1128/mBio.01441-14.
375. Durica-Mitic S, Gopel Y, Gorke B. 2018. Carbohydrate Utilization in Bacteria: Making the Most Out of Sugars with the Help of Small Regulatory RNAs. *Microbiol Spectr* 6.
376. Fujita Y. 2009. Carbon catabolite control of the metabolic network in *Bacillus subtilis*. *Biosci Biotechnol Biochem* 73:245-59.
377. Mimee M, Tucker AC, Voigt CA, Lu TK. 2015. Programming a Human Commensal Bacterium, *Bacteroides thetaiotaomicron*, to Sense and Respond to Stimuli in the Murine Gut Microbiota. *Cell Systems* 1:62-71.
378. Lim B, Zimmermann M, Barry NA, Goodman AL. 2017. Engineered Regulatory Systems Modulate Gene Expression of Human Commensals in the Gut. *Cell* 169:547-558.e15. PMID: PMC5532740.
379. Qi LS, Larson MH, Gilbert LA, Doudna JA, Weissman JS, Arkin AP, Lim WA. 2013. Repurposing CRISPR as an RNA-guided platform for sequence-specific control of gene expression. *Cell* 152:1173-83. PMC3664290.
380. Cho KH, Salyers AA. 2001. Biochemical analysis of interactions between outer membrane proteins that contribute to starch utilization by *Bacteroides thetaiotaomicron*. *Journal of Bacteriology* 183:7224-7230.
381. Townsend GE, 2nd, Han W, Schwalm ND, 3rd, Raghavan V, Barry NA, Goodman AL, Groisman EA. 2019. Dietary sugar silences a colonization factor in a mammalian gut symbiont. *Proc Natl Acad Sci U S A* 116:233-238. 6320540.
382. Brigham CJ, Malamy MH. 2005. Characterization of the RokA and HexA broad-substrate-specificity hexokinases from *Bacteroides fragilis* and their role in hexose and N-acetylglucosamine utilization. *J Bacteriol* 187:890-901. PMC545704.

383. Franklund CVG, Thomas L. 1987. Glucose Uptake by the Cellulolytic Ruminal Anaerobe *Bacteroides succinogenes*. J Bacteriol 169:500-506.
384. Koropatkin NM, Cameron EA, Martens EC. 2012. How glycan metabolism shapes the human gut microbiota. Nature Reviews Microbiology 10.
385. McNulty NP, Wu M, Erickson AR, Pan C, Erickson BK, Martens EC, Pudlo NA, Muegge BD, Henrissat B, Hettich RL, Gordon JI. 2013. Effects of diet on resource utilization by a model human gut microbiota containing *Bacteroides cellulosilyticus* WH2, a symbiont with an extensive glycobiome. PLoS Biol 11:e1001637. PMC3747994.
386. Rakoff-Nahoum S, Foster KR, Comstock LE. 2016. The evolution of cooperation within the gut microbiota. doi:10.1038/nature17626.
387. Mastropaolo MD, Thorson ML, Stevens AM. 2009. Comparison of *Bacteroides thetaiotaomicron* and *Escherichia coli* 16S rRNA gene expression signals. Microbiology (Reading) 155:2683-2693.
388. Terrapon N, Lombard V, Gilbert HJ, Henrissat B. 2015. Automatic prediction of polysaccharide utilization loci in Bacteroidetes species. Bioinformatics 31:647-55.
389. Lam KN, Martens EC, Charles TC. 2018. Developing a *Bacteroides* System for Function-Based Screening of DNA from the Human Gut Microbiome. doi:10.1128/mSystems.00195-17.
390. Donald G. Guiney KB, Patricia Hasegawa, and Barbara Matthews. 1988. Construction of Shuttle Cloning Vectors for *Bacteroides fragilis* and Use in Assaying Foreign Tetracycline Resistance Gene Expression. Plasmid 20:17-22.
391. Nadja B. Shoemaker RDB, and Abigail A. Salyers. 1989. Cloning and characterization of a *Bacteroides* conjugal tetracycline-erythromycin resistance element by using a shuttle cosmid vector. J Bacteriol 171.
392. Cheng J, Pinnell L, Engel K, Neufeld JD, Charles TC. 2014. Versatile broad-host-range cosmids for construction of high quality metagenomic libraries. J Microbiol Methods 99:27-34.
393. Zimmermann M, Zimmermann-Kogadeeva M, Wegmann R, Goodman AL. 2019. Mapping human microbiome drug metabolism by gut bacteria and their genes. Nature 570:462-467.
394. Siegel LS, Hylemon PB, Phibbs PV, Jr. 1977. Cyclic adenosine 3',5'-monophosphate levels and activities of adenylate cyclase and cyclic adenosine 3',5'-monophosphate phosphodiesterase in *Pseudomonas* and *Bacteroides*. J Bacteriol 129:87-96. 234899.
395. Bencivenga-Barry NA, Lim B, Herrera CM, Trent MS, Goodman AL. 2020. Genetic Manipulation of Wild Human Gut *Bacteroides*. J Bacteriol 202. 6964735.

396. Garcia-Bayona L, Comstock LE. 2019. Streamlined Genetic Manipulation of Diverse *Bacteroides* and *Parabacteroides* Isolates from the Human Gut Microbiota. *mBio* 10. 6692515.
397. Van Tassell RL, Lyerly DM, Wilkins TD. 1992. Purification and characterization of an enterotoxin from *Bacteroides fragilis*. *Infect Immun* 60:1343-50. 257002.

VITA

Victoria H. Pearce

Education

- 2018-2023** Pennsylvania State University College of Medicine, Hershey, PA
Ph. D. Biomedical Sciences
- 2015-2018** Youngstown State University, Youngstown, OH
B.S. Biology

Publications

1. Modesto JL, **Pearce VH**, Townsend GE. (2023). Harnessing gut microbes for glycan detection and quantification. *Nature Communications*. 14, 275.
2. **Pearce VH**, Groisman EA, Townsend GE. (2023). Dietary sugars silence the master regulator of carbohydrate utilization in human gut *Bacteroides* species. *Gut Microbes*. 15, 1.

Honors and Awards

- 2023** **Microbiome Center Conference Travel Grant**
Penn State University
- 2023** **Summer Travel Award**
Penn State University
- 2022** **Graduate Alumni Endowed Scholarship**
Penn State College of Medicine
- 2020** **Graduate Alumni Society Award**
Penn State College of Medicine

Conference Presentations

- Pearce VH**, Townsend GE. (2023 Jun 19) Host Dietary Sugar Consumption Silences the Activity of the Conserved Master Regulator of Carbohydrate Utilization in *Bacteroides*. [Oral Presentation]
American Society for Microbiology, ASM Microbe 2023, Houston, TX, United States
- Silvis VH**, Townsend GE. (2021 Jun 21) Pentose Phosphate Pathway Intermediates Control a Conserved Intestinal Colonization Mechanism in Dominant Gut Microbes. [Virtual Poster Presentation]
World Microbe Forum